INSTITUTO SUPERIOR DE ENGENHARIA DO PORTO
MESTRADO EM ENGENHARIA MECÂNICA

CONTRIBUTION TO THE VALIDATION AND VERIFICATION OF DRIVE-NEUTRAL-REVERSE SUBSYSTEM OF A CVT TRANSMISSION

PEDRO NUNO DOS SANTOS ALMEIDA
Outubro de 2017

POLITÉCNICO
DO PORTO

Instituto Superior de Engenharia do Porto

CONTRIBUTION TO THE VALIDATION AND VERIFICATION OF DRIVE-NEUTRAL-REVERSE SUBSYSTEM OF A CVT TRANSMISSION

Pedro Nuno dos Santos Almeida

2017

Instituto Superior de Engenharia do Porto – School of Engineering, Polytechnic of Porto

Mechanical Engineering Department

POLITÉCNICO DO PORTO

POLITÉCNICO
DO PORTO

Instituto Superior de Engenharia do Porto

CONTRIBUTION TO THE VALIDATION AND VERIFICATION OF DRIVE-NEUTRAL-REVERSE SUBSYSTEM OF A CVT TRANSMISSION

Pedro Nuno dos Santos Almeida

1120666

Dissertation presented to ISEP – School of Engineering to fulfill the requirements necessary to obtain a Master's degree in Mechanical Engineering, carried out under the guidance of Doctor Francisco José Gomes da Silva, Adjunct Professor.

2017

Instituto Superior de Engenharia do Porto – School of Engineering, Polytechnic of Porto

Mechanical Engineering Department

POLITÉCNICO DO PORTO

POLITÉCNICO
DO PORTO

JURY

President

Manuel Jorge Dores de Castro

Adjunct Professor, Department of Mechanical Engineering, ISEP

Advisor

Francisco José Gomes da Silva

Adjunct Professor, Department of Mechanical Engineering, ISEP

Arguing

Ricardo José Alves de Sousa

Auxiliar Professor, Department of Mechanical Engineering, University of Aveiro

ACKNOWLEDGEMENTS

I would like to start by thanking to all who contributed directly and indirectly to my personal and academic life course.

To my family and close friends who were always present even when the distance was a barrier ready to support and motivate me.

To my girlfriend, Beatriz, who was always an unconditional supporter of all my decisions and a source of courage and admiration to make me embrace new challenges.

To my university's mentor, Professor Francisco J. G. Silva, for all the academic assistance, the inexhaustible willingness to provide feedback and the motivation to me facing this challenge.

I could not forget the person who introduced me to the automotive industry, Amadeu Bastos, his knowledge, experience and advices, with no fear of sharing his vast knowledge and experience, in the internship at Simoldes Plásticos during over a year.

I would like to thank Gert Heirman who provided me the internship opportunity at Punch Powertrain NV and believed me and my potential. I would also like to thank my team at Punch Powertrain, Rudi Aerts, Wouter Tits and Ronald Vanderloo for all the experience and what they have taught me. The readiness, availability and willingness to help me to get better results and learn as much as possible are some of the factors that made this stage so important and constructive.

Finally, I would like to thank you Luiz Filipe Pereira for all the advices and to Carolien Dusar for the support.

KEYWORDS

Continuously Variable Transmission, Drive-Neutral-Reverse subsystem, Planetary Gear Set, Wet clutches, Drag losses, pre-load conditions, biting-point conditions, transmissible torque, Tolerance chain stack up

ABSTRACT

Continuously Variable Transmissions (CVT) are the synonymous for fuel economy and smooth ride. Due to these major features of this type of automatic transmission (AT) it can be easily the future of automatic transmissions since the restrictions regarding to the fuel emissions are getting stricter.

The knowledge by the student related to this thematic was developed in an internship with a duration of six months at a specialized company in the development and production of CVT transmissions. By being incorporated in the department of R&D, specifically on the team of the DNR subsystem (Drive-Neutral-Reverse subsystem), it was possible to be introduced to CVT. Punch Powertrain NV in Belgium, Sint-Truiden, was the perfect opportunity to enrich the academic experience of the student, to introduce the student to development field of automotive transmissions industry from concept to testing and also to consolidate the experience in the automotive industry previously started at Simoldes Plásticos during the master degree. Firstly, it was suggested to assist to the prototype assembly process of a complete CVT followed by the analyses to the flow chart of the DNR subsystem and the manufacturability of all the components of the subsystem in order to get introduced to the subsystem. Secondly it was proposed to develop a showcase model which would be a great tool to explain people the working principle of a DNR subsystem in detail. At the same time, the student decided to start some calculations related to the DNR subsystem not only to better understand the subsystem and apply the knowledge obtained during the graduation but also to learn more specific subjects related to this field of study. This task would later allow the student to verify the mechanical requirements. After asking for quotations and getting in contact with several suppliers it was time to assemble the entire showcase getting in contact with different manufacturing processes and difficulties. At the end, it is irrefutable the amount of knowledge acquired during the internship. Undoubtedly, the support from all the colleagues was very important by transmitting me all their knowledge and experience.

PALAVRAS CHAVE

Transmissão Continuamente Variável, Subsistema Drive-Neutral-Reverse, Conjunto de engrenagens planetárias, Pratos de embraiagem húmidos, Perdas por arraste, Condições de pré-carga, condições de biting-point, torque transmissível, Cadeia de tolerância em série

RESUMO

Transmissões Continuamente Variáveis (CVT) são sinónimo de economia de combustível e condução suave. Devido a estas grandes características deste tipo de transmissão, podemos estar facilmente perante o futuro das transmissões automáticas visto que as restrições relativamente às emissões de combustível se estão a tornar mais apertadas.

O conhecimento adquirido pelo estudante nesta temática foi desenvolvido num estágio com duração de seis meses numa empresa especializada no desenvolvimento e produção de transmissões CVT. Ao estar incorporado no departamento de I&D, mais especificamente na equipa de desenvolvimento do subsistema DNR, foi possível familiarizar-se com as Transmissões de Continuamente Variáveis. Punch Powertrain NV na Bélgica, Sint-Truiden, foi a oportunidade perfeita para enriquecer a experiência do estudante, introduzi-lo à área de desenvolvimento da indústria das transmissões automóveis desde o conceito até à fase de testes, e também para consolidar a experiência na indústria automóvel previamente iniciada num estágio na Simoldes Plásticos durante o percurso de mestrado. Em primeiro lugar, foi sugerido assistir à montagem da fase protótipo de uma CVT seguida da análise do esquema do fluxo do óleo do subsistema DNR e os processos de fabrico de todos os componentes do subsistema com vista a integrar-se no subsistema. Em segundo lugar foi proposto desenvolver um equipamento de amostra que seria uma ótima ferramenta para explicar detalhadamente às pessoas o princípio de funcionamento de um subsistema DNR. Ao mesmo tempo, o estudante decidiu começar alguns cálculos relativos ao subsistema DNR não só para melhor compreender o subsistema, mas também para aplicar o conhecimento adquirido durante o seu percurso académico com vista a aprender campos mais específicos sobre este tema de estudo. Esta tarefa iria mais tarde permitir ao estudante a verificação dos requisitos. Após de alguns pedidos de orçamentação e de

ter entrado em contacto com alguns fornecedores, era tempo da montagem do equipamento de amostra estando diretamente em contacto com diferentes processos de fabrico e respetivas dificuldades. No final, é irrefutável a proporção de conhecimento adquirido durante este estágio. Sem dúvida alguma o apoio dos colegas foi bastante importante ao transmitirem todo o seu conhecimento e experiência.

LIST OF SYMBOLS AND ABBREVIATIONS

List of abbreviations

AMT	Automated manual transmission
Assy	Assembly
AT	Automatic Transmission
BOM	Bill of materials
CAFE	Corporate Average Fuel Economy
CC	Clutch Carrier
CO	Carbon monoxide
CO_2	Carbon dioxide
CP	Clutch plates
CVT	Continuously Variable Transmission
D	Drive Gear
DCT	Dual Clutch Transmission
DNR	Drive-Neutral-Reverse subsystem
EOP	Engine operating point
EPA	Environmental Protection Agency
EPT	Epicyclic Gear Train
EU	European Union
EUDC	Extra urban cycle
EV	Electric vehicle
FBD	Free body diagram
FEA	Finite Elements Analysis
FFOR	Fully Functional Operating Range
FL	Free length
FWD	Forward
HC	Hydrocarbons
IC	Internal combustion
ICE	Internal Combustion Engine
ID	Inner diameter
ISO	International Standard Organization
LCV	Low carbon vehicle

MT	Manual Transmission
N	Neutral Gear
NO_x	Oxides of nitrogen
NV	*Naamloze Vennootschap*
OD	Outer diameter
PGS	Planetary Gear Set
PGT	Planetary Gear Train
PHEV	Plug-in hybrid electric vehicle
R	Reverse Gear
REV	Reverse
RSS	Root Sum Square
SF	Safety Factor
SP	Spring pack
TRH	Transmission Housing
UK	United Kingdom
USA	United States of America

List of units

^oC	Celsius degrees
cm	Centimetre
cP	Centipoise
g	Gram
hp	Horsepower
Hz	Hertz
K	Kelvin degrees
kg	Kilogram
km	Kilometre
m	Meter
mm	Millimetre
MPa	Megapascal
mpg	Miles per galon
N	Newton
Nm	Newton meter (torque)
Pa	Pascal
rad	Radian
rpm	Revolutions per minute
s	Second
t	Tons

List of symbols

A	Elongation
A_F	Friction area
A_H	Hydraulic area
A_n	Extension of a bar up to the point of fracture measured over an initial gauge length of n times the bar diameter
b	Thickness
b_W	Radial wall (width) (wavy washer)
C	Spring index (compression spring)
d	Deflection
d_c	Coil diameter (compression springs)
d_m	Limit spring deflection
D_m	Mean diameter
d_{max}	Limit spring deflection
D_p	Fluid entry diameter
E	Young's Modulus or Modulus of Elasticity
F	Load
F_a	Amplitude force
F_{ax}	Axial force
F_C	Centrifugal force
F_H	Hydraulic force
FL	Free length (springs)
F_m	Midrange force
F_n	Load at height n
F_S	Load at solid height
G	Material shear modulus
h	Height
H	Unloaded spring height (Belleville washer)
h_0	Initial cone height of disc springs without ground ends (equal to free overall height, FL, minus b)
h_B	Unloaded height of truncated cone of free spring (Belleville washer)
h_P	Clearance between consecutive clutch plates
i	Ratio (gears)
ID	Inner diameter
ID_c	Compression springs inner diameter
ID_F	Inner friction surface diameter
$ID_{F\ tol}$	Inner friction surface diameter tolerance
ID_H	Inner hydraulic diameter
$ID_{H\ tol}$	Inner hydraulic diameter tolerance
IR	Inner radius
IR_F	Inner friction surface radius
IR_H	Inner hydraulic radius

K_1, K_2, K_3, K_4	Coefficients used for the calculation of fatigue disc springs
K_B	Bergsträsser factor
K_C	Wahl correction factor (compression spring)
K_W	Multiple wave factor (wavy washer)
L	Length
N	Number of springs
N_A	Number of active coils
N_P	Number of clutch pads
N_S	Number of frictional surfaces (clutches)
N_T	Total number of coils
N_W	Number of waves per turn (wavy washer)
OD	Outer diameter
OD_c	Compression springs outer diameter
OD_F	Outer friction surface diameter
$OD_{F\ tol}$	Outer friction surface diameter tolerance
OD_H	Outer hydraulic diameter
$OD_{H\ tol}$	Outer hydraulic diameter tolerance
OR	Outer radius
OR_F	Outer friction surface radius
OR_H	Outer hydraulic radius
p	Pitch
Q	Needing feed flow rate
Q_i	Input flow rate
r	Slope line
R	Radius
R_1	Inner radius of the friction plates
R_2	Outer radius of the friction plates
R_F	Mean friction radius
RF	Reaction force
r_m	Mean radius
R_m	Tensile strength
r_p	Fluid entry radius
R_p	Yield strength
$R_{p\ 0.2\%}$	0.2% offset yield strength
R_s	Equivalent radius of oil film
R_W	Effective wave radius (wavy washer)
SF_f	Safety factor against fatigue
SH	Solid height
SR	Spring rate/stiffness
S_{sa}	Shear stress amplitude limit
S_{sa}^{Gerber}	Shear stress amplitude limit according to Gerber
$S_{sa}^{Goodman}$	Shear stress amplitude limit according to Goodman

S_{sa}^{Sines}	Shear stress amplitude limit according to Sines
S_{se}	Shear endurance limit
S_{se}^{Gerber}	Shear endurance limit according to Gerber
$S_{se}^{Goodman}$	Shear endurance limit according to Goodman
S_{sm}	Maximum endurance strength component for infinite life
S_{su}	Torsional modulus of rupture
T	Temperature
t	Time instant
T_C	Transmissible torque
T_D	Drag torque
t_W	Wire thickness (wavy washer)
w	Width
W_H	Half wave free height (wavy washer)
W_L	Half wave length (wavy washer)
X	Fatigue stress ratio (wavy washer)
Z	Number of teeth (gears)
Z_w	Number of turns (wavy washer)
γ_1, γ_2, γ_3	Calculation coefficients (Belleville washer)
δ	Diameter ratio
ζ	Friction coefficient
ζ_{max}	Max. Friction coefficient
ζ_{min}	Min. Friction coefficient
Θ_W	Included wave angle (wavy washer)
λ	Fluid's kinematic viscosity
μ	Fluid's dynamic viscosity
ν	Poisson's ratio
ρ	Density
ρ	Density
σ	Stress
σ_I, σ_{II}, σ_{III}, σ_{IV}, σ_{OM},	Calculated material stresses at the point I to OM of the disc spring cross section
σ_S	Stress at solid height
τ_a	Shear stress amplitude
τ_m	Midrange shear stress
ω	Rotating speed

GLOSSARY OF TERMS

Allow for set	Spring is supplied longer than specified to compensate for length loss when fully compressed in assembly by customer. Recommended for large quantity order to reduce cost (Spring, 2011)
Barge	A long boat with a flat bottom, used for carrying heavy objects on rivers or canals (Cambridge Dictionary, n.d.)
Biting point	Biting point is known as the moment when there is contact between clutch plates starting to transmit torque
Commercial vehicle	Motor vehicle designed for the purpose of: − transporting people − Bus; − for transporting goods and pulling trailers − Truck; or just for pulling trailers − Tractor. This excludes passenger cars. (Naunheimer, Bertsche, Ryborz, & Novak, 2010)
Crawling	To move at an unusually slow pace
Engine Idling	Engine running with no load and the vehicle is steady
Fully functional operating range	The range of temperatures between -20 and 120 ^{o}C. This is the range that maximum torque and maximum efficiency need to be guaranteed. From -25 to -20 ^{o}C it needs to be driveable as so from 120 to 140 ^{o}C (Punch Powertrain NV)
Gradeability	Gradeability is defined as the highest grade a vehicle can ascend maintaining a particular speed (Akilesh Yamsani, 2014)
Gridlock	a situation where roads in a town become so blocked by cars that it is impossible for any traffic to move (Dictionary, n.d.)
Hybrid (vehicle)	A vehicle that can be powered by both electricity and an internal-combustion engine (Hillier, 2012)
Passenger car	Motor vehicle designed and equipped mainly for transporting people, with a maximum of nine seats. (Naunheimer *et al*., 2010)
Preset	Presetting consists of coiling the spring to a longer length than the ultimate desired free length and then compressing it beyond its elastic limit. Presetting allows the use of higher design stresses with the added cost of the secondary operation. Some of this added cost,

	however, is sometimes offset by using less material within a given envelope. (Corp, n.d.)
Set	Length loss in operation due to high stress condition in the spring (Spring, 2011)
Tensile strength	The maximum engineering stress, in tension, that may be sustained without fracture. Often termed ultimate (tensile) strength. (William D. Callister & David G. Rethiwsch, 2010)
Torque converter	a device that transmits or multiplies the torque generated by an engine (Hillier, 2012)
Yield strength	The stress required to produce a very slight yet specified amount of plastic strain; a strain offset of 0.002 is commonly used. (William D. Callister & David G. Rethiwsch, 2010)

INDEX OF FIGURES

INDEX OF TABLES

INDEX

INTRODUCTION

1 INTRODUCTION

1.1 Contextualization

1.1.1 Fundamental Principles of Traffic and Vehicle Engineering

The interrelations between traffic and traffic engineering and the economy is not only close but also fundamental, when considered a whole. An example of this interrelation is illustrated on Figure 1.

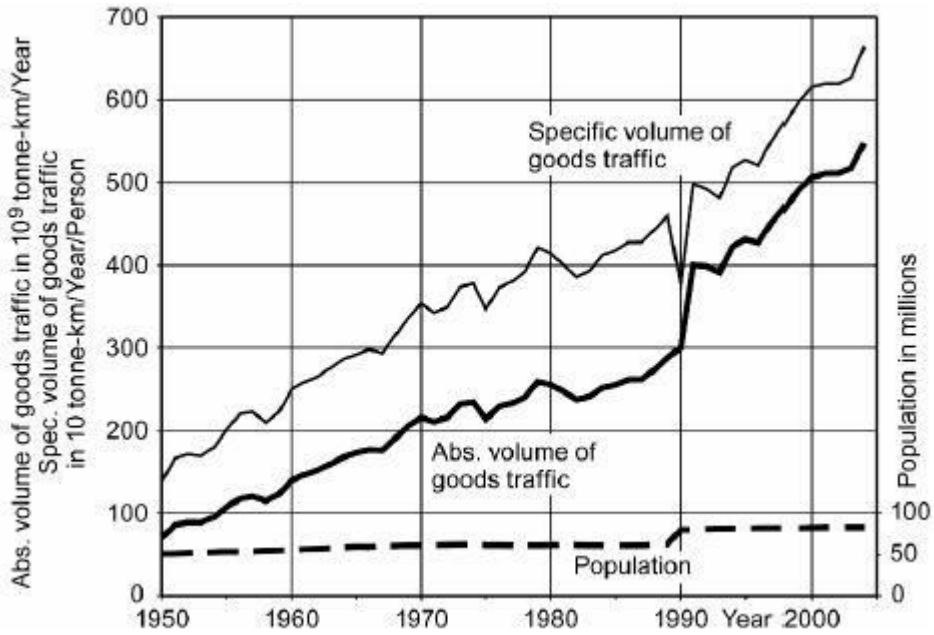

Figure 1 - Development of goods traffic and population in Germany; figures for the whole of Germany from 1990 (Naunheimer *et al.*, 2010)

Figure 1 illustrates a constant increase in goods traffic performance, both universally and with reference to the population of Germany. The largest part of this goods traffic takes place on the road (Naunheimer *et al*., 2010).

1.1.2 The significance of motor vehicles in our mobile world

Mobility is assumed as a basic and human need. There are two factors which have an influence on human choice of means of transport. The first one is the satisfaction of his objective needs like transportation performance, door-to-door access and destination

attainability. The second one is the satisfaction of perceived subjective needs such as comfort, convenience and freedom to decide the means, destination and timing of the journey (Naunheimer *et al*., 2010).

Automotive industry has quite an important significance in the economy regarding to employment and human sustenance. As an example, in 2005, one in seven German citizens worked for the automobile industry. Furthermore, the sales volume of the automotive industry in Germany is twelve times greater than the industry of machine tool (Naunheimer *et al*., 2010).

In Figure 2, it is presented the portion of jobs that are direct or indirectly dependent on the transport industry.

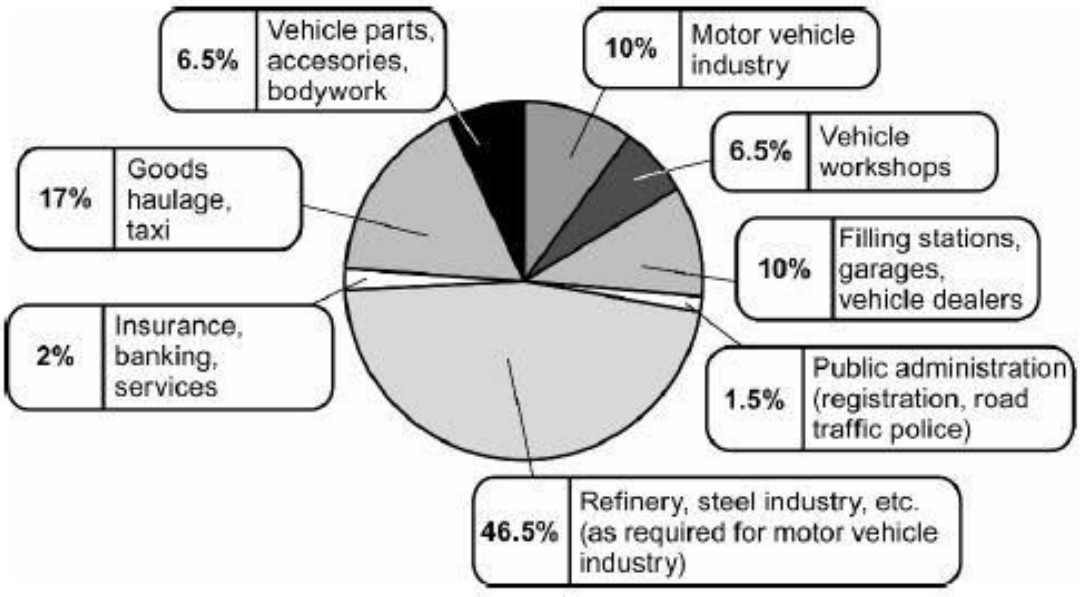

Figure 2 – Breakdown of jobs dependent on the motor transport industry in Germany (Naunheimer *et al*., 2010)

It is important to underline that on the graph above it is only considered employment since the gasoline station although the chain is longer than what is visible in Figure 3.

Before the gasoline pump, also the fossil fuel reservoir, fuel refinery and road transport create a considerable amount of employment. Although it is desired to get an alternative option to fossil fuels due to the fact of their extinction, new employment will be certainly created.

Motor vehicles have gained great significance for humanity not only because they fulfil the basic human need for mobility but also because they allow door-to-door transport of both people and goods. There are no alternatives to motor vehicles in sight (Naunheimer *et al*., 2010).

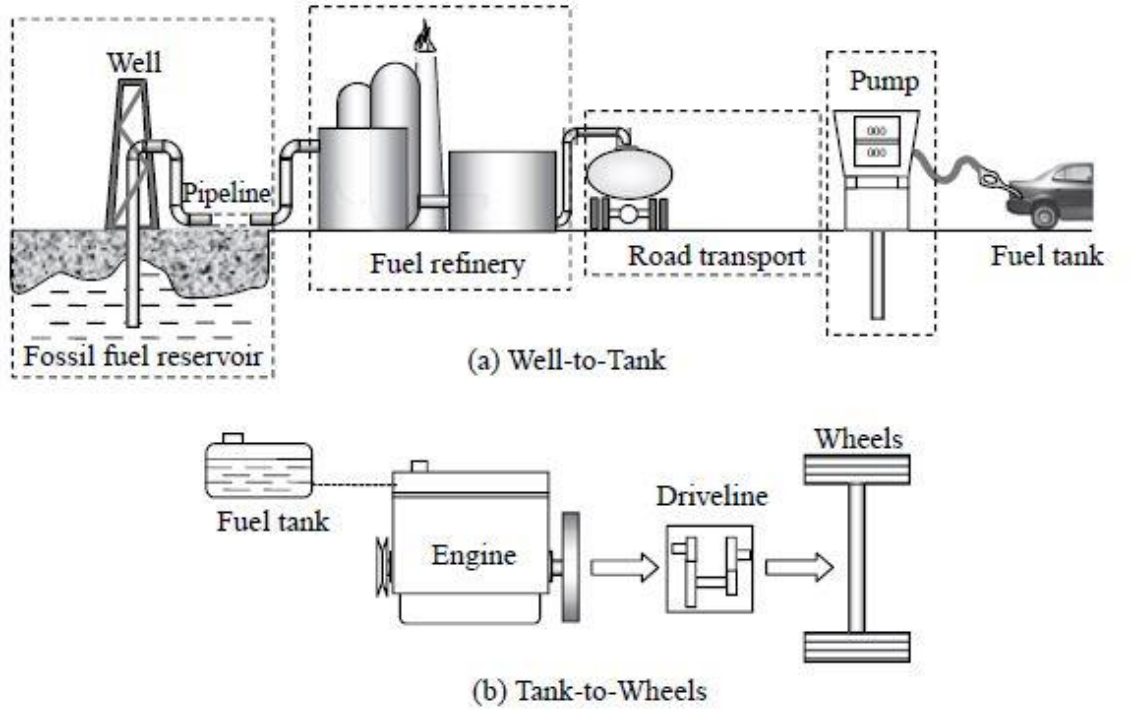

Figure 3 – Overall energy conversion process in vehicle transportation – the Well-to-wheels idea (Mashadi & Crolla, 2012)

In Figure 4, it is shown the various vehicles types and the way road vehicles are divided.

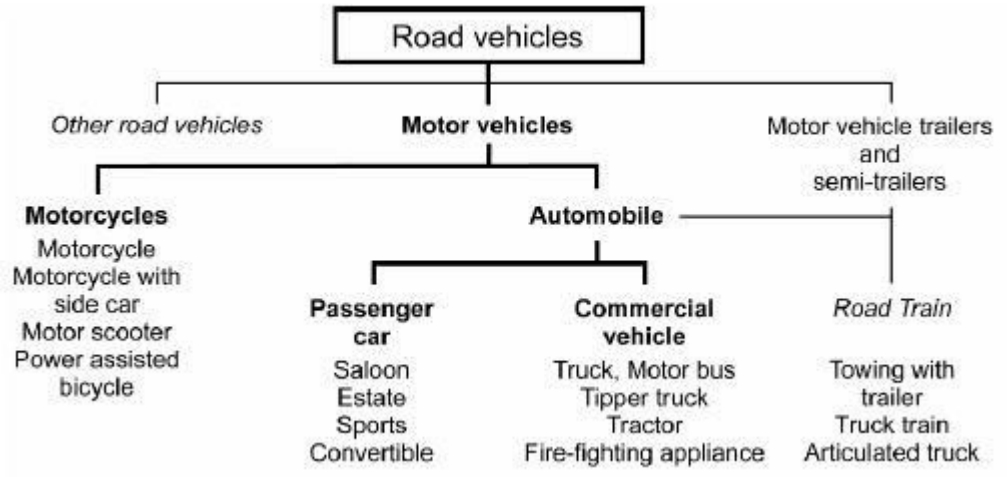

Figure 4 – Classification of road vehicles and motor vehicles to German standard DIN 70010 (Naunheimer *et al.*, 2010)

Statistics refer that motor vehicles are an imperfect trend. Neither environmental negligence or destruction nor the threat of gridlock have alerted people for such dependency and desire of mobility. The number of motor vehicles in the world has risen 10% per year as can be seen on Figure 5, since 1946 (Naunheimer et al., 2010).

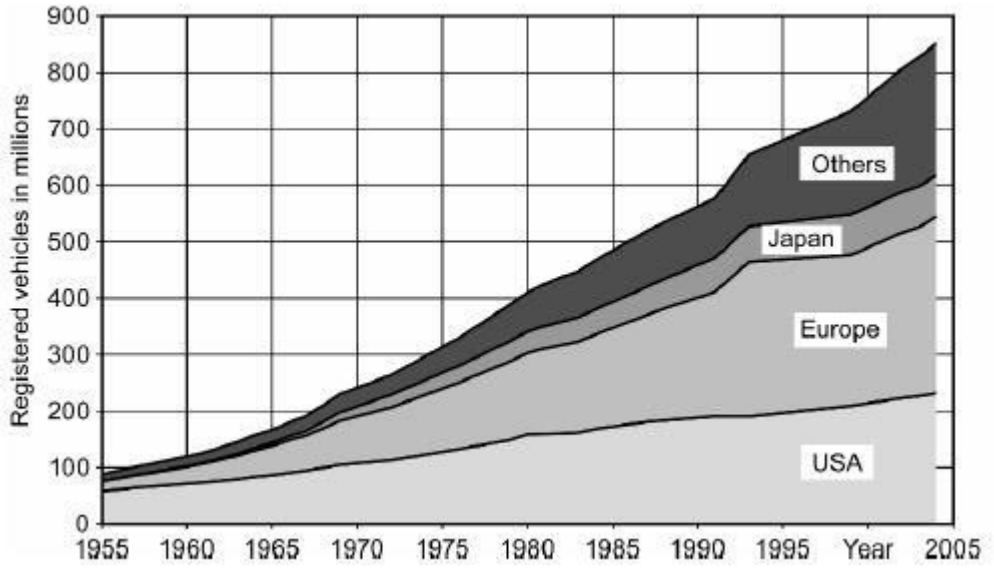

Figure 5 – Increase in the number of motor vehicles worldwide (Naunheimer *et al*., 2010)

According to the graph of Figure 5, Europe market is the one who presents the highest rise. It is expected the demand for motor vehicles in Eastern Europe and Asia to keep climbing even with the intensive promotion of mass transit. However not so significantly as in industrial countries in the past. It is jussive that the vehicles that are produced and exported in these developing countries be as resource-conserving and efficient as possible to prevent spreading environmental issues to other parts of the globe (Naunheimer *et al*., 2010). As seen before, automotive industry is a crucial factor in the global economy. In 2004, about 63 million motor vehicles were manufactured: 53 million correspond to passenger cars and 10 million to commercial vehicles (Naunheimer *et al*., 2010).

There are three centres competing in the development of motor vehicles: Europe, US and Japan/South Korea/China. Europe is the largest manufacturer of passenger cars. In the various European producer countries, the proportion of passenger car production accounted for by small, mid-range and luxury passenger cars varies greatly. In France and Italy are produced mostly small and mid-range passenger cars, in Germany are produced mostly mid-range and luxury passenger cars. In Germany are produced more luxury passenger cars than in the rest of Europe put together (Naunheimer *et al*., 2010). Each market has specific conditions based on socioeconomic situation of buyers, social values, geographical factors and, not the least, legislation. In order to succeed, motor

vehicles need to fulfil all the requirements of the respective market. Transmission system has a key role as it is the link between the road and the engine. For example, in US over 85% of passenger cars are equipped with automatic transmissions while in Europe it is only 13%. For commercial vehicles over 3.5t gross weight, the gearbox is selected specifically for the particular case of application. There are often different numbers of speeds and different methods of operation (manual or automatic) available for a commercial vehicle gearbox. Assuming that for spare parts, 10% of gearboxes are manufactured in excess, the number of transmission components such as gears and synchronizer packs can be estimated. In 2004, about 240 million gearwheels and 46 million synchronizer packs were produced for passenger car synchromesh gearboxes in Europe. For commercial vehicle constant-mesh and synchromesh transmissions, about 38 million gearwheels and 7.5 million synchronizer packs were manufactured (Naunheimer *et al*., 2010). In 2009, the total population in the world of cars and light trucks was estimated at around 900 million, with a production in the same year of about 61 million units. More than 99% per cent of these vehicles are equipped with conventional powertrains (Mashadi & Crolla, 2012).

1.1.3 Statistics

1.1.3.1 *Vehicles in use*

In 2015, 294.2 million motor vehicles were driven in European Union of which 256.1 million were passenger cars. This corresponds to a motorisation rate of 573 units per 1000 inhabitants. Compared to 2005, the amount of passenger cars in use increased 27 million units ((ACEA), 2017).

1.1.3.2 *Employment*

In terms of employment, automotive industry provides direct and indirect jobs for 12.6 million European citizens where 2.5 million are direct jobs. The number of jobs provided by automotive industry has been rising since 2013 until at least 2015 ((ACEA), 2017).

1.1.3.3 *Production*

In 2016, Greater China was the most productive continent followed by Europe. In fact, the amount of units produced by Great China has increased significantly, as so South

Asia. For the other continents, it has been oscillating. As a whole, the production of passenger cars around the world has increased on a significant way. This type of vehicle is the most produced in the EU (European Union) (86%) ((ACEA), 2017).

1.1.3.4 *Trade*

In 2016 North America exported 32.7% of their produced cars, while Asia/Oceania exported 33.1% and EU 20.7. In fact, EU exported 6.3 million vehicles in 2016. Automotive industry generated in 2016 a trade surplus of about 90 billion euros for the EU. Most of the vehicles imported by the EU come from Turkey (about 1 million) and Japan (2nd place) with a significant percentage difference. Annually, about 3 million motor vehicles are imported to the EU. The main market of exportation from the EU is the US (about 1.2 million) ((ACEA), 2017).

1.1.3.5 *Environment*

The average emission of new cars in the EU is 118.1 gCO_2/km. In 2016, Germany was the country with higher emissions of CO_2. It is evident that there is a higher market demand for more fuel-efficient cars. It has been verified that the number of new cars in the EU with emissions of CO_2 greater than 130 g/km is decreased exponentially. At this moment, most of the cars present emissions in the range of 96-130 g/km and the number of vehicles within this range has increased significantly. The number of new passenger cars in the EU with emissions lower than 95 g/km is increasing slowly ((ACEA), 2017).

1.1.4 Trends in Traffic Engineering

Traffic is “the sum of all processes serving to overcome distance, comprising all relocation of persons, goods and information”. The environment of the automotive transmissions systems is defined by the traffic system. Traffic can be divided in five categories (Naunheimer *et al*., 2010):

- local traffic: urban traffic;
- regional traffic: traffic within agglomeration areas;
- long-distance traffic: traffic between agglomeration areas;
- continental traffic: long-distance traffic;
- intercontinental traffic.

For passenger and commercial vehicles transmissions, they can only be distinguished between local and long-distance traffic while for buses there is a three-fold distinction between city traffic, local traffic and long-distance traffic (coaches).

The term “transportation performance” defines traffic performance and is related to goods traffic. Since always, the increase of transportation performance has been greater than the population growth.

Modern traffic engineering has a main purpose of solving the following issues (Naunheimer *et al.*, 2010):

- satisfying all transportation requirements;
- increasing the environmental friendliness of the means of transportation;
- reducing primary and secondary energy consumption;
- realising the potentials of electronic communication.

The several means of transport (road, rail, canal and pipeline) can be distinguished into transport systems having in account their purpose or technology (Naunheimer *et al.*, 2010).

1.1.5 Passenger and Goods Transport Systems

Traffic engineering purpose is to develop and provide reliable transport systems. It can be divided in passenger and goods traffic. For passengers, the main transport means are walking, bicycle, motorcycle, private car, taxis, public transport, railways, airplanes and ships. There is a low percentage of people who is carried by public transport and railway as it can be seen in Figure 6.

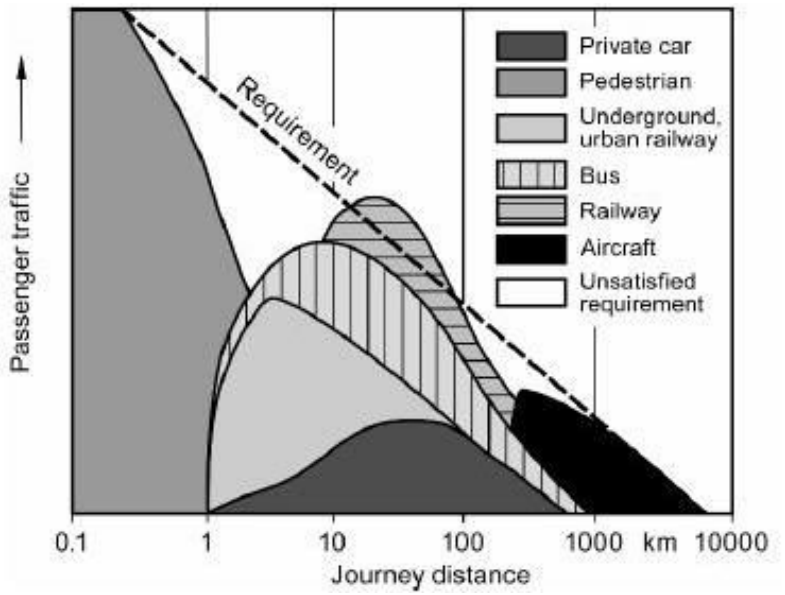

Figure 6 - Comparison of passenger transport supply and demand related to length of journey (Naunheimer *et al.*, 2010)

According to Figure 6, it is conclusive that there is no adequate means of transport in the two distance ranges: between 1 to 10 km and between 100 to 1000 km. Nowadays, passenger cars and taxis are the fastest means of transport for short-distance passenger trips. Because of low average driving speed, city buses are significantly slower than urban high-speed railways given equal idle times. From about 14 km (longer journey distances) high-speed city railways provide shorter travel times than passenger cars and taxis.

There are five means of transport for goods transport:

- Railways;
- Commercial vehicles (road traffic);
- Ships (canals, maritime transport);
- Airplanes (airfreight);
- Pipelines.

Usually some means of transport are joined in order to create a transport chain. Goods traffic on roads needs to be urgently limited. Transport speed, transport flow, space required and transport flow related to the space requirement are the characteristics used to compare the several means of transport of goods. In terms of transport speed and flow, the railway takes the lead followed by trucks. Pipelines, on the other hand, perform unfavourably. Commercial vehicles carry most of the annual volume of goods traffic with rail and barge well behind (Naunheimer *et al*., 2010).

Similar to passengers' transport, a key feature for goods transport is door-to-door access. This parameter together with speed, economic efficiency and just-in-time delivery to assembly lines are the reasons behind the expressive increase in the number of trucks on roads. Three main points should be considered at the time of choosing a transport system: transportation needs, environmental impact and energy efficiency (Naunheimer *et al*., 2010).

1.1.6 Classification of vehicles and vehicle use

In a first instance, vehicles are split into passenger cars, commercial vehicles, construction-site vehicles, agricultural tractors and special vehicles.

Passenger cars can be divided into three main groups: under 75 kW engine size, over 75 kW engine size and vans smaller than 3.5t. The commercial vehicle category can be split into buses and trucks. The truck category can then be divided by gross weight. Buses category can be divided according to the stops per kilometre. All this data can be seen of Table 1.

Table 1 – Transmission-oriented classification of motor vehicles by type of vehicle and type of use (Naunheimer *et al.*, 2010)

Type of vehicle			Type of use		
Passenger cars		Power P < 75 kW	On-road	On-/off-road (building sites)	Off-road
		Power P > 75 kW			
		Vans < 3.5 t			
Commercial vehicles	Trucks	Light-duty commercial vehicles: GVW < 7.5 t			
		Medium-duty commercial vehicles: GVW < 16 t			
		Heavy-duty commercial vehicles: GVW > 16 t			
	Buses *)	Urban bus			
		Interurban bus			
		Multi-purpose bus			
		Coach			
Agricultural tractors					
Construction-site vehicles					
Special vehicles					

1.1.7 Vehicle performance

Since the first road vehicles developed by, for example, Daimler, Benz, Peugeot and Panhard & Levassore in the 1890s and 1900s, people introduced performance features in order to be able to compare different models and vehicles. In the beginning these features were top speed and fuel range. When more powerful engines started to come out, new measures were defined such as acceleration, gradeability and towing performance. Performance could be easily predicted based on the Newton's Second Law of Motion (Mashadi & Crolla, 2012).

According to the pioneering automobile engineer Olley (review paper of 1936), a typical American car of that period weighed about 2 tons (2000 kg) and the engine power was about 100 hp (75 kW). This resulted in an acceleration of approximately 3 m/s^2, a gradeability of about 11% and a top speed about 140 km/h. The accuracy of these predictions started getting better since 1930 because measurement techniques for engine performance, tyre rolling resistance characteristics and aerodynamic drag effects were significantly improved (Mashadi & Crolla, 2012).

In Figure 7, it is illustrated where all the energy is used in a vehicle longitudinal performance for typical urban and highway conditions (Mashadi & Crolla, 2012).

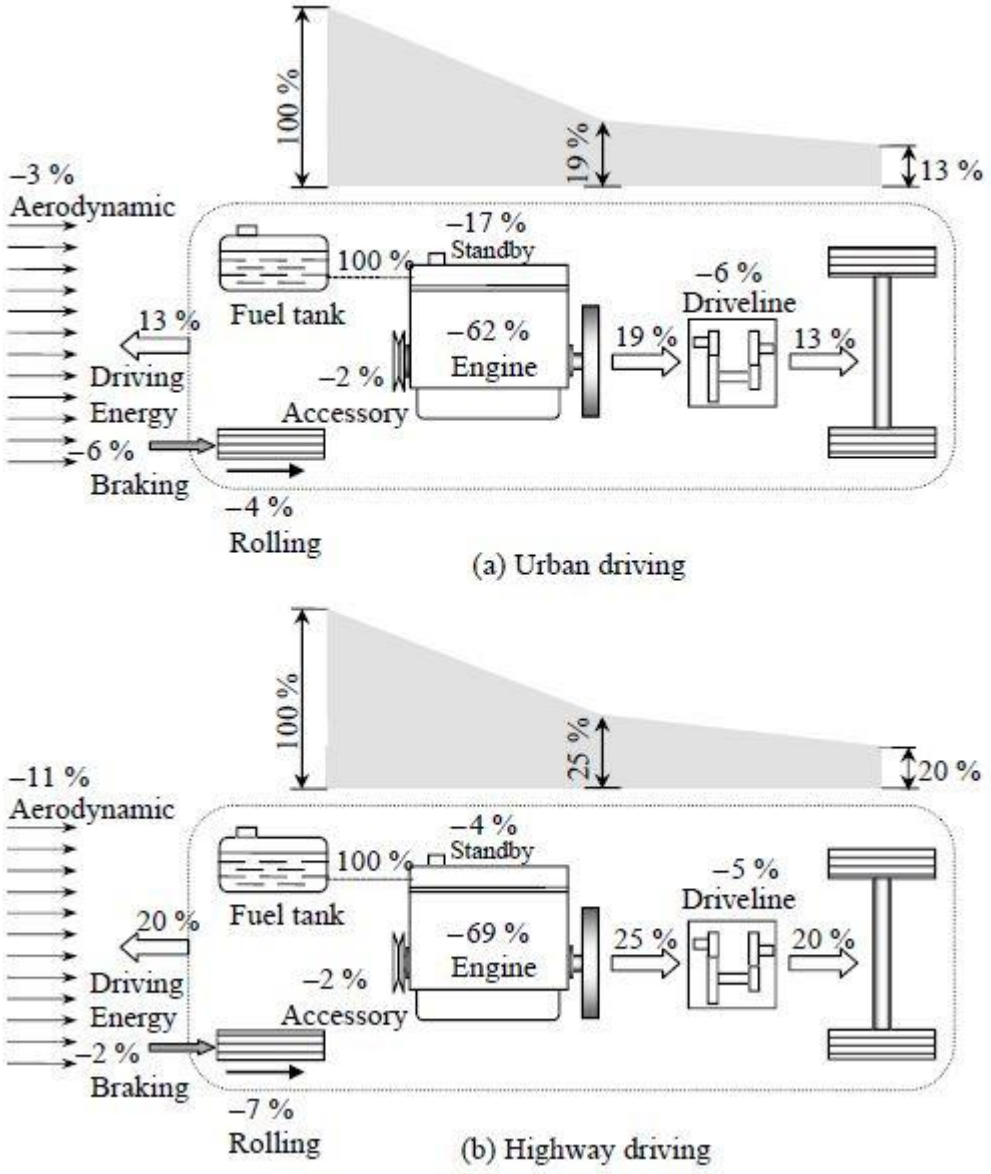

Figure 7 – Example of typical energy flows during urban (a) and highway (b) driving (Mashadi & Crolla, 2012)

In the 1970s, it started to be paid more attention to the fuel economy calculations than vehicle performance. In 1975, as a consequence of the oil crisis of 1973, CAFE (Corporate Average Fuel Economy) by Congress determined federal regulations whose main purpose was to improve the average fuel economy of cars and light trucks sold in the USA (United States of America). This point is the beginning of the interest in both fuel economy and the topic of emissions. Governments became very active in legislating for

the measurement and control of both these aspects of vehicle performance. In recent decades, it started to be required by the consumers data and performance figures to compare different models. Longitudinal performance such as maximum speed, acceleration, hill climbing, towing ability, etc are straight forward to measure. In contrast, comparative data on fuel economy and hence emissions are extremely controversial. The actual method to measure the fuel economy of a vehicle consists on to mount the vehicle on the instrumented dynamometer a drive a standard cycle. The drive cycle consists of a set of data points which specify a speed vs distance travelled profile. Different drive cycles have been developed in order to simulate as close as possible the different types of vehicle operation such as extra-urban, urban, highway and combined urban-highway (Mashadi & Crolla, 2012).

In recent decades, it started to be required by the consumers data and performance figures to compare different models. Longitudinal performance such as maximum speed, acceleration, hill climbing, towing ability, etc are straight forward to measure. In contrast, comparative data on fuel economy and hence emissions are extremely controversial (Mashadi & Crolla, 2012).

The actual method to measure the fuel economy of a vehicle consists on to mount the vehicle on the instrumented dynamometer a drive a standard cycle. The drive cycle consists of a set of data points which specify a speed vs travelled distance profile. Different drive cycles have been defined having in account the different types of vehicle operation such as extra-urban, urban, highway and combined urban-highway. Despite this approach being internationally accepted, there are some differences in the different countries and regions of the world. The current range of standard drive cycles was defined by the world's large three automotive markets: Europe, USA and Asia. The differences between the approaches of each region is based on the driving patterns of the regions. Furthermore, different countries and regions have defined different targets for fuel economy and emissions. This makes difficult for the manufacturers whose vehicles are sold worldwide to fulfil the requirements of all the markets (Mashadi & Crolla, 2012).

Due to these regional differences, it has been a source of considerable controversy and it has been quite difficult to reach a unanimous standard test. In addition, in real-world driving it is very difficult to achieve the ideal results obtained on standard test conditions. This fact comes out with no surprise as the tests and measurements are carried out in laboratory conditions over a repeatable drive cycle. Consumer organizations and popular car publications defend that the data displayed on the windscreen while on sale must be reasonably achievable in real drive conditions. In the EU, the fuel economy of passenger vehicles is measured using two different drive cycles: urban and extra-urban. The urban test-cycle (ECE-15) was introduced in 1999 and simulates a 4 km journey at an average speed of 18.7 km/h and a maximum speed of 50 km/h. The extra urban cycle (EUDC) simulates a mix between urban and highway driving.

The duration of the test is 400 seconds with an average speed of 62.6 km/h and a top speed of 120 km/h. In the USA, procedures are organized by the EPA (Environmental Protection Agency) and were updated in 2008 to include five distinct tests. The information of these tests is then presented on the car sales information. Some say that this information is more objective and reflective of the real-world driving fuel economy performance than the information obtained on the EU tests. In addition to the controversy of tests and measurements between the different markets, there is another issue: fuel economy is quoted in different units around the world. For example, USA and UK (United Kingdom) use apparently the same unit, mpg, although these are not comparable since the US gallon is 0.83 of an imperial gallon. In Europe and Asia, fuel consumption is quoted in l/100 km. A large mpg is comparable to a low l/100 km, which translates itself as : 30 mpg = 9.4 l/100km and 50 mpg = 5.6 l/100 km (Mashadi & Crolla, 2012). In general, drive cycles used in tests are less aggressive than the real-world driving as it is believed in tests are simulated lower values of acceleration and deceleration.

Regarding to emissions, there are two aspects which are commonly referred as “tailpipe emissions”. This name is the consequence of the fact that these emissions emerge from the exhaust pipe as product of the combustion process. The first aspect is the pollutant emissions which includes CO (Carbon monoxide), unburnt HC (Hydro carbons) and NO_x (Oxides of nitrogen). In Europe, in order to reduce the emissions of these pollutants, engine emission standards were defined. This measured lead to significant improvements in harmful emissions from passenger cars. The second aspect is related to CO_2 emission levels of vehicles. A lot of attention have been dedicated to this issue on the early part of the twenty-first century due to global concerns about the environment directly linked to the carbon footprint calculations which are nowadays embedded in all aspects of life. In the UK from 2001, the vehicle taxes were linked to the CO_2 emissions of the vehicle. Vehicles with emissions lower than 100 g/km were free of road taxes. In 2008, some legislation was determined to force European car manufacturers to reduce the average CO_2 emissions of new cars to 130 g/km by 2015 (Mashadi & Crolla, 2012).

1.2 Main goals

Two main goals were proposed for this work. The first one was the contribution to the validation of the DNR subsystem by verifying all the mechanical requirements. The other main goal was to develop a showcase model whose major purpose was to be able to show people all the details of the working principle of a DNR subsystem by allowing interaction with the user and visualization of the inside components of the subsystem.

1.3 Methodology

In order to achieve the proposed goals many other tasks were necessary to be done. For the validation of the DNR subsystem it was necessary to:

- Do intense research about all the mechanisms, components and theoretical topics directly and indirectly related to CVT and DNR subsystems;
- Study the function of the exterior adjacent components of the DNR (for example: torque converter and variator);
- Deeply study the working principle of the proposed DNR subsystem;
- Collect all the necessary information related to the components in study (for example: dimensions and materials);
- Develop numerical models which would lead to results which would be compared to the requirements as also some intermediate calculations to understand the influence of some parameters;
- Do a ramp-down test to compare to the calculated drag torque;

For the development of the showcase model the following tasks were done:

- Research and study of some mechanisms which allow the transmission of motion between the cams and the shifting lever;
- To understand the main requirements and desired function for the showcase;
- To design and calculate the several components of the showcase;
- 3D modelling;
- FEA (Finite elements analysis) to validate the crucial components;
- Technical drawings to ask for quotation;
- Assembly at the supplier.

In this dissertation, it will be explained the working principle of the DNR subsystem which is the base of this thesis. Firstly, it will be studied the DNR schematics in order to understand the principle of a DNR subsystem. Secondly it will be studied the hydraulic circuit to understand the oil flow and by this way to understand which components are pressurized. Having in account the previous point it will be possible to understand the kinematics of the subsystem. During this dissertation, it is also expected to understand the function of some special components. By doing this introduction to the subsystem it will be easier to complete all the tasks previously stated.

1.4 Thesis structure

The thesis structure is divided in seven main chapters. The first one is a contextualization with the topic of study as well as about the work in general. The second chapter is related to the theoretical aspects which imply a deep research of all the mechanisms and components in use in the DNR subsystem. This research it was also useful to

understand the main difference between some transmission and gearboxes' architectures. In the third chapter it is presented all the necessary calculation models and formulas which will be useful in the intermediate calculations for the verification of the mechanical requirements of the DNR. In the fourth chapter it is presented the working principle of the DNR as also all the calculations of the DNR and intermediate tasks. In the same chapter it is also presented the description of the showcase as also all the necessary calculations and FEA for validation. In the conclusion chapter it was done a resume of all the calculations achieved during the thesis development. In the sixth chapter it is presented all the consulted sources of information. Finally, in the last chapter it is presented all the auxiliary information for the thesis development, some extra technical aspects and all the technical drawings of the showcase as also some photos of the final result.

1.5 Welcoming company

Punch Powertrain NV (*Naamloze Vennootschap*), located in Sint-Truiden, Belgium, is an independent full system supplier of powertrains. With over than 40 years of experience in the production of CVT Transmissions, this company also offers electric powertrains for New Energy Vehicles such as Plugin Hybrids (PHs) and Electric Vehicles (EVs), as well as DCT (Dual clutch transmission). Since 2013 Punch Powertrain has achieved an average annual growth of over 50%. This is with no doubt, a challenging and enriching company to develop the master thesis in the field of automotive industry not only because of the enormous amount of knowledge than can be transmitted to student but also because the clear view that can be taken be the student of the complete process of a CVT transmission, from the R&D (Research and Development) to the production line.

LITERATURE REVIEW

2 LITERATURE REVIEW

2.1 Theoretical aspects

2.1.1 Power sources

The most implemented source of power so far developed for driving road vehicles is the internal-combustion engine (ICE) with cyclical combustion, working on the spark-ignition or diesel principle. The power developed by the ICE is generated by the burning of fuel inside the engine itself. There are some alternative power units such as the steam engine and the electric motor (Hillier, 2012; Naunheimer et al., 2010). The former requires a boiler to generate the steam, in addition to the engine itself, making the complete installation rather bulky. Furthermore, there are heat losses in the boiler as well as in the engine, therefore it is less efficient than the ICE. During temporary halts, the steam engine continues to consume fuel in order to maintain steam pressure, whereas the internal-combustion engine consumes fuel only when it is actually running (Hillier, 2012).

To operate an electric motor, it is necessary a supply of electrical energy. If this energy is to be carried on the vehicle, it must be in the form of batteries or accumulators. Although, these are both heavy and bulky in relation to the amount of energy they can store, limiting the range, speed and load-carrying capacity of the vehicle. If an external supply of electrical energy is to be used, the vehicle must be connected to a distant power station by some means such as a system of wires, suspended at a safe height above the road, with which contact is made by suitable arms mounted on top of the vehicle and provided with some form of sliding connection to the wires. Such a system has obvious limitations and because of that it cannot be implemented in everyday particular vehicles. It has been invested in the development of more practical electric cars and of hybrid vehicles due to the ecological advantages these types of vehicles offer (Hillier, 2012).

ICE is known for some advantages such as high power-to-weight ratio, relatively good efficiency and relatively compact energy storage. However, there are three fundamental disadvantages (Naunheimer *et al*., 2010):

- Unlike steam engines or electric motors, the ICE is incapable of producing torque from rest (zero engine speed);
- ICE only produces maximum power at a certain engine speed;
- Fuel consumption is strongly dependent on the operating point in the engine's performance map.

At the late 1800s and early 1900s steam had a long history of development and there wasn't any problem installing enough power to give an adequate performance. On the other hand, fuel economy was poor, the boiler needed firing up prior to a journey and both water storage and usage were problematic. However, electric cars look extremely promising: they are quiet, clean and remarkably easy to operate. The major problem was the range which was limited by the amount of energy that could be stored on the batteries. This problem is even today the subject of many researches. Gasoline cars in that period were less well developed and looked extremely troublesome: they were difficult to start and when running they were noisy, dirty and unreliable. However, they were distinct by a fundamental advantage: energy density of gasoline is about 300 times better than a lead-acid battery. This means that it was worthwhile to invest in the refinement of the gasoline-based powertrain. This refinement has continued to nowadays (Mashadi & Crolla, 2012).

2.1.2 Vehicle powertrain concepts

2.1.2.1 *Introduction*

The output from the power source dominated by ICE is controlled by a transmission system and driveline to deliver tractive effort to the wheels. All these components, collectively referred to as powertrain system are controlled by the driver. It is the engineering behind powertrain systems which provide the driving force behind the mobility (Mashadi & Crolla, 2012).

Drivers have a range of performance criteria such as: acceleration, top speed, fuel economy, gradeability and towing capacity. These are quantitative features. However, there are also subjective features which have a great impact in the commercial success of a certain model such as driveability, fun to drive, refinement and driving pleasure. Recently, new demands were imposed like emissions (Mashadi & Crolla, 2012).

2.1.2.2 *Powertrain subsystems*

All the subsystems of a powertrain system are subject to constant research and development in order to improve their performance and the performance of the whole system in terms of efficiency, emissions control, refinement and overall cost.

A powertrain system is composed by four subsystems such as (Mashadi & Crolla, 2012):

- Engine;
- Transmission;
- Vehicle structure;
- Systems operation.

2.1.2.3 *Conventional powertrains*

A conventional powertrain is defined to be composed by an IC engine that the vehicle wheels through a transmission, incorporating a gearbox and a final drive unit. The most common layout of a small passenger car is front-engine, front wheel drive. However, the principles associated with powertrain analysis are applicable to other kinds of layout (Mashadi & Crolla, 2012).

It is known that more than 99% of the 61 million of new cars and light trucks produced in 2009 were equipped with a conventional powertrain. Despite the considerable interest from 2000 onwards in alternative powertrains, described under the general heading of LCVs (Low carbon vehicles), it is known that the principles to analyse and understand conventional powertrain systems will keep being applied for some more decades (Mashadi & Crolla, 2012).

2.1.2.4 *Hybrid powertrains*

During the late 1800s and early 1900s, steam, electric and petrol were the three competing technologies for the powerplant. As expected, each of these had their own advantages and disadvantages which make it unclear to predict which one would be implemented in the future (Mashadi & Crolla, 2012).

The notion of a hybrid vehicle was born between nineteenth and twentieth centuries when it was suggested to combine two powerplants in order to extract the best features of each one. Initially it was not called hybrid. In 1902 Woods gas-electric car realize what is nowadays known as an electric hybrid layout. This vehicle was driven by a motor which doubled as a generator. The vehicle could run on battery power alone at low speeds while the gasoline engine could be used to charge the battery and taking advantage of regenerative breaking (Mashadi & Crolla, 2012).

There are plenty of different powertrain architectures for hybrid vehicles. In 2011, there were three main architectures which were already equipping some vehicle models. These three different architectures are presented in Figure 8. The example of Figure 8

(a) was equipped in Nissan leaf, in (b) it is presented the architecture of Chevrolet Volt and in (c) it is illustrated the architecture of Toyota Prius (Mashadi & Crolla, 2012).

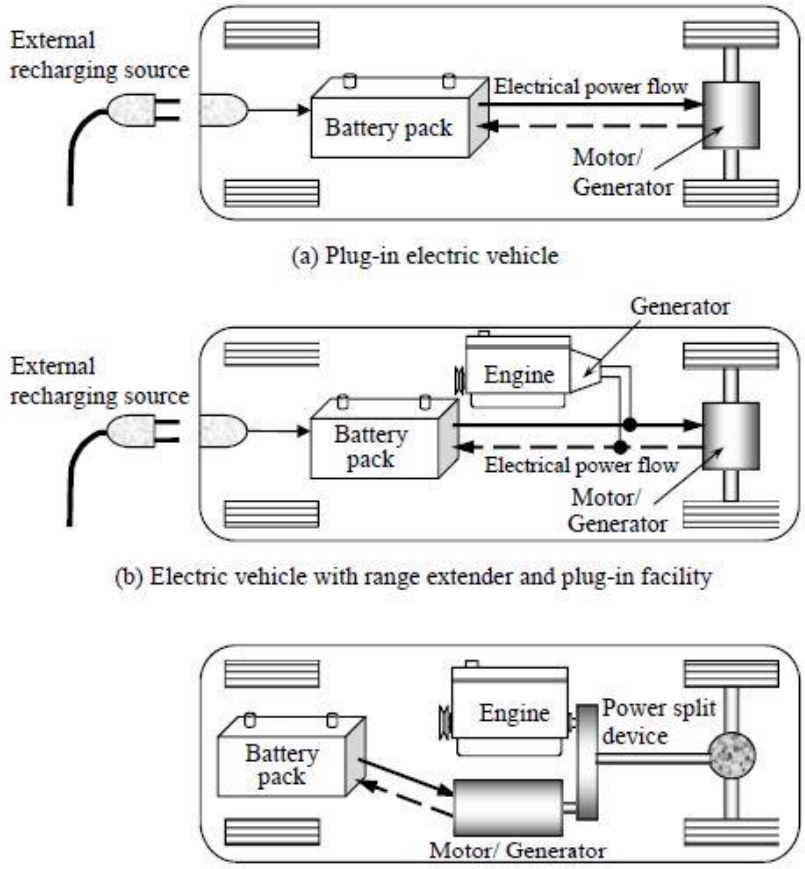

Figure 8 – Three types of typical hybrid/electric vehicle architectures available in 2011 (Mashadi & Crolla, 2012)

2.1.3 Transmissions

2.1.3.1 *Introduction*

The main goal a vehicle transmission is to transfer engine power to the driving wheels of the vehicle. Shifting which happens inside the transmission allows matching the engine torque and speed with the vehicle's load and speed conditions (Mashadi & Crolla, 2012). The most recent developments have been focused on AMT (Automated manual transmission), DCT and CVT.

In the UK, the transmission system is understood to refer to the complete driveline between the engine and the road wheels. However, in many other countries the term 'transmission' refers to the gearbox unit and applies in particular to the type of arrangement used on a given vehicle (i.e. whether the selection of the gears has to be

carried out manually by the driver or uses automatic means) (Hillier, 2012). On this thesis, “transmission” system is to be understood according to the UK terminology: the complete driveline between the engine and the road wheels. The complete transmission system is composed for different subsystems:

- Gearbox;
- Clutch;
- Propeller shaft;
- Final drive and differential;
- Drive shafts to each driven wheel;
- Universal joints.

The development of a transmission system takes in account the type of vehicle, its power unit and intended use. A classification of vehicles oriented to transmission development can be consulted on chapter 1.1.6 (Naunheimer *et al*., 2010).

2.1.3.2 *Functions of transmissions*

Development engineer team should consider the vehicle transmission as a functional whole, in order to guarantee an adequate link between the engine and the drive wheels. The transmission system includes gearbox and moving-off elements, i.e. the entire system to adapt speed and torque including changing gear and starting. The four main functions of a vehicle transmission are to (Naunheimer *et al*., 2010):

- Enable the vehicle to move-off from rest;
- Adapt power flow;
- Convert output torque T2 and output speed n2;
- Enable reverse motion;
- Enable permanent power transmission;
- Positive or force locking engine power transmission with minimal loss;
- Control power matching.

In addition to these main requirements there are also other kind of requirements, known as operational requirements, such as (Naunheimer *et al*., 2010):

- Operational reliability;
- Gearbox costs;
- Ease of repair;
- Ease of operation;
- Power matching;
- Efficiency;
- Installation dimensions and weight;
- Customisability;
- Emissions (noise, oil etc.).

The operational requirements can partially dictate the competitiveness of the transmission.

2.1.3.3 *Key factors and Conventions*

The key factors of a gearbox are the direction of rotation, the transmission ratio and the torque. In order to be able to compare different transmission architectures, designs and variants, some definitions need to be used as a standard.

2.1.3.3.1 Direction of rotation

The direction of rotation of a powertrain is considered to be positive when the direction of rotation is clockwise in a right-hand Cartesian system of co-ordinates. This is as viewed against the forward direction of movement related to the vehicle, as shown on Figure 9.

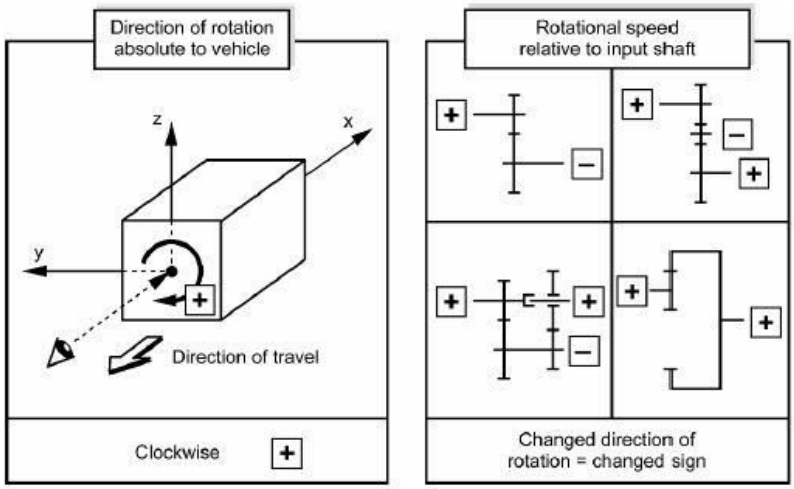

Figure 9 – Definition of direction of rotation in a powertrain (Naunheimer *et al.*, 2010)

2.1.3.3.2 Transmission ratio

The transmission ratio, i_G, is defined as the relationship between the angular velocity ω_1 of the input shaft of a gearbox and ω_2 of the output shaft and can be calculated as follows:

$$i_G = \frac{\omega_1}{\omega_2} = \frac{n_1}{n_2} \quad \{2.1\}$$

The relation between the output speed, n_2, and the input speed, n_1 in a powertrain component is called the speed conversion. The torque conversion gives the relation between the output torque T_2 and the input torque T_1 of a powertrain component. The following characteristic result for the transmission ratio:

- iG > 0 transmission input and output shaft rotate in the same direction;
- iG < 0 change of direction of rotation in the transmission;
- |iG| > 1 speed reducing ratio;
- |iG| < 1 speed increasing ratio.

In the case of CVT and with transmission combinations:

- iG = ∞ stationary output with rotating input;
- iG = 0 stationary input with rotating output.

The ratios in a gearbox are designated by gear ratio, u. The gear ratio of a gear pair is the ratio of the number of teeth z_2 of the larger wheel to the number of teeth z_1 of the smaller wheel (pinion) (Naunheimer *et al*., 2010):

$$u = \frac{z_2}{z_1} \text{ with } z_2 \geq z_1 \quad \{2.2\}$$

German standard DIN 3990 states that in the case of spur gears the number of teeth of a wheel with external gearing is positive, and that the number of teeth of a wheel with internal teeth (ring gear) is to be taken as negative (Naunheimer *et al*., 2010).

2.1.3.3.3 Torque

The torque direction of the transmission input shaft is usually defined as positive. As illustrated in Figure 10, the torque direction changes along a transmission component but not the direction of rotation.

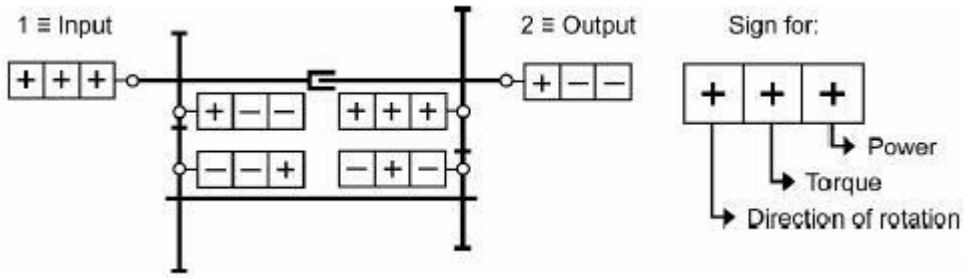

Figure 10 - Sign rules for rotational speed, torque and power (Naunheimer *et al*., 2010)

The sign of the power P absorbed (positive) and delivered (negative) at a particular point can be determined from the speed of rotation and the torque at that point in the transmission as follows:

$$P = T\omega = 2\pi nT\left[W\right] \quad \{2.3\}$$

Müller HW proposed four rules for speeds of rotation, torque values and power values in a transmission:

- All parallel shafts in a transmission rotating in the same direction will have speeds with the same sign;
- In an "input shaft", the signs for speed of rotation and torque are the same; in an "output shaft", they are opposite to each other;
- "Input power" is always positive; "output power" is always negative;
- The two equal connecting torque values of a free connecting shaft have opposite signs at the connecting ends.

A transmission consists of three parts. One is the frame. This condition is important because it is necessary to provide a reaction for the difference in force or torque between the input and output side resulting from the conversion of movement. In vehicle transmission, the frame corresponds to the gearbox housing.

In Figure 11, it is illustrated the symbolic representation proposed by Wolf.

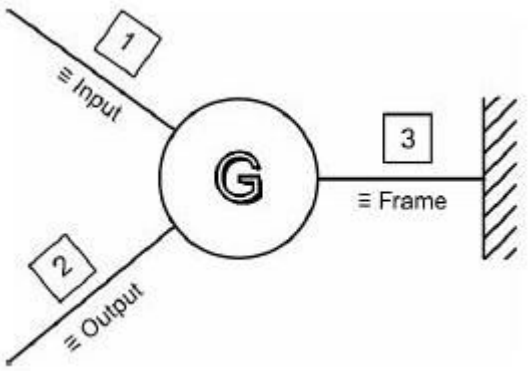

Figure 11 – Wolf transmission symbols (Naunheimer *et al*., 2010)

2.1.3.4 *Latest developments*

The most recent developments in transmission systems are (Herdman, 1995; Mashadi & Crolla, 2012):

- Lower-friction lubricants (engine oil, transmission fluid, axle fluid);
- Hydraulic losses in the torque converter;
- Continuously variable transmission (CVT);
- Automated manual gearbox;
- Dual clutch gearbox;
- Increase in the ratio spread between top and first gear.

Systems operation is another subsystem of a powertrain system. This subsystem is also related to the transmission. And also in this subsystem it has been made some effort to improve the performance by (Mashadi & Crolla, 2012):

- Automatically shutting off engine when vehicle is stopped;
- Recapturing wasted energy while braking (regenerative braking);
- Augmenting a downsized engine with an electric drive system and battery (mild hybrid vehicles);
- Improved control of water-based cooling systems so that engines reach their efficient operating temperature sooner.

2.1.3.5 *Manual transmissions*

Manual transmissions are the oldest type of transmissions and even after new architectures have been developed they are still very popular. Simplicity, low cost and efficiency are the main advantages of this kind of transmissions. Manual transmissions are still the most efficient transmissions although their usage depends on the ability of the driver as frequent shifting is necessary mainly on urban regions (Mashadi & Crolla, 2012). In this type of transmissions the driver of the vehicle is responsible for the shifting (changing from one gear ratio to another) according to the vehicle need (D. A. Crolla, 2009).

2.1.3.5.1 Design and Working Principle

According to Figure 12, transmission is fastened to the engine body by bolts through the bell housing. Inside the bell housing it is assembled the clutch system. The clutch system is bolted to the engine flywheel so by this way the torque and speed of the engine is transmitted to the clutch plate (CP). Consequently, the clutch plate transmits the power from the engine to the input shaft of the transmission. When the clutch is engaged, the

input shaft and the clutch rotate at the same speed as the engine. When clutch is disengaged, the transmission input is disconnected from the engine and shifting can be performed. Shifting is then performed by means of a shifting mechanism (Mashadi & Crolla, 2012).

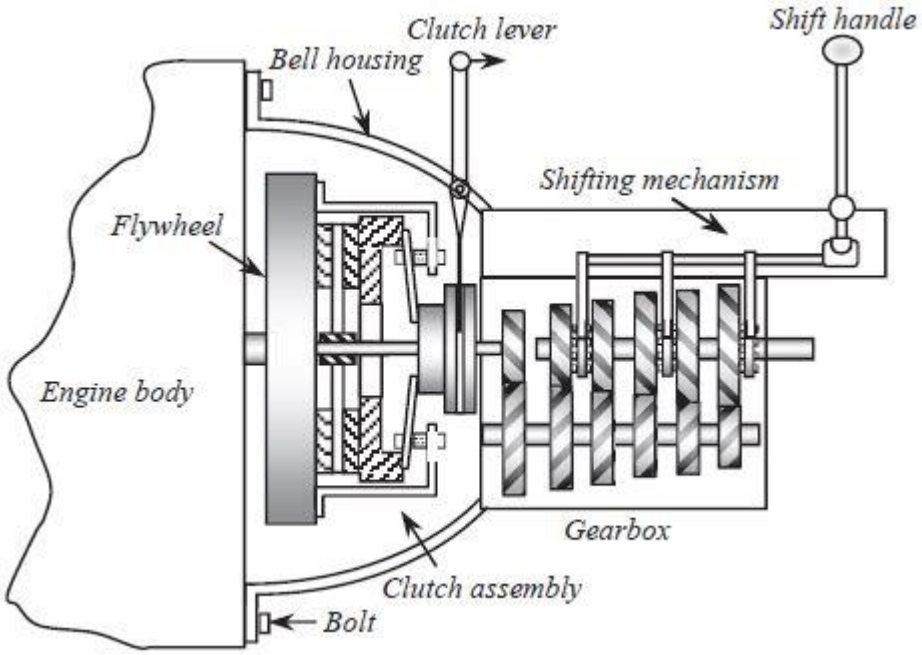

Figure 12 – Manual transmission assembly (Mashadi & Crolla, 2012)

Clutch system is activated when the clutch pedal is released and the gear lever is pulled back, forcing the release bearing to push the diaphragm spring. The seesaw effect on the spring pulls back the pressure plate and consequently the clutch plate is released. The input shaft of the transmission and the clutch plate are directly connected through the splines and both rotate with the same speed (Mashadi & Crolla, 2012).

There are two types of gear change: moving a gear to mesh the opposing gear, or moving a linking member to deliver torque to already meshing gears. The first type is called the “sliding-mesh”. This shifting method is already obsolete. Its concept is illustrated in Figure 14 (a). The second shifting method is called “constant-mesh” and it is used in all modern manual transmissions. Its concept is showed in Figure 14 (b) (Mashadi & Crolla, 2012). In Figure 14, it is illustrated a layshaft type gearbox with in-line input and output shafts.

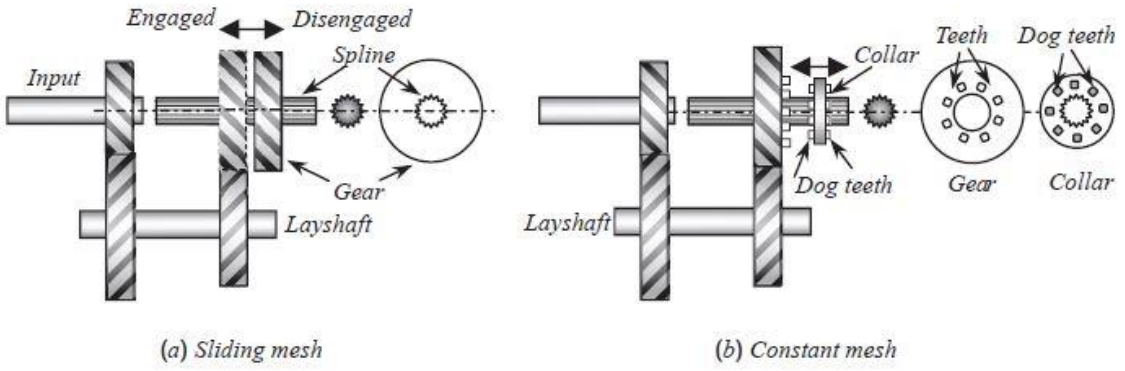

Figure 14 – Sliding mesh and constant-mesh gear meshing methods (Mashadi & Crolla, 2012)

When the clutch is released the power is transferred to the output shaft of the transmission. In the constant mesh gearing method both gears are in constant mesh. However, the gear located on the output shaft has a hole in the centre which means that it is not connected to the output shaft. Not torque is transferred between the gear and the output shaft. The power is transferred by means of a sliding collar with a spline in its core and dog teeth over its sides (Figure 14 (b)). The collar is always turning with the output shaft through the splines and when it is shifted to the side, its dog teeth fit into the matching teeth on the side of the gear and the three (shaft, collar and gear) get connected to each other and power is transferred. Prior to the engagement of the gear and output shaft in constant mesh design, both rotate with different speeds. Due to this fact it is necessary synchronize the speeds of both. The device which is responsible for this action is called synchronizer and it is illustrated in Figure 13 (Mashadi & Crolla, 2012).

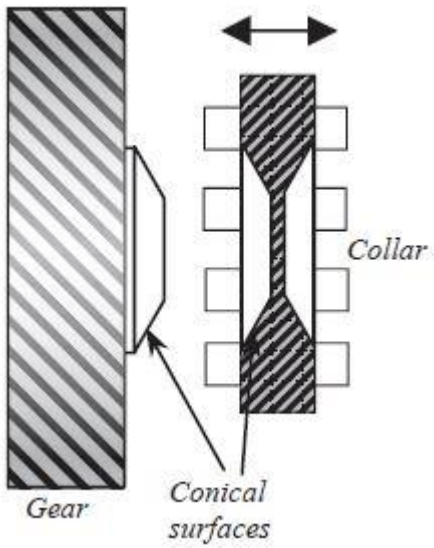

Figure 13 – Synchronizing concept (Mashadi & Crolla, 2012)

In Figure 13, it is presented the concept of two matching conical surfaces which get in contact gradually while the collar slides towards the gear. When, finally, both surfaces get in contact, the speeds gradually synchronize and the teeth subsequently engage (Mashadi & Crolla, 2012).

In Figure 15, it is showed the gear selecting and shifting mechanism in three different views: front, top and left. Usually, for a five-speed transmission there are three forks that control the three collars. Each collar is used to connect two gears when they are moved to the left or right side. The forks are fixed on three rods that can move back and forward. The correct rod is chosen by left-right movement of the shift handle. The choice between two gears is made by moving the shifting handle front or back (Mashadi & Crolla, 2012).

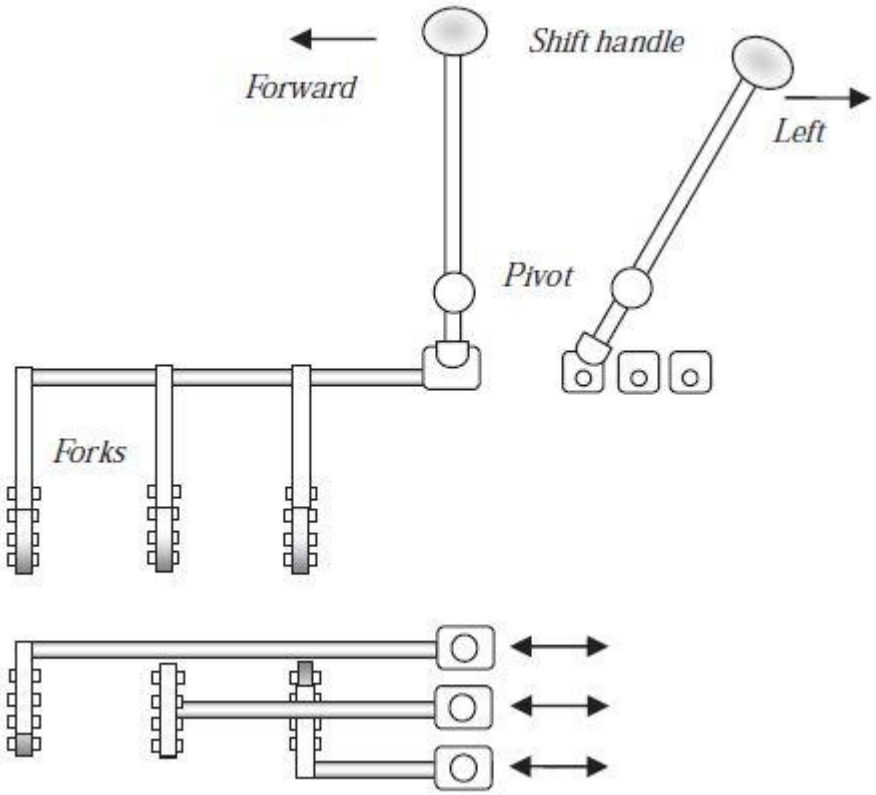

Figure 15 – Shifting mechanism (Mashadi & Crolla, 2012)

2.1.3.6 *Automatic transmission*

2.1.3.6.1 Introduction

Automatic transmissions make driving an easier task as the driver does not need to worry about shifting. It is only necessary to select a gear when the driver wants to

change from driving forward to backwards and vice-versa or when the driver wants to park (D. A. Crolla, 2009). In automatic transmission, it is required that the driver also choose a gear, but not frequently since there are only four gears: Drive, Neutral, Park and Reverse. While for manual transmissions it is necessary to constantly shift having in account the desired speed, speed limits, road slope and so on, for automatic transmission the driver rarely needs to shift because the transmission itself takes in account the parameters mentioned before. So, the driver is mainly responsible for steering and choose the gear pattern needed to suit the general driving conditions. The automatic gearbox system allows the vehicle to be either moved off or brought to rest in a smooth manner, without the driver having to do anything except press the accelerator or brake pedal. Automatic gearboxes can have a selection of drive methods, ranging from a fluid flywheel or torque converter to conventional gear sets, similar to manual gearboxes but with electronic control of clutch and gear shift (Hillier, 2012).

Early automatic transmissions had limited gear selection such as ‘drive’ for forwards, ‘reverse’ for backwards and ‘park’ and ‘neutral’ for stationary situations where no drive was transmitted to the road wheels. More modern automatic gearboxes have up to eight forward-moving gears to improve overall performance and fuel efficiency. The conventional reverse, park and neutral complete the automatic transmission assembly (Hillier, 2012).

Despite existing more than one forward moving gears, the shifting can be performed automatically without driver interaction. In Figure 16, it is illustrated an inside view of an automatic gearbox.

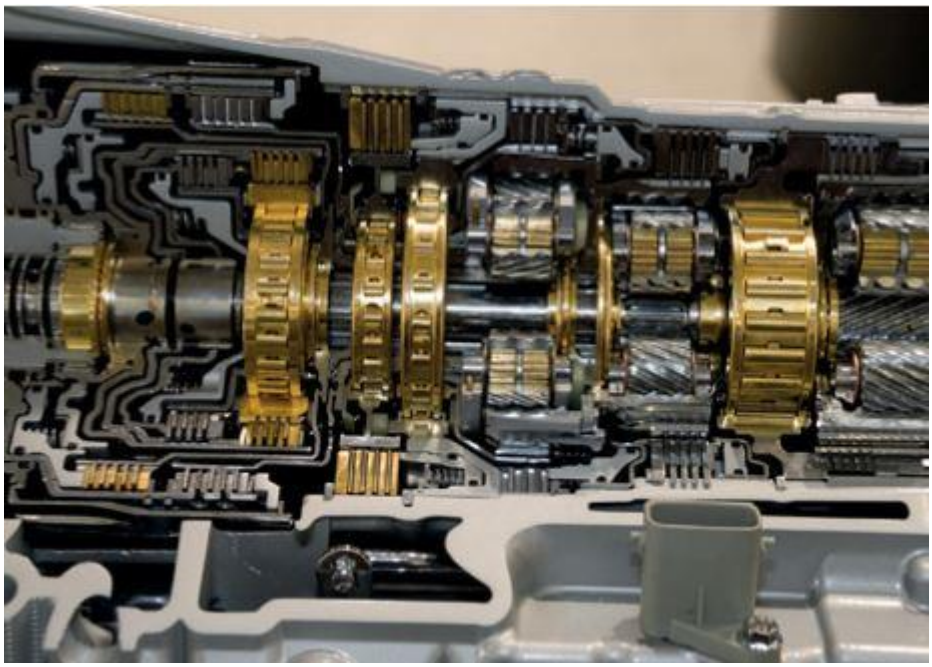

Figure 16 - Automatic gearbox internals (Hillier, 2012)

The inclusion of electronic control systems in modern vehicles gives the driver the option of an automatic gearbox that can also be driven manually. This option can be easily selected (Hillier, 2012).

Due to the recent progress in electronics new types of automatic transmissions have been developed. The first example of this progress is the development of the AMT where well-developed manual transmissions (MT) which are highly efficient, are electronically controlled. Another derivation from manual transmissions is the DCT, known to have a continuous torque flow (Mashadi & Crolla, 2012).

2.1.3.6.2 Conventional automatic transmissions

In a conventional automatic transmission, the clutch system is replaced by a fluid coupling or torque converter in order to eliminate engaging/disengaging movements during gear change. The gearing system is completely different from the other architectures. Instead of conventional gears, planetary or epicyclic gears are used to perform gear ratio. These changes make conventional automatic transmissions totally different from the manual transmissions internally as the external shape is quite similar, as can be seen in Figure 17 (Mashadi & Crolla, 2012).

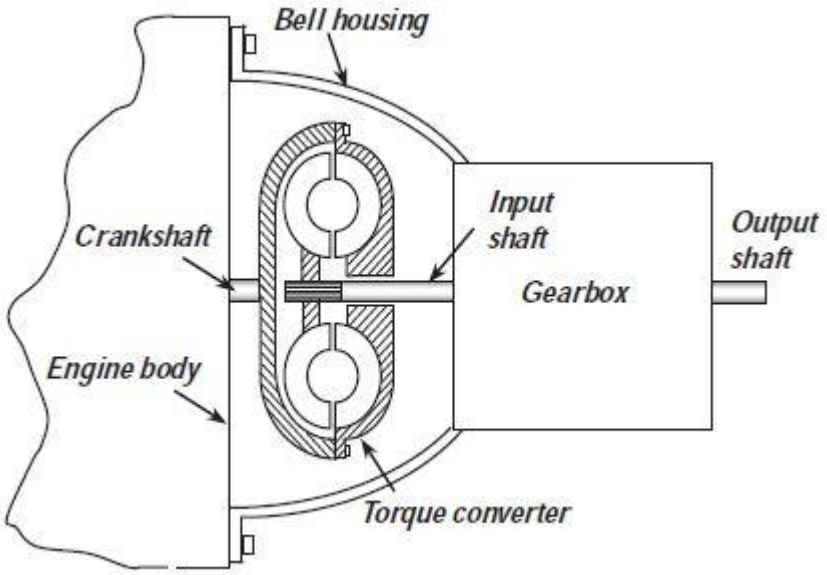

Figure 17 - Overall construction of a conventional automatic (Mashadi & Crolla, 2012)

By using epicyclic gears it is possible to achieve several gear ratios. For multi-speed transmission, several Planetary Gear Sets are necessary. When two sets of PGS are connected, it results in coupled gears (Mashadi & Crolla, 2012).

2.1.3.6.3 AMTs

AMT means “automated manual transmission”. This kind of transmission combines the best characteristics of manual and automatic transmissions: the high efficiency of manual transmissions and the easy operating of automatic transmissions (Mashadi & Crolla, 2012). In addition, there is an economical advantage when compared to MT and AT. AMTs are more efficient than ATs and are programmed to shift more effectively than a regular driver. This transmission architecture is quite linked to Formula 1 (D. A. Crolla, 2009). An AMT is developed from a manual transmission with the addition of electronic controls. The clutch actuation which is the most difficult part of gear changing, is performed automatically while in manual transmission is performed manually. This makes gear shifting more comfortable and driving less exhaustive, so the driver can focus on other operations (Mashadi & Crolla, 2012). This is one more reason why this transmission architecture is being implemented in trucks (D. A. Crolla, 2009).

As gear shifting is performed automatically (shift-by-wire), the mechanical connection between selector lever and transmission is eliminated. When compared to an automatic transmission, AMT presents the following advantages: possibility to use manual transmission manufacturing facilities which results in lower production costs; high efficiency and lower weight. The interruption of flow during shift actuation is presented as the main disadvantage of an AMT (Mashadi & Crolla, 2012).

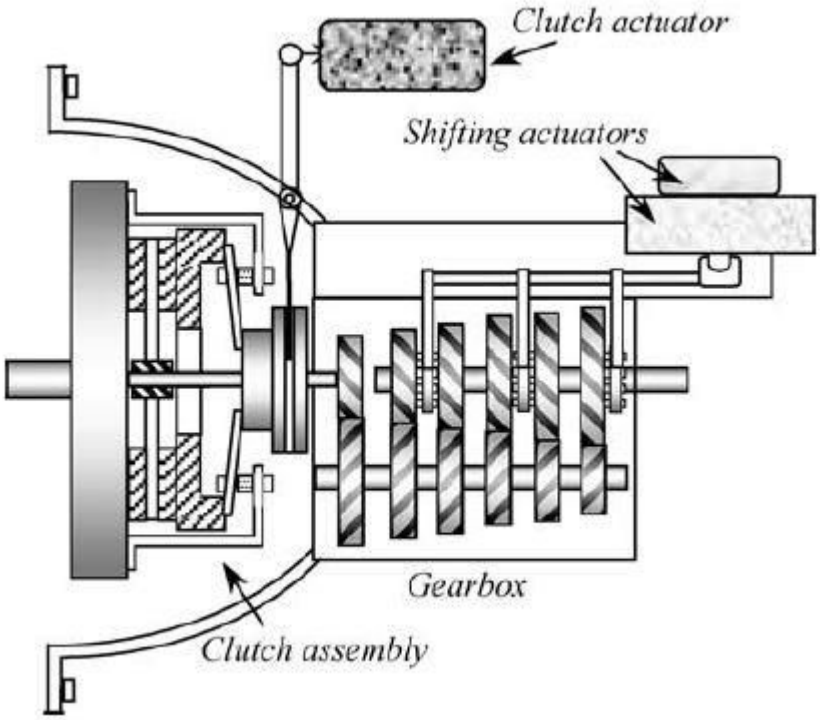

Figure 18 – Actuators for AMT (Mashadi & Crolla, 2012)

It is required two tasks to convert a manual transmission to an AMT (Mashadi & Crolla, 2012):

- Installing three actuator systems for the three actions a driver usually performs: 1 for clutching plus 2 for two movements in gear selection (Figure 18);
- Adding a control unit to make shifting decisions.

2.1.3.6.4 DCTs

DCT are the initials for "dual clutch transmission". As mentioned before, the main disadvantage of manual transmissions is the torque interruption during gear shifting. According to the working principle of a manual transmission, to perform gear shifting it is necessary to disengage the clutch in order to eliminate transmission of engine's torque to the gearbox. By this way, gear meshing can be performed by means of a sliding motion. When the next gear is selected, the clutch is engaged (released) to re-stablish the torque transmission between the engine and the gearbox. With the concept of sliding motion for gear shifting it is inevitable the torque interruption (Mashadi & Crolla, 2012).

DCT design is based on the concept of manual transmissions. Basically, a DCT is a layshaft-type gearbox with two input shafts. It is necessary a clutch system for each shaft. Clutch systems are controlled hydraulic and electronically. The biggest challenge of DCT is the coordination between engagement of one clutch and disengagement of the other one. Usually, in DCTs odd gears are attached to one shaft and the even gears to the other. By doing this, gear shifting can be performed with no torque interruption. The torque interruption is roughly eliminated because of the engagement of one clutch and disengagement of the other one is performed simultaneously. The results are smooth accelerations comparing to manual and even automatic transmissions (Mashadi & Crolla, 2012).

Contrarily to automatic transmissions in which torque converters transmit the engine torque to the gearbox, in DCTS dry clutches or multi-plate wet clutches are used (Mashadi & Crolla, 2012). This type of transmission presents the following advantages when compared to conventional automatic transmissions (Halderman, 2012):

- Quicker throttle response;
- No drop in engine speed when the driver releases the throttle;
- Instant gear changes;
- Improved fuel economy.

When compared to CVT or conventional AT the disadvantages are the following (Halderman, 2012):

- No torque multiplication advantage of a torque converter;
- Not as fuel efficient as a CVT or transaxle.

Function

As seen before, odd and even gears are places in distinct shafts. Two input shafts and two power paths are present on DCT. At the end of each input shaft there is a clutch to allow power interruption for gear shifting. In Figure 19, it is illustrated a schematic of a 6-speed DCT.

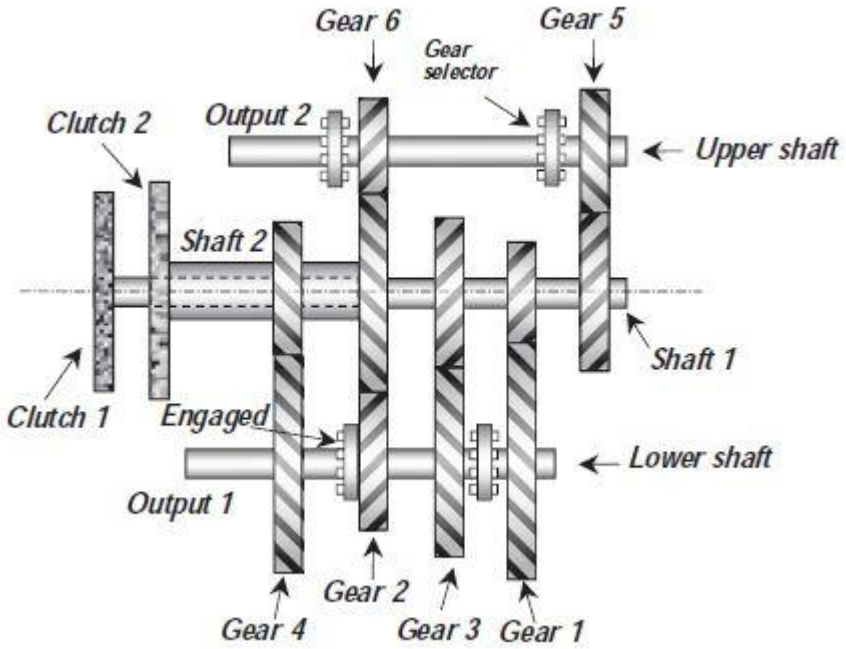

Figure 19 – Schematic of a 6-speed DCT (Mashadi & Crolla, 2012)

According to Figure 19, both input shafts are placed coaxially with one solid shaft (shaft 1). Therefore, shaft 1 is places inside the shaft 2 (hollow shaft). Each shaft (1 and 2) has a clutch from where the engine power is transmitted. Lower and upper shafts are the output shafts. The power is transferred to each of these shafts by selecting one gear. Like a typical layshaft gearbox, the gears of the output shaft rotate freely until they are connected to the shaft by the gear selector. Only one gear is connected to the output at a time.

Based on Figure 19, if the vehicle is in gear 2, clutch 2 is engaged (released) and shaft 2 is transmitting power to the output shaft 1. To shift to gear 3, the gear selector which is located between gear 1 and 3, will move in direction to gear 3. After that, when output

shaft 1 starts rotating, so does gear 3 and mating gear of input shaft 1. Clutch 1 rotates while it is not engaged. Pre-selecting a gear will force the free clutch to rotate. To shift the gear after pre-selection both clutches need to swap over releasing the clutch which is engaged and engaging the free one. In the example of Figure 19, the engine power is transmitted through shaft 1 and gear 3 to the lower output shaft. The other gear selector is still connected to gear 2 and the input shaft 2 will also rotate freely due to the rotation of gear 2. In a DCT there are two paths for torque flow and during gear shifting torque flow is complex. Torque flow depends on several factors such as: clutch clamp forces, layshaft angular velocity and the type of gear shift (upshift or downshift). Since both clutches engage and disengage simultaneously, if the pressure profiles are not appropriate, high torque variations will be induced which results in undesired longitudinal acceleration inputs to the vehicle and its passengers (Mashadi & Crolla, 2012).

2.1.3.6.5 CVTs

CVT are the initials for “Continuously Variable Transmission”.

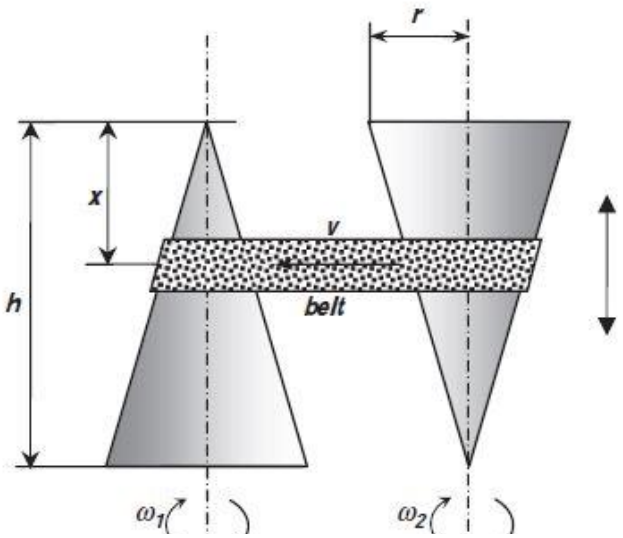

Figure 20 – Conceptual CVT (Mashadi & Crolla, 2012)

CVT concept is based on a principle to transmit power from one rotating shaft to another with continuously variable speeds. The concept is basically two similar cones with a flat wrapped belt around them as showed in Figure 20 (Mashadi & Crolla, 2012).

When the belt moves along the axes of the cones, the value of x varies and for a given speed ω_1 of input shaft, the output angular speed ω_2 can be obtained as follows (Mashadi & Crolla, 2012):

$$\omega_2 = \frac{x}{h-x}\omega_1 \left[rad / s \right] \quad \{2.4\}$$

In eq. {2.4}, it is considered zero slip.

For a fixed value of input angular speed, the output speed ranges from low values near zero up to high values. This feature of a CVT is useful in applications where different gear ratios and smooth shifting between ratios are required. The concept illustrated in Figure 20 does not fulfil the requirements of all the applications mainly when high duty cycles and durability requirements are to be fulfilled (Mashadi & Crolla, 2012).

Classification

CVTs can be classified based on different parameters. In Figure 21, it is presented the classification flowchart based on the nature of the production of the output torque.

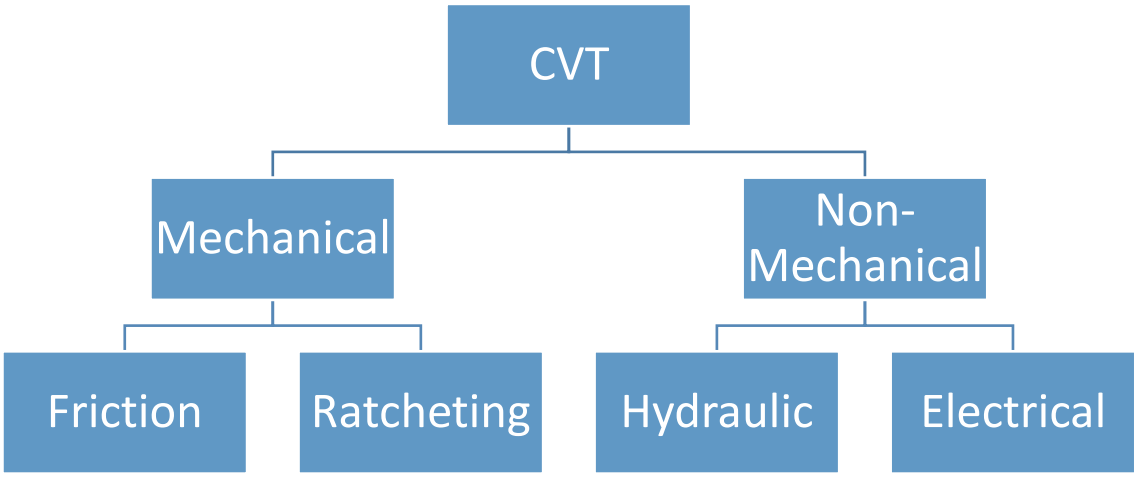

Figure 21 – Automotive CVTs' classification (adapted from (Mashadi & Crolla, 2012))

Friction CVTs

The power provided by an ICE cannot be fully exploited by a traditional gearbox due to the finite number of gears. With an infinite number of gears that is achieved with a CVT the engine can be operated at the ideal operating point in terms of economy or

performance as required (Naunheimer *et al*., 2010). Friction CVTs produce torque due to the friction between mating surfaces by means of belts or rollers. There are two types of friction CVTs in use in automobiles: belt and toroidal CVTs. A belt CVT system is similar to belt-pulley drive with the exception that the pulleys are not fixed and are able to move apart. In Figure 22 is presented the geometry of a typical belt CVT.

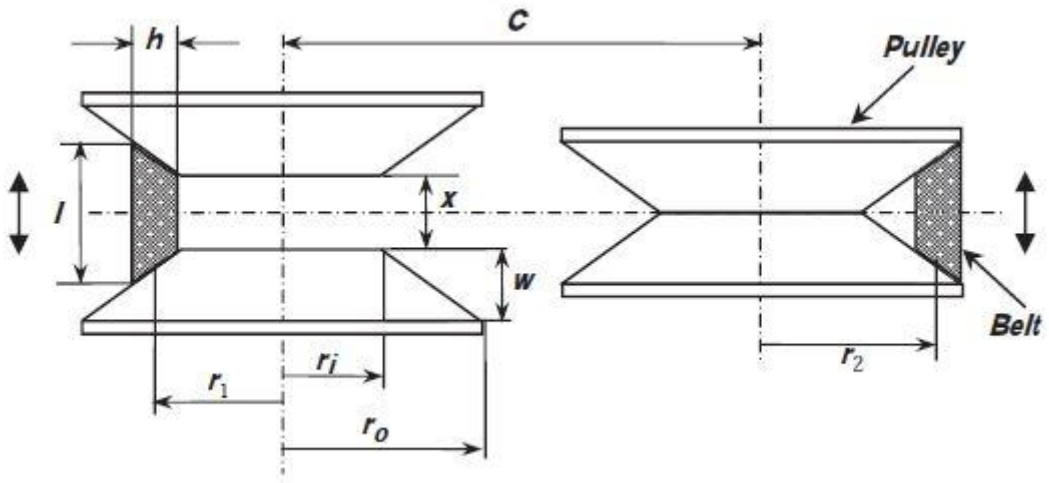

Figure 22 – Geometry of a typical belt CVT (Mashadi & Crolla, 2012)

Pulley transmissions are used in most of the mass-produced passenger cars. The main component of the pulley transmission is the variator. It consists on taper discs and a chain. Power is transmitted by means of friction through the chain. The chain runs between two axially adjustable taper discs (Naunheimer *et al*., 2010). Both pulleys have fixed axes of rotation at a certain distance from each other. The sides of each pulley are controlled to move apart or together laterally, but the displacements of each pulley are the opposite of the other (Mashadi & Crolla, 2012). This axial adjustment provides variable diameters infinitely varying the ratio (Naunheimer *et al*., 2010). In Figure 22 it is illustrated an extreme case when the sides of one pulley are fully apart and the sides of the other pulley are fully closed (Mashadi & Crolla, 2012).

One of the crucial issues in friction CVTs is the amount of friction generated at the contacting surfaces or points. Friction is used to create traction forces at the contact region which creates a torque. However, friction is associated to two disadvantages: build-up of heat and sensitivity to wear. Lubricating oil can be a solution but as a consequence it will reduce the friction and torque capacity of the system. Friction force depends not only on coefficient of friction but also on normal load. If the normal load is increased, coefficient of friction can be compensated (Mashadi & Crolla, 2012).

The torque-related pressure is a parameter to take in deep attention since excessive pressure reduces the efficiency of the chain, leading to increased power consumption, power loss by the contact pressure pump and increased stress on the transmission. Chain slipping is undesirable as this can would lead to the destruction of the

transmission. In conclusion, design and reliability of the pressure pump (and its control) is a crucial factor in CVT of this type (Naunheimer *et al*., 2010).

In the case of chains there are two types: tensional link chains and thrust link chains (Figure 23). The first type is more efficient as less power is required to adapt the chain to the ratio radii and they are better suited to higher torques. For this purpose, short pitch of thrust link chains requires more work. In terms of meshing impact and noise generation, this type of chains play a better role (Naunheimer *et al*., 2010).

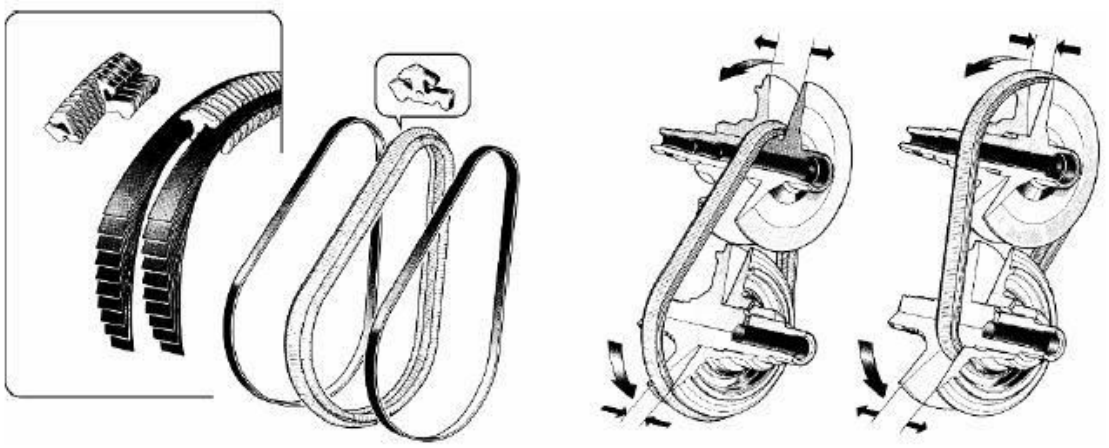

Figure 23 – Elements of a thrust link chain and principle of operation of the variator (Naunheimer *et al*., 2010)

Ratcheting CVTs

A ratchet is a mechanism that produces rotation in one direction regardless of the direction of the input rotation. The originated output is non-uniform and oscillatory. Ratcheting gearboxes' concept is based on the production of the output rotation from a series of discontinuous rotations summed up at the output. Several mechanisms are built in order to produce a gearbox (Mashadi & Crolla, 2012).

Non-mechanical CVTs

There are two distinct types of non-mechanical CVTs which are based on hydraulic and electrical components. A hydraulic system composed by a pump and a hydraulic motor constitutes a gearbox. The pump is responsible for the production of oil flow and turning the motor. The input mechanical power is transformed to fluid power by the pump and once again to mechanical power by the motor. This system can be converted to a CVT

by selecting a pump and/or a motor of variable displacement type. On the other hand, an electric system consists of a generator and a motor which makes it similar to the hydraulic gearbox. The mechanical input power can rotate the generator and produce electric current that can drive an electric motor and produce mechanical power at the output. The conversion of this system to a CVT is achieved by using electric power circuits that control the motor's voltage or frequency.

2.1.3.7 *Gearbox*

2.1.3.7.1 Introduction

As seen before, gearbox is one subsystem of a transmission system. The transmission is a subsystem of powertrain.

Modern vehicles equipped with ICE require a gearbox and a differential. Gearboxes provide a range of gear ratios to maintain engine power and speed to allow the vehicle to travel at appropriate road speeds relevant to the driver and environmental requirements. The differential provides a constant torque amplification ratio (final drive) and acts as a power split device for left and right wheels. The role of the gearbox is to provide different torque amplification ratios from the engine to the wheels when it is necessary and at different driving conditions (Hillier, 2012; Mashadi & Crolla, 2012). The number of gears in a vehicle range from three (old cars) to eight (recent models) (Mashadi & Crolla, 2012).

The gearbox can be manual or automatic. The lowest forward gear (first gear) allows the engine to operate at peak power and torque, but produces low road speed. By moving up the gears, the ratio allows the engine revolutions to remain fairly constant within the peak operating efficiency, while increasing road speed. Using a high gear will allow the vehicle to travel at higher road speeds, but lower engine speeds, resulting in increased fuel efficiency and lower emissions (Hillier, 2012).

First gear is generally used to accelerate the vehicle from a standstill position or manoeuvre the vehicle at low speed, such as when parking. That is one more reason why a gearbox is necessary: to help in the acceleration of a vehicle from standstill (Hillier, 2012).

A well-known benchmark for the overall performance of a vehicle is the 0-100km/h time. A reference value can be considered 10 seconds. This implies an acceleration of 2.7 m/s^2. For this acceleration, for a typical vehicle with a mass of 1000 kg and wheel radius of 30 cm it is required a torque of 710 Nm at the wheel centre. In an electric motor, the maximum acceleration is achieved at start of motion and is up to 2-3 times the average

acceleration. If an acceleration of 2.5 times the average acceleration, the maximum torque at the wheel would be 1775 Nm. In Table 2, it is presented the results comparison between IC engines and EV engines in terms of maximum torques they generate. For this comparison, it was considered engines with an average power of 60 kW (80 hp) (Mashadi & Crolla, 2012).

Table 2 – Gear ratios for different power sources (Mashadi & Crolla, 2012)

Power source (60 kW)	Max torque [Nm]	Overall gear ratio (n)	Gearbox ratio (n_g)
SI Engine (Petrol)	100-120	15-18	4.3-5.1
CI Engine (Diesel)	170-200	9-10	2.6-2.9
Electric motor	250-500	3.5-7	1-2

According to Table 2, the engines (torque sources) have insufficient torque and so they are not suitable to connect directly to the driving wheels (Mashadi & Crolla, 2012).

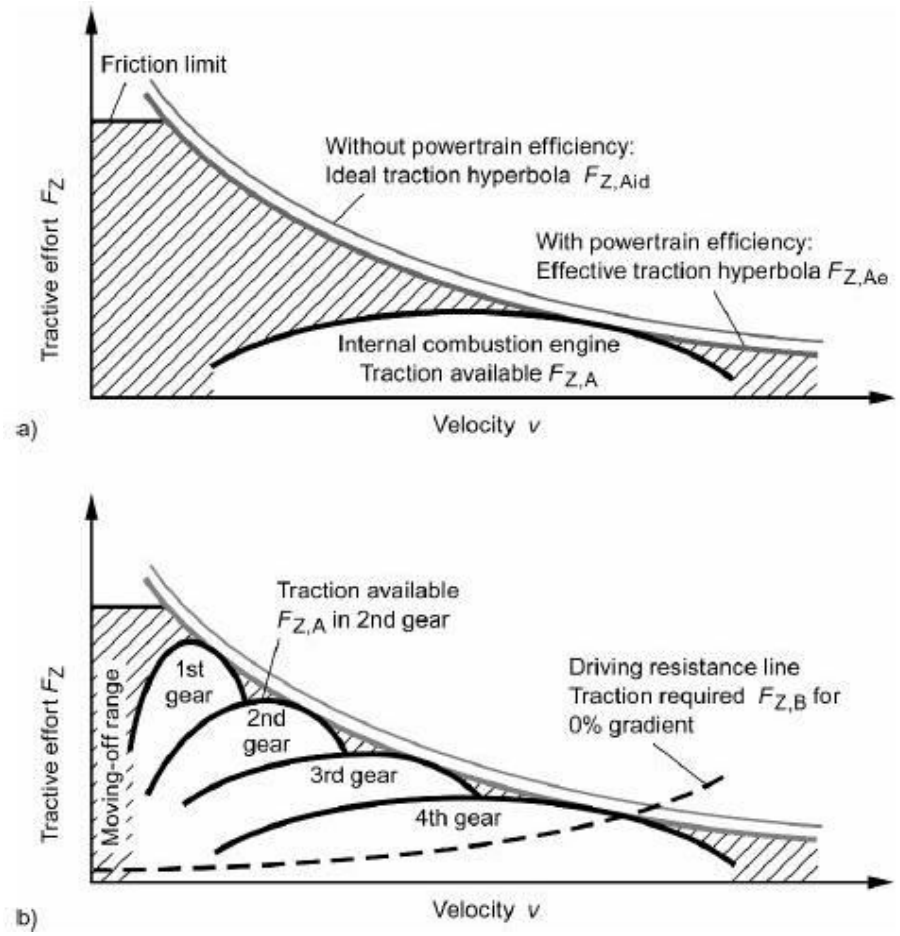

Figure 24 – a) secondary map of an ICE without a gearbox; b) secondary map of an ICE with rear-mounted 4-speed gearbox: traction diagram (Naunheimer *et al.*, 2010)

Another function of the gears is to allow the engine to run at higher speeds when the car is moving slowly, so making use of the vehicle's maximum power and torque for climbing steep hills or accelerating rapidly from low speeds (Hillier, 2012). There is a more technical reason why gearbox use is imperative when the vehicle is equipped with an ICE. If the full-load engine power (P_{max}) was available over the whole speed range, the traction hyperbolas shown in Figure 24 a) would result successfully.

For the ICE, the traction profile would result too. The maximum traction between tyres and road is limited by the friction limit. The whole shaded area of Figure 24 a) cannot be applied without an additional output converter. The output converter must convert the characteristic of the ICE in a way that approximates as closely as possible the traction hyperbola (Figure 24 b)).

There are two possible examples of output converters (Naunheimer *et al*., 2010):

- Speed converter: mechanical or hydrodynamic clutch;
- Speed-torque converter: geared transmission or continuously variable transmission.

The proportion of impossible driving states (proportion of shaded area) is significantly smaller when an output converter is applied and the power potential of the engine can be better applied.

Based on Figure 24 b), increasing the number of speeds as much as possible gives a correspondingly better approximation to the traction hyperbola. With CVT, the traction hyperbola can correspond to the traction characteristic curve over the range of ratios (Naunheimer *et al*., 2010).

The second fundamental disadvantage of the ICE presented on chapter 2.1.1 is solved by means of a moving-off element (force locking clutch). The moving-off clutch (master clutch) is generally mounted between the engine and the transmission in the powertrain (Naunheimer *et al*., 2010).

The purpose of the transmission is to define engine operating points (EOP) that are favourable in terms of efficiency and performance. Low gears are used at low speeds, and should provide high tractions for accelerating and hill climbing. On the other hand, high gears, are used at higher speeds and must allow proper matching between engine torque-speed characteristics with vehicle speed and acceleration (Mashadi & Crolla, 2012).

2.1.3.7.2 Manual gearbox

The manual gearbox consists of sets of gears that amplify the output given by the engine to enable the driving force at the road wheels to be increased sufficiently to overcome the resistance to movement of the vehicle. The gearbox enables the engine speed to be

kept within its working limits irrespective of the speed of the vehicle. It also allows a 'neutral' position where the engine can run without moving the vehicle.

Early manual gearboxes had four forward-moving gears and a reverse gear to drive the vehicle backwards. Modern gearboxes now consist of up to six forward-moving gears in manual gearboxes (up to eight in automatic gearboxes). This enhances the vehicle's overall performance and fuel efficiency. By having more gear ratios, the engine's power can be kept within the peak power band to improve acceleration and performance (Hillier, 2012).

2.1.4 Planetary gear set

Planetary gear sets or Epicyclic gear sets are responsible for the gear ratios in automatic transmissions. Figure 25 shows a typical PGS composed by a sun gear S, a ring gear (or annulus gear) R and a number of planets P that have their rotation axle on a common carrier known as planet carrier C. The example of PGS presented on Figure 25 is similar to the one studied in this thesis. The PGS has three sets of concentric gears meshing at two different diameters. The R has internal teeth and the other gears have external teeth. Most of the times in ATs the PGS are operated with one of the shafts fixed to the gearbox housing making the remaining shafts the input and output (D. A. Crolla, 2009).

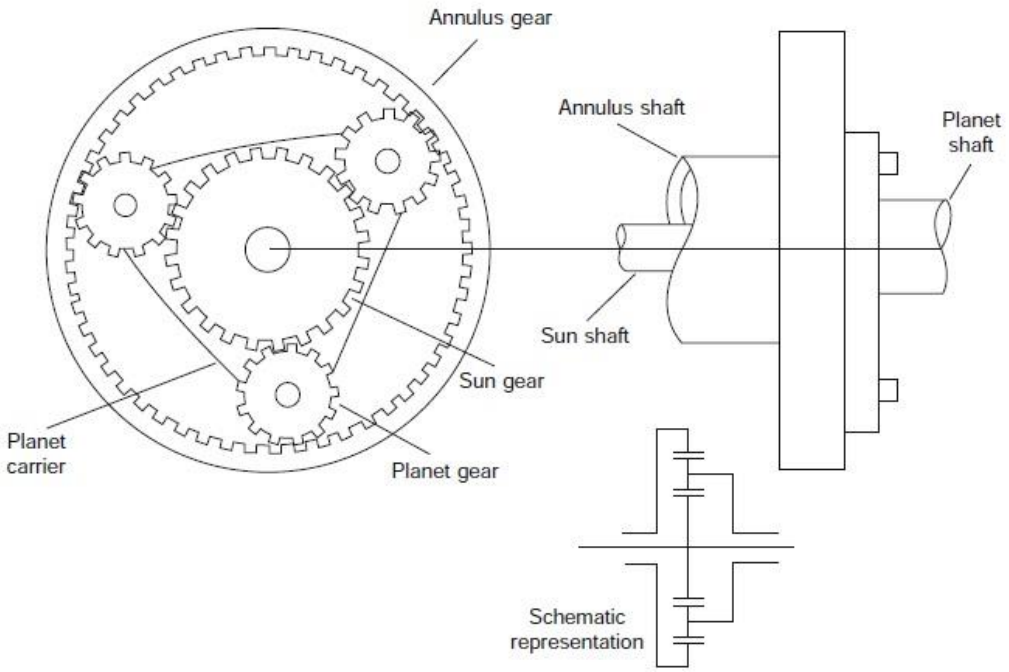

Figure 25 – Planetary gear set (D. A. Crolla, 2009)

In addition to the presented information in this chapter, more topics were studied due to its importance in the understanding of the system in study. The extra topics are presented on Appendix (Extra theoretical aspects).

2.2 Calculations' methods and expressions

2.2.1 Springs

2.2.1.1 *Introduction*

Springs are elastic components which exert reaction forces, or torques, and absorb energy, which is usually stored and later released, infrequently or over continuous cycles. Usually, springs are made of metal however they can also be made of plastic for application with light loads (Juvinall & Marshek, 2012).

In engineering, springs are commonly used to control movement, apply (reaction) forces (to external loads), limit impact forces, reduce vibration and force measurement (Carvil, 1993). Springs have been intensively studied. They are mass-produced and consequently low cost, and different configurations have been found for a variety of applications (Shigley, Mischke & Budynas, 2002).

In the design development, both the level of stress and the amount of deflection are important, usually at the same time (T. H. Brown, 2005).

There are several types of mechanical springs, such as:

- Spiral springs;
- Leaf springs;
- Helical springs;
- Spring washers;
- Moulded springs.

Helical springs can be organized in three distinct categories: compression, tension and torsion springs. Diverse types of spring washers can be seen in Figure 26.

Figure 26 – Types of spring washers (Juvinall & Marshek, 2012)

In this report, only Belleville washers, Wave springs and compression springs will be studied as only these were used in the design of the Drive-Neutral-Reverse subsystem. Below it can be found specific information related to these three types of springs.

2.2.1.2 *Diaphragm springs*

This type of springs is mainly used in dry clutches to generate force for the generation of friction on the clutch plate. These springs have a conical shape with a number of slots cut out in the upper part as can be seen in Figure 27. The tips of the fingers come in contact with the release bearing when clutch pedal is depressed. At the engaging stage the release bearing is held away from the diaphragm spring's fingers (Mashadi & Crolla, 2012).

Figure 27 – Simple form of a diaphragm spring
(Mashadi & Crolla, 2012)

2.2.1.3 *Compression springs*

When the word spring is used, its image is always associated to the image of a helical spring. Typically, they have circular cross sections and their coils are cylindrical, though other shapes are possible. Although other cross sections such as square are also common (T. H. Brown, 2005).

A compression spring is an open-coil helical spring that reacts to a compressive load applied axially. As expected, when a compression coil spring is loaded, making It shorter, it pushes back against the load and tries to get back to the original length.

2.2.1.3.1 Applications

Compression springs can be applied on automotive engines and stamping presses as well as in medical devices, cell phones, electronics and sensitive instrumentation

devices. Cone shape metal springs are generally used in applications where low solid height and increased resistance to surging are required (Spring, 2011).

2.2.1.3.2 Direction of wind

Similar to a screw type thread, coil spring can be wound in either left or right-hand direction. For applications where a spring operates inside another one, it is necessary to coil the springs in opposite directions. If a spring is screwed onto a thread, the direction of the helix must match the one of the thread, i.e., a left hand wound spring will spiral in the same direction as a left hand threaded screw (Spring, 2011).

2.2.1.3.3 End types

In Figure 28 it is presented the four types of ends which are usually applied with compression springs.

A spring with plain ends has a noninterrupted helicoid. The ends are the same as if a long spring has been cut into sections. Springs with plain ends which are squared or closed are obtained by deforming the ends to a zero-degree helix angle.

For important applications, where a better transfer of load is required, springs should be both squared and ground (Shigley *et al.*, 2002).

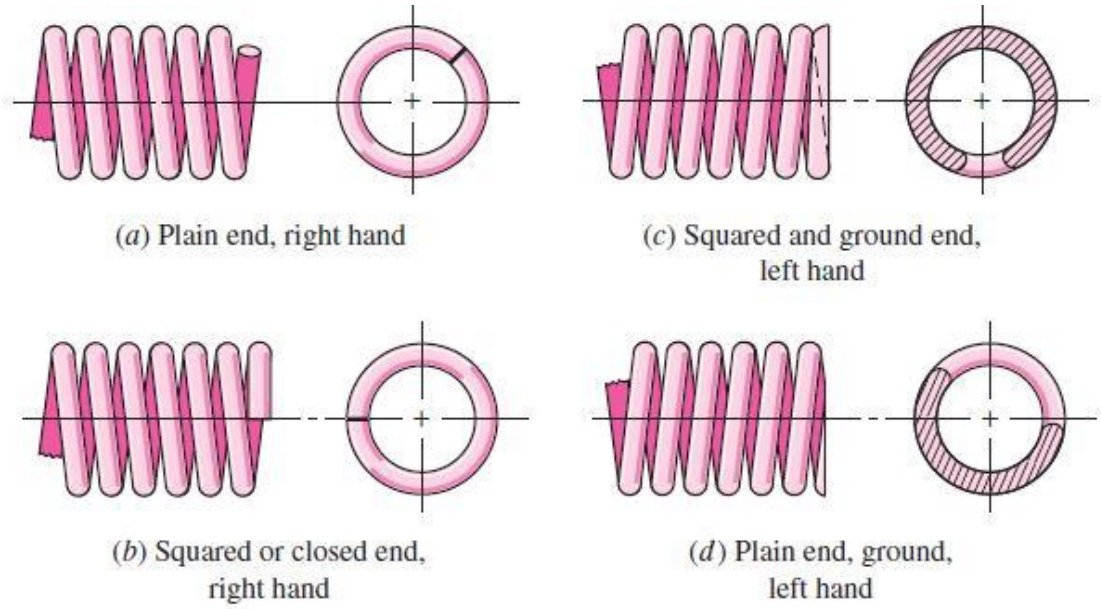

Figure 28 – Types of ends for compression springs (Shigley *et al.*, 2002)

2.2.1.3.4 Counting coils

The total number of coils is counted from consecutive tips according to Figure 29.

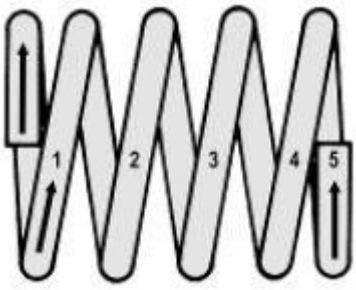

Figure 29 – Counting coils for compression springs (Spring, 2011)

The number of coils and the spring length are directed affected by the type of end used. Consequently, solid height and the pitch will be affected, too. These relations can be visualized in Figure 30.

Term	Type of Spring Ends			
	Plain	Plain and Ground	Squared or Closed	Squared and Ground
End coils, N_e	0	1	2	2
Total coils, N_t	N_a	$N_a + 1$	$N_a + 2$	$N_a + 2$
Free length, L_0	$pN_a + d$	$p(N_a + 1)$	$pN_a + 3d$	$pN_a + 2d$
Solid length, L_s	$d(N_t + 1)$	dN_t	$d(N_t + 1)$	dN_t
Pitch, p	$(L_0 - d)/N_a$	$L_0/(N_a + 1)$	$(L_0 - 3d)/N_a$	$(L_0 - 2d)/N_a$

Figure 30 – Influence of the types of ends of compression springs (Shigley *et al.*, 2002)

2.2.1.3.5 Induced residual stresses

Set removal or presetting is a process applied during the manufacturing process of the compression springs in order to induce useful residual stresses. This process consists in producing the spring longer than needed and afterwards compressing it to its solid height. By doing this, the required final free length it set. Furthermore, since the yield

strength of the springs' material has been exceeded, residual stresses are induced opposite in direction to those induced in service.

During design development, it is recommended to consider an excess of 10 to 30 percent of the initial free length, for springs to be preset.

If the stress at the solid height is greater than 1.3 times the torsional yield strength, distortion may occur. If this stress is much less than 1.1 times, it is difficult to control the resulting free length.

Set removal is especially useful when the spring is used for energy-storage applications, as this process increases the strength of the spring. For applications where the springs are submitted to fatigue, set removal should not be applied (Shigley *et al*., 2002).

2.2.1.3.6 Spring materials

Springs can be manufactured either by hot or cold forming. The choice of the manufacturing process depends on the size of the material, spring index and desired properties.

Winding of the spring induces residual stresses through bending on the mechanical spring, although these are normal to the direction of the torsional working stresses in a coil spring. It is quite frequent in spring manufacture to relieve the springs after winding by mean of a thermal treatment. There is a vast variety of materials suitable for the manufacturing of springs, such as:

- Plain carbon steels;
- Alloy steels;
- Corrosion-resisting steels;
- Phosphor bronze;
- Spring brass;
- Beryllium copper;
- Nickel alloys.

The main and more common property for comparison of the different materials is the tensile strength. However, to know the tensile strength of a certain material, the diameter of the wire must me known because the tensile strength varies significantly with the wire diameter.

The processing of the material influences the tensile strength too. Although the torsional strength is a necessary property to the spring design and its performance's analysis, spring materials are most of the times tested only for tensile strength. A reasonable explanation for this is the low cost of this kind of tests. Posteriorly a rough deduction of

the torsional yield strength may be obtained by assuming that the tensile yield strength is between 60 and 90 per cent of the tensile strength (Shigley *et al*., 2002).

2.2.1.3.7 General calculations

In this chapter, it is presented a calculation process for compression springs and some formulas. There are several ways to calculate the different parameters of a compression spring. Not always, this method was followed, however the formulas were based on the ones presented above. This is because sometimes some parameters were already defined. The process presented here was useful to understand the calculation process of a compression spring design.

First of all, to design a spring is necessary to define the appropriate material taking in account the working environment and kind of application. Shear modulus and tensile strength depends on the material and these values will be crucial on the spring design.

The next step is about calculating the mean diameter and the inner or outer diameter of the spring. At this time, it is necessary to do an assumption of the value of the coil diameter. To find out the optimum value of the coil diameter some iterations should be done. It is important to compare the ID (Inner diameter) of the spring to any work over rod requirements. Furthermore, lowest OD (Outer diameter) (or ID) dimension (having in account the tolerances) should be incorporated when examining the work over rod requirements (Spring, 2011).

Mean diameter and *ID* can be calculated by means of the following equation (Spring, 2011):

$$D_m = OD - d_c \left[m\right] \quad \{2.5\}$$

$$ID = OD - 2d_c \left[m\right] \quad \{2.6\}$$

Where *OD* represents the outer diameter of the spring and is expressed in meters [m]; d_c represents the coil diameter and is expressed in meters [m].

As expected, the diameter of a compression spring increases when compressed. The value of this increment depends on the pitch. At this step, OD expansion is calculated and then this value is compared to any work in hole requirements. It is necessary to consider the great side of the OD tolerance when examining the work in hole requirements (Spring, 2011).

$$OD_{\exp ansion} = \left[\sqrt{D_m^2 + \frac{p^2 - d_c^2}{\pi^2}} + d_c \right] - OD[m] \quad \{2.7\}$$

In which D_m represents the mean diameter of the spring and is expressed in meters [m]; p corresponds to the pitch and is a nondimensionalise variable; and π corresponds to the mathematical constant.

In the following step, pitch is calculated and consequently coils per mm, and spring index. It must be verified that pitch of the spring is not greater than the OD, otherwise coiling difficulties will appear during the manufacturing. As previously mentioned, some factors depend on the type of end of the spring so as a consequence spring index depends on the type of end, too (T. H. Brown, 2005; Spring, 2011). Spring index formulas as a function of the type of end are presented on Table 3.

Table 3 – Spring index of compression springs (adapted from (Spring, 2011))

Type of end			
Open	Open/Ground	Closed	Closed/Ground
$\frac{FL - d_c}{N_A}$	$\frac{FL}{N_T}$	$\frac{FL - 3d_c}{N_A}$	$\frac{FL - 2d_c}{N_A}$

$$\text{Coils per inch} = {}^{1}\!/_{p} \ [1/m] \quad \{2.8\}$$

$$\text{Spring index} = C = \frac{D_m}{d_c} \quad \{2.9\}$$

It is crucial to analyse the spring index value. If it is not between 4 and 10, further examination and considerations are required, such as (Spring, 2011):

- Special tooling (pencil arbors for tight index springs);
- Special packaging (for flimsy or slinky type-high index springs);
- Stress relieving (would either not be applicable for springs with indexes over 25 or would require special handling to prevent distortion);
- Tangling issues;
- No grinding (because grinding high index springs will actually worsen squareness);
- No additional operations, such as plating or tumbling (because of tangling issues);

So, it is recommended to do some iterations changing some initial estimated values in order to avoid manufacturing difficulties and price rise.

Next step is about choosing the design criteria because each criteria has its own calculation method (Spring, 2011):

- Design based on physical dimensions;
- Design based on spring rate;
- Design based on two loads;
- Design based on one load and spring rate;
- Design based on one load and free length.

After defining the spring rate and the number of active coils, the number of total coils can be calculated. This does not apply to designs that are based on physical dimensions (Spring, 2011).

The formulas to calculate the N_T are presented on the table of Figure 30. To calculate *SH* and verify that all the requirements are fulfilled and that the all the load heights are above solid height. It is necessary to consider a variation of 3% to the nominal solid height to calculate the maximum solid height. Formulas to calculate the *SH* is presented on the table of Figure 30 but in this table "solid length" was used instead of "solid height".

As most of the times, there are load requirements. The stress at the load heights must be calculated and compared to the tensile strength of the spring's material. If the percent stress (formula presented below) at any load height is greater than 40% (and the spring will not be compressed more than this particular height) then a set operation or allow for set should be considered. If the percent stress is greater than 60% a re-design must be considered (T. H. Brown, 2005; Spring, 2011).

$$\sigma = \frac{8F \cdot D_m}{\pi d_c^3}\left[Pa\right] \quad \{2.10\}$$

$$\text{Corrected stress} = \frac{8F \cdot D_m}{\pi d_c^3} K\left[Pa\right] \quad \{2.11\}$$

In which *F* corresponds to the load and is expressed in Newtons [N], where (T. H. Brown, 2005):

$$K = \frac{4C-1}{4C-4} + \frac{0.615}{C}[\ ] \quad \{2.12\}$$

Where *C* corresponds to the spring index and is a nondimensionalized variable.

The percent stress can be calculated as follows (Spring, 2011):

$$\text{Percent stress} = \frac{\sigma}{R_m} \cdot 100 \left[\%\right] \quad \{2.13\}$$

Where σ corresponds to the stress and is expressed in Pascal [Pa]; R_m corresponds to the material tensile strength and is expressed in Pascal [Pa].

Unless the working range is specifically known, the stress at solid height must be examined. If the percent stress at solid height is greater than 40% then a set operation or allow for set should be considered. If the percent stress is greater than 60%, a re-design must be done. If an overstressed situation is presented, it must be known how the spring will be used in order to see if it is possible to avoid the overstress. Overstress load and respective stress can be calculates as follows (Spring, 2011):

$$F_S = SR(FL - SH) \left[N\right] \quad \{2.14\}$$

$$\sigma_S = \frac{8F_S \cdot D_m}{\pi \cdot d_c^3} \left[Pa\right] \quad \{2.15\}$$

$$\text{Percent stress at solid height} = 100 \cdot \frac{\sigma_S}{R_m} \left[\%\right] \quad \{2.16\}$$

Where *FL* (Free length) corresponds to the free length of the spring and is expressed in meters [m]; *SR* corresponds to the spring stiffness and is expressed in Newton per meter [N/m]; and *SH* corresponds to the solid height of the spring and is expressed in meters [m].

Design to physical dimensions

In order to calculate the main properties of a spring based on the physical dimensions the following information is required:

- Wire diameter;
- Outside diameter or hole diameter or inside diameter or rod size;
- Free length;
- Number of coils (active/inactive)
- Ends configuration;
- Solid height.

In addition to the general considerations presented above, spring rate must be calculated (T. H. Brown, 2005):

$$SR = \frac{G \cdot d_c^4}{8 N_A \cdot D_m^3} \left[N / mm \right] \quad \{2.17\}$$

Where G corresponds to the material's shear modulus and is expressed in Pascal [Pa]; N_A corresponds to the number of active coils and is a nondimensionalize variable.

Spring rate is generally defined between 20 and 80% of the available deflection where it is linear (Spring, 2011).

Design to spring rate

With the purpose to calculate the number of active coils of a compression spring the following information is required:

- Wire diameter;
- Outside diameter or hole diameter or inside diameter or rod size;
- Free length;
- Spring rate;
- Number of inactive coils;
- Ends configuration;
- Solid height;

In addition to the general considerations presented above, number of active coils must be calculated (T. H. Brown, 2005).

$$N_A = \frac{G \cdot d_c^4}{8 \cdot SR \cdot D_m^3} \left[\ \right] \quad \{2.18\}$$

Design to two loads

The following information is necessary to design a compression spring for two loads:

- Wire diameter;
- Outside diameter or hole diameter or inside diameter or rod size;
- Load at height 1;
- Load at height 2;
- Ends configurations;
- Solid height;
- Number of inactive coils.

In addition to the general considerations presented above, the following parameters must be calculated:

- Spring rate:

$$SR = \frac{\Delta F}{\Delta h} = \frac{F_2 - F_1}{h_1 - h_2}\left[N/m\right] \quad \{2.19\}$$

Where F_2 corresponds to the load at working height 2 and is expressed in Newton [N]; F_1 corresponds to the load at working height 1 and is expressed in Newton [N]; h_1 corresponds to the working height 1 and is expressed in meters [m]; and h_2 corresponds to the working height 2 and is expressed in meters [m].

- Number of active coils is calculated according to equation {2.18}.
- Free length:

$$FL = h_1 + \frac{F_1}{SR}\left[m\right] \quad \{2.20\}$$

Design to one load/rate

When is the intention of the designer to calculate a spring for one load or based on its rate the following information is necessary:

- Wire diameter;
- Outside diameter or hole diameter or inside diameter or rod size;
- Load at height 1;
- Spring rate;
- Ends configurations;
- Solid height;
- Number of inactive coils.

In addition to the general considerations presented above, the following parameters must be calculated:

- Number of active coils can be calculated according to equation {2.18};
- Free length can be calculated based on equation {2.20}.

Design to one load/free length

The following information is required to calculate the compression spring for one load and with the free length as a requirement:

- Wire diameter;
- Outside diameter or hole diameter or inside diameter or rod size;
- Load at height 1;
- Free length;
- Ends configurations;
- Solid height;
- Number of inactive coils.

In addition to the general considerations presented above, the following parameters must be calculated:

- Spring rate:

$$SR = \frac{\Delta F}{\Delta h} = \frac{F_1}{FL - h_1}\left[N / m\right] \quad \{2.21\}$$

- Number of active coils according to equation {2.18}

2.2.1.3.8 Fatigue

Springs are almost always subject to fatigue loading. In fact, all the springs applied on the DNR subsystem are under dynamic loading conditions. In case of an expected life of millions of cycles without failure, spring must be designed for an infinite life. This is the case of the valve springs of a combustion engine (Shigley *et al*., 2002).

Shot peening can be applied on springs dynamically loaded in order to improve fatigue strength. It may increase the torsional strength at least twenty per cent. Shot size is about 1/64 inches, so spring coil wire diameter and pitch must allow for complete coverage of the spring surface (Shigley *et al*., 2002). The highest values of torsional endurance limits of springs steels are those reported by Zimmerli. He discovered that

size, material and tensile strength haven't any effect on the endurance limits (infinite life only) of spring steels in sizes under 10 mm. Endurance limits tend to level out at high tensile strengths however the justification for this phenomenon is still unknown (Shigley *et al*., 2002). Unpeened springs were tested from a minimum torsional stress of approximately 138 MPa to a maximum of 621 MPa. Peened springs were tested from a range of approximately 138 MPa to 931 MPa (Shigley *et al*., 2002). The following endurance strength components for infinite life were found to be:

- Unpeened:

S_{sa} = 241 MPa and S_{sm} = 379 MPa

- Peened:

S_{sa} = 398 MPa and S_{sm} = 534 MPa

The torsional modulus of rupture S_{su} is necessary for the designer's torsional fatigue diagram and may be calculated as follows (Shigley *et al*., 2002):

$$S_{su} = 0.67 R_m \left[Pa \right] \quad \{2.22\}$$

For shafts and other kind of machine elements it is quite common fatigue loading in the form of completely reversed stresses. Although, compression springs are never used as both compression and extension springs. Furthermore, compression springs are usually installed with a preload so that the working load is additional.

Amplitude force must be calculated as follows (Shigley *et al*., 2002):

$$F_a = \frac{F_{\max} - F_{\min}}{2} \left[N \right] \quad \{2.23\}$$

Where F_{max} corresponds to the maximum load applied on the spring and is expressed in Newton [N] and F_{min} corresponds to the minimum load applied on the spring and is expressed in Newton [N].

Midrange force may be obtained as follows (Shigley *et al*., 2002):

$$F_m = \frac{F_{\max} + F_{\min}}{2}\left[N\right] \quad \{2.24\}$$

Shear stress amplitude is (Shigley *et al*., 2002):

$$\tau_a = K_B \frac{8F_a D_m}{\pi d^3}\left[Pa\right] \quad \{2.25\}$$

In which F_a corresponds to the amplitude force and is expressed in Newtons [N], where K_B is obtained as follows (Shigley *et al*., 2002):

$$K_B = \frac{4C+2}{4C-3} \quad \{2.26\}$$

K (eq. {2.12}) can be used instead of K_B.

Midrange shear stress is given by (Shigley *et al*., 2002):

$$\tau_m = K_B \frac{8F_m D_m}{\pi d_c^3}\left[Pa\right] \quad \{2.27\}$$

Slope line is given by ("Formulas for Compression Spring Fatigue Design," n.d.):

$$r = \frac{\tau_a}{\tau_m}\left[\ \right] \quad \{2.28\}$$

Where τ_a corresponds to the shear stress amplitude and is expressed in Pascal [Pa] and τ_m corresponds to the midrange shear stress and is expressed in Pascal [Pa].

Shear endurance limit according to Gerber is given by (Shigley *et al*., 2002):

$$S_{se}^{Gerber} = \frac{S_{sa}}{1-\left(\frac{S_{sm}}{S_{su}}\right)^2}[Pa] \quad \{2.29\}$$

Where S_{sa} corresponds to the shear stress amplitude limit and is expressed in Pascal [Pa]; S_{sm} corresponds to the maximum endurance strength component for infinite life and is expressed in Pascal [Pa] and S_{su} corresponds to the torsional modulus rupture and is expressed in Pascal [Pa].

Shear endurance limit according to Goodman is given by ("Formulas for Compression Spring Fatigue Design," n.d.):

$$S_{se}^{Goodman} = \frac{S_{sa}}{1-\left(\frac{S_{sm}}{S_{su}}\right)}[Pa] \quad \{2.30\}$$

Shear stress amplitude limit according to Gerber failure criteria can be calculated as follows ("Formulas for Compression Spring Fatigue Design," n.d.):

$$S_{sa}^{Gerber} = \frac{r^2 S_{su}^2}{2S_{se}}\left(-1+\sqrt{1+\left(\frac{2S_{se}}{r \cdot S_{su}}\right)^2}\right)[Pa] \quad \{2.31\}$$

In which *r* corresponds to the slope line and is a nondimensionalized variable.

Shear stress amplitude limit according to Goodman failure criteria can be obtained as follows ("Formulas for Compression Spring Fatigue Design," n.d.):

$$S_{sa}^{Goodman} = \frac{rS_{se}S_{su}}{rS_{su}+S_{se}}[Pa] \quad \{2.32\}$$

The value of S_{sa} according to Sines is equal to S_{sa} according to Zimmerli.

Factor of safety against fatigue is given by ("Formulas for Compression Spring Fatigue Design," n.d.):

$$SF_f = S_{sa} / \tau_a \quad \{2.33\}$$

2.2.1.4 *Wave springs*

A wave spring is like a compression spring made of coiled flat wire with waves along the coils to give it a spring effect. This kind of springs can replace conventional round wire compression springs in applications where tight load deflection in space critical environments is required. Generally, for the same load, wave springs occupy between 30 and 50% of the compressed height space compared to round wire springs. This provides not only space savings but also smaller assemblies which use less material and consequently lower production costs.

Wave springs are manufactured from a single filament of flat wire formed in continuous and precise coils with uniform diameter and waves. It must be taken in account the material for high temperatures or corrosive operating environments.

Wave springs can be found in a wide variety of applications where structural considerations restrict the installation height, where uniform force distribution is needed and/or uniform rotational pressure is required over 360°. This kind of spring washers is suitable for both static and slightly dynamic load applications. However, fatigue is critical for dynamic load applications. For higher life cycles is it necessary a stronger spring. Special solutions must be found for extremely dynamic applications, since considerable stress on the sine wave curves can cause material abrasion at the contact point. Typical applications include connectors, clutches, valves, pumps, seals, medical equipment, etc (Spring, 2011).

In Figure 31 is presented the terminology of a wave spring that will be applied in the following calculations.

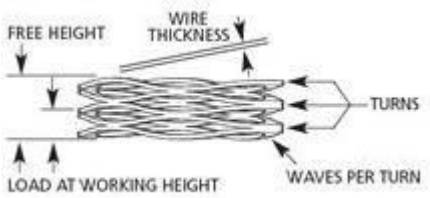

Figure 31 – Terminology of a wave spring (Spring, 2011)

There are four critical factors to be taken in account during design development of a wavy washer (Spring, 2011):

- Constraints of the application: Bore/shaft, ID/OD, etc;
- Load;
- Working height;
- Material.

2.2.1.4.1 Design general considerations

If a spring is designed to a static application, the percentage of stress at working height must be less than 100%. If this value is greater than 100%, spring will take a set. In case of dynamic application, the percentage of stress at working height must be less than 80%. If this value is greater than 80% spring will take a set. If the work height per turn is less than two times wire thickness, the spring will operate in a nonlinear range and actual loads may be higher than calculated.

Number of turns must be between 2 and 20. Number of waves per turn must be in half increment. Minimum radial wall must be equal to three times wire thickness. Maximum radial wall must be equal to ten times wire thickness.

It is not recommended to completely compress a wave spring (solid height) (Spring, 2011).

2.2.1.4.2 General calculations

Deflection, can be calculated as follows:

$$d = \frac{F \cdot K_W \cdot D_m^3 \cdot Z_W}{E \cdot b_W \cdot t_W^3 \cdot N_W^4} \cdot \frac{ID}{OD} \left[m \right] \quad \{2.34\}$$

Where F corresponds to the load and is expressed in Newton [N]; K_W corresponds to the multiple wave factor (Table 4) and is a nondimensionalized variable; D_m corresponds to the mean diameter and is expressed in meters [m]; Z_W corresponds to the number of turns and is a nondimensionalized variable; E corresponds to the materials' Young's Modulus and is expressed in Pascal [Pa]; b_W corresponds to the radial wall (width) of the wavy washer and is expressed in meters [m]; t_W corresponds to the wire thickness and

is expressed in meters [m]; N_W corresponds to the number of waver per turn and is a nondimensionalized variable; *ID* corresponds to the inner diameter of the wavy washer and is expressed in meters [m] and *OD* corresponds to the outer diameter and is expressed in meters [m].

Spring rate can be calculated according to the following formula:

$$SR = \frac{F}{d} = \frac{E \cdot b_w \cdot t_w^3 \cdot N_w^4}{K_w \cdot D_m^3 \cdot Z} \cdot \frac{OD}{ID} \left[N / m \right] \quad \{2.35\}$$

Where *d* corresponds to the deformation of the spring when compressed and is expressed in meters [m].

The value of K_w can be found via correspondence according to Table 4.

Table 4 – Multiple wave factor (Spring, 2011)

N_w	K_w
2.0-4.0	3.88
4.5-6.5	2.9
7.0-9.5	2.3
10 and over	2.13

OD expansion is a crucial factor mainly for wavy springs as this kind of springs is most of the times assembled in a housing (hole) (that is the case of the studied wavy spring).

$$OD_{\exp ansion} = (0.02222 R_W \cdot N_W \cdot t_W) + b_W \left[m \right] \quad \{2.36\}$$

In which R_W corresponds to the effective wave radius and is expressed in meters [m].

Where:

$$R_W = \frac{(4W_H^2 + W_L^2)}{8W_H} \left[m \right] \quad \{2.37\}$$

In which W_H corresponds to the half wave free height and is a nondimensionalized variable; and W_L corresponds to the half wave length and is a nondimensionalized variable.

$$\theta_W = \arcsin\left(\frac{W_L}{2R_W}\right) \quad \{2.38\}$$

$$W_L = \frac{\pi D_m}{2N_W} \quad \{2.39\}$$

$$W_H = \left(\frac{\frac{FL}{Z} - t_W}{2}\right) \quad \{2.40\}$$

2.2.1.4.3 Fatigue

Operating stress can be calculated as follows:

$$\sigma = \frac{3\pi F \cdot D_m}{4b_w \cdot t_w^2 \cdot N_w^2}[Pa] \quad \{2.41\}$$

In case of a static application, need of presetting can be verified according to Table 5.

Table 5 – Wave springs design stresses for static/low cycles (Spring, 2011)

Static/Low cycles	
No preset	100% R_m
Preset springs	150% R_m

In case of dynamic applications, cycle life can be estimated according to Table 6.

Table 6 – Wave springs design stresses for dynamic service applications (Spring, 2011)

	Dynamic service
10^4 cycle life	80% R_m
10^5 cycle life	53% R_m
10^6 cycle life	50% R_m
10^7 cycle life	48% R_m

Fatigue stress ratio can be calculated based on the following formula:

$$X = \frac{\sigma - \sigma_1}{\sigma - \sigma_2} \quad \{2.42\}$$

Where σ_1 corresponds to the stress at the working height 1 and is expressed in Pascal [Pa]; σ_2 corresponds to the stress at the working height 2 and is expressed in Pascal [Pa]; and σ corresponds to the operating stress and is expressed in Pascal [Pa].

The value of σ_1 must be less than σ.

The cycle life can be estimated based on Table 7.

Table 7 - Wavy spring estimated cycle life (Spring, 2011)

X	Estimated life cycle (nr. of cycles)
<0.40	Under 30000
0.40-0.49	30000-50000
0.50-0.55	50000-75000
0.56-0.60	75000-100000
0.61-0.67	100000-200000
0.68-0.7	200000-1000000
> 0.7	Over 1000000

2.2.1.5 *Belleville washers*

Belleville washers are also called by Belleville springs or Disc springs. The main advantage of these type of springs is that it occupies only a small space in height (A. A. D. Brown, 1981).

Belleville washer is an annular dished steel ring which deflects axially under load (Carvil, 1993). The slight conical shape gives the washer a spring property. When compared to

helical springs, Belleville washers' conical shape provides them the ability to support high loads with relatively small deflections and solid heights (Spring, 2011).

Several springs may be used in series or parallel arrangements to give lower or higher stiffness, respectively (Carvil, 1993).

For a given deflection, a higher reaction load may be obtained by nesting, that is, to stack the springs in parallel. On the other hand, stacking the springs in series provides a larger deflection for the same load. When stacked in series, there is danger of instability (Shigley *et al*., 2002). In Figure 32 it is shown the representation of the two stacking configurations for Belleville washers.

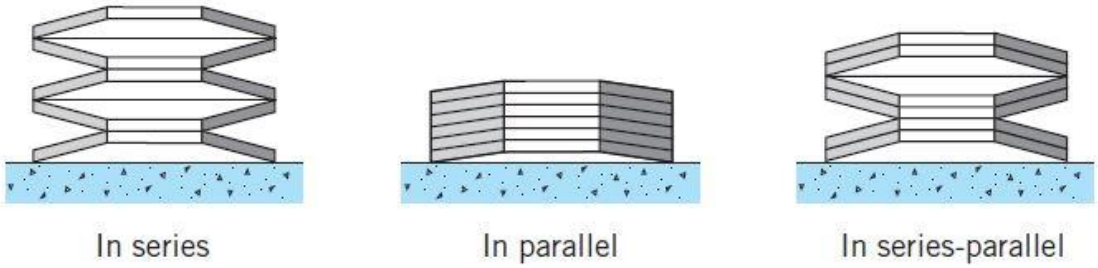

Figure 32 – Stacked Belleville washers (Juvinall & Marshek, 2012)

This kind of spring washers can also be applied as locking devices, but only in applications with low dynamic loads (Spring, 2011).

In this chapter, all the necessary data related to the disc springs can be found.

In Figure 33, it is illustrated a cross section of a Belleville washer and the nomenclature adopted for the following calculations.

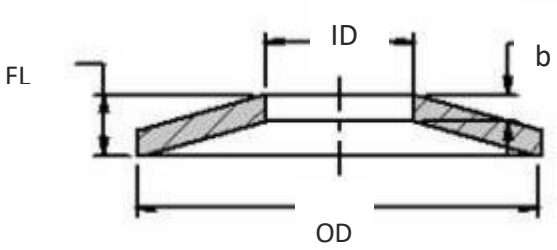

Figure 33 – Main dimensions for Belleville washers (Spring, 2011)

2.2.1.5.1 General calculations

The diameters' ratio can be calculated according to the following equation (Spring, 2011):

$$\delta = \frac{OD}{ID} \qquad \{2.43\}$$

Where *OD* corresponds to the outer diameter of the disc spring and is expressed in meters [m]; *ID* corresponds to the inner diameter and is expressed in meters [m].

The load at maximum working height can be calculated as follows (Spring, 2011):

$$F_{h_{\max}} = \frac{4E \cdot b^3 \cdot d_{\max}}{(1-\nu^2) \cdot \gamma_1 \cdot OD^2}\left[N\right] \qquad \{2.44\}$$

Where *E* represents the material's Young's modulus and is expressed in Pascal [Pa]; *b* corresponds to the thickness and is expressed in meters [m]; d_{max} represents the maximum allowed deflection and is expressed in meters [m]; *v* corresponds to the material's Young's Modulus and is expressed in Pascal [Pa]; γ_1 represents the calculation coefficient and is a nondimensionalized variable.

The load at any working height can be obtained as follows (Spring, 2011):

$$F = \frac{4E \cdot b^4}{(1-\nu^2) \cdot \gamma_1 \cdot OD^2} \cdot \frac{d}{b} \cdot \left[\left(\frac{h_B}{b} - \frac{d}{b}\right) \cdot \left(\frac{h_B}{b} - \frac{d}{2b}\right) + 1\right]\left[N\right] \qquad \{2.45\}$$

In which *d* represents the spring's deflection and is expressed in meters [m]; h_B represents the unloaded height of truncated cone of free spring and is expressed in meters [m]. Where:

$$h_B = FL - b\left[m\right] \qquad \{2.46\}$$

In which *FL* corresponds to the unloaded spring height and is expressed in meters [m].

The stress at a certain point can be calculated as follows (Spring, 2011):

$$\sigma = \frac{4E \cdot b \cdot d}{(1-\nu^2) \cdot \gamma_1 \cdot OD^2} \cdot \left[\gamma_2 \left(\frac{h_B}{b} - \frac{d}{2b} \right) + \gamma_3 \right] [Pa] \quad \{2.47\}$$

In which γ_2 and γ_3 represent calculation coefficients and are nondimensionalized variables. Where (Spring, 2011):

$$\gamma_1 = \frac{1}{\pi} \cdot \frac{\left(\frac{\delta - 1}{\delta} \right)^2}{\frac{\delta + 1}{\delta - 1} - \frac{2}{\ln \delta}} \quad \{2.48\}$$

$$\gamma_2 = \frac{1}{\pi} \cdot \frac{6}{\ln \delta} \left(\frac{\delta - 1}{\ln \delta} - 1 \right) \quad \{2.49\}$$

$$\gamma_3 = \frac{\delta - 1}{\pi} \cdot \frac{3}{\ln \delta} \quad \{2.50\}$$

In which δ represents the diameter's ratio and is a nondimensionalized variable.

2.2.1.5.2 Fatigue

Static stress

In the case of disc springs made of spring steel (DIN EN 10 132-4), stress σ_{OM} in a flattened condition should not exceed the tensile strength of approximately 1600 MPa of the material (*Disc springs - theory and practice*, n.d.). In the case of springs made from DIN 17 221 or DIN 17 222 steel that are submitted to static loading or to moderate fatigue conditions, the stress at the point designated OM (Figure 34) shall be approximately equal to the yield strength of the material used (i.e. 1400 to 1600 N/mm^2) (DIN 2093, 1992).

When submitted to higher stresses, it is likely that the springs will suffer from creep or relaxation (DIN 2093, 1992). In case of higher levels of stress, high deflection may be expected with a minor degree of direct resetting. Up to around 5000 load cycles, it is still considered a static application (*Disc springs - theory and practice*, n.d.).

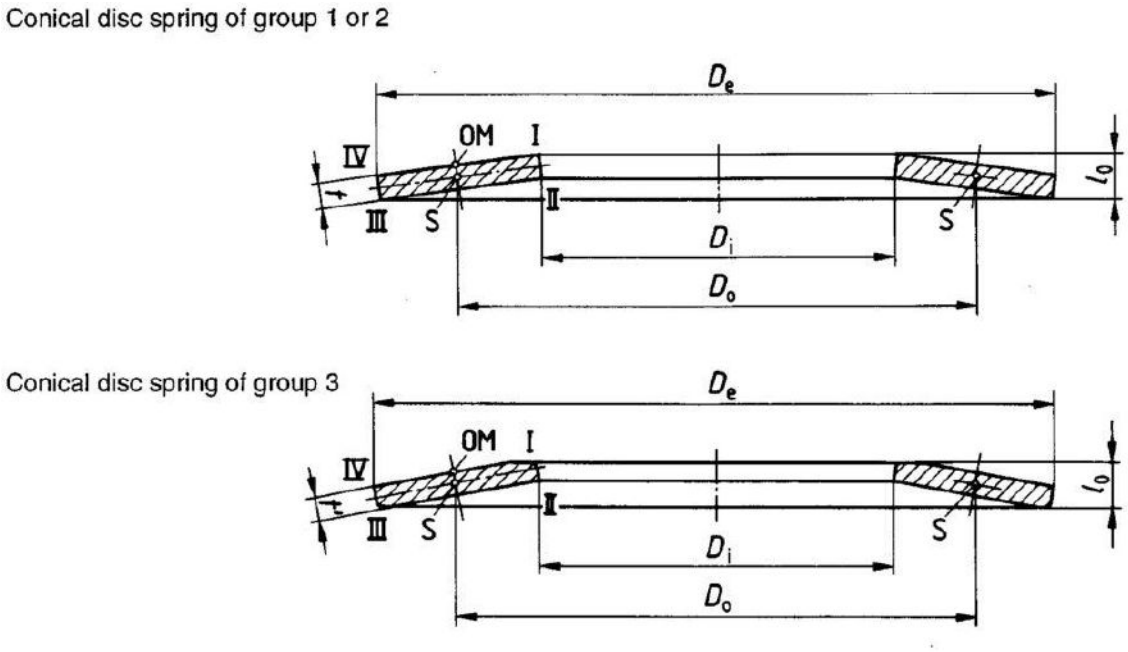

Figure 34 – Cross section of a single disc spring, including the relevant points of loading ("DIN 2093," 1992)

Dynamic stress

Minimum pre-stress to avoid cracking

Springs that are subject to fatigue loading must be designed and installed in such a way that the initial deflection is from about $0.15h_0$ to $0.20h_0$ in order to avoid cracking at the upper inner edge (point I of Figure 34) as a result of residual stresses from the setting processes (DIN 2093, 1992).

It is possible to counteract the influence of residual tensile strength by providing enough pre-stress in the spring. Depending on the stress level of the disc springs, a greater pretension deflection may be necessary, or a smaller deflection may be enough (*Disc springs - theory and practice*, n.d.).

Stress in the work range

When submitted to vibrating stress, the response of a disc spring is determined by the tensile stress occurring on the underneath of the spring. The number of load cycles to fracture results from the minimum stress limit σ_u assigned to the maximum spring deflection. Whether the stress levels occurring at cross section point II or III are decisive depends on the dimensioning of the disc spring. (*Disc springs - theory and practice*, n.d.)

Endurance and fatigue strength diagrams

The graphs from Figure 35 to Figure 36 illustrate the endurance life of conical disc springs submitted to fatigue loading that have not been shot peened.

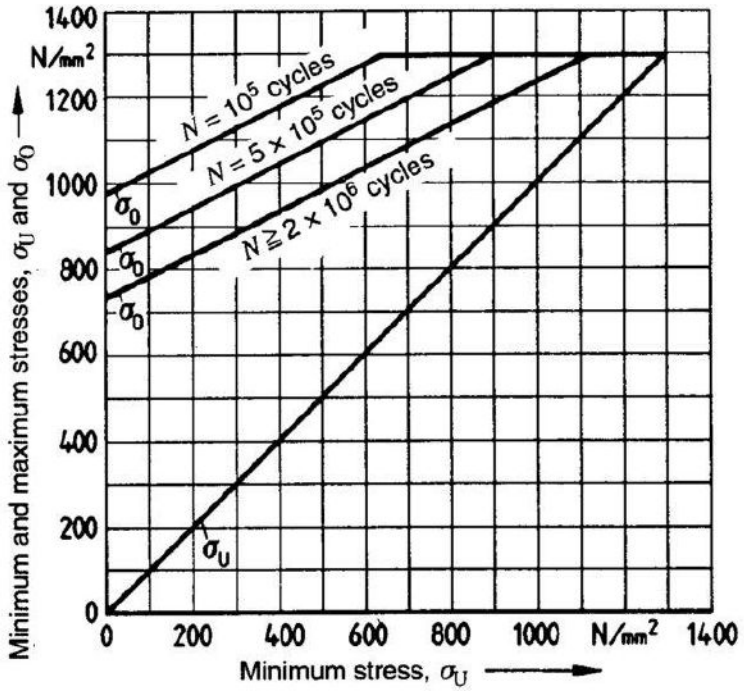

Figure 35 – Graphical representation of endurance life of springs where thickness is less than 1,25 mm (DIN 2093, 1992)

The information provided on these graphs represents the results of laboratory testing using fatigue testing equipment capable of producing sinusoidal loading cycles and the statistical results obtained for a 99% probability of endurance life. The test pieces were ten single discs with hardened surfaces, stacked in series, designed for use at ambient temperature, provided with an internal or external centring element with a smooth finish, having a minimal initial deflection from about $0.15h_0$ to $0.20h_0$.

These graphs specify guideline values for the range of stress, σ_H, as a function of the minimum stress, σ_u, at three different numbers of stress cycles, N_C, namely where N_C is less than or equal to $2 \cdot 10^6$, equal to 10^5, and equal to $5 \cdot 10^5$. Intermediate values for other values of stress cycles may be estimated based on this information.

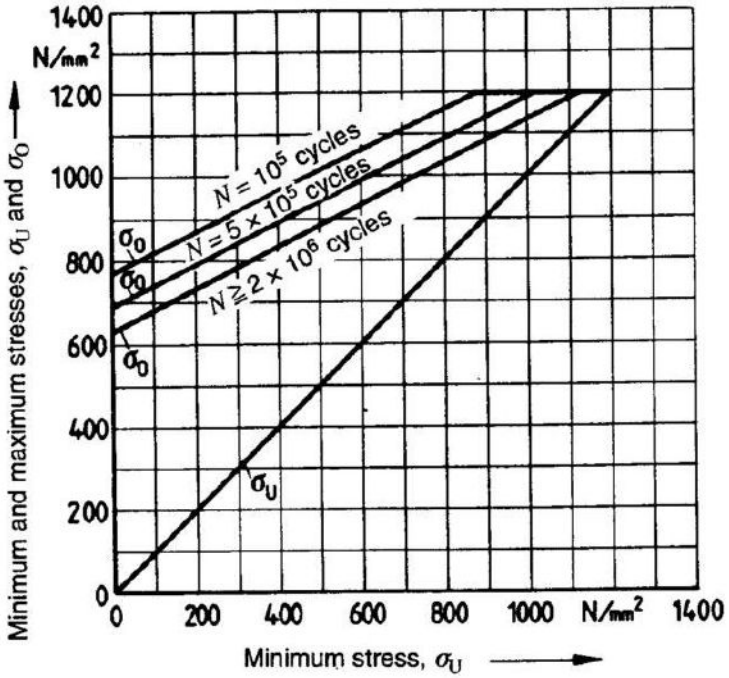

Figure 37 – Graphical representation of endurance life of springs where 6 mm < thickness < 14 mm (DIN 2093, 1992)

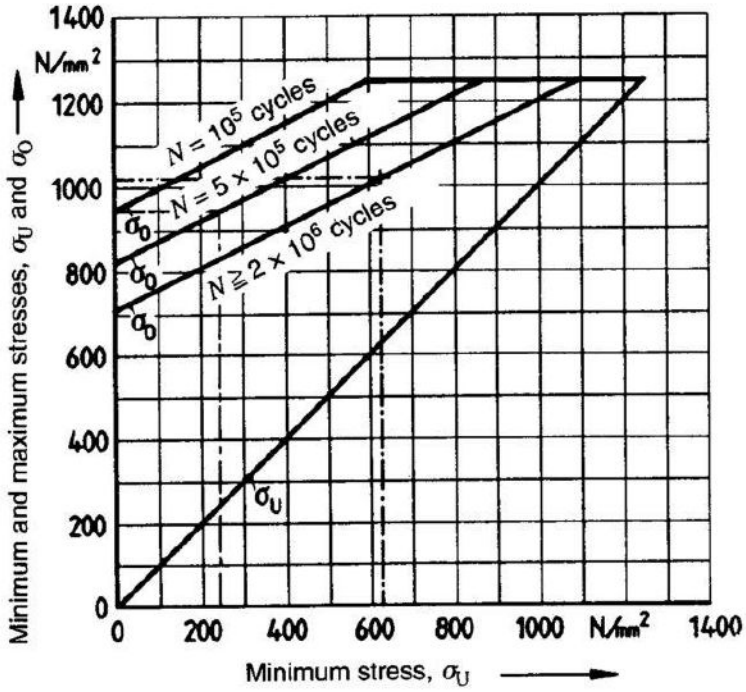

Figure 36 – Graphical representation of endurance life of springs where 1,25 mm ≤ thickness ≤ 6 mm (DIN 2093, 1992)

Calculations

On this chapter are presented all the necessary equations to study the fatigue of disc springs. First of all, it is necessary to calculate all the four coefficients, as follows (*Disc springs - theory and practice*, n.d.):

$$K_1 = \frac{1}{\pi} \cdot \frac{\left(\frac{\delta - 1}{\delta}\right)^2}{\frac{\delta + 1}{\delta - 1} - \frac{2}{\ln \delta}} \quad \{2.51\}$$

$$K_2 = \frac{6}{\pi} \cdot \frac{\frac{\delta - 1}{\ln \delta} - 1}{\ln \delta} \quad \{2.52\}$$

$$K_3 = \frac{3}{\pi} \cdot \frac{\delta - 1}{\ln \delta} \quad \{2.53\}$$

In which δ represents the diameter's ratio and is a nondimensionalized variable.

The value of K_4 is not calculated directly because this value depends if there are contact surfaces between disc springs and other components. As the disc spring used on the DNR subsystem has no contact surfaces with other components, the value of *K4* can be considered as follows (*Disc springs - theory and practice*, n.d.):

$$K_4 = 1 \quad \{2.54\}$$

After that, stresses at different points may be calculated as follows (*Disc springs - theory and practice*, n.d.):

$$\sigma_{OM} = -\frac{4E}{1 - \nu^2} \cdot \frac{b^2}{K_1 \cdot OD^2} \cdot K_4 \cdot \frac{d}{b} \cdot \frac{3}{\pi} [Pa] \quad \{2.55\}$$

$$\sigma_I = -\frac{4E}{1-\nu^2}\cdot\frac{b^2}{K_1\cdot OD^2}\cdot K_4\cdot\frac{d}{b}\cdot\left[K_4\cdot K_2\left(\frac{h_0}{b}-\frac{d}{2b}\right)+K_3\right][Pa] \quad \{2.56\}$$

$$\sigma_{II} = -\frac{4E}{1-\nu^2}\cdot\frac{b^2}{K_1\cdot OD^2}\cdot K_4\cdot\frac{d}{b}\cdot\left[K_4\cdot K_2\left(\frac{h_0}{b}-\frac{d}{2b}\right)-K_3\right][Pa] \quad \{2.57\}$$

$$\sigma_{III} = -\frac{4E}{1-\nu^2}\cdot\frac{b^2}{K_1\cdot OD^2}\cdot K_4\cdot\frac{1}{\delta}\cdot\frac{d}{b}\left[K_4\left(K_2-2K_3\right)\left(\frac{h_0}{b}-\frac{d}{2b}\right)-K_3\right][Pa] \quad \{2.58\}$$

$$\sigma_{IV} = -\frac{4E}{1-\nu^2}\cdot\frac{b^2}{K_1\cdot OD^2}\cdot K_4\cdot\frac{1}{\delta}\cdot\frac{d}{b}\left[K_4\left(K_2-2K_3\right)\left(\frac{h_0}{b}-\frac{d}{2b}\right)+K_3\right][Pa] \quad \{2.59\}$$

Where K_1, K_2, K_3 and K_4 represent calculation coefficients and are nondimensionalized variables; h_0 corresponds to the initial cone height of disc springs without ground ends.

Positive stress values correspond to tensile stress and negative stress values correspond to compressive stresses.

Where the value of h_0 is given by (DIN 2093, 1992):

$$h_0 = FL - b[m] \quad \{2.60\}$$

2.2.2 Centrifugal force in rotating cylinder

Centrifugal force in rotating cylinder is the centrifugal force exerted by a fluid in a piston, if the cylinder rotates about its symmetry axis("Centrifugal force in rotating hydraulic cylinders - MATLAB," n.d.). This kind of cylinders are used in control mechanism, friction clutches, brakes, etc.

Some basic assumptions and limitations need to be taken in account:

- No inertial effects are considered in the model which means that the angular velocity of the cylinder is constant or changing at very low speed;
- Fluid inertia is neglected;
- Fluid compressibility is neglected.

Centrifugal force in a cylinder can be calculated as follows ("Centrifugal force in rotating hydraulic cylinders - MATLAB," n.d.):

$$F_c = \frac{\pi\rho\omega^2}{4}\left(OR^4 - IR^4 - 2r_p^2\left(OR^2 - IR^2\right)\right) \quad \{2.61\}$$

Where π represents the mathematical constant; ρ represents the density of the fluid and is expressed in kilogram per cubic meter [kg/m^3]; ω represents the rotating speed and is expressed in radians per second [rad/s]; *OR* represents the outer hydraulic radius and is expressed in meters [m]; *IR* represents the inner hydraulic radius and is expressed in meters [m]; r_p represents the fluid entry radius and is expressed in meters [m].

In terms of design, the following relation must be achieved ("Centrifugal force in rotating hydraulic cylinders - MATLAB," n.d.):

$$r_p < \sqrt{\left(OR^2 + IR^2\right)/2} \quad \{2.62\}$$

In Figure 38, it is illustrated the effect of a rotating cylinder in a fluid (White, 2010).

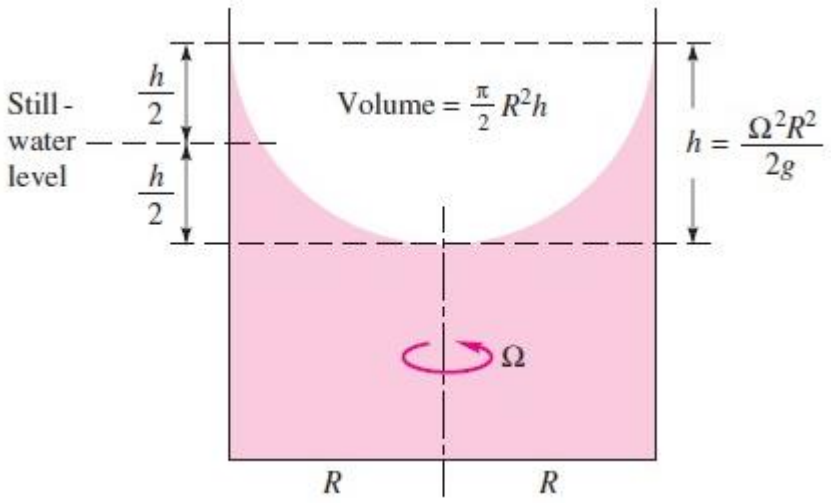

Figure 38 - Effect of centrifugal force on a fluid (White, 2010)

2.2.3 Transmissible torque

The transmissible torque of a wet clutch in multi-plate design can be obtained with the axial force, mean friction radius, friction coefficient and the number of friction surfaces, as follows (Naunheimer *et al*., 2010):

$$T_C = F_{ax} \cdot R_F \cdot \zeta \cdot N_S \left[N.m \right] \quad \{2.63\}$$

In which F_{ax} represents the axial force applied on the clutch plates and is expressed in Newtons [N]; R_F represents the mean friction radius and is expressed in meters [m]; ς represents the friction coefficient between clutch plates and is a nondimensionalized variable and N_S corresponds to the number of frictional surfaces and is a nondimensionalized variable. Where the mean friction radius can be obtained, as follows (Naunheimer *et al*., 2010):

$$R_F = \frac{2}{3} \cdot \frac{\left(OR_F^3 - IR_F^3 \right)}{\left(OR_F^2 - IR_F^2 \right)} \left[m \right] \quad \{2.64\}$$

Where OR_F and IR_F represent the outer and inner friction surface radius, respectively and are expressed in meters [m].

2.2.4 Drag torque of wet clutches

A lot of research has already been made in this field of study. Despite not being completely dominated the mathematical models are feasible and are getting closer to the real values. The actual models are enough accurate for an approximate prediction of the drag torque while for validation of the system is advisable to use real tests.

Reduction of drag torque of wet clutches is a significant factor to improve transmission efficiency. Reduction of drag torque in disengaged wet clutches is the focus of transmission research because it is one of the potentials to improve transmission efficiency (Shihua & Zengxiong, 2010).

There was already a model for drag losses before research in this topic has been made by (Shihua & Zengxiong, 2010). This model is called by “Traditional model”. Traditional model is not accurate to predict the decrease after oil film shrinking due to the difficulty

in modelling the flow pattern between two plates. In this model flow pattern was considered as laminar flow and full oil film in the gap between two plates.

In conclusion, traditional model is not accurate at high speed region (Shihua & Zengxiong, 2010). The equation of the tradition model can be seen below (Shihua & Zengxiong, 2010):

$$T_D = \frac{N_S \cdot \mu \cdot \pi \left(R_2^2 - R_1^2 \right) \cdot \omega \cdot r_m^2}{h_P} \left[N.m \right] \quad \{2.65\}$$

Where N_S represents the number of friction surfaces and is a nondimensionalized variable; μ represents the fluid's dynamic viscosity and is expressed in Pascal second [Pa.s]; π represents the mathematical constant; R_2 and R_1 represent the outer and inner radius of the friction plates, respectively and is expressed in meters [m]; ω represents the rotating speed and is expressed in radians per second [rad/s]; r_m represents the mean radius and is expressed in meters [m]; and h_p represents the clearance between consecutive clutch plates and is expressed in meters [m].

This equation can only represent the rising portion of a typical drag torque curve at the low speed region when the clearance between clutch plates is full of oil film (Shihua & Zengxiong, 2010). Due to poor accuracy of the traditional model it was necessary to reveal the flow pattern through the clearance between the rotating plate and the stationary one and build a precise mathematical model to predict the characteristics of the drag torque. A lot of research on this topic was done by (Shihua & Zengxiong, 2010). It was developed a mathematical model using experimental verification. A test rig was set up to test the drag torque of disengaged wet clutch consisting of single plate and separate plate. In order to study the flow pattern, it was installed a high-speed camera. By this way it was possible to study the characteristics of oil film shrinking.

Visual test reveal that the oil film begins to shrink from outer to inner radius at the stationary plate and only flows along the rotating plate after shrinking. Meanwhile, drag torque decreases sharply due to little contact area between stationary plate and oil. According to the model analysis, the acceleration of the flow in radial direction caused by centrifugal force is the main reason for the shrinking at the constant feeding flow rate. It is important to underline the fact that the results of the model agree well with test data for non-grooved wet clutch. The wet clutch plates in study are grooved (Shihua & Zengxiong, 2010).

In Figure 39 it is presented the behaviour of oil film at different rotating speeds between the rotating plate and the stationary plate.

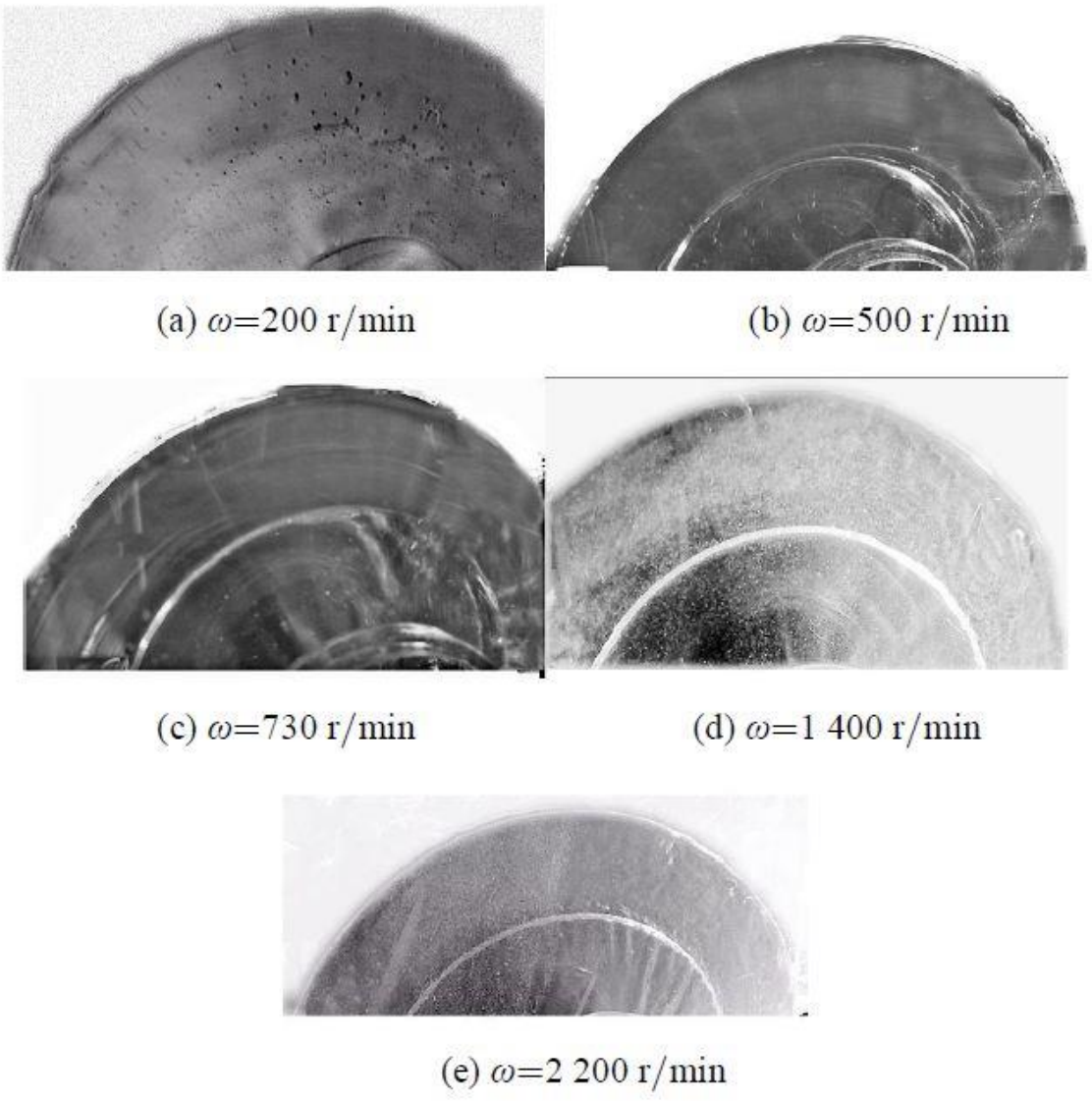

Figure 39 – Plate-view flow pattern in the gap at different rotating speed (Shihua & Zengxiong, 2010)

At low rotating speed, screwed flow in the clearance appears, especially in the inner radius region. It is also possible to state the clearance is full of oil. Increasing the speed Figure 39 (b) and (d), oil film in outer region starts to shrink and aeration emerges in the outer region due to centrifugal acceleration and continuity equation. In Figure 39 (d) it is possible to observe that screwed flow gradually disappears instead of radial flow. There is no oil attached to stationary plate and the oil flows radially only along rotating plate, whereas the fluid flowing near the rotating plate wall is more likely similar to the boundary layer flow over a single rotating plate. Cavity appears and flow pressure reduces caused by the radial acceleration of the fluid. In Figure 39(e), the fluid flows radially due to strong centrifugal force and becomes oil fog outside the clearance. From above visual observation, rotating speed is the most important factor on flow pattern.

On the other hand, flow pattern affects the drag torque through integral area calculation (Shihua & Zengxiong, 2010).

In Figure 40 is presented a scheme of what was explained above regarding to the flow pattern at different rotating speeds.

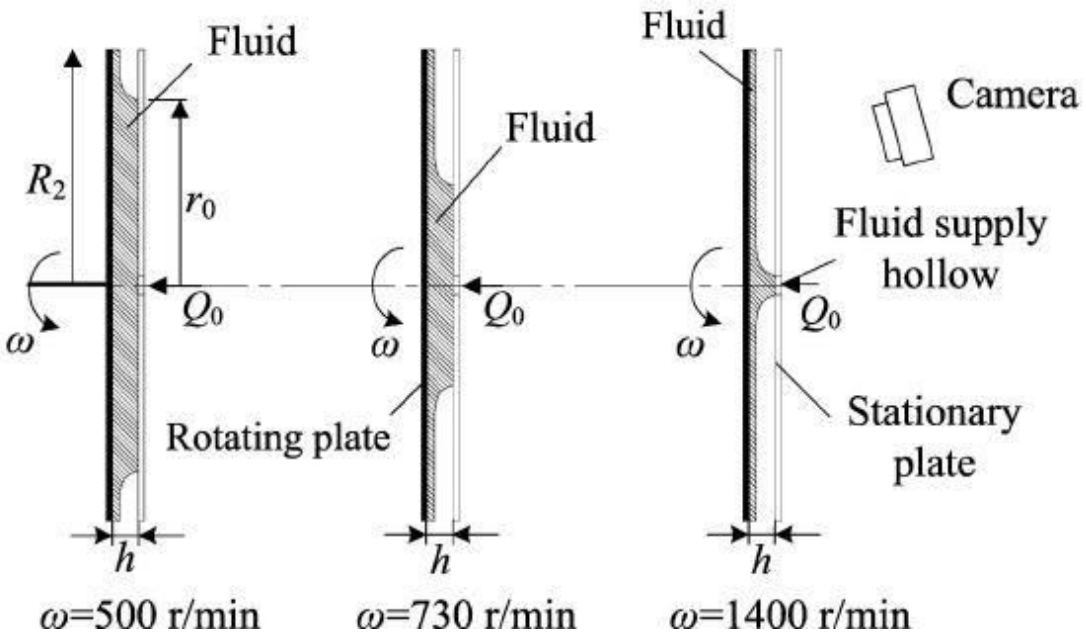

Figure 40 – Flow pattern in the clearance at different rotating speed (Shihua & Zengxiong, 2010)

Based on (Jibin & Zengxiong, 2009), drag torque increases linearly before oil film shrinking due to full oil film in the clearance.

In Figure 41 it is presented the comparison between the results of mathematical models and the experimental tests. It was applied and considered a constant feeding flow rate of 3L/min. It is conclusive that the traditional model is a straight line and is only similar to the other models until approximately 500 rpm. After that the values of drag torque are completely different. Analysing the experimental results, it is conclusive that from 1250 rpm drag torque is almost zero. This means that there is no shear stress on the plates. It is easy to conclude that no oil film leads to little shear stress (Shihua & Zengxiong, 2010). On the other hand, for circumferential degree mathematical model, the values are decreasing but do not reach zero. This means that this mathematical model is not accurate to predict the reduction of drag torque.

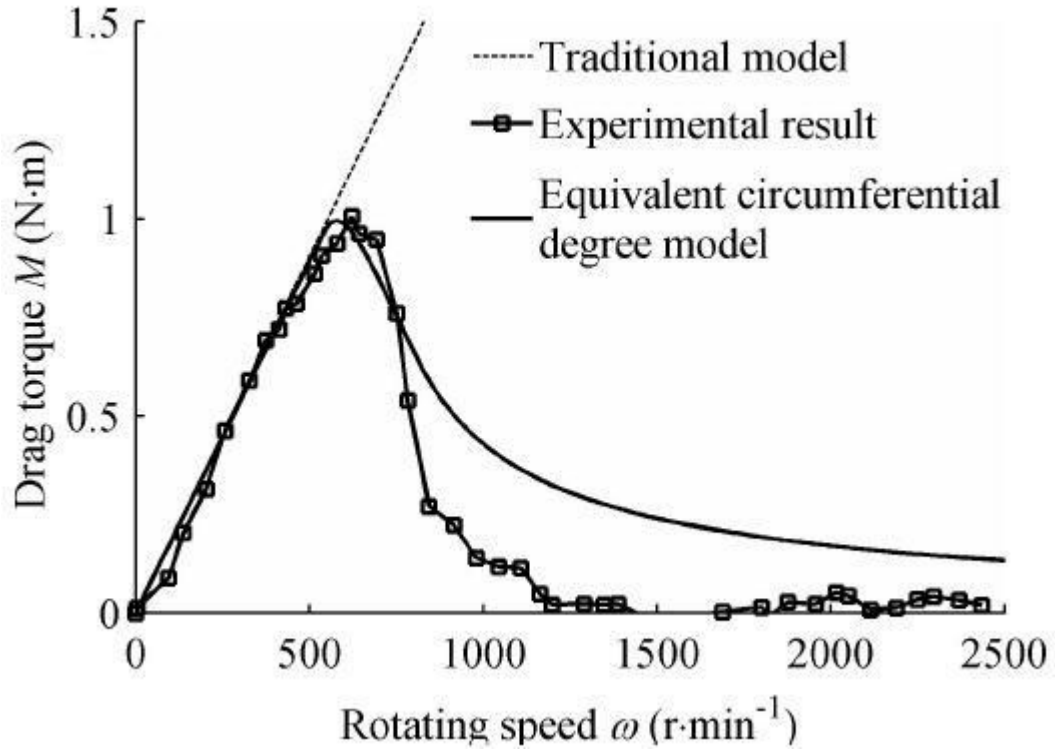

Figure 41 – Comparison between different mathematical models and experimental tests results (Shihua & Zengxiong, 2010)

Hereafter, it will be presented a mathematical model which is based on the following assumptions:

- Oil is incompressible and steady state;
- Flow in the wet clutch clearance is laminar and symmetrical;
- Gravity is neglected;
- Wet clutch plate in non-grooved;
- Friction plate and counter plate don't have any glide with its surface layer oil.

The oil motion in the radial direction between the plates is mainly driven by the centrifugal force, whereas the viscous tend to resist the motion. The relative rotating motion causes the drag torque due to oil viscosity (Heyan *et al*, 2013).

Based on the assumptions presented above and on Navier-Stokes equations, boundary conditions equations can be written as (Shihua & Zengxiong, 2010):

$$\begin{cases} v_r(r,0)=0, v_r(r,h_P)=0 \\ v_\theta(r,0)=0, v_\theta(r,h_P)=\omega R \\ p_2=p_0, p_1=0 \end{cases} \quad \{2.66\}$$

Where p_1 is the existing pressure at outer radius, p_2 is the flow pressure at inner radius, p_0 is the feeding pressure and h_P is the axial gap or clearance between consecutive plates.

In Figure 42, it can be found an auxiliary schematic of disengaged wet clutch with all the terminology that will be used on this mathematical model.

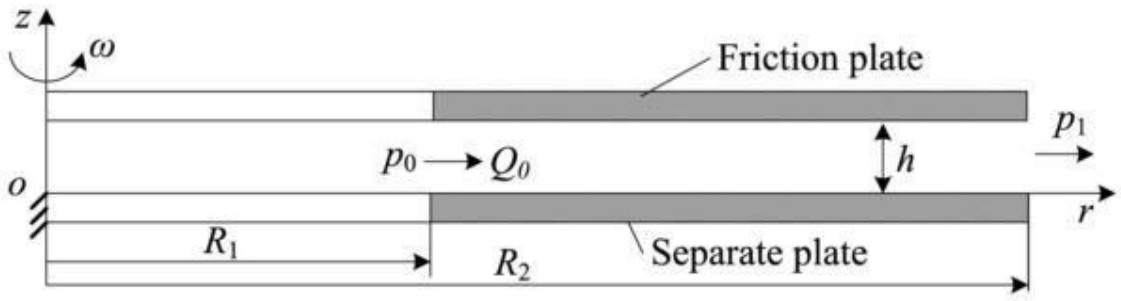

Figure 42 – Schematic of disengaged wet clutch (Yuan Shihua, Peng Zengxiong, 2010)

Radial speed distribution can be divided in three distinct stages. The first stage is caused by steady flow between two fixed plates. In this stage flow speed becomes lower when radius increases. The second stage is a consequence of centrifugal force. Its speed increases with the rise of rotating speed and radius. Finally, third stage is caused by flow inertia. It cannot be neglected when flow rate is very large. Therefore, centrifugal inertia and flow inertia accelerate the radial speed of oil in the clearance. As rotating speed increases, centrifugal speed distribution becomes dominant so that radial speed is strongly accelerated as it can be seen in Figure 39 (e) (Shihua & Zengxiong, 2010).

According to (Shihua & Zengxiong, 2010), radial oil pressure distribution along the radial direction can be calculated based on eq. {2.67}.

$$p(R)=\frac{6\mu Q}{\pi h_P^3}\ln\frac{R_1}{R}-\frac{3\rho\omega^2}{20}\left(R_1^2-R^2\right)-\frac{27\rho Q^2}{140\pi^2 h_P^2}\left(\frac{1}{R^2}-\frac{1}{R_1^2}\right)[Pa] \quad \{2.67\}$$

Where Q represents the needing feed flow rate and is expressed in cubic meters per second [m^3/s]; R corresponds to an arbitrary radius and is expressed meters [m].

According to eq. {2.67}, it is possible to conclude that the rotating speed and flow rate affect pressure distribution of the fluid, especially when Q and ω are very high. This

equation is a junction of four pressure distributions. The first is caused by feeding pressure, the second one is caused by the steady flow between two fixed plates, the third is caused by centrifugal inertia and the fourth is caused by fluid flow inertia. Feeding pressure can be rewritten as:

$$p_0 = \frac{6\mu Q}{\pi h_P^3}\ln\frac{R_1}{R_2} - \frac{3\rho\omega^2}{20}\left(R_1^2 - R_2^2\right) - \frac{27\rho Q^2}{140\pi^2 h_P^2}\left(\frac{1}{R_2^2} - \frac{1}{R_1^2}\right)\left[Pa\right] \quad \{2.68\}$$

There is a strong phenomenon of suction in the inner radius region as rotating speed is very high, which is running as a centrifugal pump (Shihua & Zengxiong, 2010).

In some papers, such as (Shihua & Zengxiong, 2010), import and export pressure of friction pair are considered the same. However, in the real clutch they are not the same. Pressure difference between import and export of friction pair can be considered as follows (Heyan *et al*., 2013):

$$p(R_1) - p(R_2) = \Delta p\left[MPa\right] \quad \{2.69\}$$

Where $p(R_1)$ and $p(R_2)$ represent the pressure on the outer and inner radius, respectively and are expressed in Pascal [Pa].

According to (Heyan *et al*., 2013), the following equation can be used to calculate the ideal flow rate for full oil film in the clearance. This equation was based on the Navier-Stokes equations considering the centrifugal effect.

$$Q = \frac{6\mu\cdot\ln\frac{R_1}{R_2}}{\frac{27\rho}{70\pi^2\cdot h_P^2}\left(R_2^{-2} - R_1^{-2}\right)} + \\ + \frac{\sqrt{\left(\frac{6\mu}{\pi\cdot h_P^3}\ln\frac{R_1}{R_2}\right)^2 - \frac{81\rho^2\omega^2\left(R_2^{-2} - R_1^{-2}\right)\left(R_1^2 - R_2^2\right) - 540\rho\left(R_2^{-2} - R_1^{-2}\right)\Delta p}{700\pi^2 h_P^2}}}{\frac{27\rho}{70\pi^2 h_P^2}\left(R_2^{-2} - R_1^{-2}\right)}$$

$$\left[m^3/s\right] \quad \{2.70\}$$

Where *Δp* represents the pressure difference between import and export friction pair and is expressed in Pascal [Pa].

Ideal flow rate for full oil film means the needing feed flow rate to maintain full oil film in the clearance between the plates. It is conclusive that there is a relation between the needing flow rate and rotating speed: the larger *ω* is, the larger *Q* is necessary to maintain single-phase flow in the clearance (Shihua & Zengxiong, 2010) and (Heyan *et al*., 2013). In order to visualize the relation between needing feed flow rate and rotating speed, a simulation was done. The goal of this simulation was to obtain a trend chart of needing feed flow rate. The trend chart can be found in Figure 43 and the simulation conditions can be found in Table 8.

Table 8 – Conditions of clutch simulation (Heyan *et al*., 2013)

R_1 [mm]	R_2[mm]	h_P [mm]	Q_i [L/min]	μ [Pa.s]	ρ [kg/m^3]
86	125	0.6	1/1.5	0.086	875

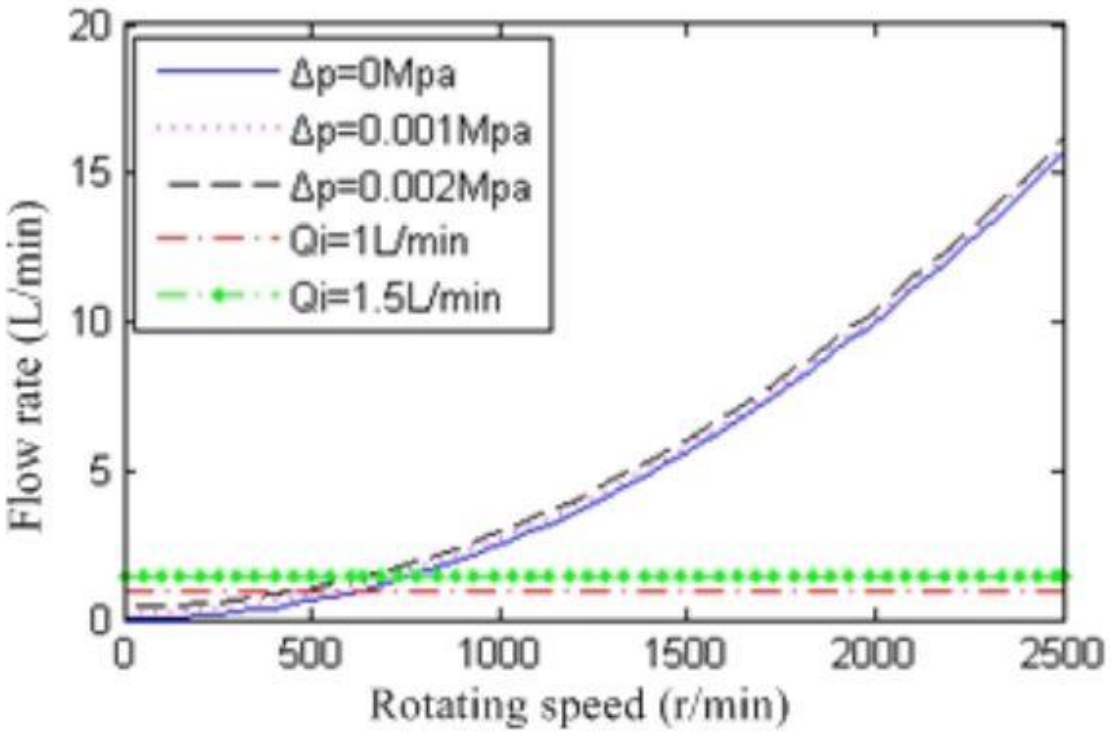

Figure 43 – Needing feed flow rate curve for full oil film (Heyan *et al*., 2013)

By observing the trend chart (Figure 43), the needing feed flow rate for full oil film increases with the rise of the rotating speed of the friction plate. But the actual feed

flow is constant regardless of the rising of rotating speed. This means that the oil film will shrink when the needing feed flow rate exceed the actual feed flow rate in high speed. This phenomenon can be seen in Figure 44 (Heyan *et al*., 2013).

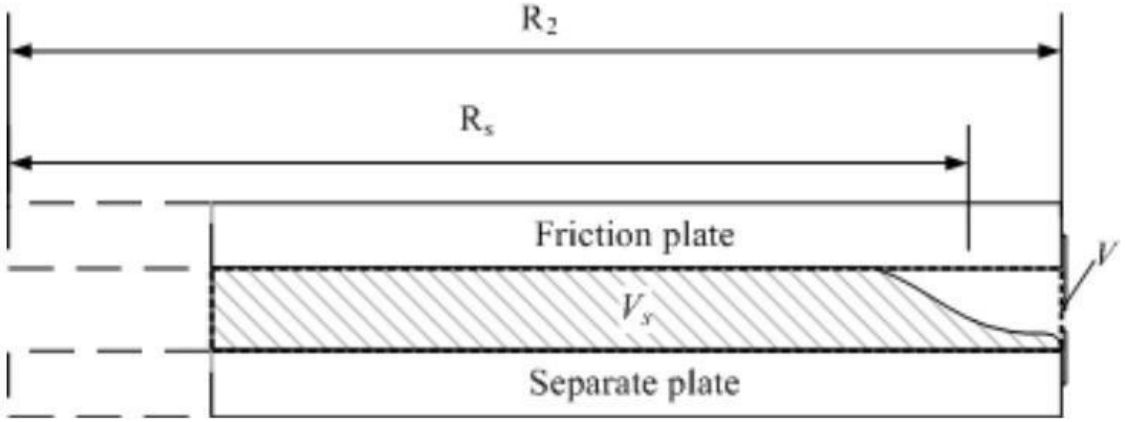

Figure 44 – Schematic diagram of partial oil filming in the clearance (Heyan *et al*., 2013)

The principle for oil film shrinking can be explained as that the clutch clearance cannot be full of oil when actual feed flow rate is lower than the needing feed flow rate (Heyan *et al*., 2013). When,

$$Q_i \geq Q, R_S = R_2 \quad \{2.71\}$$

When,

$$Q_i < Q \quad \{2.72\}$$

Where R_s represents the equivalent radius of oil film and is expressed in meters [m] and Q_i represents the input flow rate and is expressed in cubic meters per second [m^3/s].

Based on the relationship of oil flow rate and volume between import and export, equivalent radius of oil film can be defined as:

$$R_S = \sqrt{\frac{Q_i}{Q} R_2^2 + R_1^2 \left(1 - \frac{Q_i}{Q}\right)} [m] \quad \{2.73\}$$

A simulation was done by (Heyan *et al*., 2013) in order to find out what is the relation between equivalent radius and rotating speed for different Δp and Q_i. Simulation conditions are presented on Table 8. The resulting plot can is shown in Figure 45.

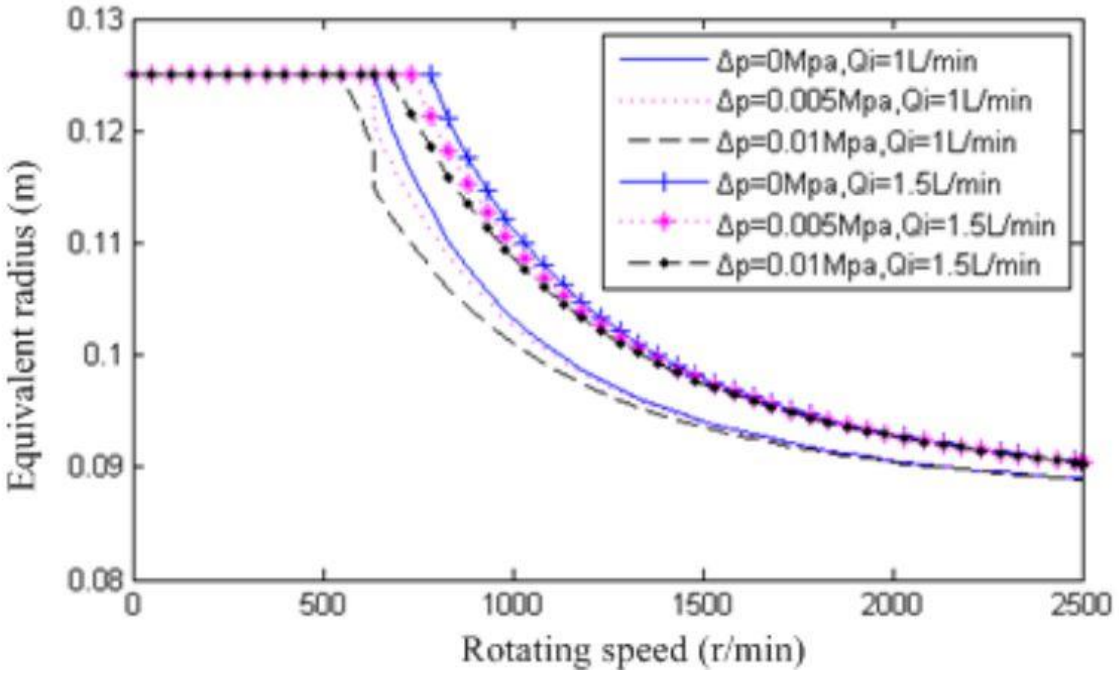

Figure 45 – Equivalent radius curve with rotating speed (Heyan *et al*., 2013)

By studying the graph above it is possible to conclude that at the beginning none of the factors (Δp and Q_i) have an effect on the value of R_s. There is an explanation for this. When the rotating speed is low, there is a full oil film and the equivalent radius equals the outer radius (eq. {2.71}). When rotating speed becomes higher, the equivalent radius starts to drop (Heyan *et al*., 2013).

According to Newton internal friction theorem, drag torque of each of the rotating plate can be expressed as:

$$T_{D_i} = \frac{\pi \mu \omega}{2h_P}\left(R_S^4 - R_1^4\right)\left[N.m\right] \qquad \{2.74\}$$

In Figure 46 a trend chart of drag torque is plotted based on the simulation conditions of Table 8.

It is expected that the resulting graphs of the actual clutch in study are similar to the shape of this: a linear rise of the drag torque with the rise of the rotating speed for low speed; when the speed increased to a certain point, the drag torque began to decrease. In high rotating speed, the drag torque decreased with the rise of the pressure difference and increased with the rise of oil flow rate.

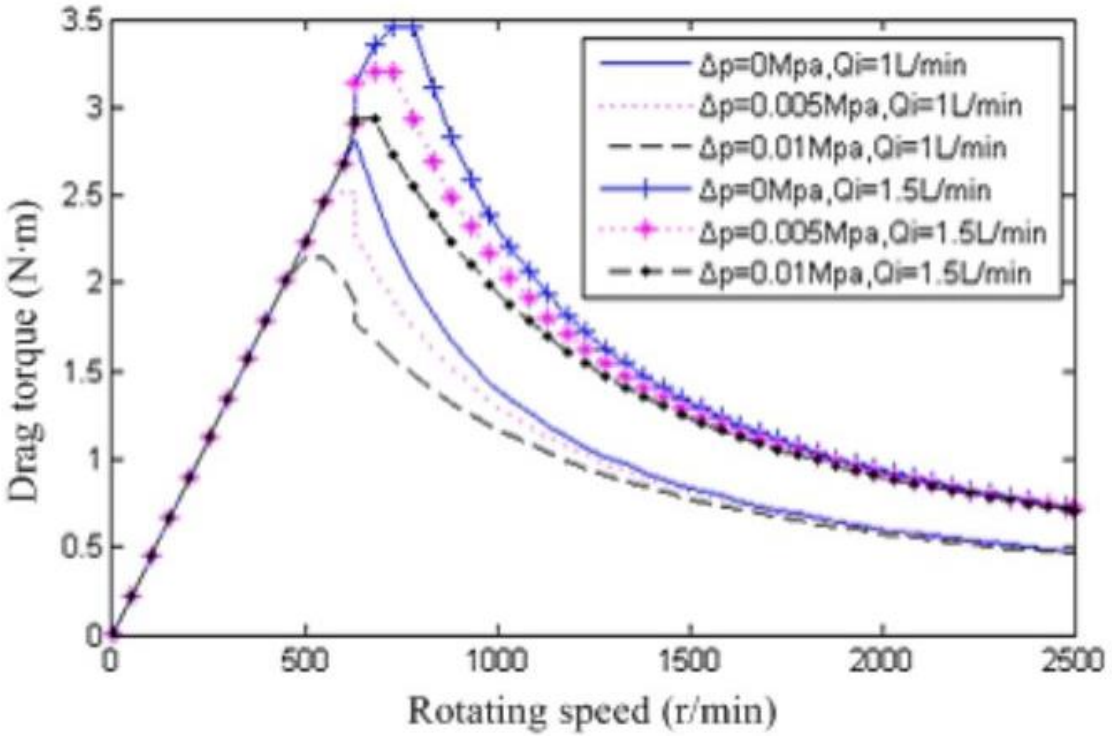

Figure 46 – Drag torque of single friction pair (Heyan *et al.*, 2013)

The resulting value of the drag torque for all the clutch plates can be obtained as follows,

$$T_D = \frac{N_S \pi \mu \omega}{2h_P}\left(R_S^4 - R_1^4\right)\left[N.m\right] \quad \{2.75\}$$

2.2.5 Planetary Gear Set ratio

PGS are complex mechanisms which great characteristics. Geared transmissions can be divided into:

- Gear sets with fixed axles;
- Epicyclic gears.

Gear sets with fixed axles refer to gearing where the positions of the axes of all the gear wheels are fixed relative to the gearbox housing. In the case of epicyclic gears or PGS, a revolving bar, which is known as the carrier or spider, carries the axes of the planetary gears. The differences between both types is explicit in Figure 47. Planetary transmissions have at least three planetary gears on a carrier or spider as shown in Figure 47. The purpose is to ensure a uniform and lower stress. The transmission ratio does not depend on the number of planetary gears or the number of teeth of each one.

Planetary gears main purpose is to reverse the direction of rotation (Naunheimer *et al.*, 2010).

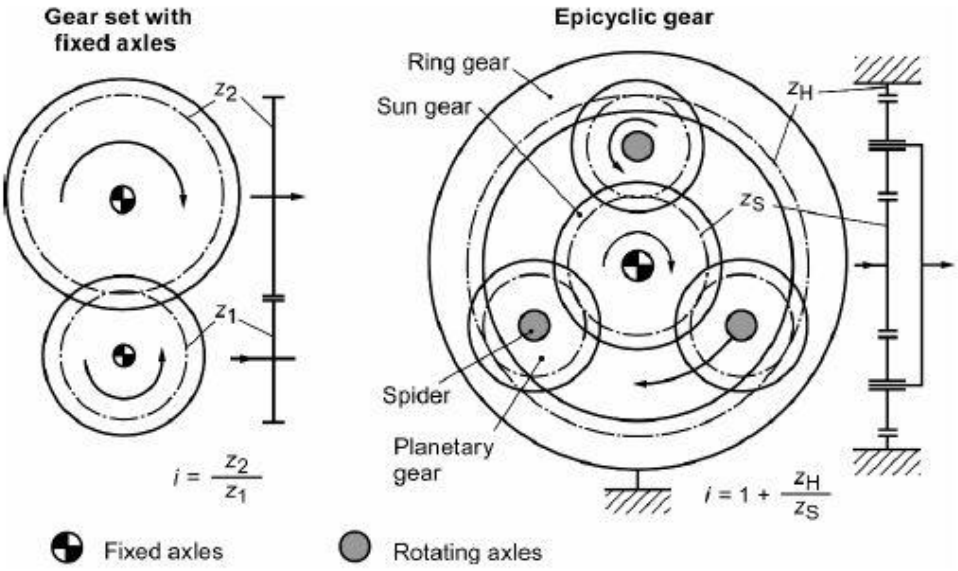

Figure 47 – Gear set with fixed axles and epicyclic gear (Naunheimer *et al.*, 2010)

When the carrier is fixed to the housing, the PGS becomes a gear set with fixed axles. With only one PGS it is possible to obtain nine different combinations. This can be achieved by fixing one by one the ring gear, sun gear and carrier acting as a frame. The remaining gear are the input and output (Naunheimer *et al.*, 2010).

The ratios of each combination or state of motion are defined by the number of teeth of the gears. The frame refers to the gear that is fixed to the housing. The different ratios can be calculated based on Table 9.

Table 9 – States of motion and ratios of a simple PGS (Naunheimer *et al.*, 2010)

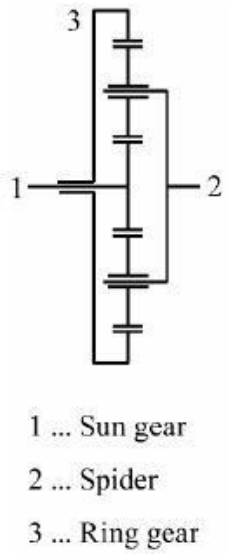

State of motion	Type of gearbox	Input	Output	Frame	Planetary step ratio
a)	Gear set with fixed axles	1	3	2	$i_P = \frac{n_1}{n_3} = i_S = -\frac{z_3}{z_1}$
b)		3	1		$i_P = \frac{n_3}{n_1} = \frac{1}{i_S} = -\frac{z_1}{z_3}$
c)	Planetary transmission single drive	1	2	3	$i_P = \frac{n_1}{n_3} = 1 - i_S = 1 + \frac{z_3}{z_1}$
d)		2	1		$i_P = \frac{n_2}{n_1} = \frac{1}{1 - i_S} = \frac{1}{1 + \frac{z_3}{z_1}}$
e)		2	3	1	$i_P = \frac{n_2}{n_3} = \frac{1}{1 - \frac{1}{i_S}} = \frac{1}{1 + \frac{z_1}{z_3}}$
f)		3	2		$i_P = \frac{n_3}{n_2} = 1 - \frac{1}{i_S} = 1 + \frac{z_1}{z_3}$

2.2.6 PGS Kinematics

PGS is a complex gearing system and to calculate the speeds (angular or linear) of each gear of this system requires to deeply understand the working principle of a PGS and particularly what happens to the PGS in the different modes of the DNR.

The generalized equation of Willis can be derived to the following equation (Müller, 1982):

$$\omega_b - i_{bc} n_c - (1 - i_{bc}) n_a = 0 \quad \{2.76\}$$

Where n_c and n_a represent the rotating speed of the gear *c* and *a*, respectively and are expressed in radians per second [rad/s]; i_{bc} represents the ratio between gear *b* and *c* and is a nondimensionalized variable. This generalized equation can be adapted as follows (Liu, 2017):

$$\omega_S + i \cdot \omega_R - (1 + i)\omega_C = 0 \quad \{2.77\}$$

In which ω_R and ω_S represent the rotating speed of the ring and sun gear, respectively and are expressed in rad/s. Where the value of *i* can be obtained by two different ways (Liu, 2017):

$$\begin{cases} i = \dfrac{Z_R}{Z_S} \\ i = \dfrac{r_R}{r_S} \end{cases} \quad \{2.78\}$$

Where Z_R and Z_S represent the number of teeth of the ring gear and sun gear, respectively; r_R and r_S represent the radius of the ring and sun gear, respectively and are expressed in meters [m].

2.2.7 Cams

A cam is one of the several types of clamping elements. Figure 48 shows a cam being actuated by a force *F*. The force is applied on a handle of length L measured from point

C (centre of the pivot). This force is exerting a clamping force *P* and a frictional force $\varsigma_1 P$ at the point of contact D (on the interface between the cam and the clamped component). These forces create a reaction force *R* with a frictional force $\varsigma_2 R$ on the pivot. The radius vector *r* and the position angle θ (measured from the low point A) define any point on the contour of the cam. The variable *e* is the initial eccentricity and together with the height *H* define the location of D relative to C. Height *H* depends on the cam geometry and θ (Henriksen, 1973).

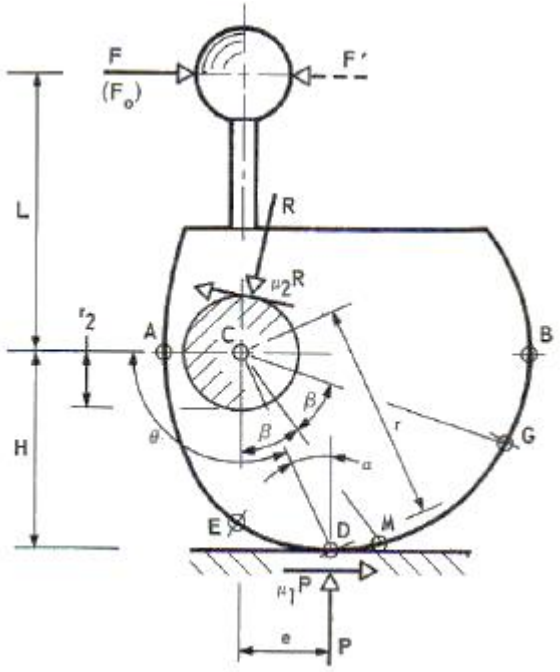

Figure 48 – The mechanics of a cam of arbitrary contour
(Henriksen, 1973)

Table 10 – Coefficients of friction μ for wedges, cams , pivots and bearings made of hardened steel (Henriksen, 1973)

Wedge or Cam Acting on	Coefficient of Friction μ_1	
	Clamping	Release
Hardened steel	0.19 to 0.20	0.19 to 0.20
Machine steel	0.17 to 0.19	0.20
Cast iron	0.15 to 0.17	0.17 to 0.19
Aluminum alloy	0.17 to 0.18	0.18 to 0.20
Laminated plastic	0.12 to 0.16	0.15 to 0.18
Pivots and bearings	Coefficient of Friction μ_2	
	Good Condition	Neglected
	0.03 to 0.06	0.10 to 0.15

The surface and lubrication conditions at point D and on the pivot, are different that is why it was used two different coefficients of friction. It was considered $\zeta_1 > \zeta_2$. The values of the coefficients of friction can be consulted on Table 10 as a reference (Henriksen, 1973). These values depend on the supplier and on other factors, so it is desirable to having in account the coefficient of frictions from the datasheets of the components.

Friction is always present on this kind of applications. In fact, the friction makes possible the self-locking of the system. The equilibrium equation for the clamping phase is (Henriksen, 1973):

$$P \cdot e + \zeta_1 \cdot P \cdot H + \zeta_2 \cdot R \cdot r_2 = F \cdot L \quad \{2.79\}$$

Where *P* represents the load at the cam and is expressed in Newton [N]; *e* represents the horizontal distance between point D and point C and is expressed in meters [m]; ζ_1 represents the friction coefficient at point D and is a nondimensionalized variable; *H* represents the vertical distance between point C and point D and is expressed in meters [m]; ζ_2 represents the frictional coefficient in the pivot and is a nondimensionalized variable; *R* represents the reaction force and is expressed in Newton [N]; r_2 represents the pivot's radius and is expressed in meters [m]; *F* corresponds to the load applied in the handle and is expressed in Newton [N]; and *L* represents the distance between point C and the handle and is expressed in meters [m].

Cams are designed in such a way to ensure that *P* is greater than *F* (10 to 20 times). As good approximation the value of *R* can be considered as follows (Henriksen, 1973):

$$R \cong 1,03P\left[N\right] \quad \{2.80\}$$

Then (Henriksen, 1973):

$$\begin{aligned} & P\left(e + \zeta_1 H + 1.03\zeta_2 r_2\right) = FL \Leftrightarrow \\ \Leftrightarrow & \frac{P}{F} = \frac{L}{e + \zeta_1 H + 1.03\zeta_2 r_2} \end{aligned} \quad \{2.81\}$$

Assuming that the cam at this point is clamped in a self-locking position with the force *P* it is necessary to find out what is the necessary force *F'* applied on the handle to release the cam. This values can be calculated based on the following equation (Henriksen, 1973):

$$Pe-\zeta_1 PH-\zeta_2 Rr_2=-F'L \Leftrightarrow$$
$$\Leftrightarrow \frac{F'}{P}=\frac{-e+\zeta_1 H+1.03\zeta_2 r_2}{L} \quad \{2.82\}$$

If the returned values of *F'* is positive, it means that the cam was self-locked. The theoretical limit for self-locking is when *F'* = 0 and consequently *R* = *P*. The theoretical condition for self-locking is given by (Henriksen, 1973):

$$-e+\zeta_1 H+\zeta_2 r_2=0 \Leftrightarrow$$
$$\Leftrightarrow \frac{\zeta_1 H+\zeta_2 r_2}{e}=1 \quad \{2.83\}$$

The safety factor is obtained as follows (Henriksen, 1973):

$$\frac{\zeta_1 H+\zeta_2 r_2}{e}=SF \quad \{2.84\}$$

The efficiency of the cam, which is dictated by the friction losses, is given by (Henriksen, 1973):

$$\frac{F_0}{F}=\frac{e}{e+\zeta_1 H+1.03\zeta_2 r_2} \quad \{2.85\}$$

2.2.7.1 *Spiral cam*

Cams used for fixture clamping can be of two types: Archimedes spirals or circular eccentrics. An example of an Archimedes spiral is illustrated in Figure 49. Figure 49 is an auxiliary to the following calculations relative to the Archimedes spiral cam.

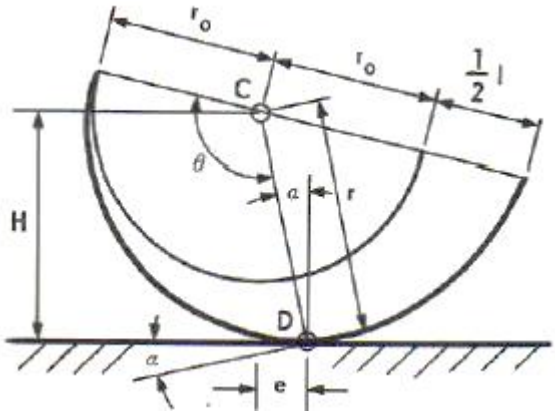

Figure 49 – The mechanics of an Archimedes spiral cam
(Henriksen, 1973)

The fundamental equation for an Archimedes spiral is given by (Henriksen, 1973):

$$r = \frac{l}{2\pi}\theta\left[m\right] \qquad \{2.86\}$$

In which θ represents an angle and is expressed in radians [rad]. Where the angle θ is in radians and *l* is the increase in radius vector *r* for one revolution.

The rise is the increase in *r* along a given length of contour. The rise over the entire operating range is called the "throw".

The slope of the tangent and the normal to the curve is determined by (Henriksen, 1973):

$$\tan\alpha = \frac{l}{2\pi r} \qquad \{2.87\}$$

Where *r* represents the radius of the exterior cam spline and is expressed in m. The angle *α* is equivalent to a wedge angle. While *l* is constant, *r* and *α* vary with θ; *α* increases with *l* and decreases with the increasing *r*. For fixture clamping cams the variation of the angle *α* over the useful length of the cam is small, usually around 1 degree.

At an arbitrary point D:

$$\begin{cases} e = r\sin\alpha\left[m\right] \\ H = r\cos\alpha\left[m\right] \end{cases} \qquad \{2.88\}$$

2.2.7.2 *Eccentric cam*

The circular eccentric cam (see Figure 50) is characterized by the eccentric radius R and the fixed eccentricity E.

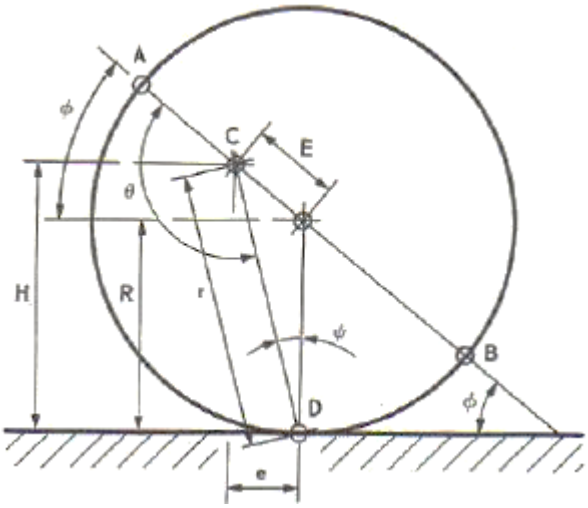

Figure 50 - The mechanics of the eccentric cam (Henriksen, 1973)

Contrarily to the spiral cams, this type of cam has low and high point, A and B, respectively. The point of contact D is defined by *r* and θ (as spiral cams). Height *H* and eccentricity *e* have the same meaning.

First of all, it is necessary to find the value of the angle ψ according to the following equation (Henriksen, 1973):

$$\frac{\sin\psi}{\sin(180-\theta)} = \frac{E}{R} \Leftrightarrow$$
$$\Leftrightarrow \sin\psi = \frac{E}{R}\sin\theta \qquad \{2.89\}$$

Where *E* represents the distance between point C and the centre of the circle and is expressed in meters [m]; *R* represents the radius of the external spline and is expressed in meters [m]; ψ and θ represent angles and are expressed in radians [rad].

It is necessary, temporarily, an auxiliary angle φ which can be calculated as follows:

$$\phi = \theta - \psi - 90\left[rad\right] \quad \{2.90\}$$

Then (Henriksen, 1973):

$$H = R - E\cos\left(\theta - \psi\right)\left[m\right] \quad \{2.91\}$$

$$e = E\cos\phi = E\sin\left(\theta - \psi\right)\left[m\right] \quad \{2.92\}$$

The variable *e* is independent of *R* and depends only on the fixed eccentricity *E* and the angle. $\Theta - \psi$ corresponds to the cam rotation angle (Henriksen, 1973). The maximum value of ψ is determined by (Henriksen, 1973):

$$\sin\psi = \frac{E}{R} \quad \{2.93\}$$

THESIS DEVELOPMENT

3 THESIS DEVELOPMENT

3.1 CVT transmission

This content cannot be presented due to confidentiality reasons.

3.2 External components

This content cannot be presented due to confidentiality reasons.

3.3 DNR working principle

3.3.1 DNR schematics

This content cannot be presented due to confidentiality reasons.

3.3.2 List of components

This content cannot be presented due to confidentiality reasons.

3.3.3 Rotational kinematics of components

This content cannot be presented due to confidentiality reasons.

3.3.4 Hydraulic circuit analysis

3.3.4.1 *Overview*

This content cannot be presented due to confidentiality reasons.

3.3.4.2 *Lubrication flow circuit*

This content cannot be presented due to confidentiality reasons.

3.3.4.3 *FWD clutch flow circuit*

This content cannot be presented due to confidentiality reasons.

3.3.4.4 *REV clutch flow circuit*

This content cannot be presented due to confidentiality reasons.

3.3.5 Kinematics of clutches

This content cannot be presented due to confidentiality reasons.

3.3.5.1 *FWD clutch*

This content cannot be presented due to confidentiality reasons.

3.3.5.2 *REV clutch*

This content cannot be presented due to confidentiality reasons.

3.3.6 Gears

This content cannot be presented due to confidentiality reasons.

3.3.6.1 *Drive gear*

This content cannot be presented due to confidentiality reasons.

3.3.6.2 *Neutral gear*

This content cannot be presented due to confidentiality reasons.

3.3.6.3 *REV gear*

This content cannot be presented due to confidentiality reasons.

3.3.7 Thrust bearings orientation

This content cannot be presented due to confidentiality reasons.

3.4 Calculations data

This content cannot be presented due to confidentiality reasons.

3.5 Analytical Calculations

3.5.1 Calculation scenarios

3.5.1.1 *FWD clutch set*

This content cannot be presented due to confidentiality reasons.

3.5.1.2 *REV clutch set*

This content cannot be presented due to confidentiality reasons.

3.5.2 Springs

3.5.2.1 *FWD spring pack*

This content cannot be presented due to confidentiality reasons.

3.5.2.1.1 General calculations

This content cannot be presented due to confidentiality reasons.

Scenarios

This content cannot be presented due to confidentiality reasons.

3.5.2.1.2 Suppliers verification

This content cannot be presented due to confidentiality reasons.

3.5.2.1.3 Pre-load conditions

This content cannot be presented due to confidentiality reasons.

Nominal scenario

This content cannot be presented due to confidentiality reasons.

Second scenario

This content cannot be presented due to confidentiality reasons.

Third scenario

This content cannot be presented due to confidentiality reasons.

Fourth scenario

This content cannot be presented due to confidentiality reasons.

3.5.2.1.4 Fatigue

This content cannot be presented due to confidentiality reasons.

3.5.2.2 *Wavy washer*

This content cannot be presented due to confidentiality reasons.

3.5.2.2.1 General calculations

This content cannot be presented due to confidentiality reasons.

3.5.2.2.2 Spring stiffness

Nominal scenario

This content cannot be presented due to confidentiality reasons.

Other Scenarios

This content cannot be presented due to confidentiality reasons.

3.5.2.2.3 Fatigue

This content cannot be presented due to confidentiality reasons.

3.5.2.3 *REV spring pack*

This content cannot be presented due to confidentiality reasons.

3.5.2.3.1 General calculations

This content cannot be presented due to confidentiality reasons.

3.5.2.3.2 Suppliers verification

This content cannot be presented due to confidentiality reasons.

3.5.2.3.3 Preload conditions

This content cannot be presented due to confidentiality reasons.

Nominal scenario

This content cannot be presented due to confidentiality reasons.

Second scenario

This content cannot be presented due to confidentiality reasons.

Third scenario

This content cannot be presented due to confidentiality reasons.

3.5.2.3.4 Fatigue

This content cannot be presented due to confidentiality reasons.

3.5.2.4 *Belleville washer*

This content cannot be presented due to confidentiality reasons.

3.5.2.4.1 General calculations

This content cannot be presented due to confidentiality reasons.

3.5.2.4.2 Fatigue

This content cannot be presented due to confidentiality reasons.

3.5.3 Transmission oil

This content cannot be presented due to confidentiality reasons.

3.5.4 Clutch slipping

This content cannot be presented due to confidentiality reasons.

3.5.5 FWD clutch set

This content cannot be presented due to confidentiality reasons.

3.5.5.1 *General calculations*

This content cannot be presented due to confidentiality reasons.

3.5.5.1.1 Nominal case

This content cannot be presented due to confidentiality reasons.

3.5.5.1.2 Second scenario

This content cannot be presented due to confidentiality reasons.

3.5.5.1.3 Third scenario

This content cannot be presented due to confidentiality reasons.

3.5.5.1.4 Fourth scenario

This content cannot be presented due to confidentiality reasons.

3.5.5.2 *Transmissible torque*

This content cannot be presented due to confidentiality reasons.

3.5.5.2.1 Nominal scenario

This content cannot be presented due to confidentiality reasons.

3.5.5.2.2 Second scenario

This content cannot be presented due to confidentiality reasons.

3.5.5.2.3 Third scenario

This content cannot be presented due to confidentiality reasons.

3.5.5.2.4 Fourth scenario

This content cannot be presented due to confidentiality reasons.

3.5.5.2.5 Scenarios' comparison

This content cannot be presented due to confidentiality reasons.

3.5.5.2.6 Creeping effect

This content cannot be presented due to confidentiality reasons.

3.5.5.2.7 Influent factors

This content cannot be presented due to confidentiality reasons.

Hydraulic force

This content cannot be presented due to confidentiality reasons.

Slipping speed

This content cannot be presented due to confidentiality reasons.

Hydraulic centrifugal force

This content cannot be presented due to confidentiality reasons.

Rotating speed

This content cannot be presented due to confidentiality reasons.

Fluid density

This content cannot be presented due to confidentiality reasons.

Fluid entry radius

This content cannot be presented due to confidentiality reasons.

3.5.5.3 *Biting-point conditions*

This content cannot be presented due to confidentiality reasons.

3.5.5.3.1 Nominal scenario

This content cannot be presented due to confidentiality reasons.

3.5.5.3.2 Second scenario

This content cannot be presented due to confidentiality reasons.

3.5.5.3.3 Third scenario

This content cannot be presented due to confidentiality reasons.

3.5.5.3.4 Fourth scenario

This content cannot be presented due to confidentiality reasons.

3.5.5.4 *Drag losses*

3.5.5.4.1 Model validation

This content cannot be presented due to confidentiality reasons.

3.5.5.4.2 Data analysis

This content cannot be presented due to confidentiality reasons.

3.5.5.4.3 Working parameters

Rotating speed

This content cannot be presented due to confidentiality reasons.

Input feed flow rate

This content cannot be presented due to confidentiality reasons.

Pressure variation

This content cannot be presented due to confidentiality reasons.

Oil temperature

This content cannot be presented due to confidentiality reasons.

3.5.6 Clutch plates

3.5.6.1 *FWD clutch*

This content cannot be presented due to confidentiality reasons.

3.5.6.2 *REV clutch*

This content cannot be presented due to confidentiality reasons.

3.5.7 REV clutch set

This content cannot be presented due to confidentiality reasons.

3.5.7.1 *General calculations*

This content cannot be presented due to confidentiality reasons.

3.5.7.1.1 Nominal case

This content cannot be presented due to confidentiality reasons.

3.5.7.1.2 Second scenario

This content cannot be presented due to confidentiality reasons.

3.5.7.1.3 Third scenario

This content cannot be presented due to confidentiality reasons.

3.5.7.2 *Transmissible torque*

This content cannot be presented due to confidentiality reasons.

3.5.7.2.1 Nominal scenario

This content cannot be presented due to confidentiality reasons.

3.5.7.2.2 Second scenario

This content cannot be presented due to confidentiality reasons.

3.5.7.2.3 Third scenario

This content cannot be presented due to confidentiality reasons.

3.5.7.2.4 Scenarios' comparison

This content cannot be presented due to confidentiality reasons.

3.5.7.3 *Biting point conditions*

This content cannot be presented due to confidentiality reasons.

3.5.7.3.1 Nominal scenario

This content cannot be presented due to confidentiality reasons.

3.5.7.3.2 Second scenario

This content cannot be presented due to confidentiality reasons.

3.5.7.3.3 Third scenario

This content cannot be presented due to confidentiality reasons.

3.5.7.4 *Drag losses*

This content cannot be presented due to confidentiality reasons.

3.5.7.4.1 Data analysis

This content cannot be presented due to confidentiality reasons.

3.5.7.4.2 Working parameters

Rotating speed

This content cannot be presented due to confidentiality reasons.

Input feed flow

This content cannot be presented due to confidentiality reasons.

Pressure variation

This content cannot be presented due to confidentiality reasons.

Oil temperature

This content cannot be presented due to confidentiality reasons.

3.5.8 Tolerance chain stack up analysis

This content cannot be presented due to confidentiality reasons.

3.5.8.1 *FWD clutch set*

This content cannot be presented due to confidentiality reasons.

3.5.8.2 *REV clutch set*

This content cannot be presented due to confidentiality reasons.

3.5.9 PGS

3.5.9.1 *Transmission ratio*

3.5.9.1.1 D gear

This content cannot be presented due to confidentiality reasons.

3.5.9.1.2 REV gear

This content cannot be presented due to confidentiality reasons.

3.5.9.2 *Kinematics analysis*

3.5.9.2.1 Drive gear

This content cannot be presented due to confidentiality reasons.

3.5.9.2.2 Neutral gear

This content cannot be presented due to confidentiality reasons.

3.5.9.2.3 REV gear

This content cannot be presented due to confidentiality reasons.

3.5.9.3 *Torque analysis*

This content cannot be presented due to confidentiality reasons.

3.5.9.3.1 Drive gear

This content cannot be presented due to confidentiality reasons.

3.5.9.3.2 Neutral gear

This content cannot be presented due to confidentiality reasons.

3.5.9.3.3 REV gear

This content cannot be presented due to confidentiality reasons.

3.5.9.4 *Loads*

This content cannot be presented due to confidentiality reasons.

3.5.10 Planetary pin

This content cannot be presented due to confidentiality reasons.

3.6 Results comparison between FWD and REV clutch

This content cannot be presented due to confidentiality reasons.

3.6.1 Transmissible torque

This content cannot be presented due to confidentiality reasons.

3.6.2 Drag losses

This content cannot be presented due to confidentiality reasons.

3.6.3 Clutches' pressure

This content cannot be presented due to confidentiality reasons.

3.7 Ramp-down test

3.7.1 Description

This content cannot be presented due to confidentiality reasons.

3.7.2 Procedure

This content cannot be presented due to confidentiality reasons.

3.7.3 Calculations

This content cannot be presented due to confidentiality reasons.

3.7.4 Results

This content cannot be presented due to confidentiality reasons.

3.7.4.1 *FWD clutch set installed*

This content cannot be presented due to confidentiality reasons.

3.7.4.2 *REV clutch set installed*

This content cannot be presented due to confidentiality reasons.

3.7.4.3 *Both clutch sets installed*

This content cannot be presented due to confidentiality reasons.

3.8 Comparison between tests and analytical calculations

This content cannot be presented due to confidentiality reasons.

3.8.1 FWD clutch set installed

This content cannot be presented due to confidentiality reasons.

3.8.2 REV clutch set installed

This content cannot be presented due to confidentiality reasons.

3.9 Requirements description

This content cannot be presented due to confidentiality reasons.

3.9.1 Resume

This content cannot be presented due to confidentiality reasons.

3.10 Design validation

3.10.1 Requirements verification

3.10.1.1 *Resume*

This content cannot be presented due to confidentiality reasons.

3.11 Development of the showcase model

3.11.1 Showcase function

The main function of the showcase is to help people to understand the working principle of a DNR subsystem of a CVT transmission. This requirement is fulfilled by allowing people to interact with the showcase. The user can simulate gear shifting by pushing or pulling the shifting lever which corresponds to the shifting lever of an automobile. There are three possible positions: Drive, Neutral and Reverse. The user can also interact with the showcase by rotating the handwheel which corresponds to the engine. So, by rotating the handwheel the user is simulating the rotational motion of the engine. With the showcase is also possible to look into the different components through some cross sections. These cross sections allow the user to better understand what changes and what is the motion chain when the different gears are selected.

3.11.2 Design

In this chapter, it will be presented all the analytical calculations and decisions which have been taken during the development process. During the design of the showcase and in order to take some decisions it was built some Excel® worksheets which makes easier the interpolation process. At the end, during the 3D design all the calculated values were adjusted and verified via Mechanism application of PTC Creo®.

One important detail is that when the shifting lever is moved from one position to another the clutch of the previous gear must be disengaged. In this aspect, the cams' system plays a vital role. The desired behaviour of the cams' system is presented on the graph of Figure 51 where the light blue line corresponds to the REV cam and the dark blue line corresponds to the FWD cam.

At the beginning of the graph, the cam is being actuated and is at its maximum travelling. On the other hand, the FWD cam is not being activated as can be seen for the line which is the zero travelling. This ensures that when the REV cam is being actuated the FWD cam not and the FWD clutch is disengaged. Between approximately 3 and 4 seconds both cams are at the zero position. During almost one second or 5 degrees both cams are at the zero position. There range corresponds to the Neutral gear position. At this position it is desirable that both clutches are disengaged and to guarantee that it is necessary that none of the cams is activated which means that they need to be at the zero position. From 4 seconds to the end, the FWD cam starts to be rotated. It is evident that at the end the desired travelling is achieved and that the REV cam is at the zero position.

It is important to underline the fact that it was not allowed the use of pneumatic of hydraulic actuation.

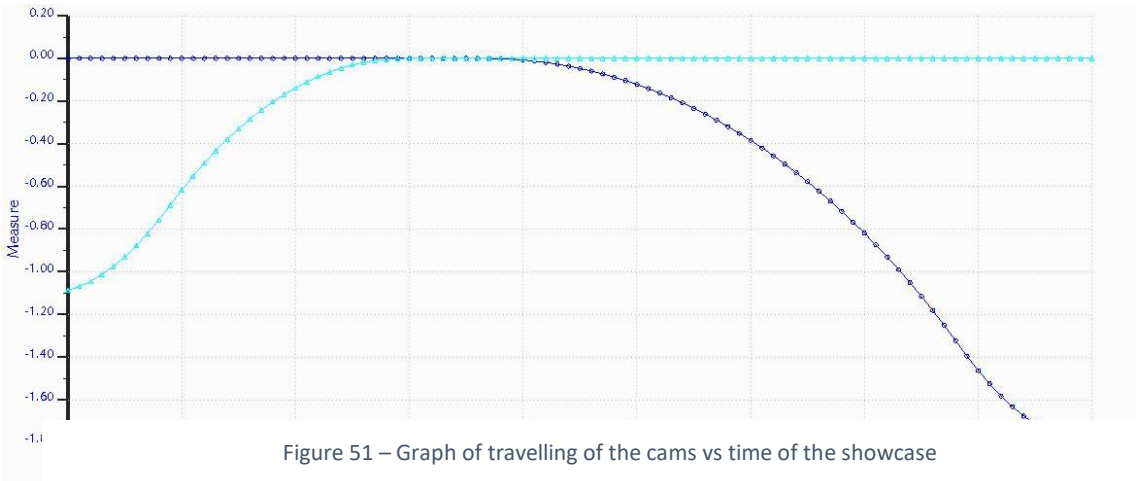

Figure 51 – Graph of travelling of the cams vs time of the showcase

3.11.2.1 *FWD*

This chapter is related to all the components which belong to the FWD clutch set.

3.11.2.1.1 Lever

During the design of the lever it was developed an Excel® worksheet with the following inputs:

- L_1;
- L_2;
- Δα.

In Figure 52, it is presented a schematic and the terminology used for the calculations of the lever.

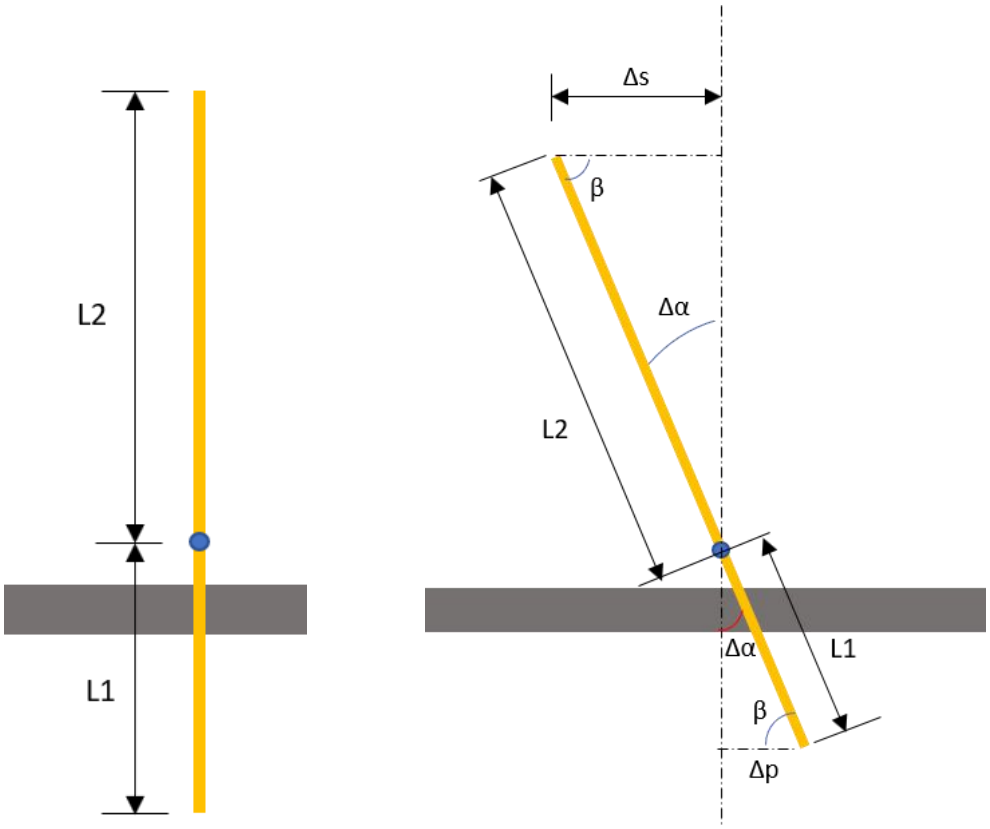

Figure 52 – Terminology for the calculations of FWD lever of the showcase

In Figure 52, the blue circle corresponds to the axis of rotation of the lever and the grey rectangle corresponds to the main plate of the showcase. On yellow, it is presented the

lever. Below, all the necessary equations for the calculations related to the lever are presented:

$$\sin \Delta\alpha = \frac{\Delta s}{L_2} \quad \{2.94\}$$

$$\begin{cases} \cos \beta = \dfrac{\Delta p}{L_1} \\ \cos \beta = \dfrac{\Delta s}{L_2} \end{cases} \quad \{2.95\}$$

$$\begin{aligned} & 180 = \beta + 90 + \Delta\alpha \Leftrightarrow \\ & \Leftrightarrow \beta = 180 - 90 - \Delta\alpha = 90 - \Delta\alpha \end{aligned} \quad \{2.96\}$$

$$\sin \Delta\alpha = \frac{\Delta p}{L_1} \Leftrightarrow \Delta\alpha = \arcsin\left(\frac{\Delta p}{L_1}\right) \quad \{2.97\}$$

The main purpose of the worksheet developed is to find out an optimum value. This value implies the minimum value of Δα, L_1 and L_2. However, it is evident that the lower the value of L_2, the higher the value of necessary force to activate FWD clutch is.

Auxiliary tables which were used for the design of FWD shifting lever are presented in chapter 6.28. The final dimensions of the lever are presented on the technical drawings.

3.11.2.1.2 Cam

Despite the final design of the cam not being exactly equal to a spiral or an eccentric cam, for the calculations during the design it was considered the calculations' method of an eccentric cam as this was the initial shape of the cam.

It is known the necessary travelling to make all the components of FWD clutch set touch each other and by this way starting to transmit torque. This amount of travelling will be guaranteed by the cam.

After defining the necessary step of the travelling it is necessary to understand how the motion will be transmitted from the lever to the cams. This system affects the amount of rotational motion that needs to be travelled by the cam in order to pull the pressing plate smoothly. The motion will be transmitted to the cam according to the schematic of Figure 53. The green circle corresponds to the centre of rotation of the cam; the blue circle corresponds to the cam; the yellow circle corresponds to the shoulder screw that transmits the motion of the red component to the cam. It is expected that the red component is connected to the shifting lever. As illustrated in the Figure 53, the red component moves to left and right, and the yellow point when the cam is rotating moves in the perpendicular direction. The white slot corresponds to the slot where the shoulder screw will slide.

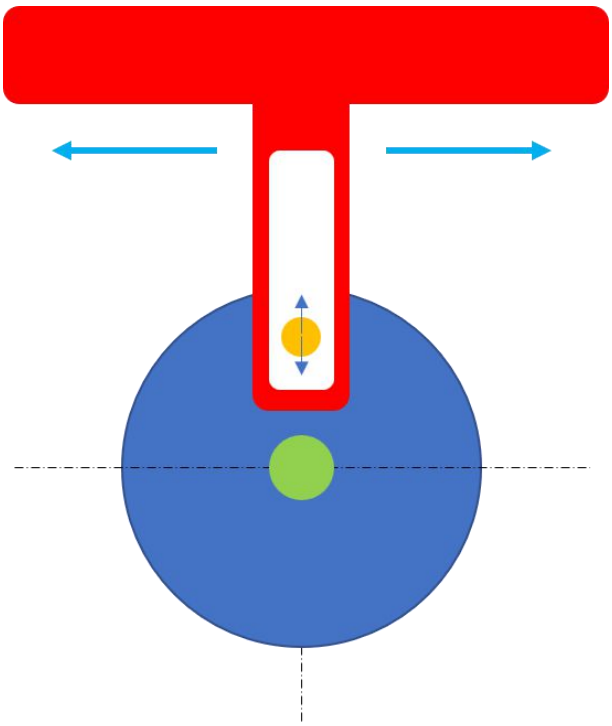

Figure 53 – Illustration of transmission of motion to the cam

In Figure 55, it is presented the FWD cam mechanism where the shoulder screw (grey circle), cam (purple) and transmitting component (blue) are presented. As can be seen, the cam does not touch directly on the pressing plate. It was screwed a stopper in the FWD and REV pressing plates in order to guarantee as less wear as possible. The cam, in fact, touches a stopper that is a standard hardened part. Both, stopper and the cam, are hardened and have the same hardiness. All the details about the stopper can be consulted on the technical datasheet. A perspective view of the stopper can be seen in Figure 54.

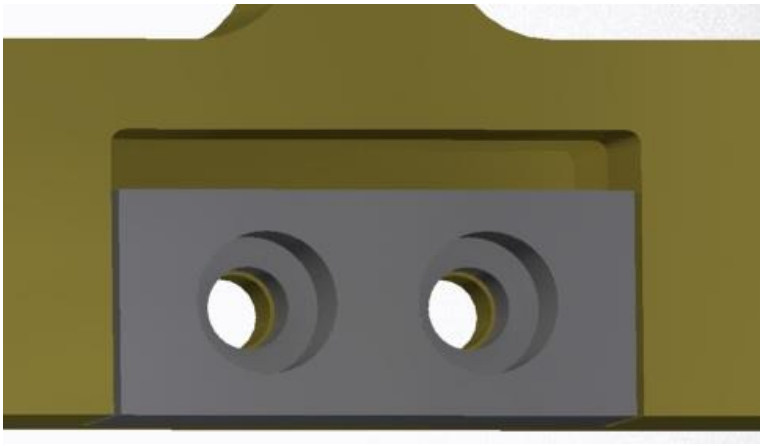

Figure 54 - Perspective view of FWD stopper

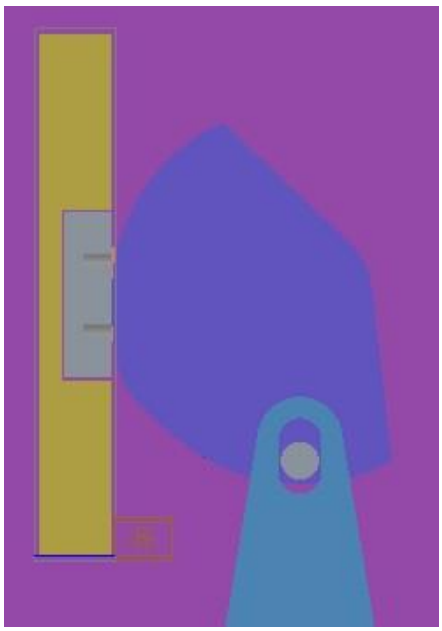

Figure 55 – FWD cam mechanism

3.11.2.1.3 FWD load

Regarding to the loads, it is known that the FWD SP was already calculated. However, it was calculated for all the springs. It was reduced the number of installed springs in order to decrease significantly the necessary force to compress the spring pack since it will be compressed by human force and not by hydraulic pressure.

The necessary travelling to make all components to touch each other was seen before.

Table 11 – FWD load input data of showcase

This content cannot be presented due to confidentiality reasons.

With the data of Table 11 the value of load was obtained for the FWD SP.

It was also considered a compression of the wavy washer in order to make sure that the torque is really transmitted. It was considered that the final SR of the wavy washer is approximately two thirds of the initial SR. With the added compression a parallel association of springs will be verified as seen before.

The final results are presented on Table 12.

Table 12 – Obtained results for FWD load of showcase

This content cannot be presented due to confidentiality reasons.

The final reaction load by the springs is calculated.

3.11.2.1.4 FWD guiding blocks

As the guiding blocks are standard components it is necessary to find a model or reference which fulfils the requirements in terms of loads. In order to calculate the loads applied on the guiding plates it was sketched the FBD of the FWD pressing plate system. All the loads, reactions forces and dimensions are expressed on Figure 56. The vertical yellow rectangle corresponds to the pressing plate while the horizontal purple rectangle corresponds to the guiding plate where the guiding blocks are screwed.

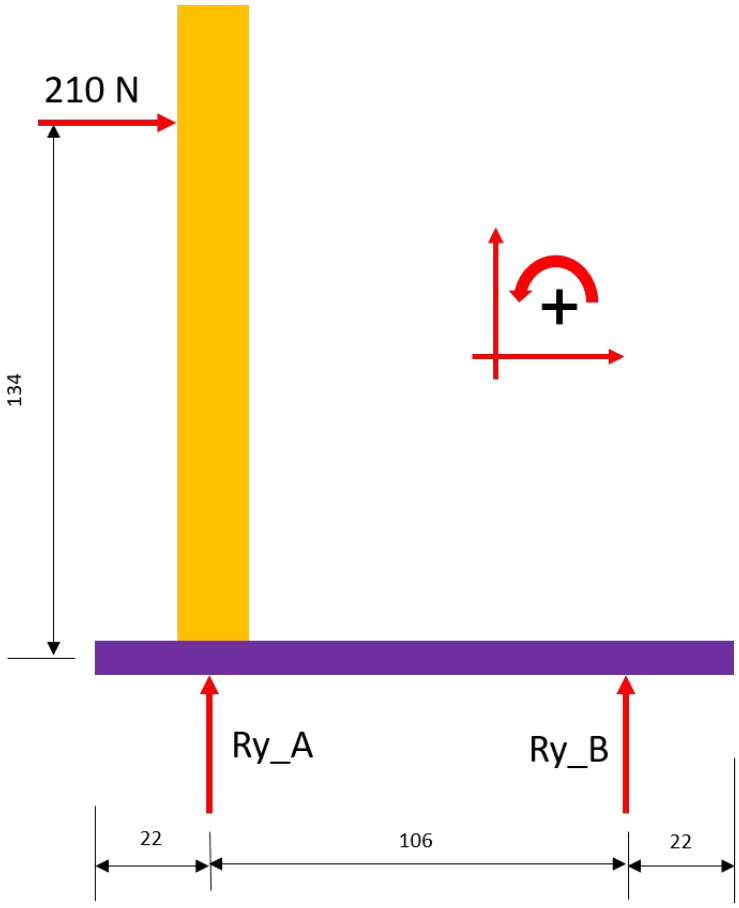

Figure 56 – FBD of FWD pressing plate system

The following conditions must be fulfilled to guarantee a static equilibrium.

$$\begin{cases} \sum M_A = 0 \\ \sum F_y = 0 \end{cases}$$

By substituting the values:

$$\begin{cases} -210 \times 134 + R_y^B \times 106 = 0 \\ R_y^A + R_y^B = 0 \end{cases} \Leftrightarrow \begin{cases} R_y^B = 265,472N \\ R_y^A = -265,472N \end{cases}$$

According to the technical datasheet of the guiding blocks, for a shaft of 16 mm of diameter, it is allowed a dynamic load of 775 N. By dynamic load it is intended to be a

load applied on the blocks during the travelling. Having this in account the SF is equal to 2.9 which is reasonable. Having in account the guiding blocks in use can be validated.

3.11.2.2 *REV*

3.11.2.2.1 Lever

For the calculations of the lever which are related to REV activation of the clutch it was used the same Excel® worksheet developed for FWD.

It was expected to obtain a negative value since that to activate the REV clutch it is necessary to pull the lever to the opposite direction.

3.11.2.2.2 Cam

Some content cannot be presented due to confidentiality reasons.

This amount of travelling will be guaranteed by the cam. The motion from the shifting lever will be transmitted to the REV cam by the same way of FWD system.

In Figure 57, it is presented the REV cam mechanism where the shoulder screw (grey circle), cam (green) and transmitting component (blue) are presented. As can be seen, the cam does not touch directly on the pressing plate (pink).

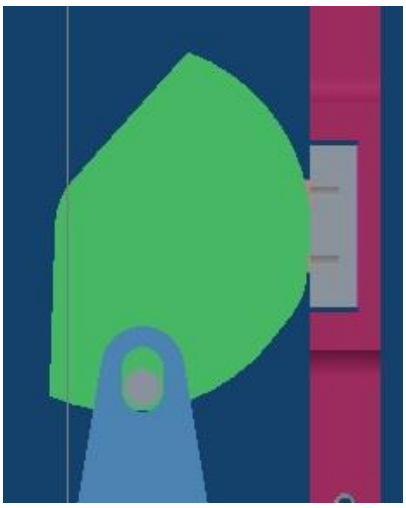

Figure 57 – REV cam mechanism

3.11.2.2.3 REV load

All the calculations regarding to the REV SP are spring disc were already presented. However, it was calculated for all the springs. It was reduced the number of installed springs in order to decrease significantly the necessary force to compress the spring pack since it will be compressed by human force and not by hydraulic pressure. The necessary travelling to make all components to touch each other was seen before.

Table 13 – REV load input data for showcase design

This content cannot be presented due to confidentiality reasons.

With the data of Table 13 the value of load obtained for the REV SP is calculated.

It was also considered a compression of the disc spring in order to make sure that the torque is really transmitted. As the spring disc will be cut out the SR will decrease significantly. With the added compression a parallel association of springs will be verified as seen before.

The final results are presented on Table 14.

Table 14 – Obtained results for FWD load of showcase

This content cannot be presented due to confidentiality reasons.

The final reaction load by the springs is calculated.

3.11.2.2.4 REV guiding blocks

In order to calculate the loads applied on the guiding plates it was sketched the FBD of the REV pressing plate system. All the loads, reactions forces and dimensions are expressed on Figure 58. The vertical purple rectangle corresponds to the pressing plate while the horizontal dark blue rectangle corresponds to the guiding plate where the guiding blocks are screwed.

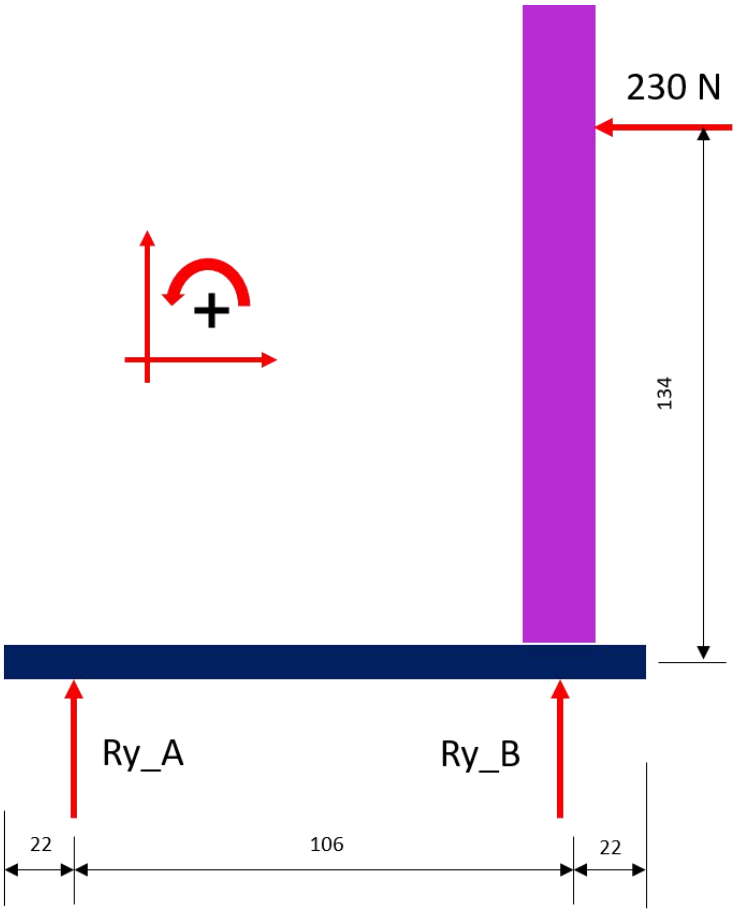

Figure 58 – FBD of REV pressing plate system

The following conditions must be fulfilled to guarantee a static equilibrium.

$$\begin{cases} \sum M_B = 0 \\ \sum F_y = 0 \end{cases}$$

By substituting the values:

$$\begin{cases} 230 \times 134 - R_y^A \times 106 = 0 \\ R_y^A + R_y^B = 0 \end{cases} \Leftrightarrow \begin{cases} R_y^A = 290,755N \\ R_y^B = -290,755N \end{cases}$$

Both guiding systems (FWD and REV) slide on the same shafts which means that the guiding blocks of both systems must be identical. This means that the maximum allowed dynamic load on the blocks is 775N that is quite higher than the applied load. Having this in account the SF is equal to 2.6 which is reasonable. Having in account the guiding blocks in use can be validated

The technical datasheet of the guiding blocks is presented in the Appendix chapter.

3.11.2.3 *Ball transfer units*

The number of ball transfer units assembled on the showcase is six. This means that the load applies in each of them is equal to 35 N. According to the datasheet of the ball transfer units the maximum allowed load supported by this component is equal to 150 N. There were other options with lower maximum allowed loads however it was decided to risk on a higher SF just in the case it was decided at the last minute to increase the number of springs on the FWD spring pack which would increase significantly the applied load on each ball transfer unit. Another solution would be to increase the amount of applied ball transfer units but there wasn't enough room for that. The final SF is 4.3.

3.11.2.4 *Cam*

In order to understand the amount of force necessary to actuate the cam for a load of 300 N, it was built a table where it is possible to see the relation between the different angles and the amount of necessary force. The table is illustrated on chapter 6.30. For the calculations it was considered an eccentric cam and all the equations are expressed on 2.2.7.

The input data for the calculations is expressed on Table 15.

Table 15 – Input data for the calculations of the forces on the cam

Variable	Unit	Value
L	mm	30
H	mm	50
r2	mm	20
e	mm	0
P	N	300
μ_1		0.18
μ_2		0.05

3.11.2.5 *Lever's load*

At the end it is necessary to know the amount of force that was necessary to apply on the shifting lever to actuate the cams. In order to find out that value it was built the table of chapter 6.31. In this table is expressed the value of the force related to the amount of degrees. In the same table it is expressed the values of reaction forces of the shoulder screws and the shifting lever. The maximum amount of force that needs to be applied on the shifting lever is amount 7 N. This seems to be an allowable value. After assembling the complete showcase, it was tested and in fact the amount of necessary force to actuate the cams was achievable by everyone. It is important to underline the fact that in these calculations it was not considered friction between metallic components. It was only considered the coefficient of friction between the cam and the stopper.

3.11.2.6 *Fittings*

In this chapter, it will be explained all the decisions regarding to fittings of the components. All the fittings were defined according to (Krulikowski, 2010).

3.11.2.6.1 Cam and bearing

The cam will be assembled in the bearing via a press fitting. It was chosen this type of fitting because it is easy to do, cheap and it guarantees that there is no motion between the cam and the inner ring of the bearing. This means that the inner ring of the bearing and the cam rotate solidary.

In Figure 59, it is presented the assembly of the cam and bearing.

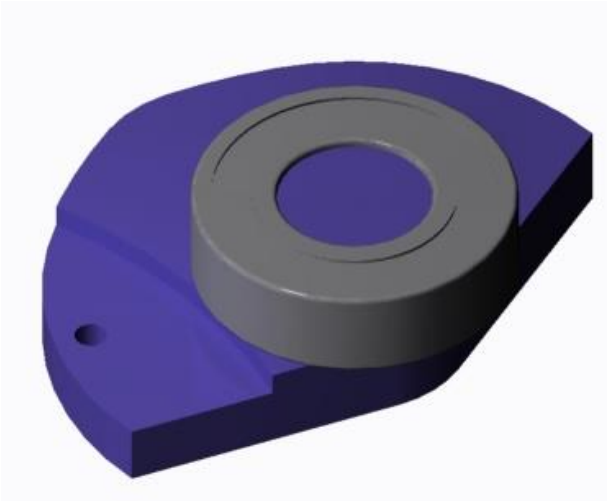

Figure 59 – Fitting between FWD cam and bearing

In Table 16, it is presented all the calculations regarding to the fitting. The hole corresponds to the bearing and the shaft corresponds to the cam. By cam it means the cylindrical surface designed on purpose to fit inside the inner ring of the bearing. The nominal diameter is 20 mm. The resulting fitting is H7/s6 (hole basis). Besides being a standard component, the tolerance of the inner ring can be selected from a range of options.

Table 16 – Fitting between cam and bearing

Hole (bearing)	Shaft (cam)	Fit
19.990	20.015	-0.038
20.000	20.028	-0.015

3.11.2.6.2 Bearing and plate

In Figure 60, it is illustrated the fitting between the bearing and the main plate. It was machined a hole for housing the bearing in the main plate. Both components will be glued. At a first sight, they could be pressed fit however, as previously explained, the cam was assembled in the bearing by press fit. This assembly process is done firstly and

then the assembly cam-bearing is assembled in the main plate. The only possible way to press the bearing into the main plate would be applying the press load on the cam. This would force the inner ring of the bearing and could damage the bearing. In order to avoid damaging the bearing it was decided to glue the assembly in the main plate. By this way it is not necessary to apply to much force on the bearing. In fact, it was previewed a certain amount of gap in order to be possible to apply the glue and not be necessary to apply to much force on the bearing.

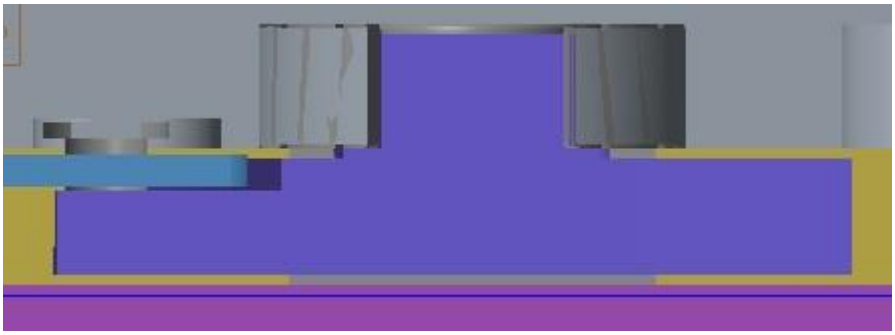

Figure 60 – Illustration of fitting between bearing and main plate

In Table 17, it is presented all the calculations regarding to the fitting. The hole corresponds to the main plate and the shaft corresponds to the bearing. The nominal diameter is 42 mm. The resulting tolerance for the main plate is H7. The tolerance of the bearing is presented on the datasheet since it is a standard component.

Table 17 – Fitting between bearing and main plate

Hole H9	Shaft	Fit
42.062	42.000	0.073
42.000	41.989	0.000

These calculations are important to understand if there is enough gap for the glue. According to the datasheets of the available glues (6.30 and 0) the minimum gap that ensures a correct bonding interface is 0.05 mm. Both glues are suitable for bonding of cylindrical fitting parts.

3.11.2.6.3 Handwheel and turbine shaft

The handwheel and the turbine shaft will be screwed to guarantee that there is no relative motion. However, it is necessary to guarantee that both components fit together. In Figure 61, it is illustrated the fitting between both components. The primary shaft needs to be machined so that both nominal dimensions of the diameter are the same. As it is necessary to assemble the handwheel in the turbine shaft smoothly and easily it was selected a free running fitting. In a hole basis, the fitting is H9/d9. The tolerance of the handwheel hole is based on the datasheet of the component. In this case the hole corresponds to the handwheel and the shaft to the turbine shaft.

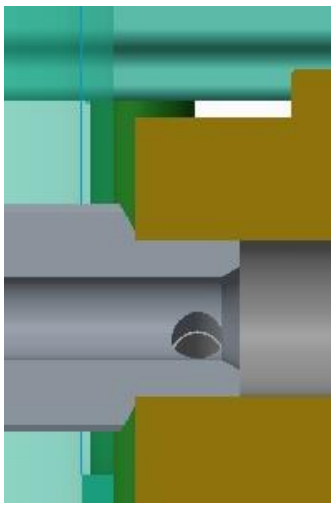

Figure 61 – Fitting between bushing support and handwheel

3.11.2.6.4 Ball transfer units' support and DNR FWD piston

Due to the complexity and lack of room, the only option which seem to be suitable is to glue the adapter to the piston. It will not be glued on the cylindrical surface but on the flat surface where the adapter faces the piston. The fitting in the cylindrical surface is quite important as it determines the correct position of the adapter. The perpendicular is defined by the flat surface. In order to guarantee a easy assembly it was selected a free running fit such as H9/d9 (hole basis). In this case the shaft corresponds to the adapter and the hole to the FWD piston.

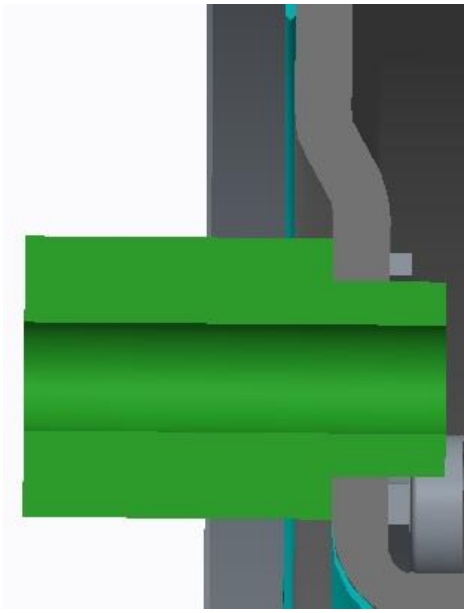

Figure 62 – Fitting between ball transfer unit's adapter and DNR FWD piston

3.11.2.6.5 Gear selector's joining and shoulder screw

The yellow part of Figure 63 corresponds to the joining and the horizontal screw is the shoulder screw.

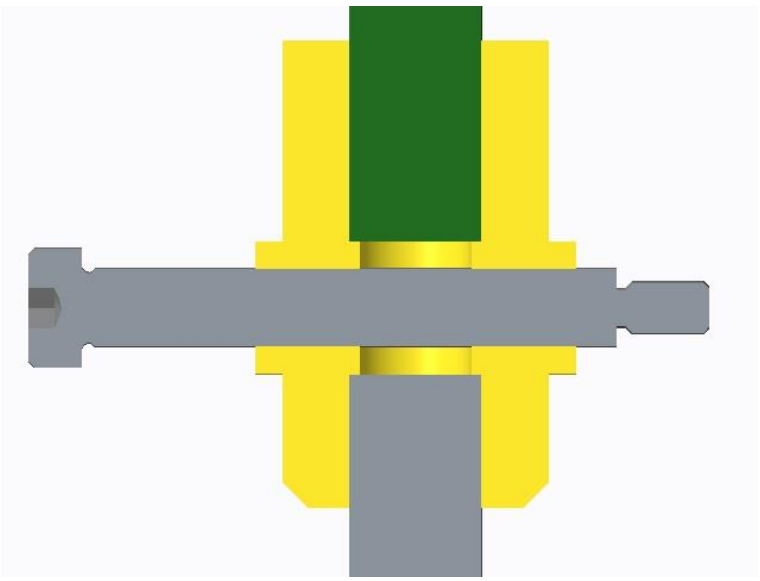

Figure 63 – Fitting between gear selector's joining and shoulder screw

When the shifting lever is pushed or pulled the joining will rotate around the shoulder screw. This means that the shoulder screw is the axis of rotation. It is desirable that the shoulder screw does not rotate. This means that it is necessary a gap between the joining and the shoulder screw so that the joining can rotate freely. In addition, the gap cannot not be exaggerated since the rotating motion needs to be accurate because the correct travelling must be guaranteed on the cams. Having this in account it was selected a clearance fit, H8/g6 (hole basis). In this case the hole corresponds to the joining and the shaft to the shoulder screw.

3.11.2.6.6 Gear selector's support and shoulder screw

As seen before, it is expected that the shoulder screw keeps steady. The thread of the shoulder screw that is placed in the gear selector's support guarantees this condition. However, a correct positioning of the shoulder screw is important since it defines the perpendicular of the joining (yellow). Having this account, it was selected a sliding fit, H7/g6 (hole basis). In this case the hole corresponds to the support and the shaft to the shoulder screw.

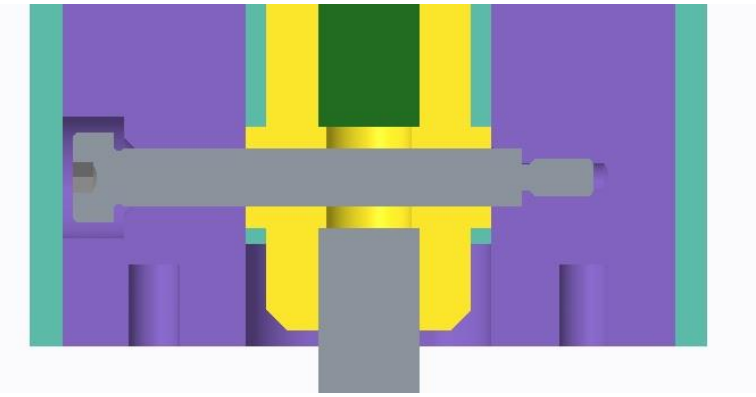

Figure 64 – Fitting between gear selector's support and shoulder screw

3.11.2.6.7 Ring and FWD pressing plate

The ring is where the ball transfer units touch when the cam is pulling the FWD pressing plate. This ring is hardened and made of steel as the ball transfer units are hardened too. As the pressing plate is made of aluminium alloy in order to save some weight it was necessary to insert a part made of steel to prevent wear. The ring is assembled in the FWD pressing plate with a medium drive fit. It is glued in the cylindrical surface and then pressed into the pressing plate in order to guarantee the correct position. The

tolerance is H7/s6 (hole basis). In this case the hole corresponds to the ring and the shaft to the FWD pressing plate.

Figure 65 - Fitting between ring and FWD pressing plate

3.11.2.6.8 Bushing support and bushing

The bushing support is a component that is used on the CVT transmission in study. As the goal of the showcase is to show people the working principle of the DNR subsystem it was decided to use as many as possible components from the CVT transmission. The bushing will be assembled inside the support and then assembled on the turbine shaft. Having this in account, it was decided to machine both components according to the tolerances h7/s6 (hole basis) providing a press fit. In this case the hole corresponds to the support and the shaft to the bushing.

Figure 66 – Fitting between bushing support and bushing

3.12 Preliminary assembly feasibility study

The detailed preliminary study of the feasibility of the assembly process is expressed on chapter 6.34.

3.13 Showcase FEA

For the FEA using Abaqus® it was used the same system of units that was used for the DNR analysis (Table 18).

3.13.1 Abaqus® system of units

Table 18 - Abaqus® system of units' convention

Dimension	Indicator (Abaqus)	Unit
Length	L	mm
Mass	M	kg
Time	T	s
Temperature	Θ	ºC
Force	F	N
E	Deformation	---
U	Displacement	mm
S	Stress	MPa

Table 19 – Abaqus® resulting units

Dimensions	Indicator (Abaqus)	Unit
Stress	σ	MPa (N/mm^2)
Density	ρ	kg/mm^3
Deformation	E	---
Displacement	U	mm
Mass moment of inertia	J	$kg \cdot mm^2$
Gravity acceleration	g	mm/s^2
Moment of inertia	I	mm^4

3.13.2 Pin (PNSA3401_2)

The pin is installed in the REV pressing plate (Figure 67). Its main purpose is to transmit the motion for the REV pressing plate to the REV piston. The pin is screwed in the pressing plate.

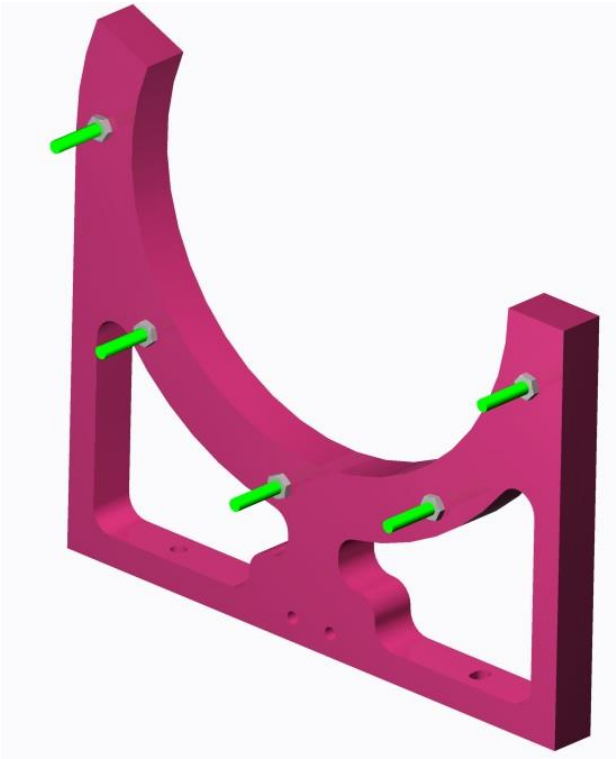

Figure 67 – REV pressing plate

Each pin presses the REV piston in a cavity purposely machined for this.

This content cannot be presented due to confidentiality reasons.

Figure 68 – Cavities of REV piston

When the REV pressing plate is being actuated by the cam, the spring pack compresses as so the disc spring as explained on the calculations. This means that this pin is subjected to the reaction of the springs to pull the pressing plate back.

In the software Abaqus®, it was simulated the working conditions of the pin. On the upper face it was applied a load of 210 N (pink arrows of Figure 69) which corresponds to the total reaction load of REV springs (REV spring pack + disc spring). The load is applied on this face because, as previously explained, this is the face which touches the cavities of the REV piston. In terms of boundary conditions, it was simulated the thread of the pin by preventing the displacement of the pin in three directions (x, y and z) as can be seen in Figure 69 (orange arrows). The input data is presented on Table 20.

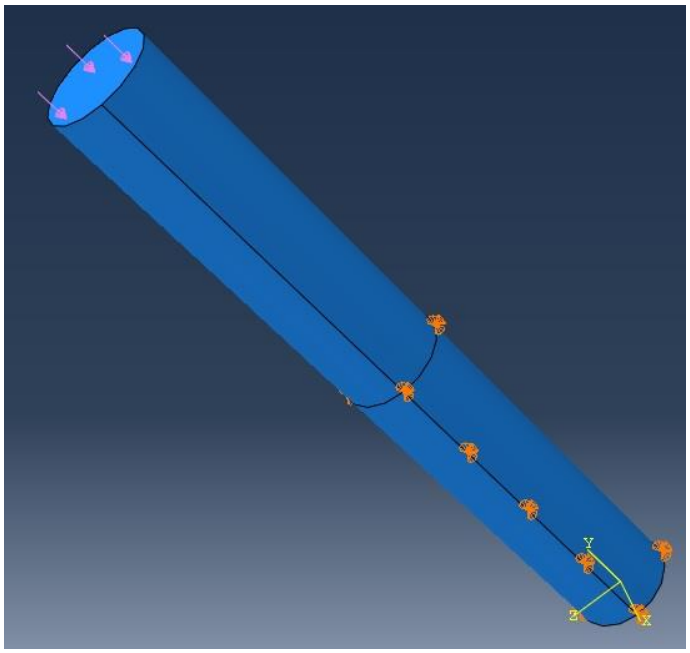

Figure 69 – Schematic of simulation conditions of the component PNSA3401_2

Table 20 – Input data of FEA of the component PNSA3401_2

Property	Value
Type of element	C3D8R (8-node linear brick, reduced integration, hourglass control)
Element size	0.4 mm
Nr. Of elements	9120
Load	230 N
Material's Young's Modulus	70 GPa
Poisson's ratio	0.33
Yield strength	240 MPa

C3D8R is a continuum element, solid element. It is Three-dimensional hexahedral element. Comparing to other tetrahedral elements, C3D8R usually provides a solution of equivalent accuracy at less cost (Simulia, 2010).

Figure 70 shows the region of the max. stress which corresponds to the red region. This region has a shape of a ring all around the pin. The value of the stress on this region is presented on

Table 21. This region corresponds to a region of stresses concentration.

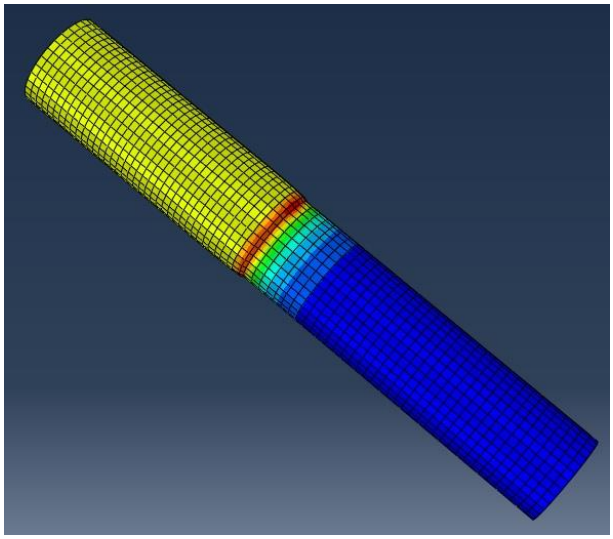

Figure 70 – Location of Von Mises max. stress area

Table 21 - Results of FEA of the component PNSA3401_2

Property	Value
S (Von Mises, Max. Principal)	25.2 MPa
U (Magnitude)	4.093×10^{-3} mm
E (Magnitude)	1.532×10^{-4}
U2	-4.078×10^{-3} mm
SF	9.54

Having in account the yield strength of the material (Table 20) and the generated Von Mises stress (

Table 21) it is conclusive that the value of the yield strength of the material was not exceeded. In fact, the SF is considerably high. In this particular application, max. stress was not the only important property. Displacement of the part along its axis is crucial. If this displacement is more than 0.1 mm, more than one shim needs to be installed.

Fortunately, the value of U2 is quite far from this limit. In conclusion, the pin can be validated.

3.13.3 Ball transfer units' adapter (PNSA1203_3)

As showed in Figure 71, this adapter transmits the load from the FWD piston the ball transfer units. In the FWD piston is applied the loads from the FWD spring pack and wavy washer. The ball transfer units will transmit the load to the ring of the FWD pressing plate. The ball transfer unit is screwed in the inner threaded hole of the adapter.

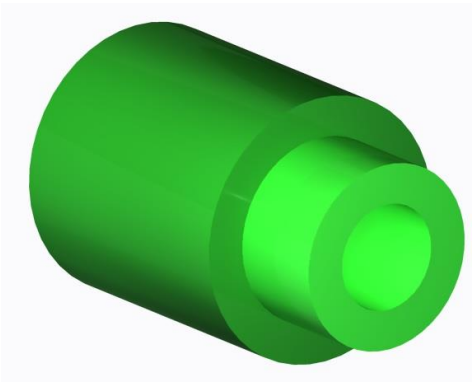

This content cannot be presented due to confidentiality reasons.

Figure 71 – Ball transfer units' adapter (left) and application (right)

There are six ball transfer units and consequently six adapters. This means that the load from the FWD springs is distributed equally for the adapters. The resulting load is presented on Table 22. Based on Figure 71, the piston presses the adapter on the contact surface. It is in this face that will be applied the load. In the left picture of Figure 72 it is illustrated the face where the load is applied (purple arrows distributed on the face). In the right picture it is illustrated the face where the boundary conditions are applied. This face corresponds to the threaded hole of the adapter.

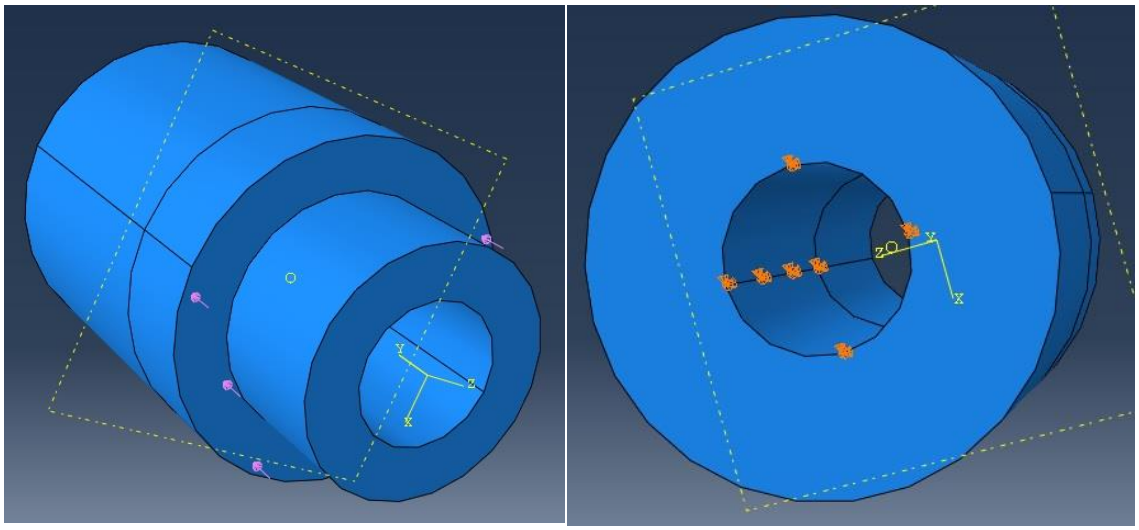

Figure 72 – Boundary conditions of component PNSA1203_3

Figure 73 shows the region of the Von Mises max. stress (left picture) which corresponds to the red region. This region has a shape of a ring all around the pin. The value of the stress on this region is presented on Table 23. This region corresponds to a region of stresses concentration on the interface between the threaded and non-threaded regions of the hole. On the right picture it is illustrated the deformed shape of the adapter.

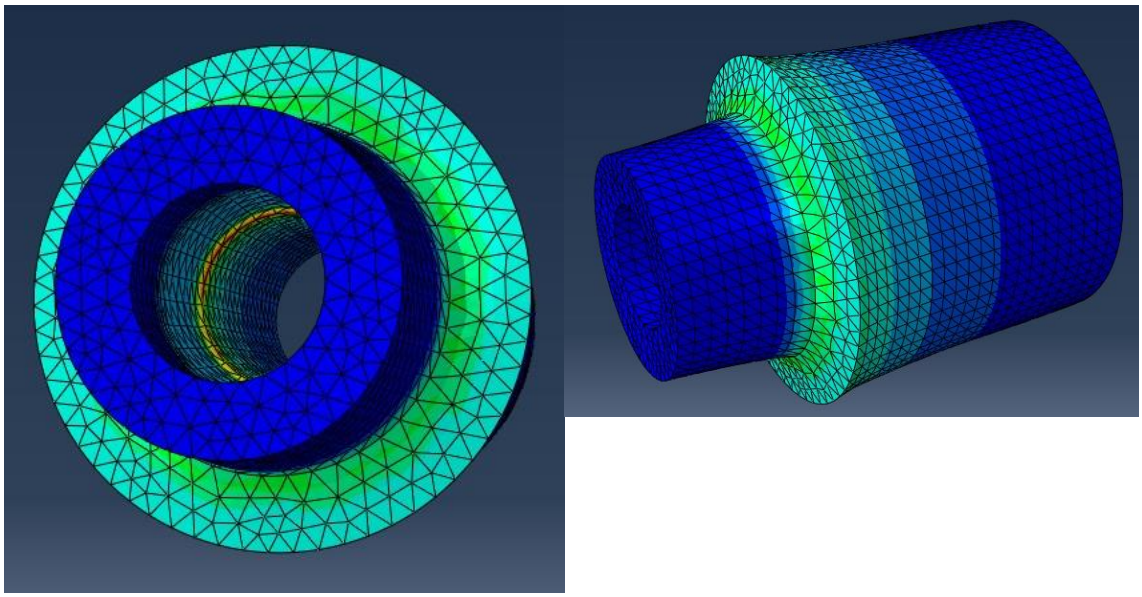

Figure 73 – Deformed shape of the adapter (scale: 2.3×10^4)

Table 22 - Input data of FEA of the component PNSA1203_3

Property	Value
Type of element	C3D10: A 10-node quadratic tetrahedron
Element size	0.5 mm
Nr. Of elements	45156
Load	35 N
Material's Young's Modulus	70 GPa
Poisson's ratio	0.33
Yield strength	240 MPa

C3D10M is a continuum element, solid element. It is a modified tetrahedral element. Comparing to the other elements of the same type, C3D10M mesh is slightly stiffer (Simulia, 2010).

Table 23 – Results of FEA of the component PNSA1203_3

Property	Value
S (Von Mises, Max. Principal)	2.675 MPa
U (Magnitude)	6.678×10^{-5} mm
E (Magnitude)	2.760×10^{-5}
U2	6.349×10^{-5} mm
SF	89.7

Having in account the yield strength of the material (Table 22) and the generated Von Mises stress (Table 23) it is conclusive that the value of the yield strength of the material was not exceeded. In fact, the SF is considerably high. In this particular application, max. stress was not the only important property. Displacement of the part along its axis is crucial. If this displacement is more than 0.1 mm, more than one shim needs to be installed. Fortunately, the value of U2 is quite far from this limit. In conclusion, the adapter can be validated.

3.13.4 FWD pressing plate (PNSA3302_5)

According to Figure 74, on the left side is located the stopper where the cam applies its load. On the upper right side is located the ring which is the interface between the ball transfer units and the FWD pressing plate. In the lower and horizontal face of the FWD pressing plate it is located four holes: two of them are for the screws that fix the pressing plate do the guiding plate.

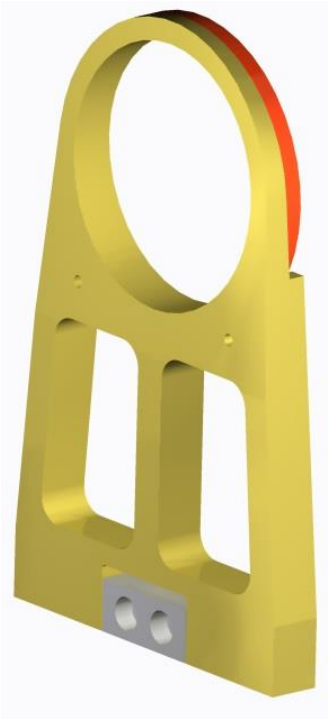

Figure 74 – FWD pressing plate assy

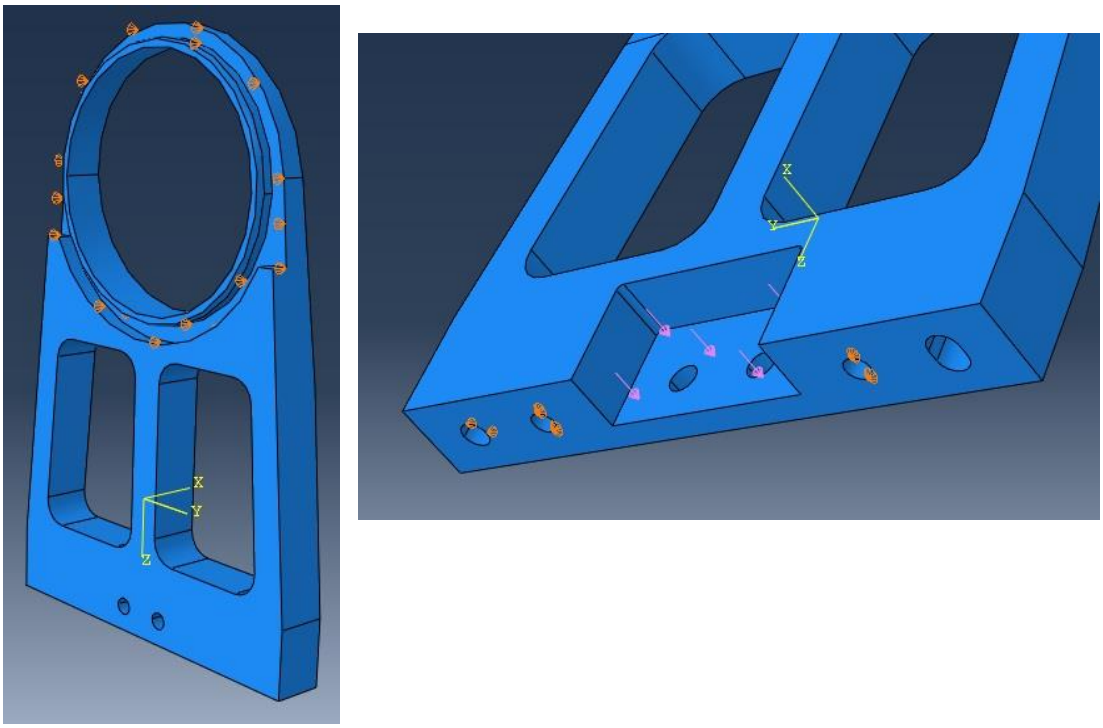

Figure 75 – Boundary conditions of component PNSA3302_5

In this case it was considered the scenario where the ring is already touching the ball transfer units and that these do not allow any kind of displacement, but the cam is still pressing the pressing plate. This means that on the interface with the ring will be not allowed any kind of displacement along the x axis. On the holes for fixation, will not be allowed any displacement along the z and y axis. The load will be applied on the interface with the stopper or the shims. All these boundary conditions are illustrated in Figure 75.

As expected and confirmed on Figure 76, the region of stress concentration is located on the holes for fixing the pressing plate to the guiding plate. On the left picture of Figure 76 it is visible that most of the component is blue and the holes are coloured of green. On a deeper look at inside the holes (left picture of Figure 76) it is evident that the concentration of stress is in the edge of the hole. The value of the maximum stress is presented on

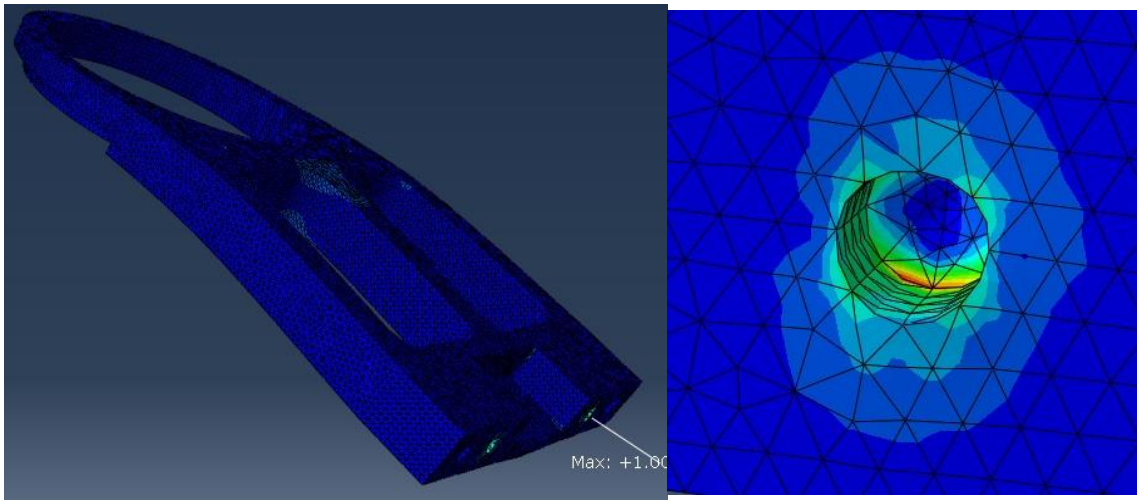

Figure 76 – Max. stress regions of FEA of component PNSA3302_5 (scale: $2.2x10^2$)

Table 24 - Input data of FEA of the component PNSA3302_5

Property	Value
Type of element	C3D10: A 10-node quadratic tetrahedron
Element size	1.5
Nr. Of elements	198135
Load	210 N
Material's Young's Modulus	70 GPa
Poisson's ratio	0.33
Yield strength	240 MPa

C3D10 is solid, quadratic tetrahedral element. It is a general purpose tetrahedral element.

Table 25 - Input data of FEA of the component PNSA3302_5

Property	Value
S (Von Mises, Max. Principal)	101 MPa
U (Magnitude)	8.310E-02 mm
E (Magnitude)	2.199E-03
SF	2.3

Having in account the yield strength of the material (Table 24) and the generated Von Mises stress (C3D10 is solid, quadratic tetrahedral element. It is a general purpose tetrahedral element.

Table 25) it is conclusive that the value of the yield strength of the material was not exceeded. In fact, the SF is higher than 1.5 that was the requirement. In conclusion, the FWD pressing plate can be validated.

3.13.5 REV pressing plate (PNSA3401_1)

As illustrated in Figure 77, on one side it is placed the stopper where the load of the cam is applied.

Figure 77 - REV pressing plate assy

On the other side pins are screwed to the plate. These pins are the interface between the pressing plate and the REV piston. This means that the load of the REV spring is applied on the pins.

In order to simulate the behaviour of the REV pressing plate in the working conditions it was applied a load on the face where the stopper is screwed (pink arrows). In terms of boundary conditions, it was defined that the threaded holes on the bottom of the pressing plate (which will be used to screw the pressing plate to the guiding plate) do not allow any motion along the x and z axis while in the threaded holes of the pins the displacement along the y axis is constraint.

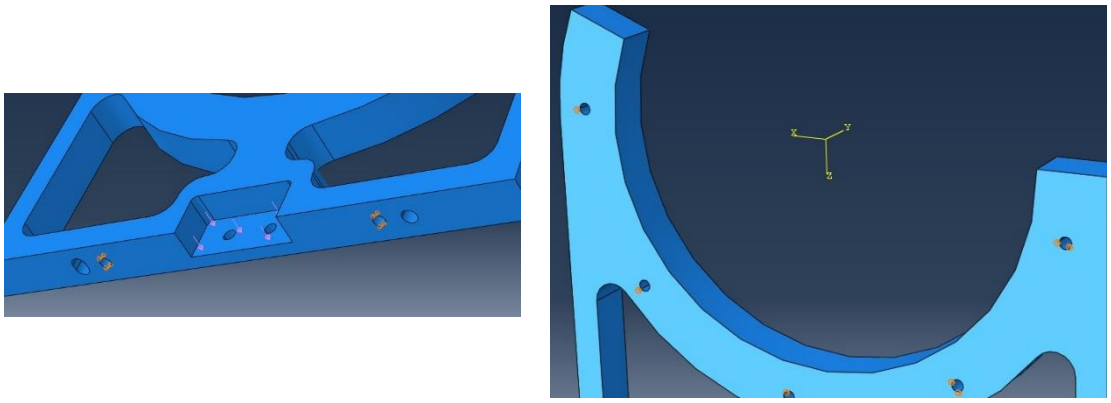

Figure 78 – Boundary conditions of the FEA of component PNSA3401_1

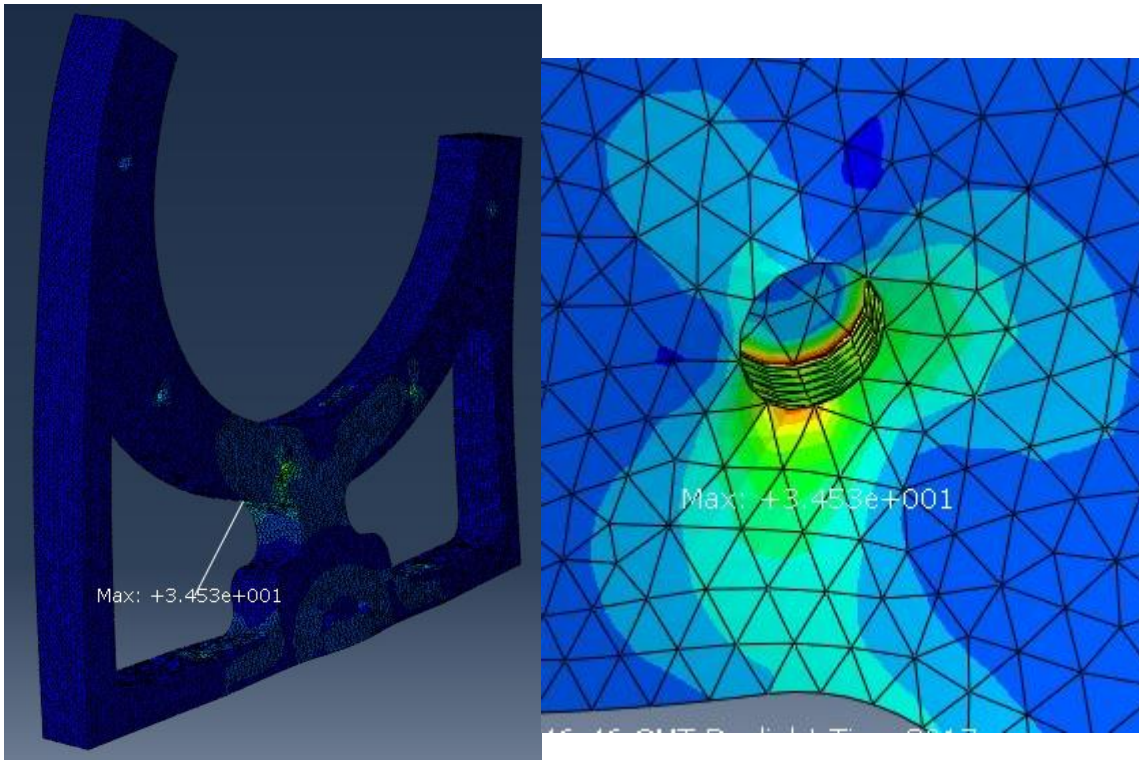

Figure 79 - Max. stress regions of the FEA of component PNSA3401_1

According to Figure 79, the max. stress region is located in the threaded holes of the pins but only on one of them (green hole of left picture). In the right picture is visible the red zones where it is the max. stress.

Table 26 - Input data of FEA of the component PNSA3401_1

Property	Value
Type of element	C3D10: A 10-node quadratic tetrahedron
Element size	1.5
Nr. Of elements	308793
Load	230 N
Material's Young's Modulus	70 GPa
Poisson's ratio	0.33
Yield strength	240 MPa

Table 27 – Results of FEA of the component PNSA3401_1

Property	Value
S (Von Mises, Max. Principal)	34.5 MPa
U (Magnitude)	3.514E-02 mm
E (Magnitude)	5.963E-04
SF	6.9

Having in account the yield strength of the material (Table 26) and the generated Von Mises stress (Table 27) it is conclusive that the value of the yield strength of the material was not exceeded. In fact, the SF is higher than 1.5 that was the requirement. In conclusion, the REV pressing plate can be validated.

3.14 Drawings

All the technical drawings of the showcase are in the appendix chapter. For all the machined parts it was used the respective standard (Standardization, 1989). All the threads were based on (BRITISH STANDARD, 1981). It is important to underline the fact the due to the lack of time for quotation it was asked to prepare the drawings only with the main dimensions, dimensions and location of holes and nonstandard tolerances of machined parts since the STEP file would be delivered to the supplier. A complete BOM of the showcase is also in the appendix chapter.

3.15 Poster

In appendix 6.39 it can be found a poster whose goal is to help people who interact with the showcase model understanding the main functions and principles of a DNR subsystem and how the showcase model works.

CONCLUSIONS

4 CONCLUSIONS AND FUTURE WORKS PROPOSAL

4.1 CONCLUSIONS

Regarding to the calculations of the DNR subsystem the following conclusions were achieved:

- This content cannot be presented due to confidentiality reasons.

Regarding to the showcase, it was obtained the following conclusions:

- All FEA prove that the parts can be validated not only in terms of stress but also in terms of displacement;
- After assembled, the showcase was tested, and it was verified that it was possible to clearly understand and see all the details of the working principle of the DNR. The necessary force to actuate the cams was easily achievable.

During the development of this thesis it was clear that there was some lack of literature regarding to automotive transmissions and related components (for example springs) with an engineering approach and with a deeper point of view.

At the end, the internship at Punch Powertrain proved to be a great experience not only by giving me a new perspective of the development process behind the automotive industry but also because it was possible to consolidate the knowledge obtained in the university. During the internship it was possible to learn theoretical subjects more related with calculations and also more practical details related to some manufacturing processes. 3D design with PTC Creo® and FEA with the software Abaqus® were two major skills acquired during the internship.

4.2 FUTURE WORKS PROPOSAL

This content cannot be presented due to confidentiality reasons.

REFERENCES AND OTHER SOURCES OF INFORMATION

5 REFERENCES AND OTHER SOURCES OF INFORMATION

5.1 SCIENTIFIC JOURNALS' ARTICLES and LITERATURE

(ACEA), E. A. M. A. (2017). The Automobile Industry Pocket Guide.

Akilesh Yamsani. (2014). Gradeability for Automobiles. *IOSR Journal of Mechanical and Civil Engineering (IOSR-JMCE)*, *11*(2), 35–41.

Ashby, M. F. (2005). *Materials Selection in Mechanical Design*. *Design*. ISBN:0750661682.

Avallone, E. A., III, T. B., & Sadegh, A. M. (2007). *Marks' Standard Handbook for Mechanical Engineers* (11th ed.). ISBN:9780071428675.

Brown, A. A. D. (1981). *Mechanical Springs* (1st ed.). ISBN:0-19-859181-0.

Brown, T. H. (2005). *Marks' calculations for machine design*. ISBN:ISBN-10: 0-07-143689-8.

Carvil, J. (1993). *Mechanical Engineer's Data Handbook*. *Butterworth Heinemann*. ISBN:0750619600.

Crolla, D. A. (2009). *Automotive engineering: powertrain, chassis system and vehicle body*. *Elsvier publications and Book AID International* (1st ed.). ISBN:1856175774.

Crolla, D., Foster, D. E., Kobayashi, T., & Vaughan, N. (2014). *Encyclopedia of Automotive Engineering*. *Encyclopedia of Automotive Engineering*. ISBN:9781118354179.

Gustafsson, F. (2014). *Wet clutch load modeling for powershift transmission bench tests*.

H. U. Jibin, Peng Zengxiong, Y. S. (2009). Drag torque prediction model for wet clutches. *Chinese Journal of Mechanical E*, *22*.

Halderman, J. (2012). *Automotive Technology : Principles, Diagnosis and Service* (4th ed.). ISBN:9780132542616.

Henriksen, E. K. (1973). *Jig and Fixture Design Manual*. ISBN:9780831110987.

Herdman, R. et all. C. (OTA). (1995). Advanced Automotive Technology: Visions of a Super-Efficient Family Car.

Heyan, L., Qi, J., & Biao, M. (2013). Modeling and Parametric Study on Drag Torque of Wet Clutch - Proceedings of the FISITA 2012 World Automotive Congress. *Automotive Concept Modelling: Optimization of the Vehicle NVH Performance*.

Hillier, V. A. W. (2012). *Hillier's Fundamental of Motor Vehicle Technology* (6th ed.). ISBN:978 1 4085 1518 1.

Juvinall, R. C., & Marshek, K. M. (2012). *Fundamentals of Machine Component Design*

(5th ed.). ISBN:9781118012895.

Krulikowski, A. (2010). *Alex Krulikowski's ISO Geometrical Tolerancing Reference Guide*. ISBN:0924520175.

Liu, W. (2017). *Hybrid Electric Vehicle System Modeling and Control* (2nd ed.). ISBN:978-1-119-27932-7.

Maki, R. (2005). *Wet clutch tribology: friction characteristics in limited slip differentials*.

Mashadi, B., & Crolla, D. (2012). *Vehicle Powertrain Systems*. ISBN:9780470666029.

Müller, H. W. (1982). *Epicyclic Drive Trains: Analysis, Synthesis, and Applications*.

Naunheimer, H., Bertsche, B., Ryborz, J., & Novak, W. (2010). *Automotive Transmissions: Fundamentals, Selection, Design and Application* (2nd ed.). ISBN:9783642162138.

Shigley, J. E., Mischke, C. R., & Budynas, R. G. (2002). *Shigley's Mechanical Engineering Design* (9th ed.). ISBN:9780070568990.

Simulia, D. (2010). *Abaqus 6.10 Analysis User's Manual - Volume IV: Elements*.

White, F. M. (2010). *Fluid Mechanics*. *McGraw-Hill,New York*. ISBN:0077422414.

William D. Callister, J., & David G. Rethiwsch. (2010). *Materials science and engineering: An introduction*. *Materials & Design* (8th ed.). ISBN:978-0470419977. https://doi.org/10.1016/0261-3069(91)90101-9

Yuan Shihua, Peng Zengxiong, J. C. (2010). Experimental Research and Mathematical Model of Drag Torque in Single-Plate Wet Clutch. *Chinese Journal of Mechanical Engineering*, *23*.

5.2 CATALOGUES

Baosteel, A. (n.d.). Baosteel auto UHSS 70.

Corporation, J. F. E. S. (n.d.). HOT ROLLED STEEL SHEET.

Datenblatt Saarstahl. (n.d.). *Datasheet - 18CrMo4*.

Dendoff Springs. (n.d.). Characteristics, Magnetic Steels, Carbon Alloys, Inconel Steels, Stainless Alloys, Titanium Modulus, Elastic Magnetic, Non Magnetic, Non, <http://www.dendoff.com/cms/wp-content/uploads/201.

Disc springs - theory and practice. (n.d.).

Founderies de Brousseval et Montreuil. (n.d.). Fonderies de brousseval et montreuil.

Kyocera. (2017). Kyocera Technical Information.

Nippon Steel & Sumitomo Metal. (2012). Hot-Rolled Steel Sheets and Coils.

Products, C. R. (n.d.). *isd dunaferr Product catalogue*.

Rods, C., Clamps, H., Various, P., Various, R., Code, C., Sizes, S., … Mpa, Y. S. (1991). 1045 MEDIUM TENSILE CARBON STEEL BAR Chemical Composition.

Saarstahl. (2011a). Material specification sheet, *4*, 7227.

Saarstahl. (2011b). Material specification sheet, 7227.

Sheet, D. (2006). Catamold ® 100Cr6, (October 2000), 1–2.

Stena Aluminium. (2010). Aluminium alloy EN AB-46000, 46000.

Tata Steel. (2010). Ympress ® S315MC Strong , consistent and highly formable.

Terms, T. (n.d.). Electrical steel strip.

5.3 STANDARDS

ASTM International. (2003). ASTM D 341 - Standard Test Method for Viscosity-Temperature Charts for Liquid Petroleum Products.

BRITISH STANDARD. (1981). Specification for ISO metric screw threads, *1981*(2), 60.

DIN 2093. (1992).

National Standard of the People's Republic of China. (2004). Structural Steels Subject to End-quench Hardenability Requirements.

Standardization, I. O. of. (1989). ISO 2768 - International standard.

5.4 WEBSITES

Cambridge Dictionary. (n.d.). Barge meaning. Retrieved August 28, 2017, from http://dictionary.cambridge.org/dictionary/english/barge

Centrifugal force in rotating hydraulic cylinders - MATLAB. (n.d.). Retrieved August 16, 2017, from https://www.mathworks.com/help/physmod/hydro/ref/centrifugalforceinrotatingcylinder.html?s_tid=gn_loc_drop

Corp, N. S. (n.d.). Presetting Coil Springs | Coil Spring Manufacturing | Newcomb Spring. Retrieved August 11, 2017, from http://www.newcombspring.com/article_presetting_springs.html

Dictionary, C. (n.d.). Gridlock definition. Retrieved August 15, 2017, from http://dictionary.cambridge.org/dictionary/english/gridlock

Formulas for Compression Spring Fatigue Design. (n.d.). Retrieved August 23, 2017, from http://www.amesweb.info/MechanicalSprings/Tables/FormulasForCompressionSpringFatigueDesign.aspx

Spring, L. (2011). Spring-I-Pedia - The Complete Guide To Spring Engineering. Retrieved August 5, 2017, from http://springipedia.com/

APPENDIX

6.41 Technical drawings of assemblies of the showcase model

6 APPENDIX

6.1 Extra theoretical aspects

6.1.1 Clutches

6.1.1.1 *Dry clutches*

Dry clutches are typically equipped on manual gearbox for manual shifting.

As can be seen in Figure 80, engine torque is transmitted to the input shaft of the gearbox via clutch plate which is locked between the flywheel and pressure plate. The clutch system is fastened to the flywheel and as consequence the pressure plate is always rotating at engine speed. When the clutch is engaged, the force exerted by the diaphragm spring is applied to the pressure plate pulling pressing it against the clutch plate. Both sides of the clutch friction plate will be loaded with the same force and the

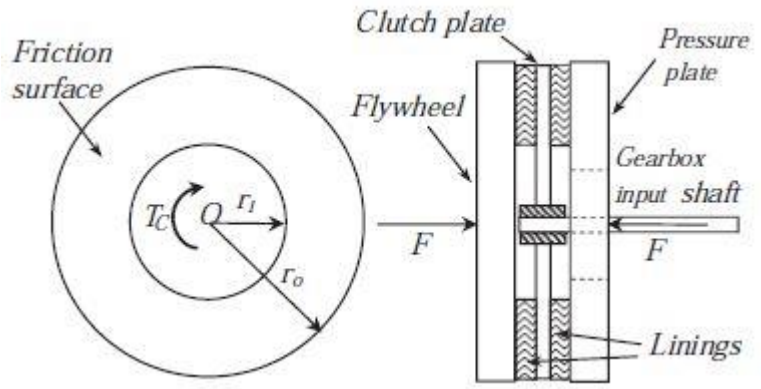

Figure 80 – Friction surfaces of as clutch plate (Mashadi & Crolla, 2012)

total produced torque is the summing up of the torque produced for each friction plate, in this case, two. Which means that each friction plate will produce half of the total torque (Mashadi & Crolla, 2012).

The phenomenon of torque generation in the clutch plate is the consequence of the existence of a normal load and slip that produce friction forces at distances from the plate centre which results in friction torque. The amount of torque depends on the normal force and slip values (Mashadi & Crolla, 2012).

6.1.1.2 *Wet clutches*

In contrast to dry clutches, wet clutches are more complex due to the oil supply. Generally, wet clutches are applied in multi-plate design, immersed by the transmission oil in the housing. The energy dissipated during the clutch engagement by the frictional contact transforms itself in heating. The transmission oil cools down the clutch plates. The other function of the oil is to reduce wear. This makes possible the clutch to operate at higher loads when compared to a dry clutch (Gustafsson, 2014).

Wet clutches are applied mainly in AT used in automobiles and trucks. Wet clutches are also used in applications where control of the torque transfer process is demanded (Maki, 2005).

This type of clutches is known for the following advantages (Naunheimer *et al*., 2010):

- small moment of inertia, depending on the type of damping system;
- small installation space requirement;
- high power/weight ratio;
- large torque capacity;
- high heat capacity as a result of higher thermal energy inputs;
- high durability at low wear;
- good controllability.

There are several important parameters in terms of durability of both dry and wet clutches such as (Naunheimer *et al*., 2010):

- lining pressure;
- specific frictional power;
- type of friction lining;
- lining thickness;
- lining grooving;
- type and amount of oil;
- shifting frequencies;
- moving-off load profiles;
- temperature.

In Figure 81, the major components that are found in a typical wet clutch device may be found.

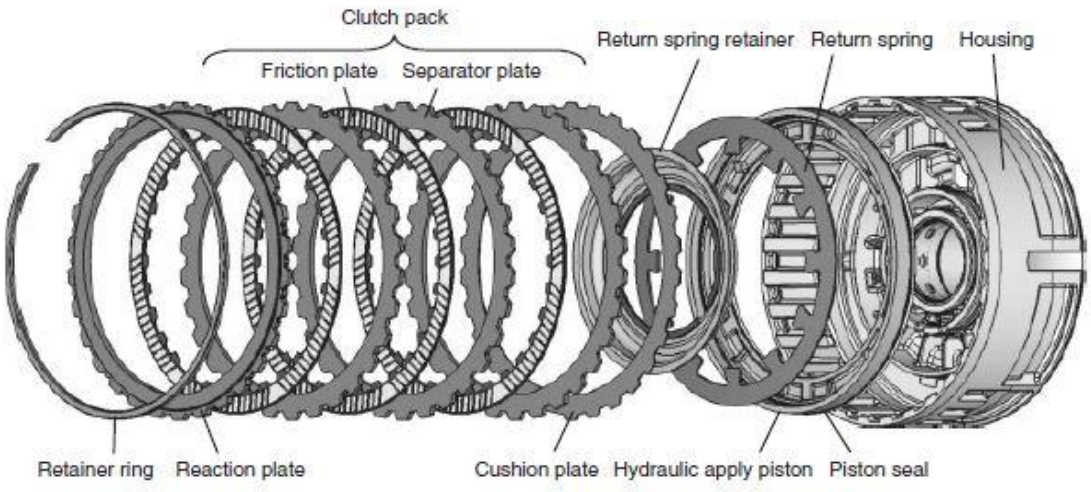

Figure 81 – Major components of wet clutch system (D. Crolla et al., 2014)

Friction plates and separator plates are alternatively placed. A clutch pack is composed by a set of friction and separator plates. The friction plates are assembled on a centre hub which is driven by a rotating drivetrain component. Separator plates are usually splined to the housing which is connected to another drivetrain component. The interface between the plates is lubricated by means of a transmission fluid. The plates are retained between the retaining ring on one side and the piston on the other end. When the clutch is open (disengaged), friction and separator plates can rotate at different speeds while spreading fluid at the interface. When the engagement of the clutch is activated, an actuator applies loading force in the piston. The piston is pulled against a return spring while squeezing oil film at the friction interface. Therefore, the torque is transmitted through viscous shear between sliding plates. A contact between the friction and separator plates takes place when the oil film is squeezed out. By this way torque is partially transmitted through mechanical friction. The clutch engagement is completed when both friction and separator plates are coupled (D. Crolla, Foster, Kobayashi, & Vaughan, 2014).

The primary function of the friction plate is to transmit torque from its spline (which is connected to a drivetrain element) to the separator plates through wet friction. The main function of the separator plate is to transit torque from its friction interface to another gear element. The other function of this component is to act as a heat sink to absorb heat generation during the engagement and releasing of the clutch. The reaction plate (or pressure plate) is located at the end of the clutch pack. The function of this component is to provide a reaction force against the clutch actuator on a uniform way supporting the friction and separator plates. Retainer ring main function is to retain clutch components such as the pressure plate and a return spring. The main purpose of

the (apply) piston is to convert the hydraulic pressure into axial force. The piston return spring pushes the piston back to its released position when the hydraulic pressure is lifted. The cushion plate normally has the shape of a wave plate or coil spring. Its main function is to absorb the initial engagement shock. The main purpose of the balance dam is to avoid or reduce the effect of the centrifugal force created on the piston (D. Crolla et al., 2014).

In Figure 82, it is presented three different geometries of the grooves of the friction plates.

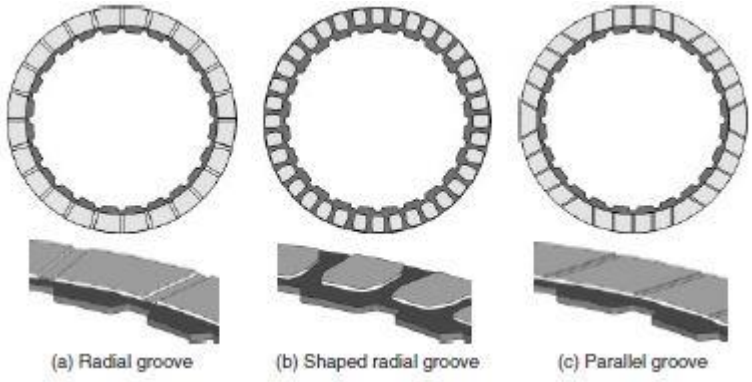

Figure 82 – Shapes of grooves of friction plates (D. Crolla et al., 2014)

The slip control of a wet clutch is the solution for a smooth launch without inducing undesirable driveline noise, vibration and harshness disturbance in the absence of torque converter (D. Crolla et al., 2014).

Due to the working principle of wet clutches (immersed on oil bath) it is inevitable the generation of drag torque. Drag torque depends strongly on the system temperature, oil viscosity. It is important to underline the fact that clutch lining do not get worn however the oil is worn and periodic oil changes are necessary to avoid clutch judder (Naunheimer *et al*., 2010).

Torsional vibration damping is necessary for wet clutch as also for dry clutches. Torsional vibration damping may be achieved by means of a torsional vibration damper, controlled slip or by combination of torsional vibration damper and continuous slip operation. Damping is considerably high in idle speeds as well as at low torques and low speeds. On the other hand, damping is low at high torques and high speeds. The exemption of damping can be achieved depending on the type of combustion engine in use. By this way the unit becomes more compact and light. Due to the high controllability of wet clutches it is possible to go through low speed range where torsional vibration is critical with light and controlled slip (Naunheimer *et al*., 2010).

Crawling or stopping on slopes is achievable with wet clutches. Power losses can be attained by the cooling oil (transmission oil). High feed flow rates are necessary for this operation. There are two different concepts for wet clutches in oil-tight housing (Naunheimer *et al*., 2010):

- the 2-line principle: one channel for the clutch pressure oil, from which the cooling oil is channelled off through suitable throttles, as well as one channel for cooling oil recirculation,
- the 3-line principle: one channel each for the clutch pressure oil, cooling oil and cooling oil recirculation.

6.1.2 Torque converter

The working principle of a torque converter is based on the transfer of momentum from a fluid (oil) to a turbine. The impeller pump is attached to the crankshaft so when the engine rotates the fluid is accelerated, moving from the inner radius to the outer radius along the vanes. This phenomenon is shown in Figure 83 (Mashadi & Crolla, 2012).

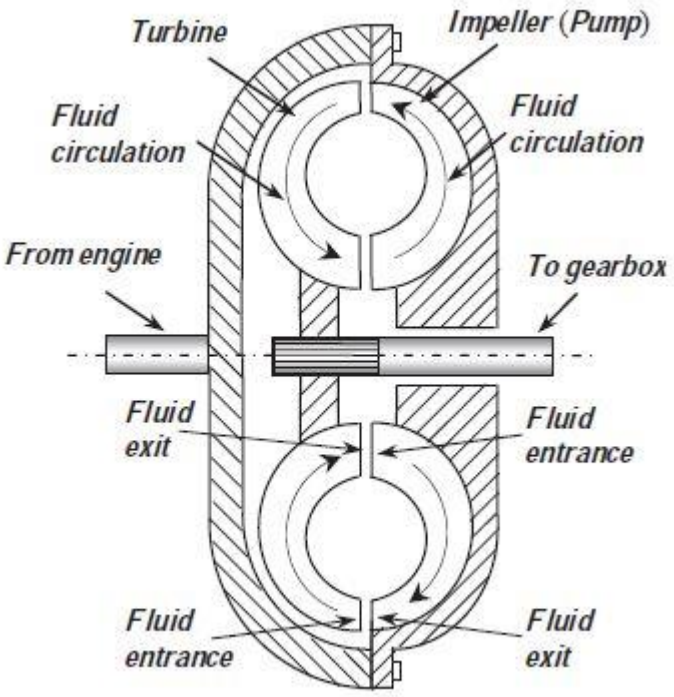

Figure 83 – Schematic of a fluid coupling (Mashadi & Crolla, 2012)

When the fluid is at the outlet of the vane, the fluid with high momentum hits the blade of the turbine. The turbine is fixed to the input shaft of the gearbox (as can be seen in

Figure 83). The momentum is transferred to the turbine while the fluid returns to the inner radius with low velocity and exits the turbine blade. After that a new cycle begins: the fluid enters to the impeller inlet channel and the fluid continuously circulates. When the input shaft of the transmission is rotating, but not the engine, the fluid is under tension but there is no mechanical connection between the engine and the gearbox. This phenomenon (slip in the fluid coupling) allows the vehicle to stop even when the engine is running. However, some torque is transmitted from the engine to the gearbox via the torque converter. When the engine is in idle state, a small amount of torque is transmitted and if the vehicle is in gear it tends to move. This motion is known as "creep". In fact, this action is desirable in automatic transmissions: when the engine speed rises, the transferred torque to the gearbox increases too which translated in a smooth acceleration of the car (Mashadi & Crolla, 2012).

6.1.3 Bearings

6.1.3.1 *Radial needle roller bearings*

Needle bearings or specifically needle roller bearings are used where low section height is a benefit (D. Crolla et al., 2014).

The length of the rollers of this type of bearing is four times their diameter. Needle bearings are available with or without inner race. Full-complement is used for high loads, oscillating or slow speeds. Needle bearings cannot support thrust loads (Avallone, III, & Sadegh, 2007).

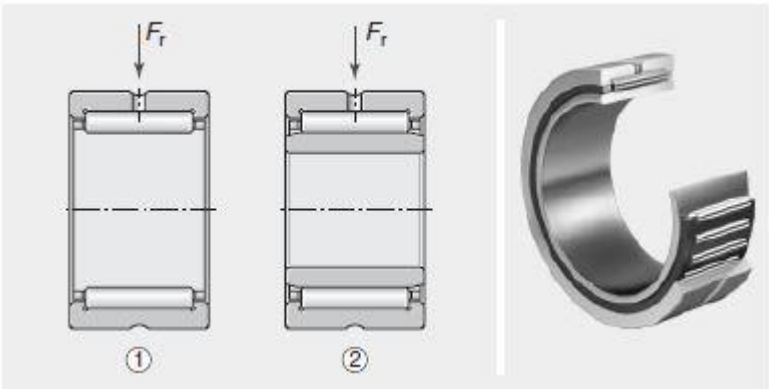

Figure 84 – Structure of a radial needle roller bearing (D. Crolla et al., 2014)

6.1.3.2 *Axial needle roller bearings*

Axial needle roller bearings or thrust bearings are widely applied in automatic transmissions. In fact, most of the bearings in an automotive transmission are of this type. The forces generated in planetary gear trains cancel each other in a large extent. This means that the bearing is responsible for supporting the axial forces that occur due to the helical gearing (D. Crolla et al., 2014).

This type of bearing should be used for moderate speeds and loads applications where other bearings carry the radial loads (Avallone *et al*., 2007).

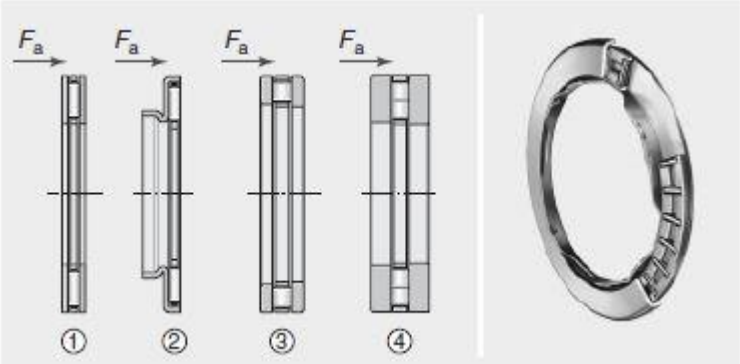

Figure 85 – Different design variants of axial needle roller bearings and cylindrical roller thrust bearings (D. Crolla et al., 2014)

6.2 Table 98 – Resulting centrifugal force of nominal and second scenario for FWD clutch

This content cannot be presented due to confidentiality reasons.

6.3 Table 99 – Auxiliary table for the study of springs' association of FWD clutch

This content cannot be presented due to confidentiality reasons.

6.4 Table 100 - Auxiliary table for calculations of the load along the travelling of the FWD springs' association

This content cannot be presented due to confidentiality reasons.

6.5 Table 101 – Results of transmissible torque of the nominal case for FWD clutch

This content cannot be presented due to confidentiality reasons.

6.6 Table 102 - Results of transmissible torque of the second scenario for FWD clutch

This content cannot be presented due to confidentiality reasons.

6.7 Table 103 - Results of transmissible torque of the third and fourth scenarios for FWD clutch

This content cannot be presented due to confidentiality reasons.

6.8 Table 104 - Resulting centrifugal force of third and fourth scenarios for FWD clutch

This content cannot be presented due to confidentiality reasons.

6.9 Table 105 – Auxiliary table to plot the graph of Figure 145

This content cannot be presented due to confidentiality reasons.

6.10 Table 106 – Auxiliary table to the calculations of pre-load conditions

This content cannot be presented due to confidentiality reasons.

6.11 Table 107 – Creeping effect on FWD clutch set

This content cannot be presented due to confidentiality reasons.

6.12 Table 108 – Resulting transmissible torque for a constant slipping speed of 200 rpm

This content cannot be presented due to confidentiality reasons.

6.13 Table 109 - Resulting transmissible torque for a constant slipping speed of 100 rpm

This content cannot be presented due to confidentiality reasons.

6.14 Auxiliary tables for the calculation of the influence of fluid entry radius in the centrifugal force

This content cannot be presented due to confidentiality reasons.

6.15 Table 113 – Excerpt of first series of tables for the calculation of FWD drag losses

This content cannot be presented due to confidentiality reasons.

6.16 Table 114 – Excerpt of second series of tables of FWD drag losses

This content cannot be presented due to confidentiality reasons.

6.17 Table 115 - Excerpt of third series of tables of FWD drag losses

This content cannot be presented due to confidentiality reasons.

6.18 Table 116 - Drive clutch zero-slip current-to-torque sensitivity expressed in Nm/bar for the nominal scenario

This content cannot be presented due to confidentiality reasons.

6.19 Table 117 - Drive clutch zero-slip current-to-torque sensitivity expressed in Nm/bar for the second scenario

This content cannot be presented due to confidentiality reasons.

6.20 Table 118 - Auxiliary tables of graphs of Figure 180 and Figure 181

This content cannot be presented due to confidentiality reasons.

6.21 Table 119 – Results of the transmissible torque for REV clutch set (nominal scenario)

This content cannot be presented due to confidentiality reasons.

6.22 Table 120 - Results of the transmissible torque for REV clutch set (second scenario)

This content cannot be presented due to confidentiality reasons.

6.23 Table 121 - Results of the transmissible torque for REV clutch set (third scenario)

This content cannot be presented due to confidentiality reasons.

6.24 Table 122 – Excerpt of first series of tables of drag losses calculations of REV clutch

This content cannot be presented due to confidentiality reasons.

6.25 Table 123 - Reverse clutch zero-slip current-to-torque sensitivity expressed in Nm/bar for the nominal scenario

This content cannot be presented due to confidentiality reasons.

6.26 Table 124 - Reverse clutch zero-slip current-to-torque sensitivity expressed in Nm/bar for the second scenario

This content cannot be presented due to confidentiality reasons.

6.27 Table 125 - Reverse clutch zero-slip current-to-torque sensitivity expressed in Nm/bar for the third scenario

This content cannot be presented due to confidentiality reasons.

6.28 Auxiliary tables of the design of FWD showcase shifting lever

In Table 28, on a first instance, it is calculated the value of Δp for different values of L_1. On the second instance, it is calculated the value of Δp for different values of Δα.

Table 28 – Auxiliary table to the design of FWD showcase shifting lever (lower lever)

Constant Δα and variable L1				Constant L1 and variable Δα			
L1 mm	Δα º	β º	Δp mm	Δα º	β º	L1 mm	Δp mm
0			0.000	5	85		6.101
10			6.428	10	80		12.155
20			12.856	15	75		18.117
30			19.284	20	70		23.941
40			25.712	25	65		29.583
50			32.139	30	60		35.000
60			38.567	35	55		40.150
70	40	50	44.995	40	50		44.995
80			51.423	45	45	70	49.497
90			57.851	50	40		53.623
100			64.279	55	35		57.341
110			70.707	60	30		60.622
120			77.135	65	25		63.442
130			83.562	70	20		65.778
140			89.990	75	15		67.615
150			96.418	80	10		68.937
				85	5		69.734

Table 29, is an auxiliary table to calculate, firstly, the value of Δs for different values of L_2 and secondly to calculate the value of Δs for different values of Δα.

Table 29 - Auxiliary table to the design of FWD showcase shifting lever (upper lever)

Constant Δα and variable L2				Constant L2 and variable Δα			
L2 mm	Δα º	β º	Δs mm	Δα º	β º	L2 mm	Δs mm
100			64.279	5	85		6.101
110			70.707	10	80		12.155
120			77.135	15	75		18.117
130			83.562	20	70		23.941
140			89.990	25	65		29.583
150			96.418	30	60		35.000
160			102.846	35	55		40.150
170	40	50	109.274	40	50		44.995
180			115.702	45	45	70	49.497
190			122.130	50	40		53.623
200			128.558	55	35		57.341
210			134.985	60	30		60.622
220			141.413	65	25		63.442
230			147.841	70	20		65.778
240			154.269	75	15		67.615
250			160.697	80	10		68.937
				85	5		69.734

Finally, during the design in PTC Creo® it was necessary to develop Table 30 where the value of Δp and Δs are quickly returned when the value of L_1, Δα and L_2 are introduced.

Table 30 – Resume auxiliary table to the design of FWD showcase shifting lever

The content of this table cannot be presented due to confidentiality reasons.

6.29 Auxiliary tables of the design of REV showcase shifting lever

In Table 31, on a first instance, it is calculated the value of Δp for different values of L_1. On the second instance, it is calculated the value of Δp for different values of Δα.

Table 31 - Auxiliary table to the design of REV showcase shifting lever (lower lever)

Constant Δα and variable L1				Constant L1 and variable Δα			
L1 mm	Δα º	β º	Δp mm	Δα º	β º	L1 mm	Δp mm
0			0.000	5	85		6.101
10			6.428	10	80		12.155
20			12.856	15	75		18.117
30			19.284	20	70		23.941
40			25.712	25	65		29.583
50			32.139	30	60		35.000
60			38.567	35	55		40.150
70	40	50	44.995	40	50		44.995
80			51.423	45	45	70	49.497
90			57.851	50	40		53.623
100			64.279	55	35		57.341
110			70.707	60	30		60.622
120			77.135	65	25		63.442
130			83.562	70	20		65.778
140			89.990	75	15		67.615
150			96.418	80	10		68.937
				85	5		69.734

Table 32, is an auxiliary table to calculate, firstly, the value of Δs for different values of L_2 and secondly to calculate the value of Δs for different values of Δα.

Table 32 - Auxiliary table to the design of REV showcase shifting lever (upper lever)

Constant Δα and variable L2				Constant L2 and variable Δα			
L2 mm	Δα º	β º	Δs mm	Δα º	β º	L2 mm	Δs mm
100			64.279	5	85		6.101
110			70.707	10	80		12.155
120			77.135	15	75		18.117
130			83.562	20	70		23.941
140			89.990	25	65		29.583
150			96.418	30	60		35.000
160			102.846	35	55		40.150
170	40	50	109.274	40	50		44.995
180			115.702	45	45	70	49.497
190			122.130	50	40		53.623
200			128.558	55	35		57.341
210			134.985	60	30		60.622
220			141.413	65	25		63.442
230			147.841	70	20		65.778
240			154.269	75	15		67.615
250			160.697	80	10		68.937
				85	5		69.734

Finally, during the design in PTC Creo® it was necessary to develop Table 33 where the value of Δp and Δs are quickly returned when the value of L_1, Δα and L_2 are introduced.

Table 33 - Resume auxiliary table to the design of REV showcase shifting lever

The content of this table cannot be presented due to confidentiality reasons.

6.30 Table 34 - Necessary force to actuate the cam

Table 34 - Necessary force to actuate the cam

Ω	H	F	Fmax
º	mm	N	N
0	40	82.3	88.44086
3.814075	40.3326	82.89867	
7.594643	40.66082	83.48947	
11.30993	40.98058	84.06505	
14.93142	41.28831	84.61896	
18.43495	41.58114	85.14605	
21.80141	41.85695	85.64252	
25.01689	42.11443	86.10597	
28.07249	42.35294	86.53529	
30.96376	42.57248	86.93046	
33.69007	42.7735	87.2923	
36.25384	42.95682	87.62227	
38.65981	43.12348	87.92226	
40.91438	43.27465	88.19437	
43.02507	43.41159	88.44086	
45	43.53553	88.66396	
46.84761	43.64769	88.86583	
48.57633	43.74919	89.04854	
50.19443	43.84111	89.21399	
51.70984	43.92441	89.36394	
53.1301	44	89.5	
54.46232	44.06867	89.6236	
55.71312	44.13114	89.73605	
56.88866	44.18805	89.8385	
57.99462	44.23999	89.93198	
59.03624	44.28746	90.01744	

6.31 Table 35 – Applied load on the shifting lever

Table 35 – Applied load on the shifting lever

Ω	β	δ	H	F	σ	Rx2	Ry2	Rx3	Ry3	Δp	Δα	U	U Perpen-dicular	Umax	U perp max
º	º	º	mm	N	º	N	N	N	N	mm	º	N	N	N	N
0.000	0.000	90.000	40.000	82.300	0.000	82.300		82.300		0.000	0.000	-9.602	-9.602	9.602	9.602
3.814	3.814	86.186	40.333	82.899	3.814	82.715		82.715		2.000	3.276	-9.650	-9.634		
7.595	7.595	82.405	40.661	83.489	7.595	82.757		82.757		4.000	6.562	-9.655	-9.592		
11.310	11.310	78.690	40.981	84.065	11.310	82.433		82.433		6.000	9.871	-9.617	-9.475		
14.931	14.931	75.069	41.288	84.619	14.931	81.762		81.762		8.000	13.213	-9.539	-9.286		
18.435	18.435	71.565	41.581	85.146	18.435	80.777		80.777		10.000	16.602	-9.424	-9.031		
21.801	21.801	68.199	41.857	85.643	21.801	79.517		79.517		12.000	20.051	-9.277	-8.715		
25.017	25.017	64.983	42.114	86.106	25.017	78.028		78.028		14.000	23.578	-9.103	-8.343		
28.072	28.072	61.928	42.353	86.535	28.072	76.355		76.355		16.000	27.203	-8.908	-7.923		
30.964	30.964	59.036	42.572	86.930	30.964	74.542		74.542		18.000	30.950	-8.697	-7.458		
33.690	33.690	56.310	42.774	87.292	33.690	72.632		72.632		20.000	34.850	-8.474	-6.954		
36.254	36.254	53.746	42.957	87.622	36.254	70.659		70.659		22.000	38.945	-8.244	-6.411		
38.660	38.660	51.340	43.123	87.922	38.660	68.656		68.656		24.000	43.292	-8.010	-5.830		
40.914	40.914	49.086	43.275	88.194	40.914	66.648		66.648		26.000	47.975	-7.776	-5.205		
43.025	43.025	46.975	43.412	88.441	43.025	64.655		64.655		28.000	53.130	-7.543	-4.526		
45.000	45.000	45.000	43.536	88.664	45.000	62.695		62.695		30.000	58.997	-7.314	-3.767		

46.848	46.848	43.152	43.648	88.866	46.848	60.779	60.779	32.000	66.104	-7.091	-2.872
48.576	48.576	41.424	43.749	89.049	48.576	58.916	58.916	34.000	76.271	-6.874	-1.631
50.194	50.194	39.806	43.841	89.214	50.194	57.113	57.113	36.000	#NÚM!	#NÚM!	#NÚM!
51.710	51.710	38.290	43.924	89.364	51.710	55.374	55.374	38.000	#NÚM!	#NÚM!	#NÚM!
53.130	53.130	36.870	44.000	89.500	53.130	53.700	53.700	40.000	#NÚM!	#NÚM!	#NÚM!
54.462	54.462	35.538	44.069	89.624	54.462	52.093	52.093	42.000	#NÚM!	#NÚM!	#NÚM!
55.713	55.713	34.287	44.131	89.736	55.713	50.552	50.552	44.000	#NÚM!	#NÚM!	#NÚM!
56.889	56.889	33.111	44.188	89.838	56.889	49.076	49.076	46.000	#NÚM!	#NÚM!	#NÚM!
57.995	57.995	32.005	44.240	89.932	57.995	47.664	47.664	48.000	#NÚM!	#NÚM!	#NÚM!
59.036	59.036	30.964	44.287	90.017	59.036	46.314	46.314	50.000	#NÚM!	#NÚM!	#NÚM!

6.32 Table 134 – Auxiliary table for the calculation of the trendline of the kinematic viscosity vs temperature

The content of this table cannot be presented due to confidentiality reasons.

6.33 Calculations data

This content cannot be presented due to confidentiality reasons.

6.33.1 Transmission oil

This content cannot be presented due to confidentiality reasons.

6.33.2 Springs

6.33.2.1 *FWD springs*

This content cannot be presented due to confidentiality reasons.

6.33.2.2 *FWD spring pack plates*

This content cannot be presented due to confidentiality reasons.

6.33.2.3 *FWD spring pack*

This content cannot be presented due to confidentiality reasons.

6.33.2.4 *Wavy washer*

This content cannot be presented due to confidentiality reasons.

6.33.2.5 *REV springs*

This content cannot be presented due to confidentiality reasons.

6.33.2.6 *REV spring pack plate*

This content cannot be presented due to confidentiality reasons.

6.33.2.7 *REV spring pack*

This content cannot be presented due to confidentiality reasons.

6.33.2.8 *Belleville washer*

This content cannot be presented due to confidentiality reasons.

6.33.3 Pistons

6.33.3.1 *FWD piston*

This content cannot be presented due to confidentiality reasons.

6.33.3.2 *Balance dam*

This content cannot be presented due to confidentiality reasons.

6.33.3.3 *REV piston*

This content cannot be presented due to confidentiality reasons.

6.33.4 Clutch plates

6.33.4.1 *FWD clutch plates*

This content cannot be presented due to confidentiality reasons.

6.33.4.2 *REV clutch plates*

This content cannot be presented due to confidentiality reasons.

6.33.5 Clutch sets

6.33.5.1 *FWD clutch set*

This content cannot be presented due to confidentiality reasons.

6.33.5.2 *REV clutch set*

This content cannot be presented due to confidentiality reasons.

6.33.6 Gears

6.33.6.1 *Ring gear*

This content cannot be presented due to confidentiality reasons.

6.33.6.2 *Sun gear*

This content cannot be presented due to confidentiality reasons.

6.33.6.3 *Planetary gear*

This content cannot be presented due to confidentiality reasons.

6.33.7 External components

6.33.7.1 *Transmission housing*

This content cannot be presented due to confidentiality reasons.

6.33.8 Materials

In this chapter are presented the mechanical properties that will be used for the analytical calculations and FEA.

It is important to underline the fact that these values are not exactly the same presented on the datasheets of each material. This means that when a range of values was presented or when there were maximum and minimum values, it was made a choice of values within the limits. Most of the times were considered the less favourable values.

All the material datasheets or extracts from catalogues are presented in the APPENDIX where more detailed information can be found.

On this chapter will be only presented the properties which are necessary for the calculations and simulations. In the case of the value of Young's Modulus and Poisson's ratio not being mentioned in the technical datasheet it will be considered the "standard" values of 210 GPa and 0.3 for steel and 70 GPa and 0.33 for aluminium alloys.

Some of this content cannot be presented due to confidentiality reasons.

6.34 Preliminary assembly feasibility study

The aim of this study is to verify the feasibility of the assembly process of the showcase model. This is an important study since the manufacturing and assembly of the model will be made in an external supplier.

The assembly process must be the following:

1. To assemble the spring pins (6x) in the respective holes of the main plate. The aim of the spring pins is to ensure the correct position and alignment of the nest components to be assembled.

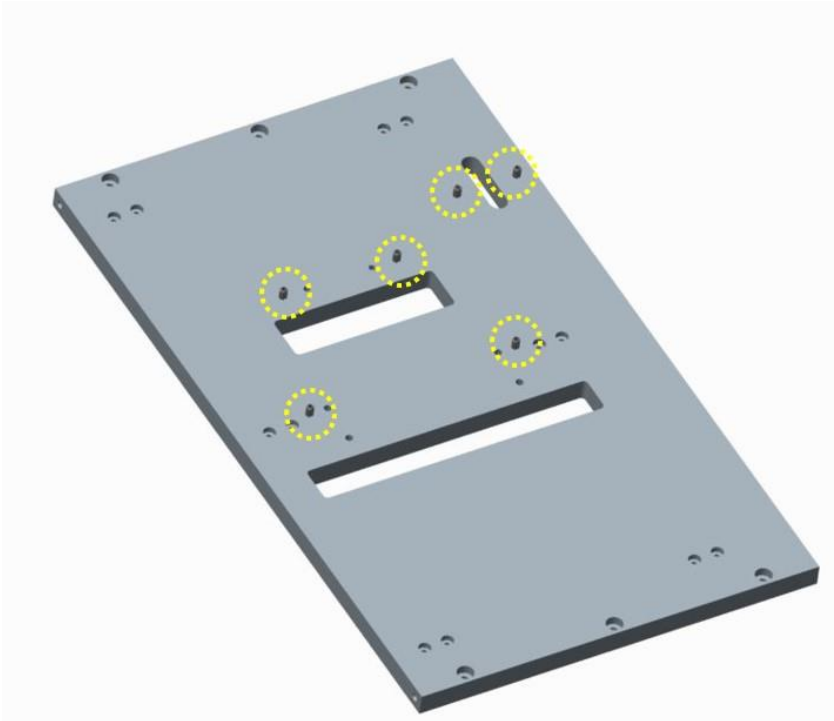

Figure 86 – Showcase assembly process: step 1

2. To assemble the guiding blocks and respective plates of FWD and REV guiding systems. Each block must be screwed with 4x M5.

3. To assemble FWD guiding system, shaft and shaft supports together. Two shaft supports must be left behind in order to allow the assemble of the next guiding system. To move for and backwards the guiding system and verify if it runs smoothly. When this condition is fulfilled, the shaft supports must be screwed to the main plate (2x M4 each unit);
4. To assemble the remaining guiding system and the two missing shaft supports. To verify if the

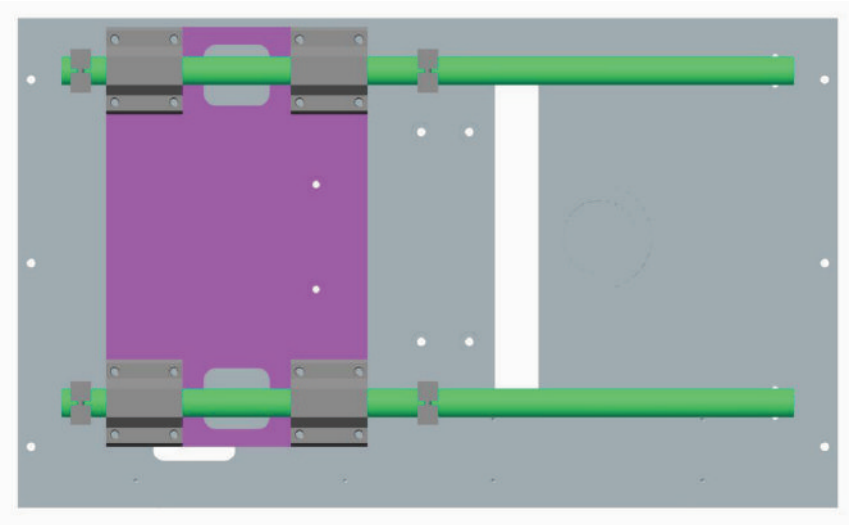

Figure 87 – Showcase assembly process: step 3

guiding system runs smoothly and then screw the shaft supports to the main plate. At this point it is supposed that the entire guidance system is perfectly aligned and running smoothly and all the shaft supports are correctly fastened to the main plate.

5. To remove the following components:
    a. FWD system plate;
    b. REV system plate;
    c. 8x guiding blocks;
    d. 2x shafts

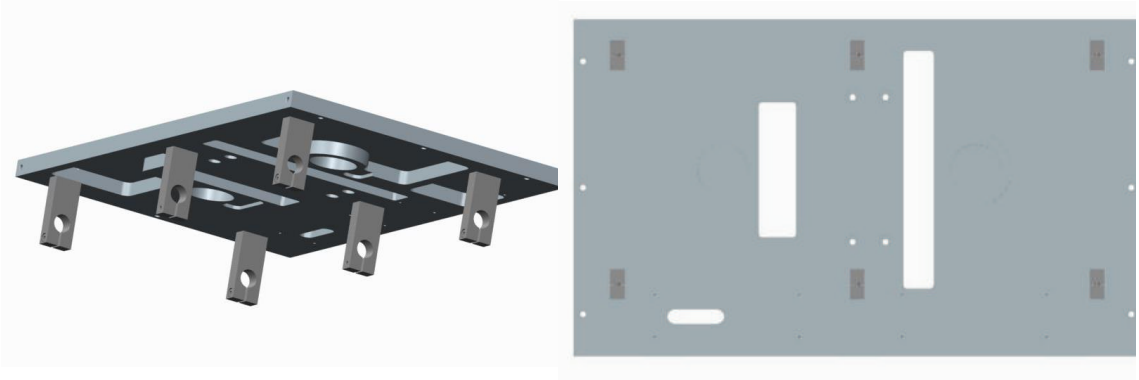

Figure 88 – Showcase assembly process: Step 5

6. To insert the spring pins in one side of the DNR housing, align both parts and screw them together with 4x M6;

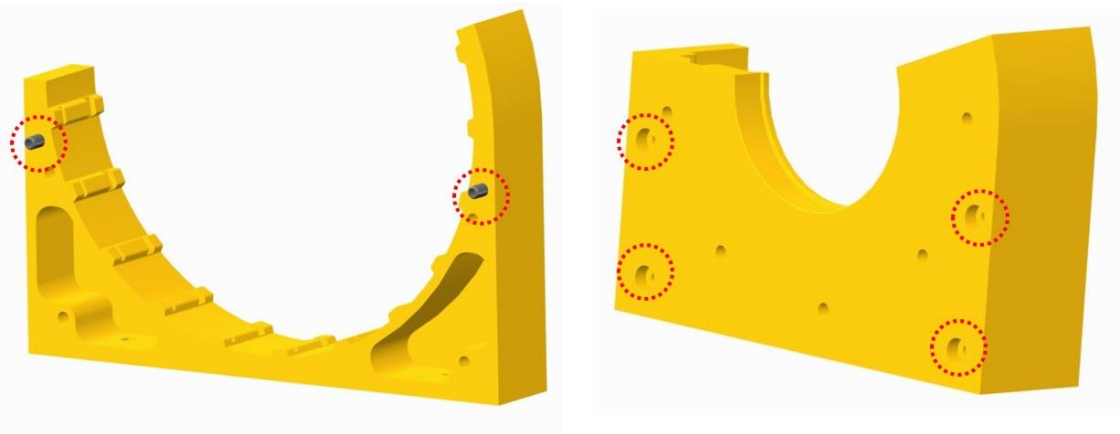

Figure 89 – Showcase assembly process: Step 6

7. To assemble the screwed pins in the REV pressing plate. By using the nuts, adjust the pins to ensure their alignment.

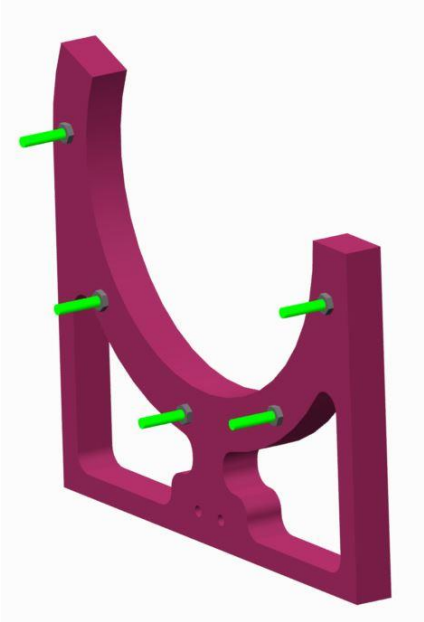

Figure 90 - Showcase assembly process: Step 7

8. To assemble the stopper and the shims in the respective concavity. The main purpose of the shims is to provide adjustment to the stroke of the pressing plate. The stopper will be in contact

with the cam. It is supposed to use only 4x shims but it will depend on the dimensional accuracy of the parts. After assembling the shims and the stopper, fasten them with 2x M5.

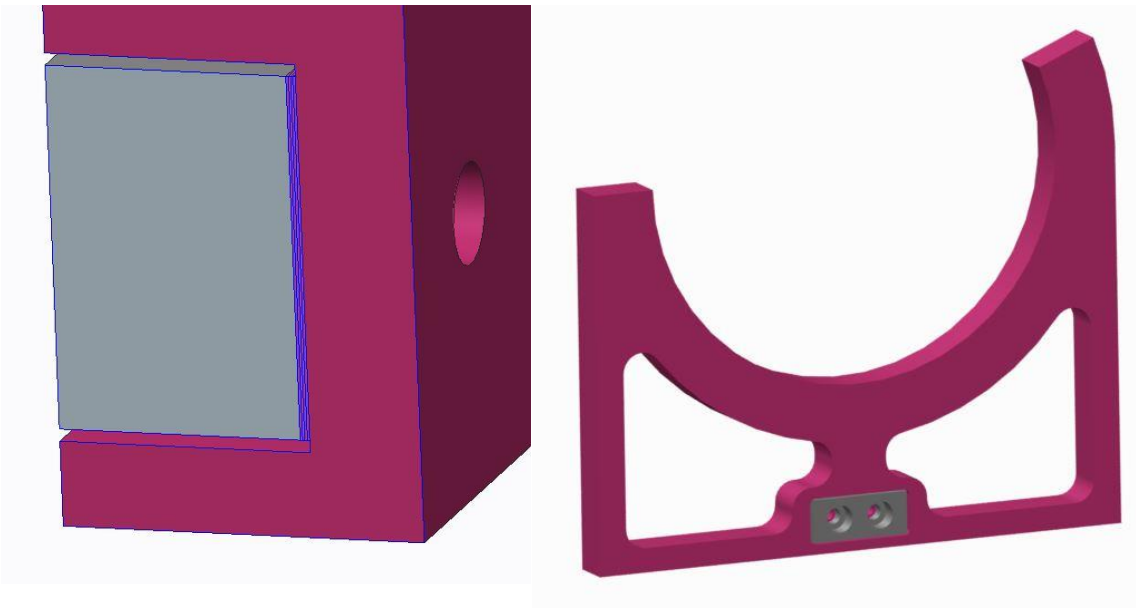

Figure 91 - Showcase assembly process: Step 8

9. To introduce the pins of the reverse pressing plate in the DNR housing in order to hold it and clamp them together. If necessary insert some spacers between the DNR housing and the pressing plate. In this operation, it is necessary to pay attention to avoid scratches on the parts since they are black anodized/oxidized.

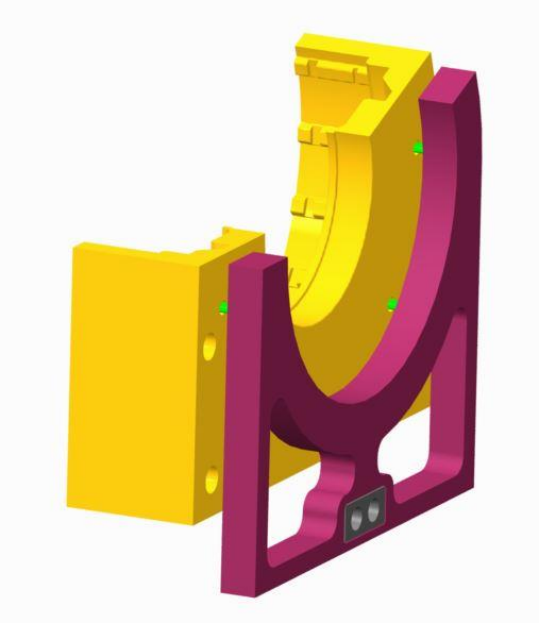

Figure 92 - Showcase assembly process: Step 9

10. To assemble both parts at the same time on the main plate. Use the spring pins (that were inserted before on the main plate) to guarantee the alignment of the DNR housing.

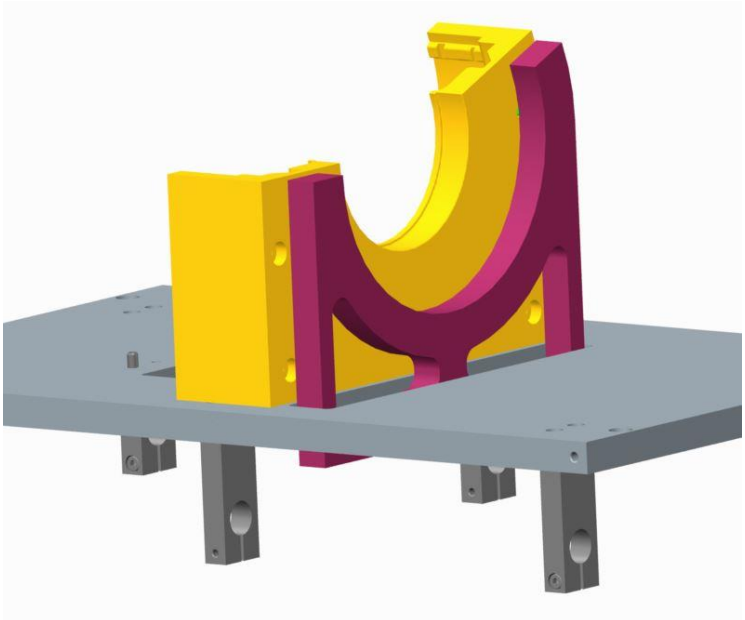

Figure 93 - Showcase assembly process: Step 10

11. To glue the 6 ball transfer units supports (contact face) to the FWD piston.

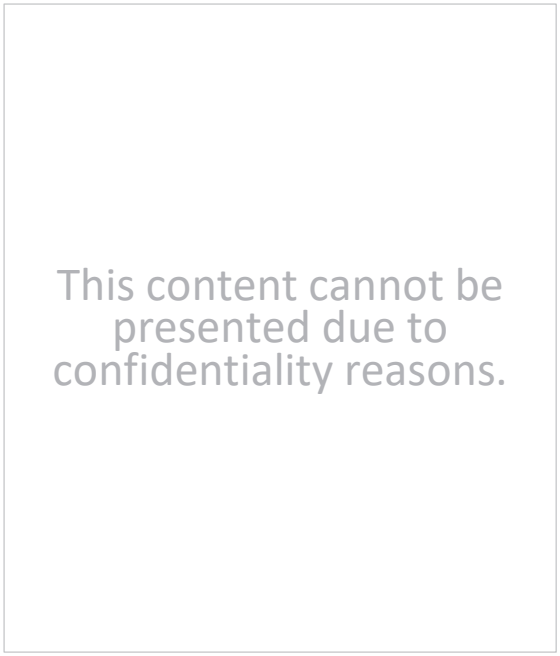

Figure 94 - Showcase assembly process: Step 11

12. To assemble the FWD piston inside the clutch carrier by aligning the ball transfer unit supports with the respective holes and the cutting sections of the CC and FWD piston.

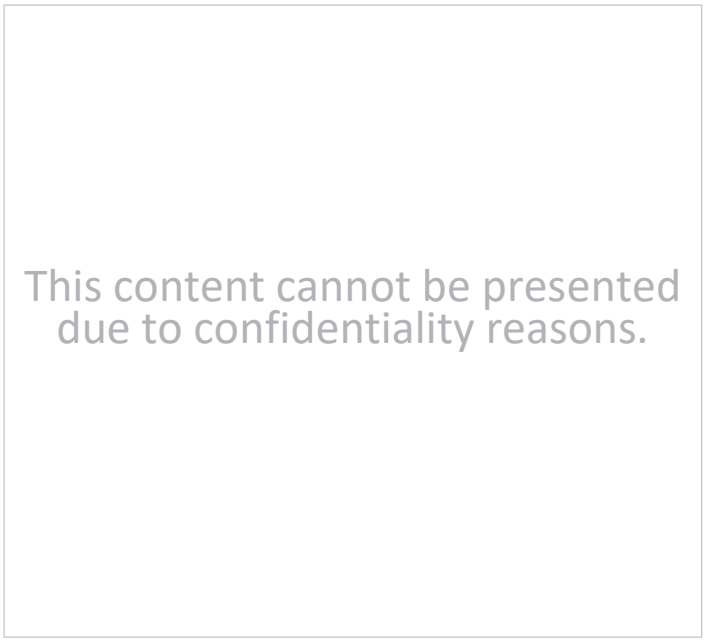

Figure 95 - Showcase assembly process: Step 12

13. To fasten the ball transfer units to their supports and verify the correct alignment.

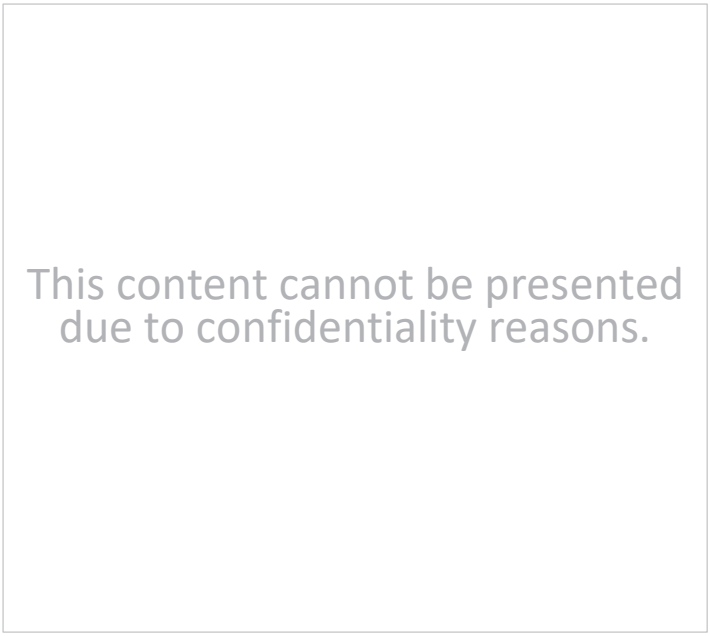

Figure 96 - Showcase assembly process: Step 13

14. To insert the plate of the spring pack and deform plastically the ball transfer unit adapter (swaging process) in order to guarantee a fixed position of the spring pack plate. In the image the adapter is not deformed.

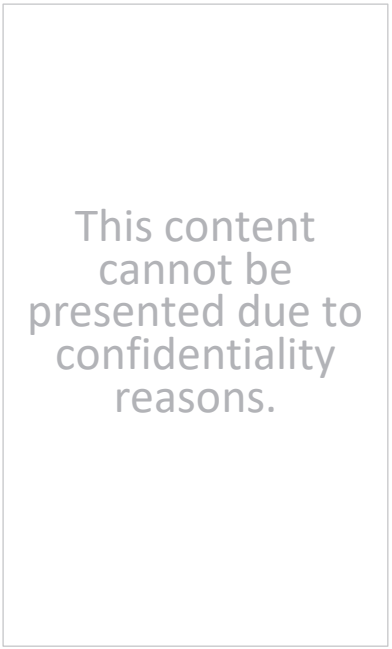

Figure 97 - Showcase assembly process: Step 14

15. To assemble the complete DNR and align the cutting section of the components.

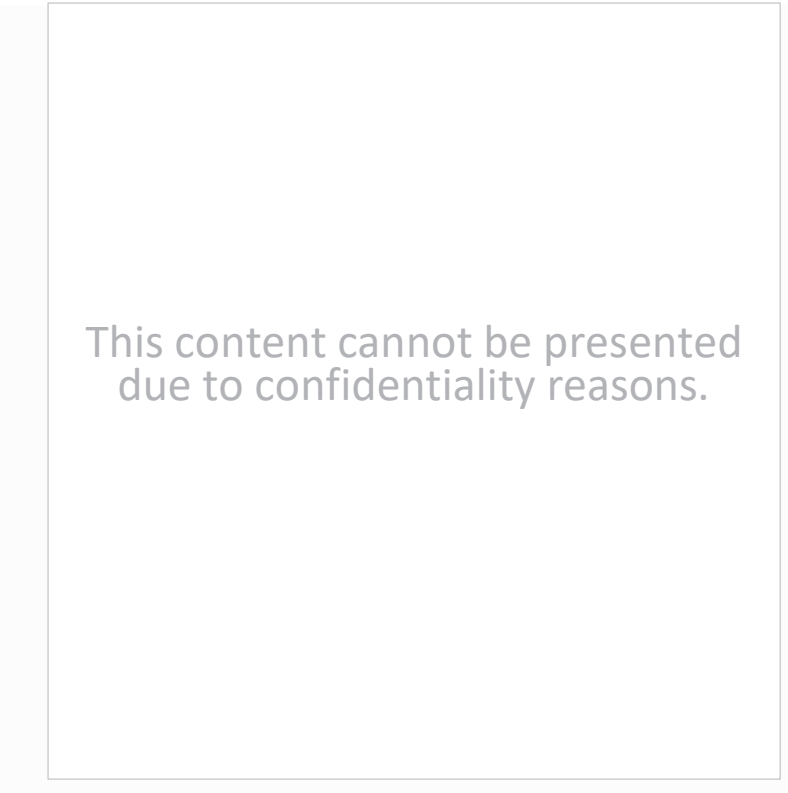

Figure 98 - Showcase assembly process: Step 15

16. To insert the DNR subsystem inside the DNR housing.

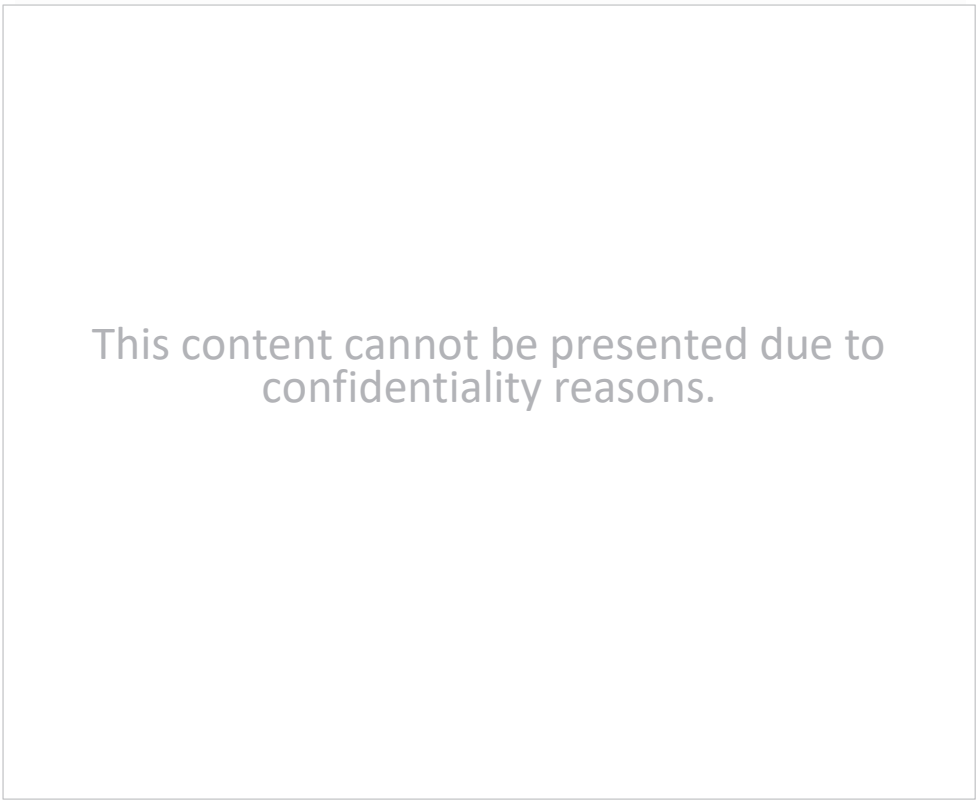

Figure 99 - Showcase assembly process: Step 16

17. To glue the ring to the FWD pressing plate.

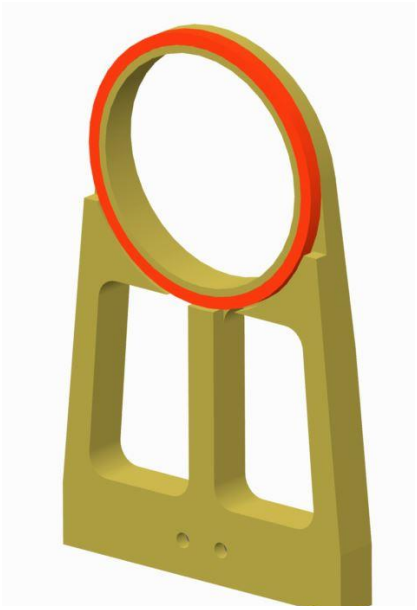

Figure 100 - Showcase assembly process: Step 17

18. To assemble the shims and the stopper in the cavity. The aim of the shims was already explained before. After assembling the shims and the stopper fasten them with 2x M5.

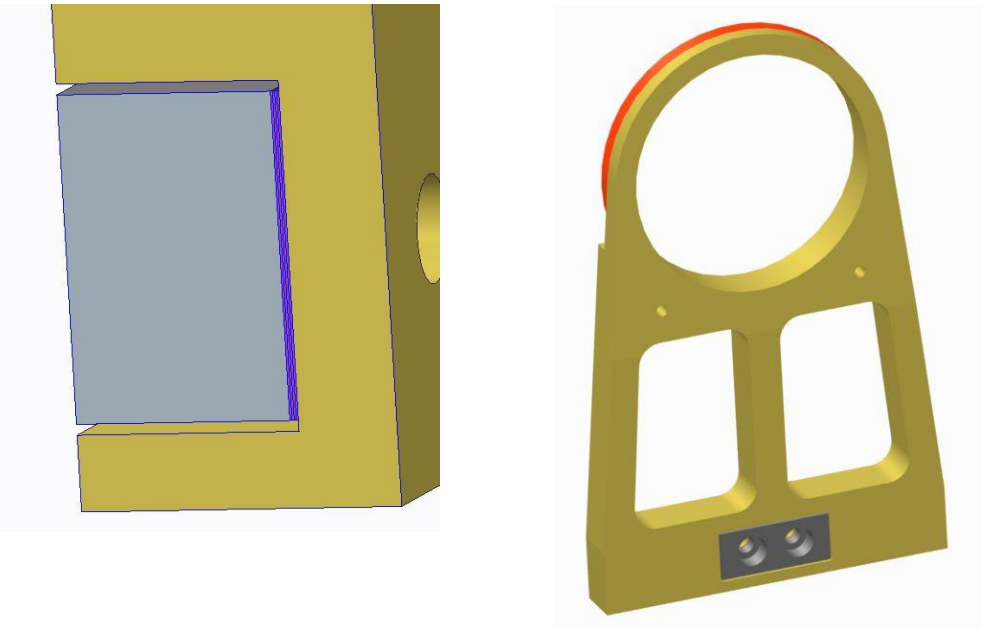

Figure 101 - Showcase assembly process: Step 18

19. To screw bushing support and FWD pressing plate together with 2x M4. These screws are auxiliary. By this way we can prevent the pressing plate to be free.

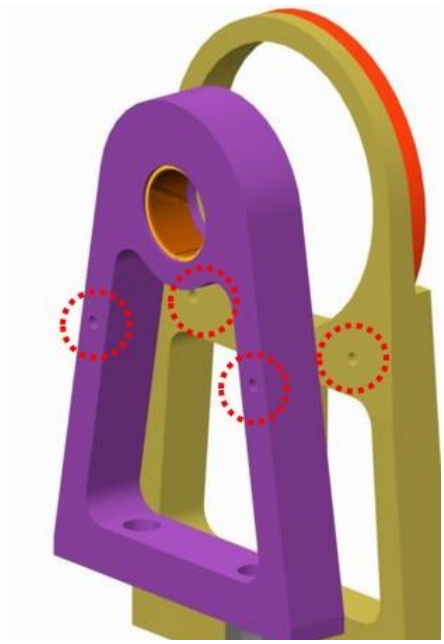

Figure 102 - Showcase assembly process: Step 19

20. The bushing support must be perfectly aligned with the auxiliary spring pins (of the main plate) and then screwed to the main plate. To check if everything is aligned and if the DNR rotates smoothly.

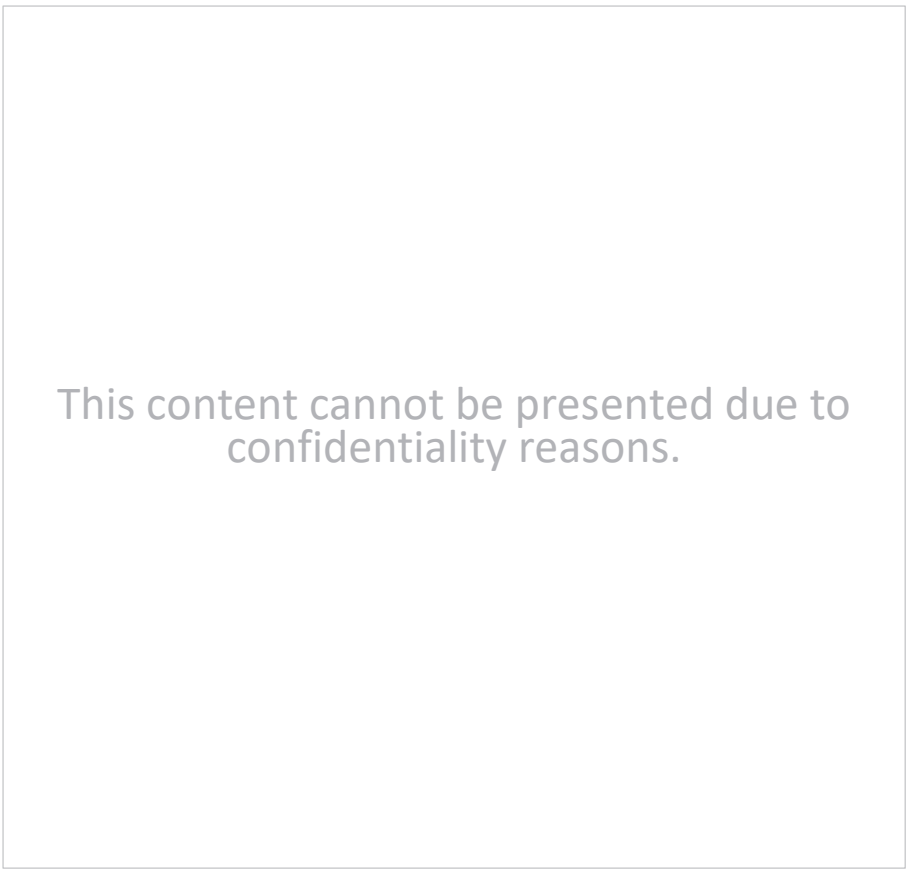

Figure 103 - Showcase assembly process: Step 20

21. To screw the supports of the sheet metal (which transmits the movement from the lever to the cams) to the main plate by means of 2x M3 (each support). To verify if the sheet metal moves with low friction to ensure there will not be extra loads.

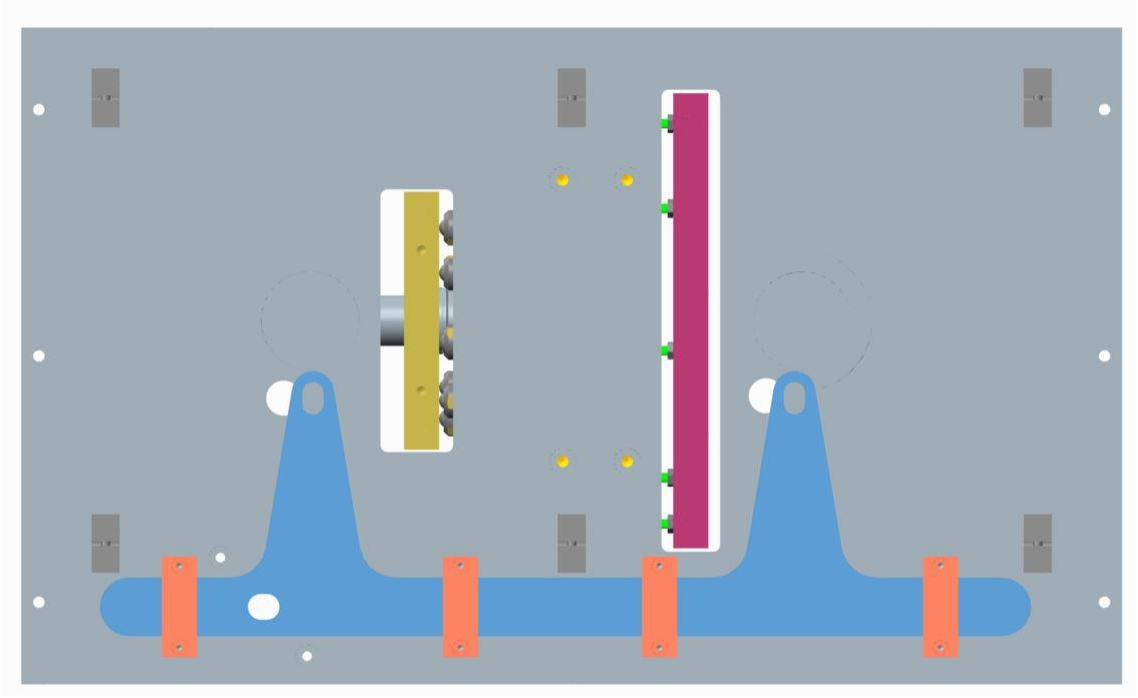

Figure 104 - Showcase assembly process: Step 21

22. To insert the cam into the bearing by means of a press.

23. After that, to glue the outer shell of the bearing to the cavity of the main plate. Guarantee that the bearing rotates freely and smoothly. At this point the cam and the sheet metal are not connected, yet. They will be screwed together forward. It is advisable to add some lubricant to the contact surfaces of the cam and stopper.

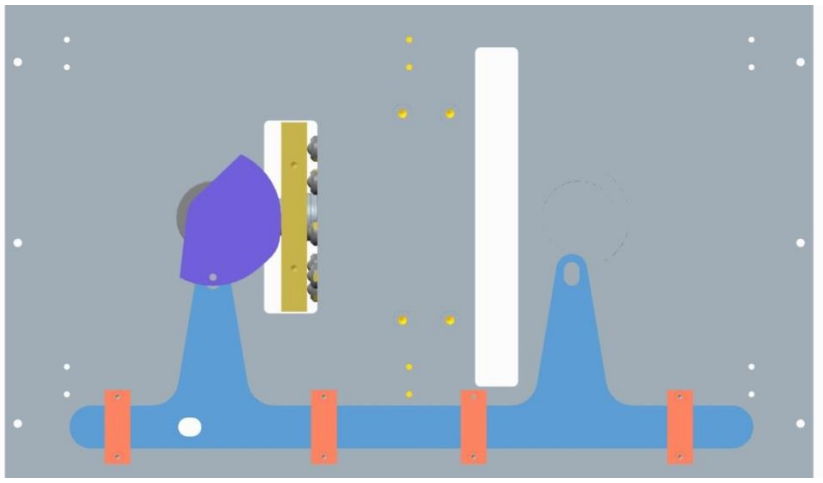

Figure 105 - Showcase assembly process: Step 23

24. To screw both shafts to originate a lever.

Figure 106 - Showcase assembly process: Step 24

25. To insert the shoulder screw MSB6-40 in the block and verify if the lever moves smoothly.

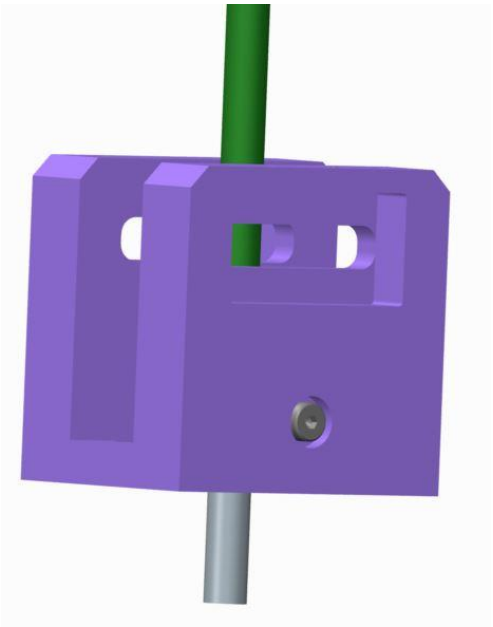

Figure 107 - Showcase assembly process: Step 25

26. To screw the spring plungers inside the square nuts. Adjust the position of the 4 square nuts in order to ensure that the user feels a “click” when it is about to leave a position (D, N or R) or about to reach one. The square nuts will be adjusted again before the assembly of the cover.

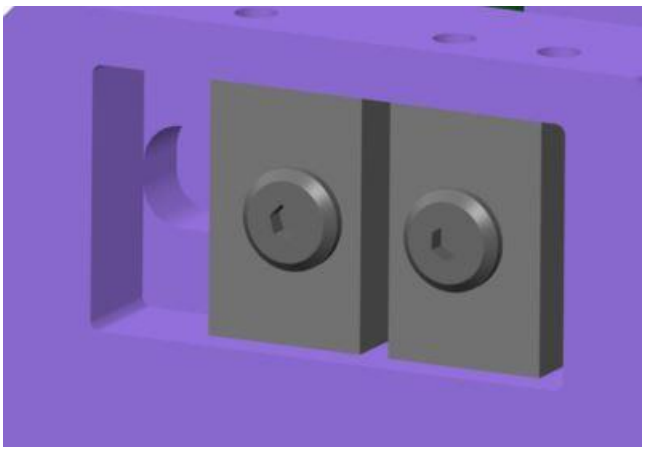

Figure 109 - Showcase assembly process: Step 26

27. To fasten the square nuts by means of the set screws after adjusting the position;

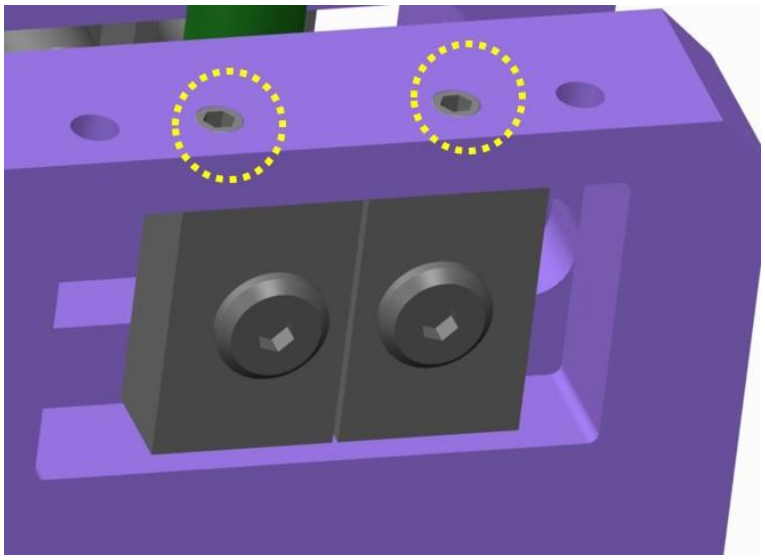

Figure 108 - Showcase assembly process: Step 27

28. It is necessary to assemble the levers system at this point to help in the fastening of the cam to the guiding sheet metal. To easily assemble the cams, it is necessary to guarantee that the cam is not being actuated by the pressing plate. By moving the lever to the REV position, we ensure that the FWD cam is not being actuated and vice-versa;

29. To move the lever to N gear.

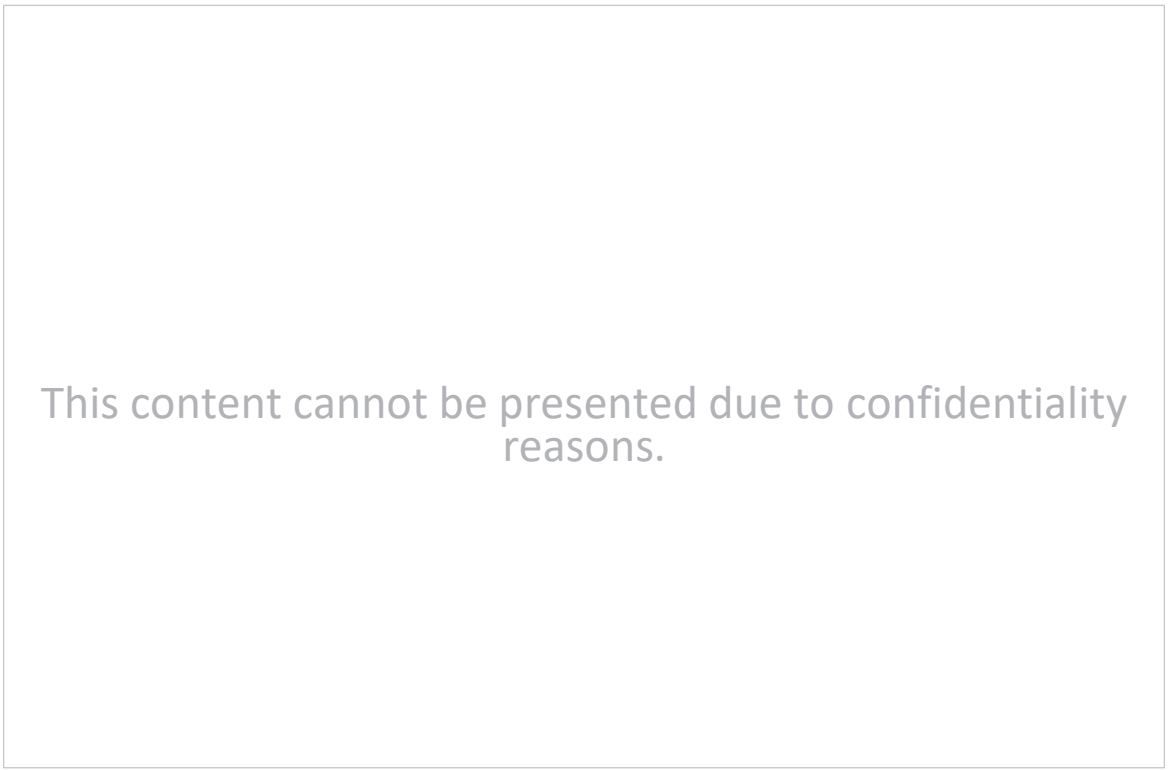

Figure 110 - Showcase assembly process: Step 29

30. To move the lever to the REV position and rotate the cam by hand, too.

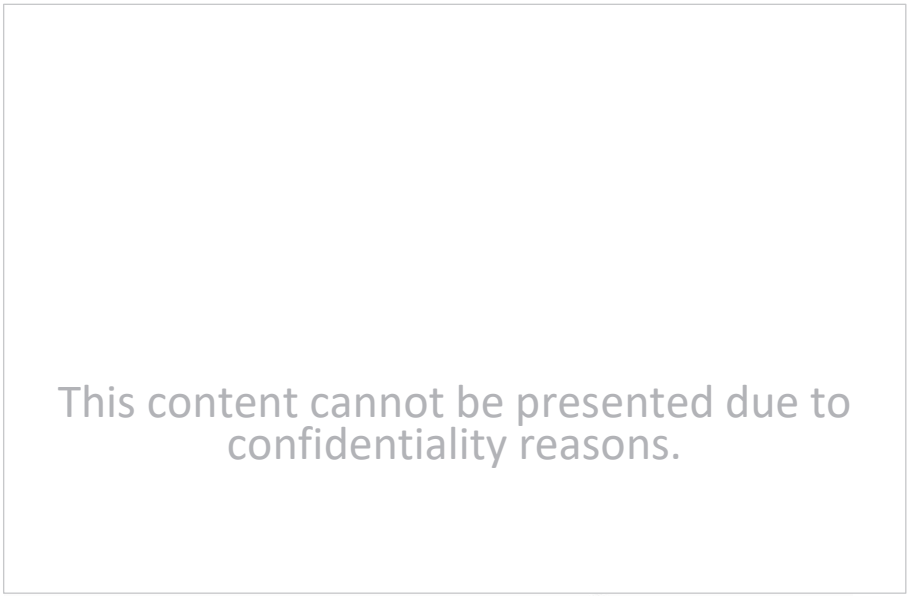

Figure 111 - Showcase assembly process: Step 30

31. In this figure, it is possible to see that in this position the FWD cam is not being actuated. There is contact but there is no transmission of force.

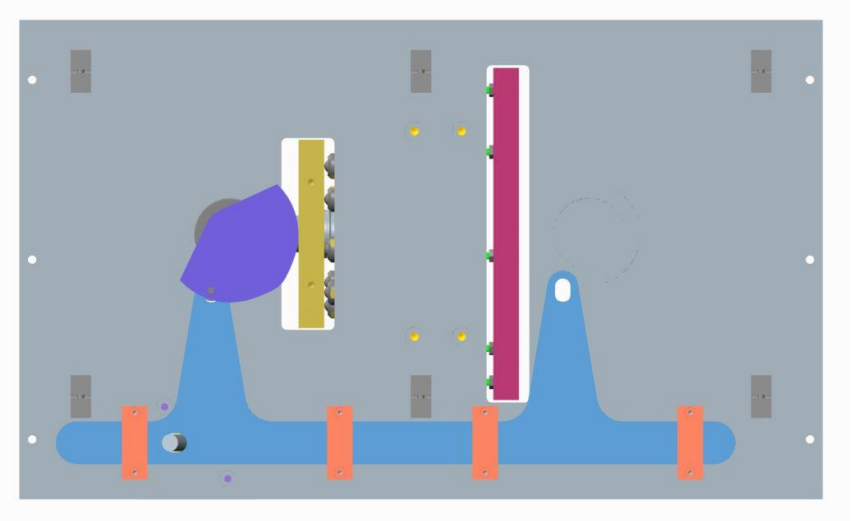

Figure 112 - Showcase assembly process: Step 31

32. To align the cam hole and the guiding plate hole. To fasten the cam to the guiding sheet (PNSA360) by mean of a shoulder screw DBGB5-8. An auxiliary hole in the main plate was created to allow the fastening of the screw. If you used a pin to help the alignment of the cam please remove it.

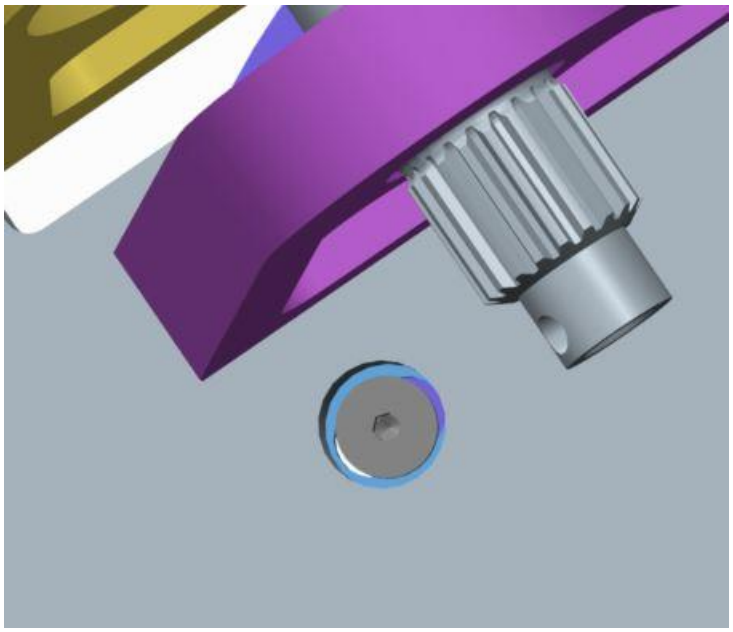

Figure 113 - Showcase assembly process: Step 32

33. To move the lever to Drive position and check if the travelling of the plate is enough to press the clutch plates and to ensure a correct working of the DNR. If necessary add or remove shims (the instructions of where these are located was previously explained). To verify at the end of the adjustment if the clutch plates are being pressed and that the DNR works correctly.

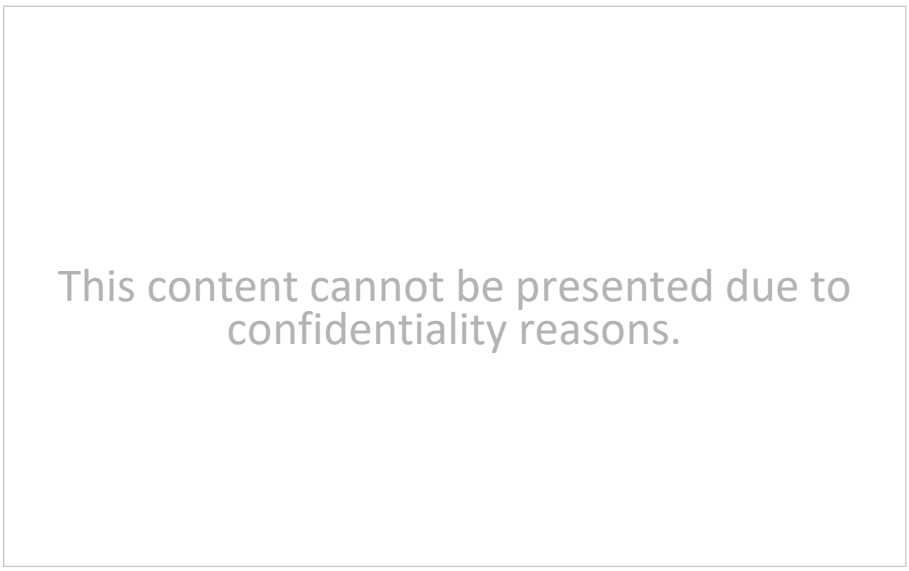

Figure 114 - Showcase assembly process: Step 33

34. To fasten the cam to the guiding sheet by mean of a shoulder screw DBGB5-8. An auxiliary hole in the base was created to allow the fastening of the screw.

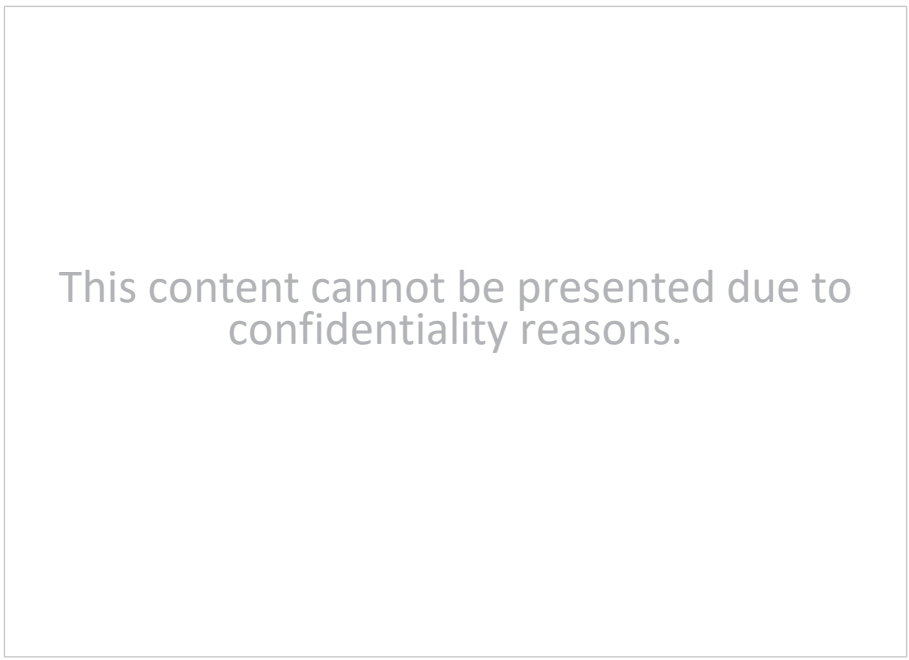

Figure 115 - Showcase assembly process: Step 34

35. To move the lever to Reverse position and check if the travelling of the plate is enough to press the clutch plates and to ensure a correct working of the DNR. If necessary add or remove shims (the instructions of where these are located was previously explained). To verify at the end of the adjustment if the clutch plates are being pressed and that the DNR works correctly. To move the lever to Drive position and verify if the forward clutches are being well pressed.

36. At this point the guiding trails need to be assembled. Remove the screws which are joining the forward pressing plate and the bushing support. Assemble the forward pressing plate with the guiding plate: align the pressing plate by the spring pins. Place the guiding bars trough the guiding blocks.

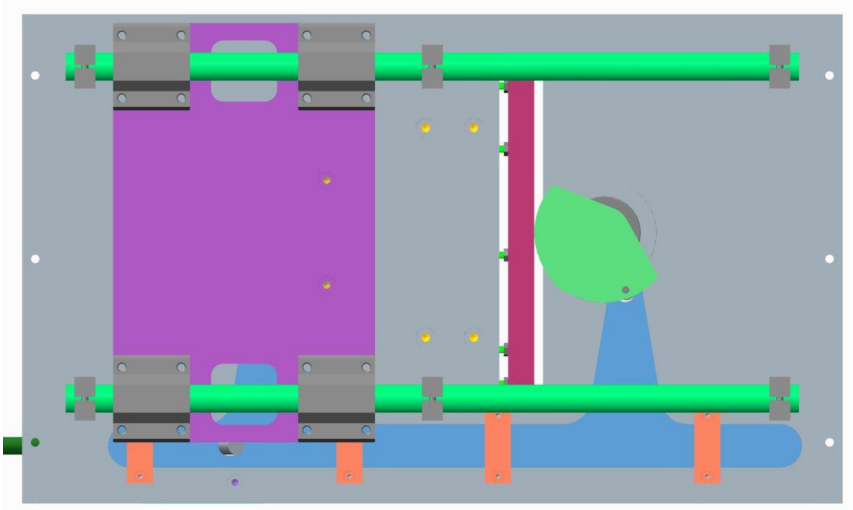

Figure 116 - Showcase assembly process: Step 36

37. To assemble the reverse pressing plate with the guiding plate: align the pressing plate by the spring pins. Place the guiding bars trough the guiding blocks. Fasten the 6 shaft supports. To check that the shafts do not move.

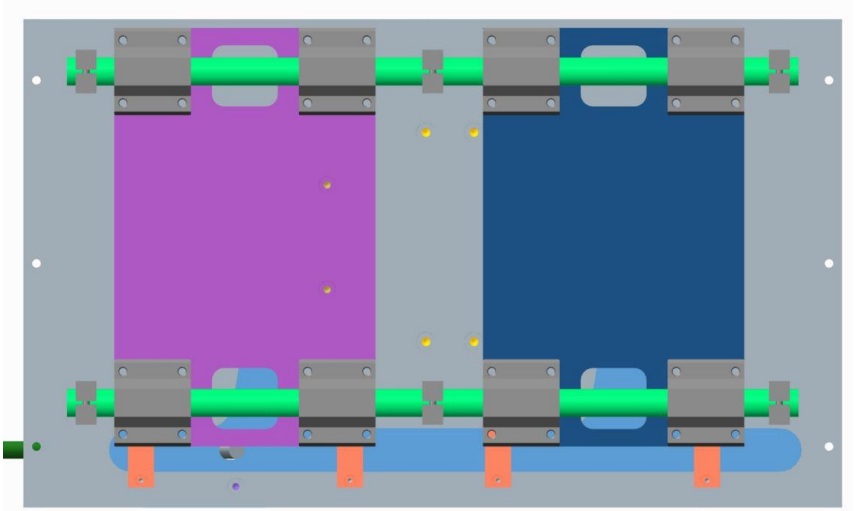

Figure 117 - Showcase assembly process: Step 37

38. To measure the play of the cam. If necessary adjust them by adding or removing shims.
39. To assemble the legs and screw them.

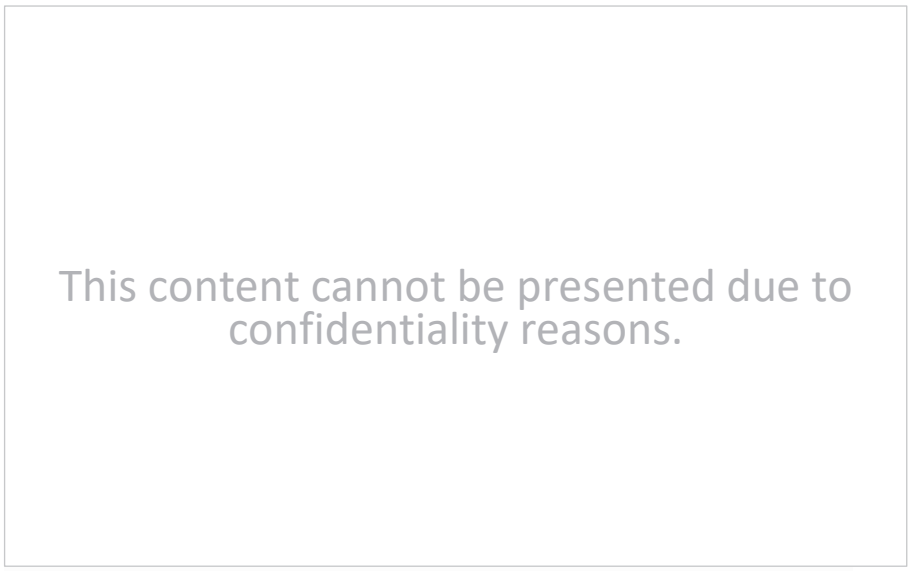

Figure 118 - Showcase assembly process: Step 39

40. To verify that there is no interference between the cams and the guiding systems.

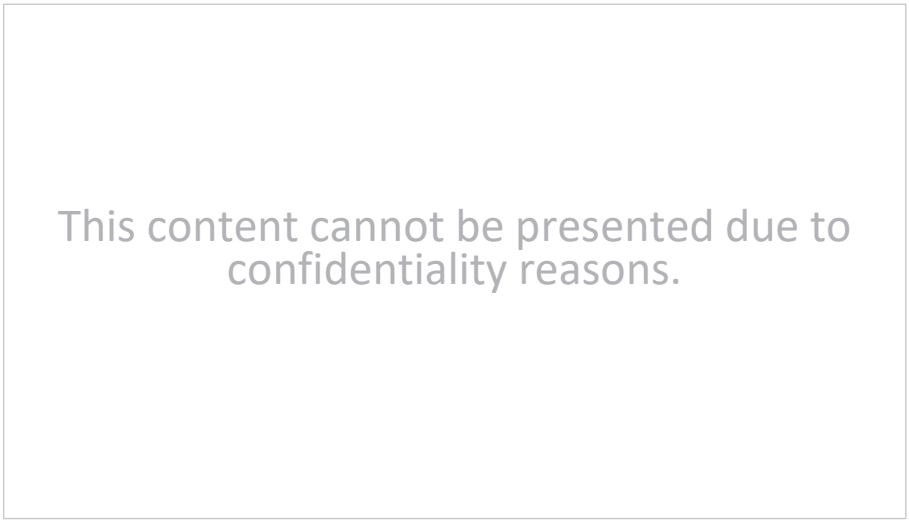

Figure 119 - Showcase assembly process: Step 40

41. To assemble and screw the side plates.

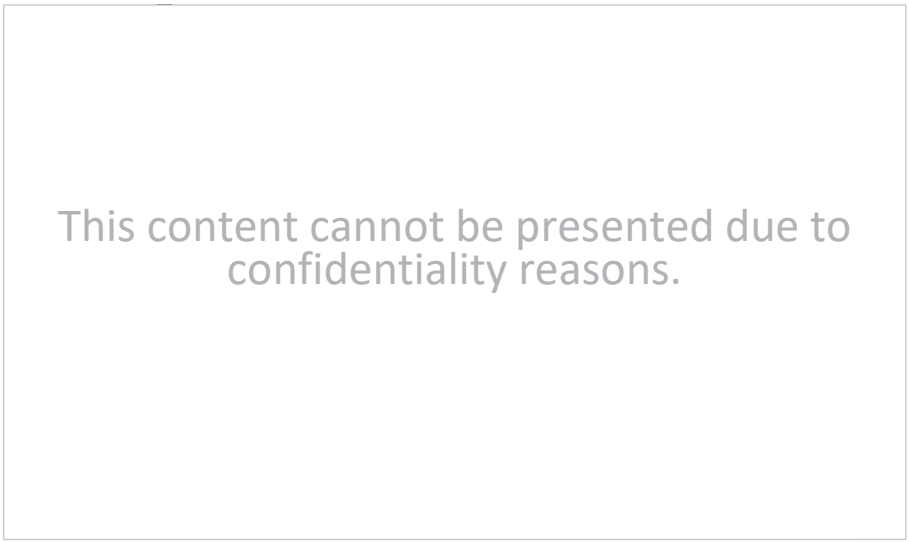

Figure 120 - Showcase assembly process: Step 41

42. To assemble and screw the transparent bottom cover.

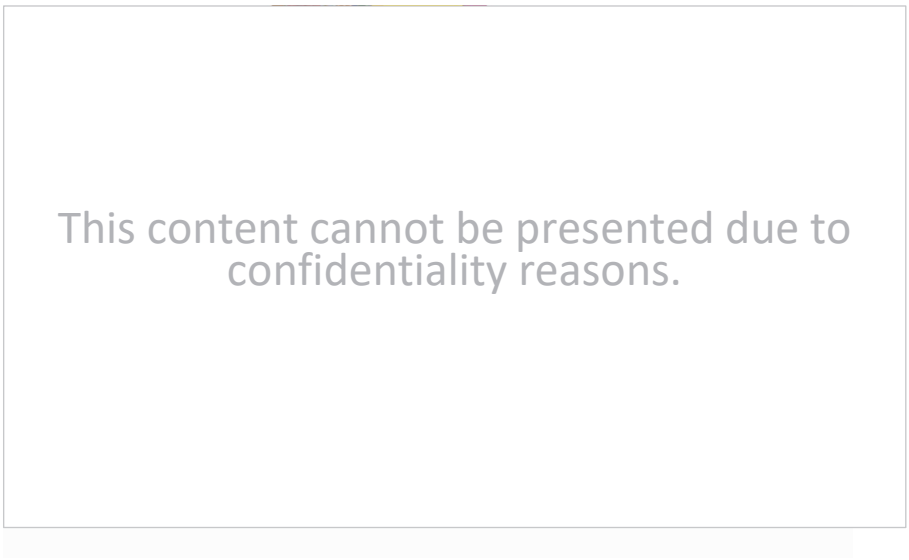

Figure 121 - Showcase assembly process: Step 42

43. To assemble the hand wheel by mean of 1x M5.

Figure 122 - Showcase assembly process: Step 43

44. To check if the travelling of both reverse and forward is enough to activate the clutches. To verify if the position of the lever is well defined and apply thread glue on the spring plungers. Assemble both covers: Lever system's cover and DNR transparent cover.

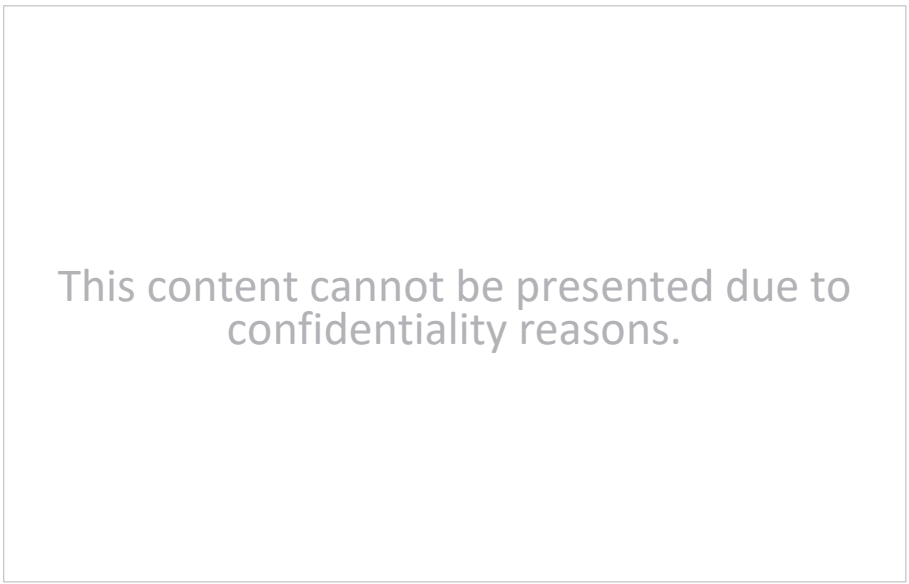

Figure 123 – Showcase assembly process: final step

6.35 Datasheet LOCTITE® 638™

Technical Data Sheet

LOCTITE® 648™

(TDS for the new formulation of LOCTITE® 648™) August 2016

PRODUCT DESCRIPTION

LOCTITE® 648™ provides the following product characteristics:

Technology	Acrylic
Chemical Type	Urethane methacrylate
Appearance (uncured)	Green liquid[LMS]
Fluorescence	Positive under UV light[LMS]
Components	One component - requires no mixing
Viscosity	Low
Cure	Anaerobic
Secondary Cure	Activator
Application	Retaining
Strength	High

This Technical Data Sheet is valid for LOCTITE® 648™ manufactured from the dates outlined in the "Manufacturing Date Reference" section.

LOCTITE® 648™ is designed for the bonding of cylindrical fitting parts. The product cures when confined in the absence of air between close fitting metal surfaces and prevents loosening and leakage from shock and vibration. Typical applications include holding gears and sprockets onto gearbox shafts and rotors on electric motor shafts. LOCTITE® 648™ provides robust curing performance. It not only works on active metals (e.g. mild steel) but also on passive substrates such as stainless steel and plated surfaces. The product offers high temperature performance and oil tolerance. It tolerates minor surface contaminations from various oils, such as cutting, lubrication, anti-corrosion and protection fluids.

TYPICAL PROPERTIES OF UNCURED MATERIAL

Specific Gravity @ 25 °C	1.1
Viscosity, Brookfield - RVT, 25 °C, mPa·s (cP):	
Spindle 2, speed 20 rpm	400 to 600[LMS]
Viscosity, Cone & Plate, 25 °C, mPa·s (cP):	
Shear rate 129 s^{-1}	400 to 600
Flash Point - See SDS	

TYPICAL CURING PERFORMANCE

Cure Speed vs. Substrate

The rate of cure will depend on the substrate used. The graph below shows the shear strength developed with time on steel pins and collars compared to different materials and tested according to ISO 10123.

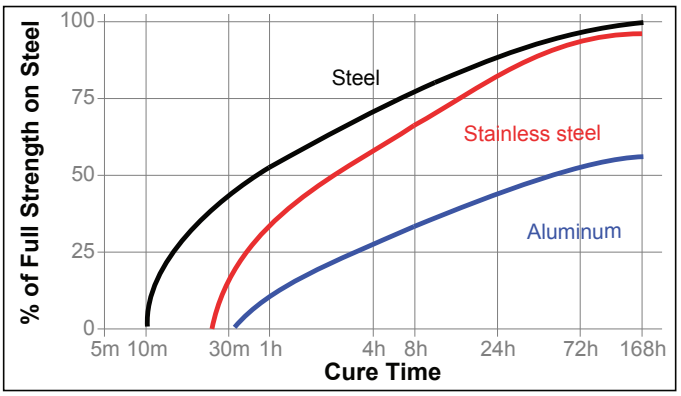

Cure Speed vs. Bond Gap

The rate of cure will depend on the bondline gap. The following graph shows shear strength developed with time on steel pins and collars at different controlled gaps and tested according to ISO 10123.

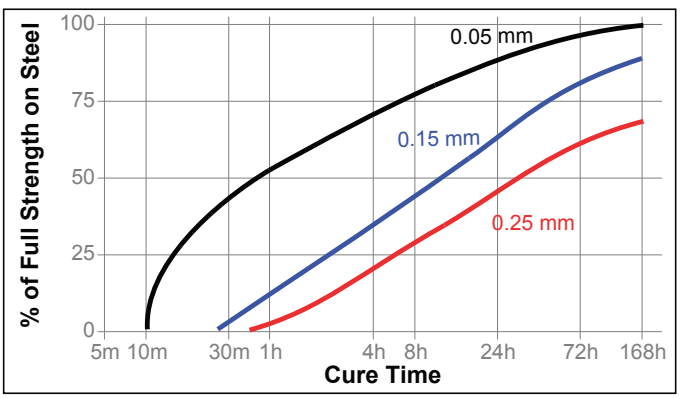

Cure Speed vs. Temperature

The rate of cure will depend on the temperature. The graph below shows the shear strength developed with time at different temperatures on steel pins and collars and tested according to ISO 10123.

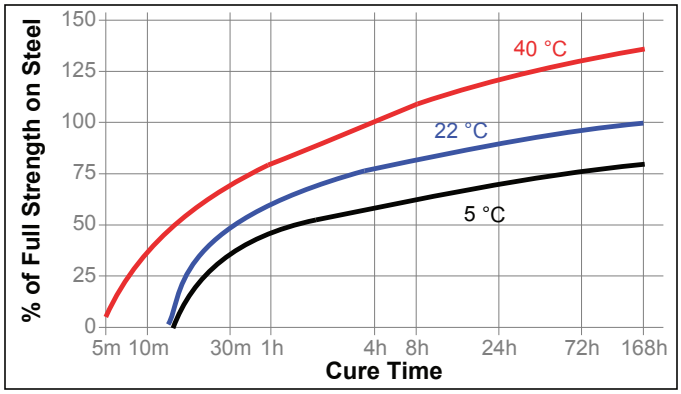

Cure Speed vs. Activator
The graph below shows the shear strength developed with time on stainless steel pins and collars using Activator SF 7471™, SF 7649™ and SF 7091™ and tested according to ISO 10123.

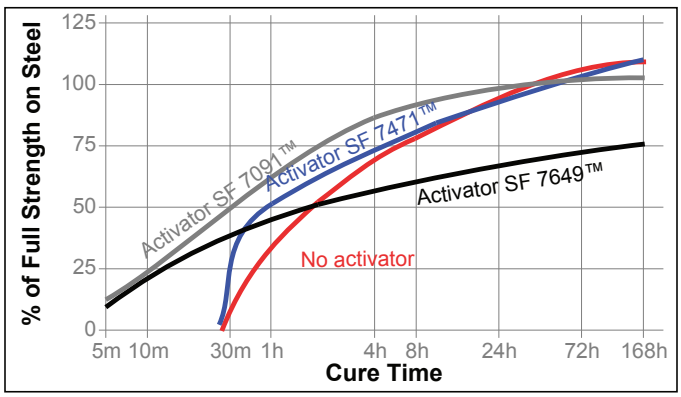

TYPICAL PROPERTIES OF CURED MATERIAL

Physical Properties:

Glass Transition Temperature ISO 11359-2, °C	76
Coefficient of Thermal Expansion, ISO 11359-2, K^{-1}:	
Below Tg	96×10^{-06}
Above Tg	192×10^{-06}

TYPICAL PERFORMANCE OF CURED MATERIAL

Adhesive Properties

After 15 minutes @ 22 °C
Compressive Shear Strength, ISO 10123:

Steel pins and collars	N/mm²	≥13.5[LMS]
	(psi)	(1,960)

After 24 hours @ 22 °C
Compressive Shear Strength, ISO 10123:

Steel pins and collars	N/mm²	≥25[LMS]
	(psi)	(3,625)

After 7 days @ 22 °C
Compressive Shear Strength, ISO 10123:

Steel pins and collars	N/mm²	29
	(psi)	(4,200)
Stainless Steel pins and collars	N/mm²	28
	(psi)	(3,990)
Aluminum pins and collars	N/mm²	17
	(psi)	(2,710)

After 24 hours @ 22 °C
Breakaway Torque, ISO 10964:

M10 black oxide bolts and mild steel nuts	N·m	57
	(lb.in.)	(505)
3/8 x 16 steel nuts (grade 2) and bolts (grade 5)	N·m	25
	(lb.in.)	(220)

Prevail Torque, ISO 10964:

M10 black oxide bolts and mild steel nuts	N·m	22
	(lb.in.)	(195)
3/8 x 16 steel nuts (grade 2) and bolts (grade 5)	N·m	9.4
	(lb.in.)	(85)

Breakloose Torque, ISO 10964, Pre-torqued to 5 N·m:

3/8 x 16 steel nuts (grade 2) and bolts (grade 5)	N·m	23
	(lb.in.)	(205)

Prevail Torque, ISO 10964, Pre-torqued to 5 N·m:

3/8 x 16 steel nuts (grade 2) and bolts (grade 5)	N·m	12
	(lb.in.)	(105)

TYPICAL ENVIRONMENTAL RESISTANCE

Cured for 1 week @ 22 °C
Compressive Shear Strength, ISO 10123:
Steel pins and collars

Hot Strength
Tested at temperature

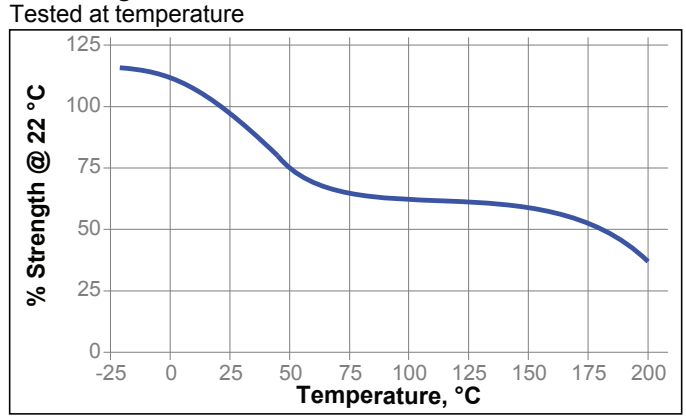

Cold Strength
This product has been tested to -75°C (-100 F). This product may work below this temperature, but has not been tested.

Heat Aging
Aged at temperature indicated and tested @ 22 °C

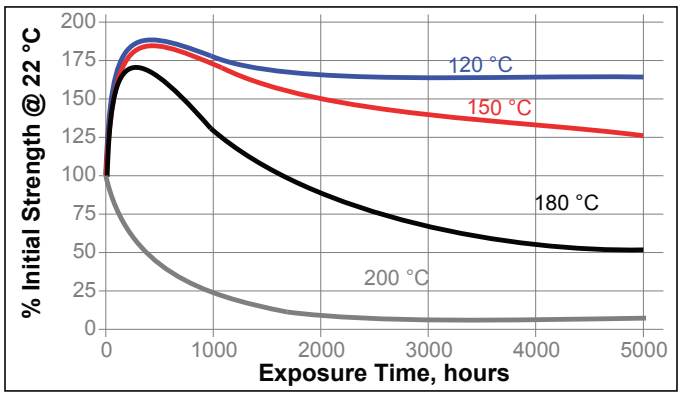

Stainless Steel pins and collars

		% of initial strength			
Environment	**°C**	**500 h**	**1000 h**	**3000 h**	**5000 h**
Sodium Hydroxide, 20%	22	100	85	60	55
Phosphoric Acid, 10%	22	95	70	40	40

Chemical/Solvent Resistance
Aged under conditions indicated and tested @ 22 °C.

		% of initial strength			
Environment	**°C**	**500 h**	**1000 h**	**3000 h**	**5000 h**
Motor oil (5W40 -Synthetic)	125	175	165	165	165
Unleaded Petrol	22	105	105	105	105
Brake fluid	22	120	115	115	115
Water/glycol 50/50	87	145	145	145	145
Ethanol	22	110	110	100	100
Acetone	22	105	105	105	105
B100 Bio-Diesel	22	115	115	115	115
DEF (AdBlue®)	22	115	105	105	105

GENERAL INFORMATION

This product is not recommended for use in pure oxygen and/or oxygen rich systems and should not be selected as a sealant for chlorine or other strong oxidizing materials.

For safe handling information on this product, consult the Safety Data Sheet (SDS).

Where aqueous washing systems are used to clean the surfaces before bonding, it is important to check for compatibility of the washing solution with the adhesive. In some cases these aqueous washes can affect the cure and performance of the adhesive.

This product is not normally recommended for use on plastics (particularly thermoplastic materials where stress cracking of the plastic could result). Users are recommended to confirm compatibility of the product with such substrates.

Directions for use:

For Assembly

1. For best results, clean all surfaces (external and internal) with a LOCTITE® cleaning solvent and allow to dry.
2. To accelerate cure speed or where large gaps are present, use activator and allow to dry.
3. **For Slip Fitted Assemblies**, apply adhesive around the leading edge of the pin and the inside of the collar and use a rotating motion during assembly to ensure good coverage.
4. **For Press Fitted Assemblies**, apply adhesive thoroughly to both bond surfaces and assemble at high press on rates.
5. **For Shrink Fitted Assemblies,** the adhesive should be coated onto the part to produce a smooth, even film of material. If heating the hub for assembly, coat the pin. If the pin is to be cooled for assembly, coat the hub. If both heating and cooling is to be done, apply material to cooled part. Avoid condensation on cooled parts.
6. Parts should not be disturbed until sufficient handling strength is achieved.

For Disassembly

1. Remove with standard hand tools.
2. If needed, apply localized heat to the assembly to approximately 250 °C. Disassemble while hot.
3. If this temperature is not possible, heat as much as possible and use mechanical aids.

For Cleanup

1. Cured product can be removed with a combination of soaking in a LOCTITE® solvent and mechanical abrasion such as a wire brush.

Loctite Material Specification[LMS]
LMS dated July 11, 2013. Test reports for each batch are available for the indicated properties. LMS test reports include selected QC test parameters considered appropriate to specifications for customer use. Additionally, comprehensive controls are in place to assure product quality and consistency. Special customer specification requirements may be coordinated through Henkel Quality.

Storage
Store product in the unopened container in a dry location. Storage information may be indicated on the product container labeling.
Optimal Storage: 8 °C to 21 °C. Storage below 8 °C or greater than 28 °C can adversely affect product properties. Material removed from containers may be contaminated during use. Do not return product to the original container. Henkel Corporation cannot assume responsibility for product which has been contaminated or stored under conditions other than those previously indicated. If additional information is required, please contact your local Technical Service Center or Customer Service Representative.

Conversions

(°C x 1.8) + 32 = °F
kV/mm x 25.4 = V/mil
mm / 25.4 = inches
µm / 25.4 = mil
N x 0.225 = lb
N/mm x 5.71 = lb/in
N/mm² x 145 = psi
MPa x 145 = psi
N·m x 8.851 = lb·in
N·m x 0.738 = lb·ft
N·mm x 0.142 = oz·in
mPa·s = cP

Manufacturing Date Reference

This Technical Data Sheet is valid for LOCTITE® 638™ manufactured from the dates below:

Made in:	First manufacturing date:
U.S.A.	September 2013
EU	Pending
China	August 2013
Brazil	November 2013
India	Pending

Note:
The information provided in this Technical Data Sheet (TDS) including the recommendations for use and application of the product are based on our knowledge and experience of the product as at the date of this TDS. The product can have a variety of different applications as well as differing application and working conditions in your environment that are beyond our control. Henkel is, therefore, not liable for the suitability of our product for the production processes and conditions in respect of which you use them, as well as the intended applications and results. We strongly recommend that you carry out your own prior trials to confirm such suitability of our product.
Any liability in respect of the information in the Technical Data Sheet or any other written or oral recommendation(s) regarding the concerned product is excluded, except if otherwise explicitly agreed and except in relation to death or personal injury caused by our negligence and any liability under any applicable mandatory product liability law.

In case products are delivered by Henkel Belgium NV, Henkel Electronic Materials NV, Henkel Nederland BV, Henkel Technologies France SAS and Henkel France SA please additionally note the following:
In case Henkel would be nevertheless held liable, on whatever legal ground, Henkel's liability will in no event exceed the amount of the concerned delivery.

In case products are delivered by Henkel Colombiana, S.A.S. the following disclaimer is applicable:
The information provided in this Technical Data Sheet (TDS) including the recommendations for use and application of the product are based on our knowledge and experience of the product as at the date of this TDS. Henkel is, therefore, not liable for the suitability of our product for the production processes and conditions in respect of which you use them, as well as the intended applications and results. We strongly recommend that you carry out your own prior trials to confirm such suitability of our product.
Any liability in respect of the information in the Technical Data Sheet or any other written or oral recommendation(s) regarding the concerned product is excluded, except if otherwise explicitly agreed and except in relation to death or personal injury caused by our negligence and any liability under any applicable mandatory product liability law.

In case products are delivered by Henkel Corporation, Resin Technology Group, Inc., or Henkel Canada Corporation, the following disclaimer is applicable:
The data contained herein are furnished for information only and are believed to be reliable. We cannot assume responsibility for the results obtained by others over whose methods we have no control. It is the user's responsibility to determine suitability for the user's purpose of any production methods mentioned herein and to adopt such precautions as may be advisable for the protection of property and of persons against any hazards that may be involved in the handling and use thereof. In light of the foregoing, **Henkel Corporation specifically disclaims all warranties expressed or implied, including warranties of merchantability or fitness for a particular purpose, arising from sale or use of Henkel Corporation's products. Henkel Corporation specifically disclaims any liability for consequential or incidental damages of any kind, including lost profits.** The discussion herein of various processes or compositions is not to be interpreted as representation that they are free from domination of patents owned by others or as a license under any Henkel Corporation patents that may cover such processes or compositions. We recommend that each prospective user test his proposed application before repetitive use, using this data as a guide. This product may be covered by one or more United States or foreign patents or patent applications.

Trademark usage

Reference N/A

6.36 Datasheet LOCTITE® 648™

Technical Data Sheet

LOCTITE® 638™

(TDS for the new formulation of LOCTITE® 638™) August 2016

PRODUCT DESCRIPTION

LOCTITE® 638™ provides the following product characteristics:

Technology	Acrylic
Chemical Type	Urethane methacrylate
Appearance (uncured)	Green liquid[LMS]
Fluorescence	Positive under UV light[LMS]
Components	One component - requires no mixing
Viscosity	High
Cure	Anaerobic
Secondary Cure	Activator
Application	Retaining
Strength	High

This Technical Data Sheet is valid for LOCTITE® 638™ manufactured from the dates outlined in the "Manufacturing Date Reference" section.

LOCTITE® 638™ is designed for the bonding of cylindrical fitting parts, particularly where bond gaps can approach 0.25 mm and where maximum strength at room temperature is required. The product cures when confined in the absence of air between close fitting metal surfaces and prevents loosening and leakage from shock and vibration. Typical applications include locking bushings and sleeves into housings and on shafts. LOCTITE® 638™ provides robust curing performance. It not only works on active metals (e.g. mild steel) but also on passive substrates such as stainless steel and plated surfaces. The product offers high temperature performance and oil tolerance. It tolerates minor surface contaminations from various oils, such as cutting, lubrication, anti-corrosion and protection fluids.

NSF International
Registered to NSF Category P1 for use as a sealant where there is no possibilty of food contact in and around food processing areas. **Note:** This is a regional approval. Please contact your local Technical Service Center for more information and clarification.

TYPICAL PROPERTIES OF UNCURED MATERIAL

Specific Gravity @ 25 °C	1.1
Flash Point - See SDS	
Viscosity, Brookfield - RVT, 25 °C, mPa·s (cP):	
Spindle 3, speed 20 rpm	2,000 to 3,000[LMS]
Viscosity, Cone & Plate, 25 °C, mPa·s (cP):	
Shear rate 129 s^{-1}	1,900 to 3,100

TYPICAL CURING PERFORMANCE

Cure Speed vs. Substrate

The rate of cure will depend on the substrate used. The graph below shows the shear strength developed with time on steel pins and collars compared to different materials and tested according to ISO 10123.

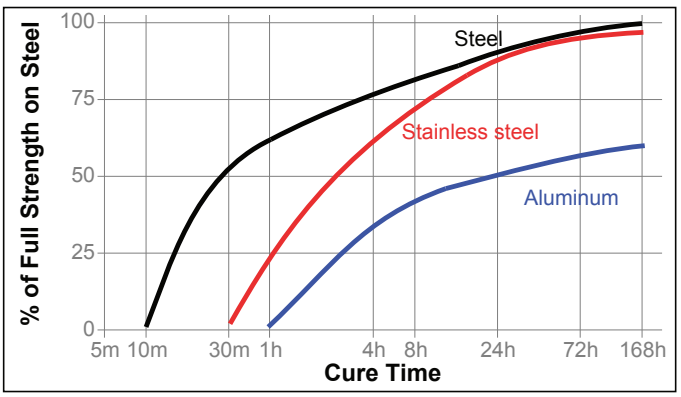

Cure Speed vs. Bond Gap

The rate of cure will depend on the bondline gap. The following graph shows shear strength developed with time on steel pins and collars at different controlled gaps and tested according to ISO 10123.

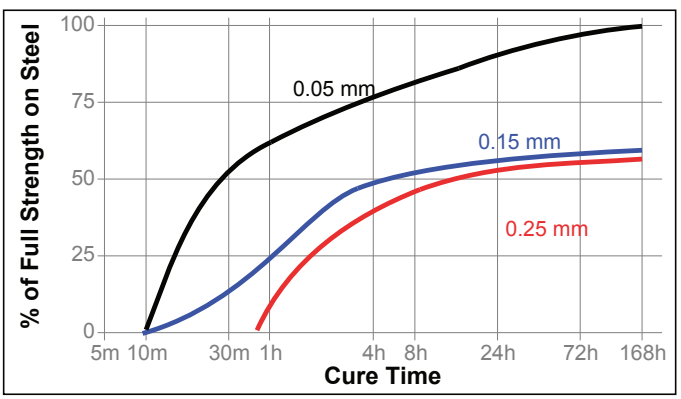

Cure Speed vs. Temperature

The rate of cure will depend on the temperature. The graph below shows the shear strength developed with time at different temperatures on steel pins and collars and tested according to ISO 10123.

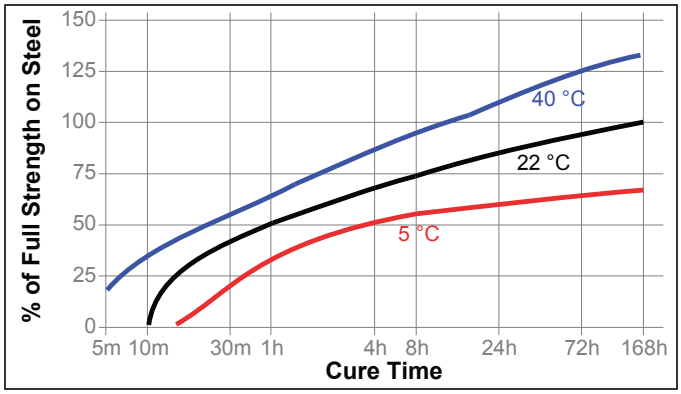

Cure Speed vs. Activator

The graph below shows the shear strength developed with time on stainless steel pins and collars using Activator SF 7471™, SF 7649™ and SF 7091™ and tested according to ISO 10123.

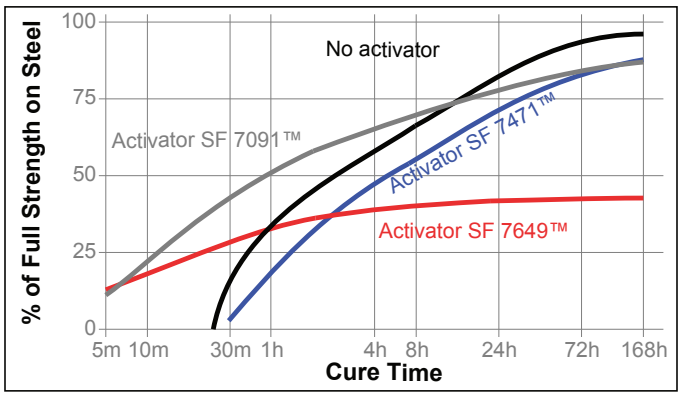

TYPICAL PROPERTIES OF CURED MATERIAL

Physical Properties:

Glass Transition Temperature ISO 11359-2, °C	100
Coefficient of Thermal Expansion, ISO 11359-2 K^{-1}:	
Below Tg	93×10^{-06}
Above Tg	184×10^{-06}

TYPICAL PERFORMANCE OF CURED MATERIAL

Adhesive Properties

Cured for 15 minutes @ 22 °C

Compressive Shear Strength, ISO 10123:

Steel pins and collars	N/mm²	≥13.5[LMS]
	(psi)	(1,960)

Cured for 24 hours @ 22 °C

Compressive Shear Strength, ISO 10123:

Steel pins and collars	N/mm²	≥25[LMS]
	(psi)	(≥3,625)

Cured for 7 days @ 22°C

Compressive Shear Strength, ISO 10123:

Steel pins and collars	N/mm²	31
	(psi)	(4,480)
Stainless Steel pins and collars	N/mm²	30
	(psi)	(4,350)
Aluminum pins and collars	N/mm²	18
	(psi)	(2,610)

Cured for 24 hours @ 22 °C

Breakaway Torque, ISO 10964:

M10 black oxide bolts and mild steel nuts	N·m	58
	(lb.in.)	(515)
3/8 x 16 steel nuts (grade 2) and bolts (grade 5)	N·m	32
	(lb.in.)	(285)

Prevail Torque, ISO 10964:

M10 black oxide bolts and mild steel nuts	N·m	40
	(lb.in.)	(355)
3/8 x 16 steel nuts (grade 2) and bolts (grade 5)	N·m	16
	(lb.in.)	(140)

Breakloose Torque, ISO 10964, Pre-torqued to 5 N·m:

3/8 x 16 steel nuts (grade 2) and bolts (grade 5)	N·m	29
	(lb.in.)	(255)

Prevail Torque, ISO 10964, Pre-torqued to 5 N·m:

3/8 x 16 steel nuts (grade 2) and bolts (grade 5)	N·m	29
	(lb.in.)	(255)

TYPICAL ENVIRONMENTAL RESISTANCE

Cured for 1 week @ 22 °C

Compressive Shear Strength, ISO 10123:

Steel pins and collars

Hot Strength

Tested at temperature

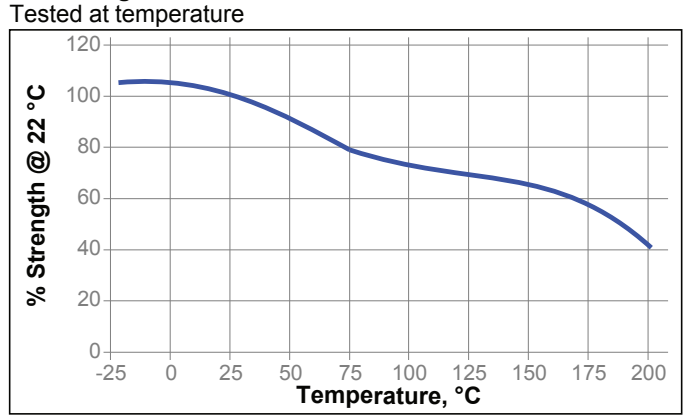

Cold Strength

This product has been tested to -75°C (-100 F). This product may work below this temperature, but has not been tested.

Heat Aging
Aged at temperature indicated and tested @ 22 °C

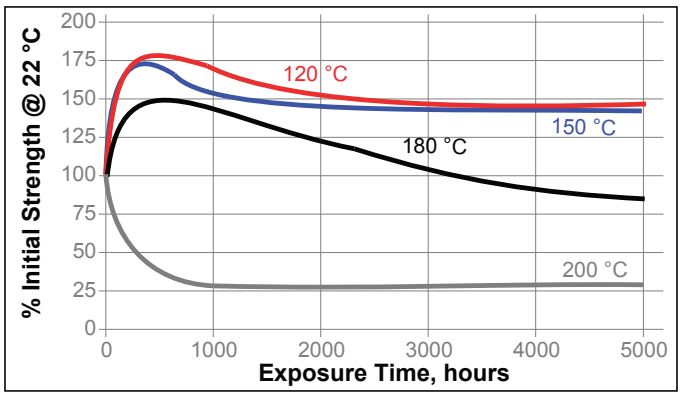

Chemical/Solvent Resistance
Aged under conditions indicated and tested @ 22 °C.

		% of initial strength			
Environment	**°C**	**500 h**	**1000 h**	**3000 h**	**5000 h**
Motor oil (5W40 -Synthetic)	125	170	165	150	145
Unleaded Petrol	22	130	130	110	105
Brake fluid	22	130	140	135	125
Water/glycol 50/50	87	85	80	80	80
Ethanol	22	130	130	125	120
Acetone	22	100	100	100	100
B100 Bio-Diesel	22	115	115	105	100
DEF (AdBlue®)	22	95	95	90	100

Stainless Steel pins and collars

		% of initial strength			
Environment	**°C**	**500 h**	**1000 h**	**3000 h**	**5000 h**
Sodium Hydroxide, 20%	22	115	105	95	90
Phosphoric Acid, 10%	22	75	60	40	35

GENERAL INFORMATION

This product is not recommended for use in pure oxygen and/or oxygen rich systems and should not be selected as a sealant for chlorine or other strong oxidizing materials.

For safe handling information on this product, consult the Safety Data Sheet (SDS).

Where aqueous washing systems are used to clean the surfaces before bonding, it is important to check for compatibility of the washing solution with the adhesive. In some cases these aqueous washes can affect the cure and performance of the adhesive.

This product is not normally recommended for use on plastics (particularly thermoplastic materials where stress cracking of the plastic could result). Users are recommended to confirm compatibility of the product with such substrates.

Directions for use:

For Assembly

1. For best results, clean all surfaces (external and internal) with a LOCTITE® cleaning solvent and allow to dry.
2. To accelerate cure speed or where large gaps are present, use activator and allow to dry.
3. **For Slip Fitted Assemblies**, apply adhesive around the leading edge of the pin and the inside of the collar and use a rotating motion during assembly to ensure good coverage.
4. **For Press Fitted Assemblies**, apply adhesive thoroughly to both bond surfaces and assemble at high press on rates.
5. **For Shrink Fitted Assemblies,** the adhesive should be coated onto the part to produce a smooth, even film of material. If heating the hub for assembly, coat the pin. If the pin is to be cooled for assembly, coat the hub. If both heating and cooling is to be done, apply material to cooled part. Avoid condensation on cooled parts.
6. Parts should not be disturbed until sufficient handling strength is achieved.

For Disassembly

1. Remove with standard hand tools.
2. If needed, apply localized heat to the assembly to approximately 250 °C. Disassemble while hot.
3. If this temperature is not possible, heat as much as possible and use mechanical aids.

For Cleanup

1. Cured product can be removed with a combination of soaking in a LOCTITE® solvent and mechanical abrasion such as a wire brush.

Loctite Material Specification[LMS]
LMS dated July 10, 2013. Test reports for each batch are available for the indicated properties. LMS test reports include selected QC test parameters considered appropriate to specifications for customer use. Additionally, comprehensive controls are in place to assure product quality and consistency. Special customer specification requirements may be coordinated through Henkel Quality.

Storage
Store product in the unopened container in a dry location. Storage information may be indicated on the product container labeling.
Optimal Storage: 8 °C to 21 °C. Storage below 8 °C or greater than 28 °C can adversely affect product properties. Material removed from containers may be contaminated during use. Do not return product to the original container. Henkel Corporation cannot assume responsibility for product which has been contaminated or stored under conditions other than those previously indicated. If additional information is required, please contact your local Technical Service Center or Customer Service Representative.

Conversions
(°C x 1.8) + 32 = °F
kV/mm x 25.4 = V/mil
mm / 25.4 = inches
µm / 25.4 = mil
N x 0.225 = lb
N/mm x 5.71 = lb/in
N/mm² x 145 = psi
MPa x 145 = psi

N·m x 8.851 = lb·in
N·m x 0.738 = lb·ft
N·mm x 0.142 = oz·in
mPa·s = cP

Manufacturing Date Reference

This Technical Data Sheet is valid for LOCTITE® 648™ manufactured from the dates below:

Made in:	First manufacturing date:
U.S.A.	September 2013
EU	Pending
China	August 2013
Brazil	November 2013
India	Pending

Note:
The information provided in this Technical Data Sheet (TDS) including the recommendations for use and application of the product are based on our knowledge and experience of the product as at the date of this TDS. The product can have a variety of different applications as well as differing application and working conditions in your environment that are beyond our control. Henkel is, therefore, not liable for the suitability of our product for the production processes and conditions in respect of which you use them, as well as the intended applications and results. We strongly recommend that you carry out your own prior trials to confirm such suitability of our product.
Any liability in respect of the information in the Technical Data Sheet or any other written or oral recommendation(s) regarding the concerned product is excluded, except if otherwise explicitly agreed and except in relation to death or personal injury caused by our negligence and any liability under any applicable mandatory product liability law.

In case products are delivered by Henkel Belgium NV, Henkel Electronic Materials NV, Henkel Nederland BV, Henkel Technologies France SAS and Henkel France SA please additionally note the following:
In case Henkel would be nevertheless held liable, on whatever legal ground, Henkel's liability will in no event exceed the amount of the concerned delivery.

In case products are delivered by Henkel Colombiana, S.A.S. the following disclaimer is applicable:
The information provided in this Technical Data Sheet (TDS) including the recommendations for use and application of the product are based on our knowledge and experience of the product as at the date of this TDS. Henkel is, therefore, not liable for the suitability of our product for the production processes and conditions in respect of which you use them, as well as the intended applications and results. We strongly recommend that you carry out your own prior trials to confirm such suitability of our product.
Any liability in respect of the information in the Technical Data Sheet or any other written or oral recommendation(s) regarding the concerned product is excluded, except if otherwise explicitly agreed and except in relation to death or personal injury caused by our negligence and any liability under any applicable mandatory product liability law.

In case products are delivered by Henkel Corporation, Resin Technology Group, Inc., or Henkel Canada Corporation, the following disclaimer is applicable:
The data contained herein are furnished for information only and are believed to be reliable. We cannot assume responsibility for the results obtained by others over whose methods we have no control. It is the user's responsibility to determine suitability for the user's purpose of any production methods mentioned herein and to adopt such precautions as may be advisable for the protection of property and of persons against any hazards that may be involved in the handling and use thereof. In light of the foregoing, **Henkel Corporation specifically disclaims all warranties expressed or implied, including warranties of merchantability or fitness for a particular purpose, arising from sale or use of Henkel Corporation's products. Henkel Corporation specifically disclaims any liability for consequential or incidental damages of any kind, including lost profits.** The discussion herein of various processes or compositions is not to be interpreted as representation that they are free from domination of patents owned by others or as a license under any Henkel Corporation patents that may cover such processes or compositions. We recommend that each prospective user test his proposed application before repetitive use, using this data as a guide. This product may be covered by one or more United States or foreign patents or patent applications.

Reference N/A

6.37 Showcase model's BOM

	Qty	Part code	Code
DNR showcase		pnsax.xx.x-x	
DNR subsystem		pnsa1	
Planetary gear set assy	1	pnsa110	
Planet carrier welding assembly	1	pnsa1101	
Planet thrust washer	6	pnsa1102	
Needle bearing	6	pnsa1103	
Planet gear	3	pnsa1104	
Planetary pin	3	pnsa1105	
Turbine shaft assembly	1	pnsa120	
Clutch carrier welded assembly	1	pnsa1201	
Clutch carrier		pnsa1201-1	
Turbine shaft		pnsa1201-2	
Piston forward clutch	1	pnsa1202	
Forward spring pack	1	pnsa1203	
Spring pack		pnsa1203_1	
Springs		pnsa1203-2	
Ball transfer unit adapter	6	pnsa1203-3	
Compensation chamber forward clutch	1	pnsa1204	
Snap ring compensation chamber forward clutch	1	pnsa1205	
Wavy washer forward clutch	1	pnsa1206	
Forward separator plate	3	pnsa1207	
Friction plate forward clutch	3	pnsa1208	
Endplate forward clutch	1	pnsa1209	
Snap ring forward clutch	1	pnsa12010	
Ring rear	1	pnsa12011	
Snap ring forward clutch narrow	1	pnsa12012	
Seal	3	pnsa12013	
Seal	1	pnsa12014	
Reverse clutch		pnsa130	
Reverse piston	1	pnsa1301	
Spring pack reverse clutch	1	pnsa1302	
Snap ring reverse piston	1	pnsa1303	
Disc spring reverse clutch	1	pnsa1304	
Reverse separator plate	1	pnsa1305	
Friction plate reverse clutch	2	pnsa1306	
Endplate reverse clutch	1	pnsa1307	
Snap ring reverse clutch	1	pnsa1308	
Needle roller thrust bearing	4	pnsa1309	
Sun gear assembly	1	pnsa1311	
Structure	1	pnsa2	
Platform	1	pnsa210	
Main plate	1	pnsa2101	
Table legs	2	pnsa2102	
DNR Housing	1	pnsa2103	
DNR Housing 1	1	pnsa2103_1	
DNR Housing 2	1	pnsa2103_2	
Spring pin	2	PNSA2104	SSPR5-14
Side cover	2	pnsa2107	
Spring pin	6	PNSA2104	SSPR5-14
Bearing		pnsa250	
Bushing support	1	pnsa270	
Support	1	pnsa2701	
Bushing	1	pnsa2702	
Safety cage	1	pnsa280	
Bottom plate	1	PNSA290	
Mechanism		pnsa3	
Gear selector system		pnsa310	
Gear selector	1	pnsa3102	
Cover	1	pnsa3102_1	
selector shaft	1	pnsa3102_2	
Joining	1	pnsa3102_5	
Secondary shaft	1	pnsa3102_6	
Car gear selector	1	pnsa3102_7	
Spring plunger	4	pnsa3102_10	PJLS 10-5
Support	1	pnsa3102_11	
Shoulder screw	1	pnsa3102_12	MSB6 - 40 - F7
Square nut	4	pnsa3102_13	FKTS25 - A16 - P7
Hex socket set screws	4	pnsa3102_14	MSSF5-6
Activating system Forward clutch		pnsa330	
Ball transfer units	6	PNSA3301_1	95180-2208
Forward pressing plate	1	pnsa3302	
Ring	1	pnsa3302-1	
Stopper	1	pnsa3302-2	FSWNF 15 - 10 - 35
Shims	4	pnsa3302-3	

Pressing plate	1	pnsa3302-5	
Cam system	1	pnsa 3306	
FWD Cam	1	pnsa3306_1	
Bearing	1	pnsa3306_4	B6004ZZ
Shoulder screw	1	PNSA3403_3	DBGB 5 - 5 - 8
Activating system Reverse clutch		pnsa340	
Reverse pressing plate		pnsa3401	
Reverse pressing plate	1	pnsa3401-1	
Pin	5	pnsa3401-2	
Stopper	1	pnsa3302-2	FSWNF 15 - 10 - 35
Shims	4	pnsa3302-3	
Nuts	5	PNSA3401_3	KNTR4
reverse guiding system	1	pnsa3402	
Reverse plate	1	pnsa3402_1	
Guiding trails	4	PNSA3702	LHBB 16
Shaft supports	2	PNSA3704	SHSBK 16-40
Spring pin	2	PNSA2104	SSPR5-14
Reverse cam system	1	PNSA3403	
Bearing	1	pnsa3306_4	B6004ZZ
Reverse cam	1	PNSA3403_1	
Shoulder screw	1	PNSA3403_3	DBGB 5 - 5 - 8
Lever system		pnsa360	
Transmission plate	1	pnsa3601	
Transmission blocks	4	pnsa3608	
Forward Guiding system	1	pnsa370	
Fwd plate	1	pnsa3701	
Linear bushing	4	pnsa3702	LHBB 16
Shafts	2	pnsa3703	SPJ16 - 420
Shaft supports	4	pnsa3704	SHSBK 16-40
Spring pin	2	PNSA2104	SSPR5-14
Handwheel	1	pnsa380	PHSFM 150-15
Primary shaft	1	PNSA390	
Primary shaft bushing	1	PNSA400	

6.38 Poster

6.39 Showcase photos

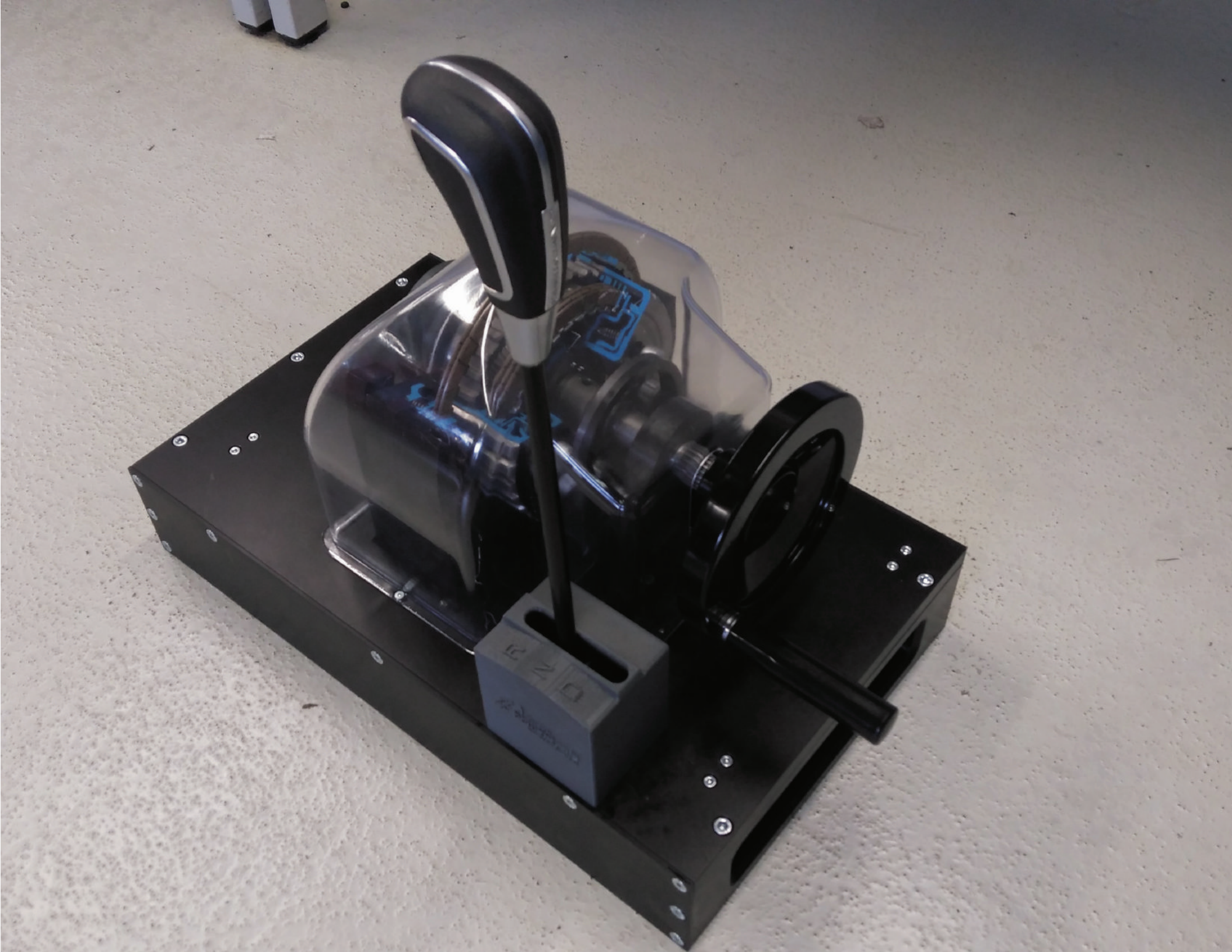

6.41 Technical drawings of individual parts of the showcase model

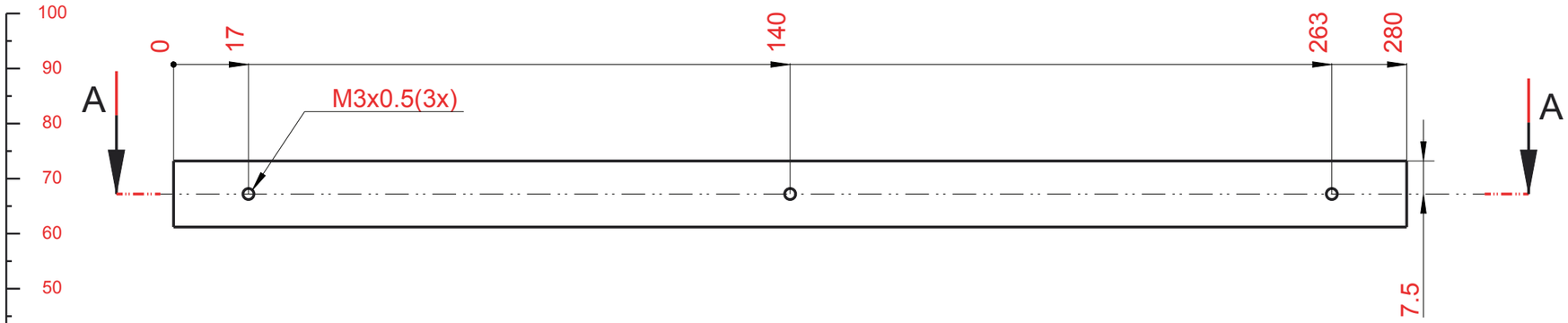

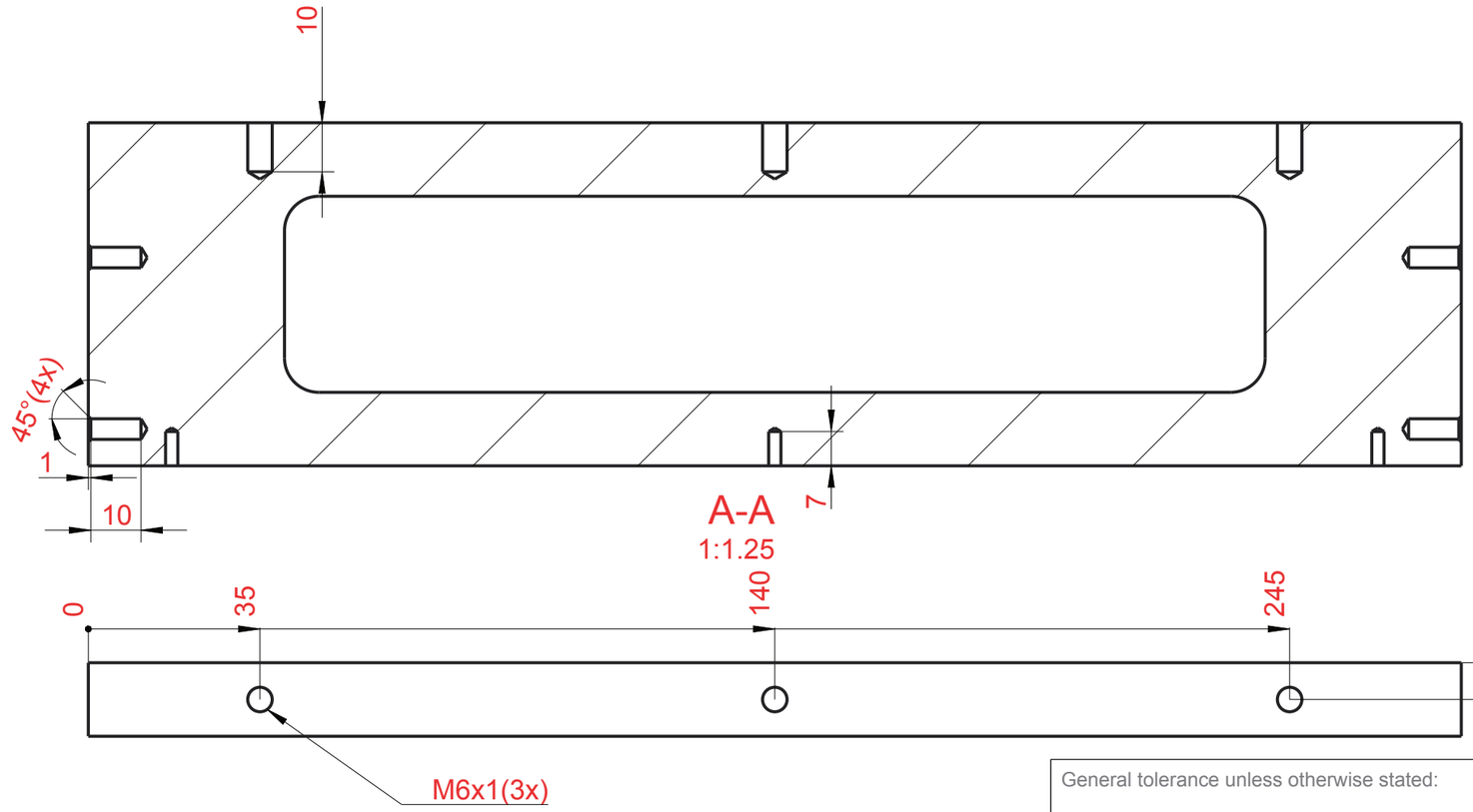

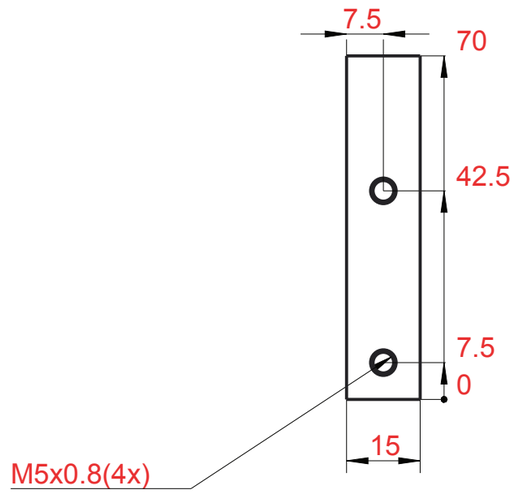

For missing dimensions, please check 3D file and apply general dimensional tolerances
Surface treatment: Black anodising

General tolerance unless otherwise stated: DIN ISO 2768 - mH	General surface roughness unless otherwise stated:	
Material: Alu	Date: 10-May-17	Surf. roughness acc. to ISO 1302
	Drawn: Pedro Almeida	CAD system: Creo Parametric; Sheet: 1 of 2
Name: Table legs	Design Resp.: Rudi Aerts	Copied from; Scale: 1:1; Mass: ( )kg
This drawing is property of Punch Powertrain NV and can't be used, copied or shown to third parties without written permission.	Article number: PNSA2102	Index: 0
PUNCH POWERTRAIN NV	Document number: PNSA2102	Index: 0; DIN: A3

model name: PNSA2102 [PART]

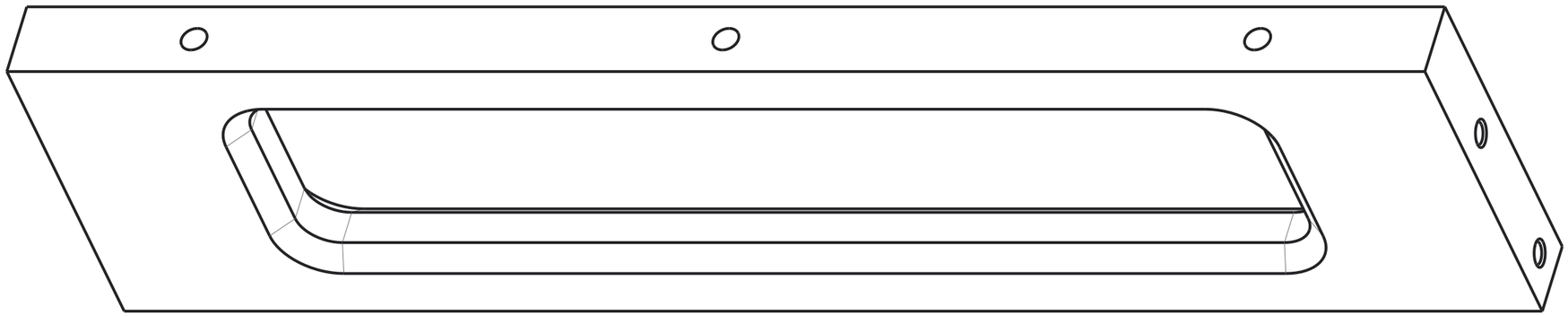

General tolerance unless otherwise stated: DIN ISO 2768 - mH	General surface roughness unless otherwise stated:		
Material: Alu	Date: 10-May-17	Surf. roughness acc. to ISO 1302	
	Drawn: Pedro Almeida	CAD system: Creo Parametric	Sheet: 2 of 2
Name: Table legs	Design Resp.: Rudi Aerts		
	Copied from: PNSA2102	Scale: 1:1	Mass: ( )kg
This drawing is property of Punch Powertrain NV and can't be used, copied or shown to third parties without written permission.	Article number: PNSA2102	Index: 0	
PUNCH POWERTRAIN NV	Document number: PNSA2102	Index: 0	DIN: A3

model name: PNSA2102 [PART]

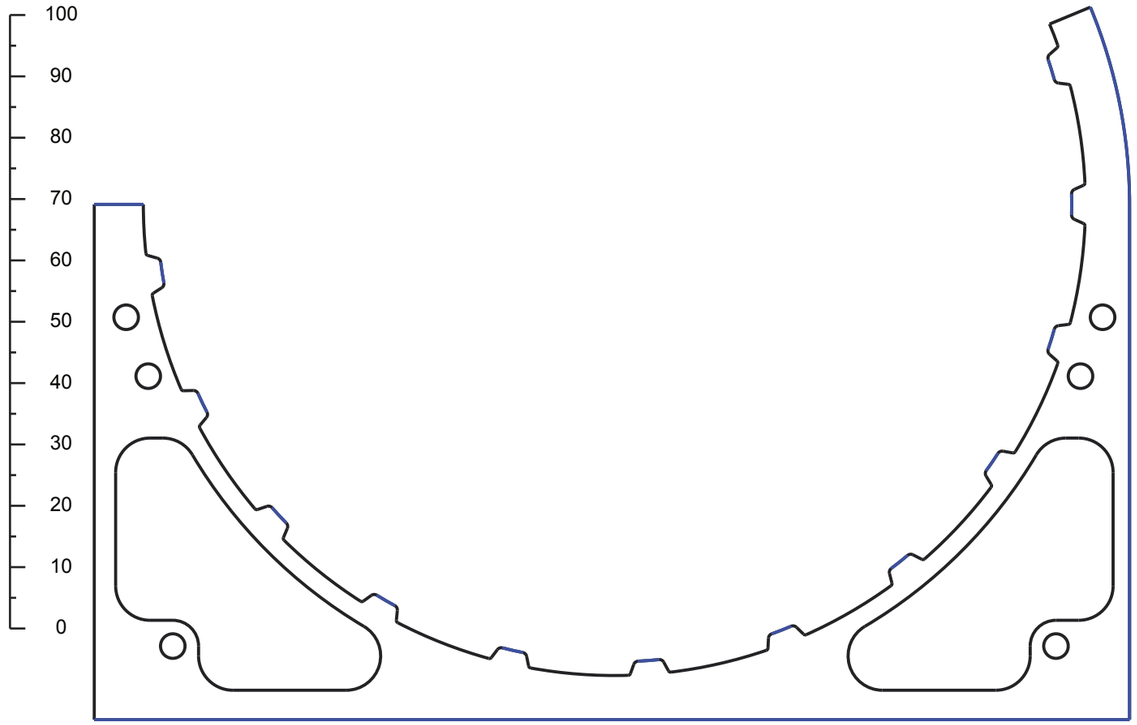

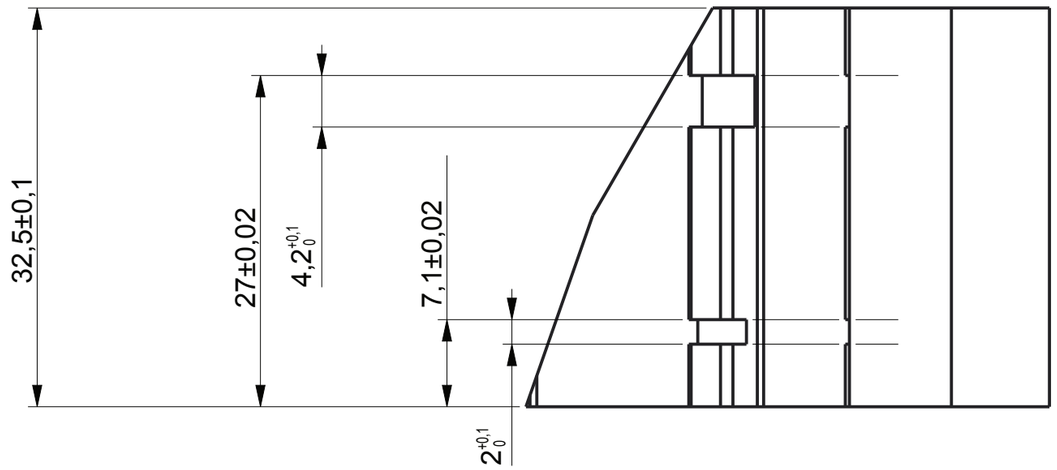

DETAIL A
SCALE 2,000

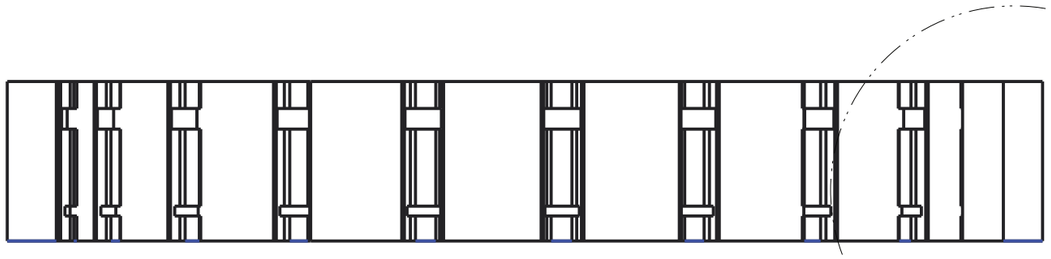

SCALE 0,800

SEE DETAIL A

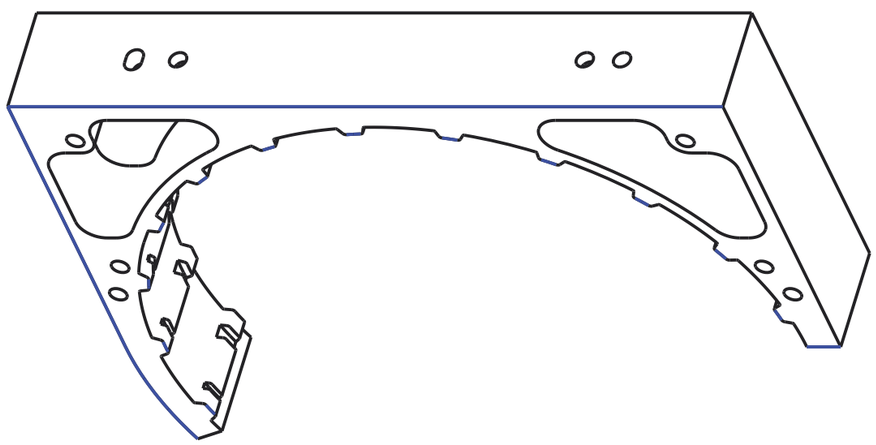

For missing dimensions, please check 3D file and apply general dimensional tolerances
Surface treatment: Black anodising

General tolerance unless otherwise stated: DIN ISO 2768 - mH	General surface roughness unless otherwise stated:		
Material: Alu	Date: 2017-05-05	Surf. roughness acc. to ISO 1302	
	Drawn: Pedro Almeida	CAD system: Creo Parametric	Sheet: 1 of 3
Name: DNR Housing 1	Design Resp.: Rudi Aerts	Copied from	Scale: 1,000 / Mass: ( )kg
This drawing is property of Punch Powertrain NV and can't be used, copied or shown to third parties without written permission.	Article number: PNSA2103_1	Index: 0	
PUNCH POWERTRAIN NV	Document number: PNSA2103_1	Index: 0	DIN: A3

model name: PNSA2103_1 [PART]

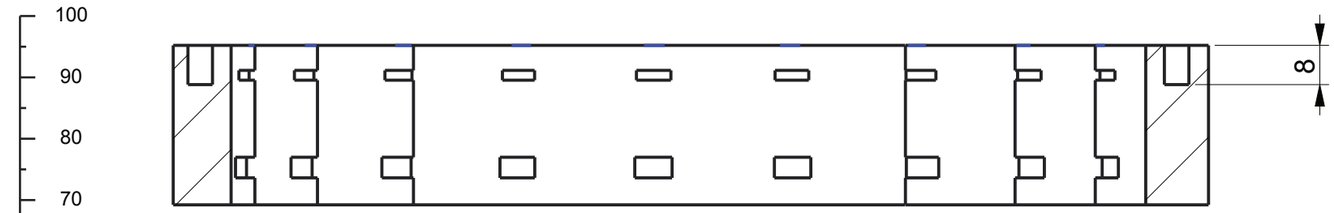

SECTION C-C

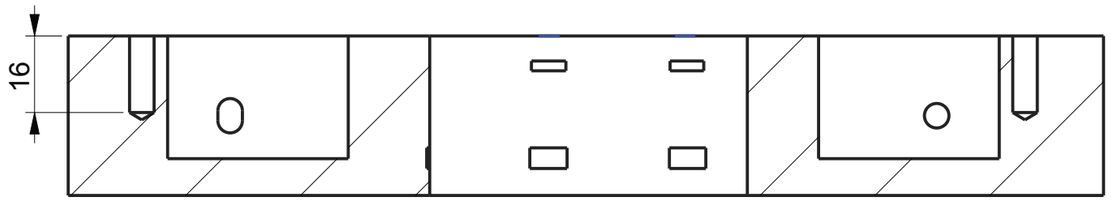

SECTION A-A

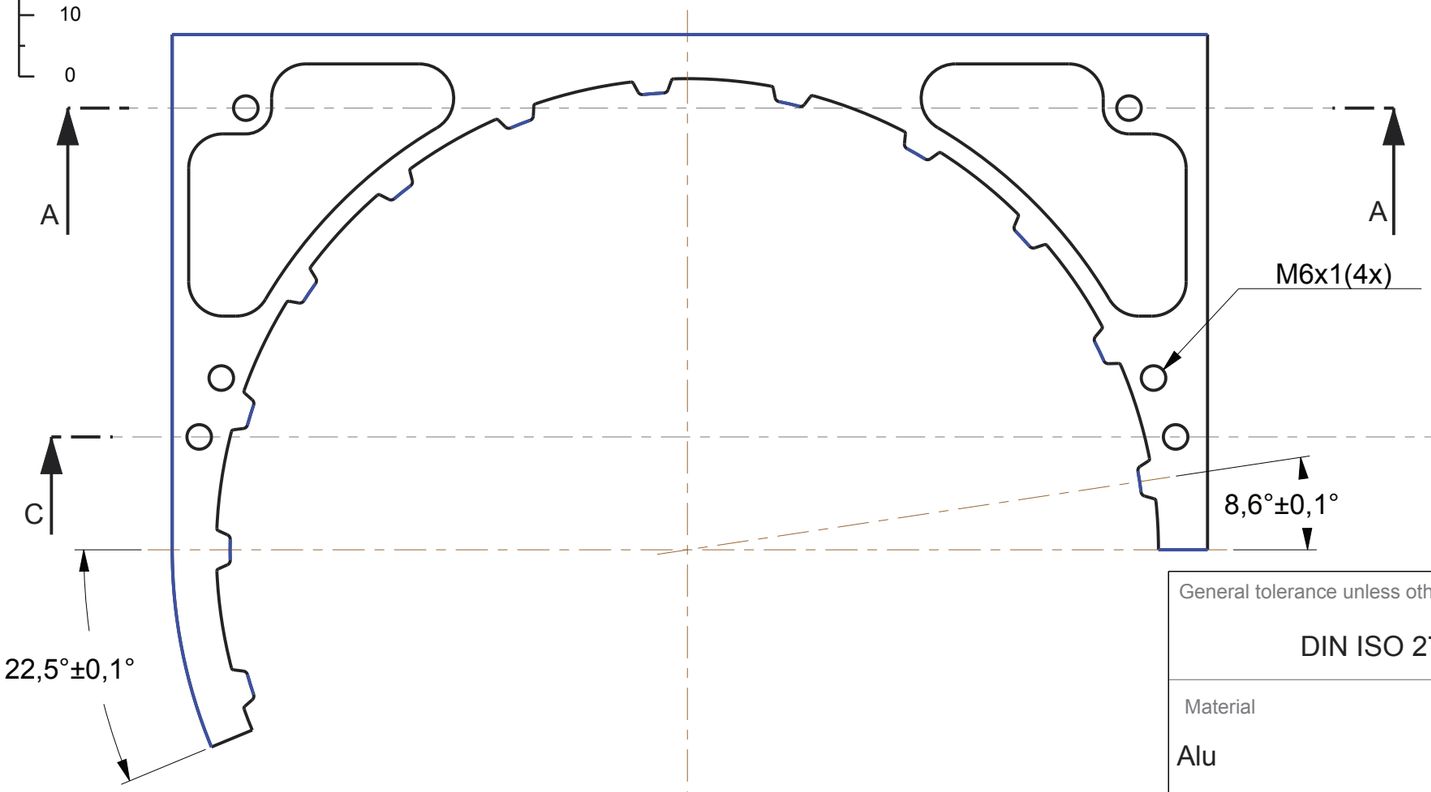

SCALE 0,800

General tolerance unless otherwise stated: DIN ISO 2768 - mH	General surface roughness unless otherwise stated:		
Material: Alu	Date: 2017-05-05	Surf. roughness acc. to ISO 1302	
	Drawn:	CAD system: Creo Parametric	Sheet: 2 of 3
Name	Design Resp.: Rudi Aerts		
	Copied from	Scale: 1,000	Mass: ( )kg
This drawing is property of Punch Powertrain NV and can't be used, copied or shown to third parties without written permission.	Article number	Index	
PUNCH POWERTRAIN NV	Document number: PNSA2103_1	Index: 0	DIN: A3

model name: PNSA2103_1 [PART]

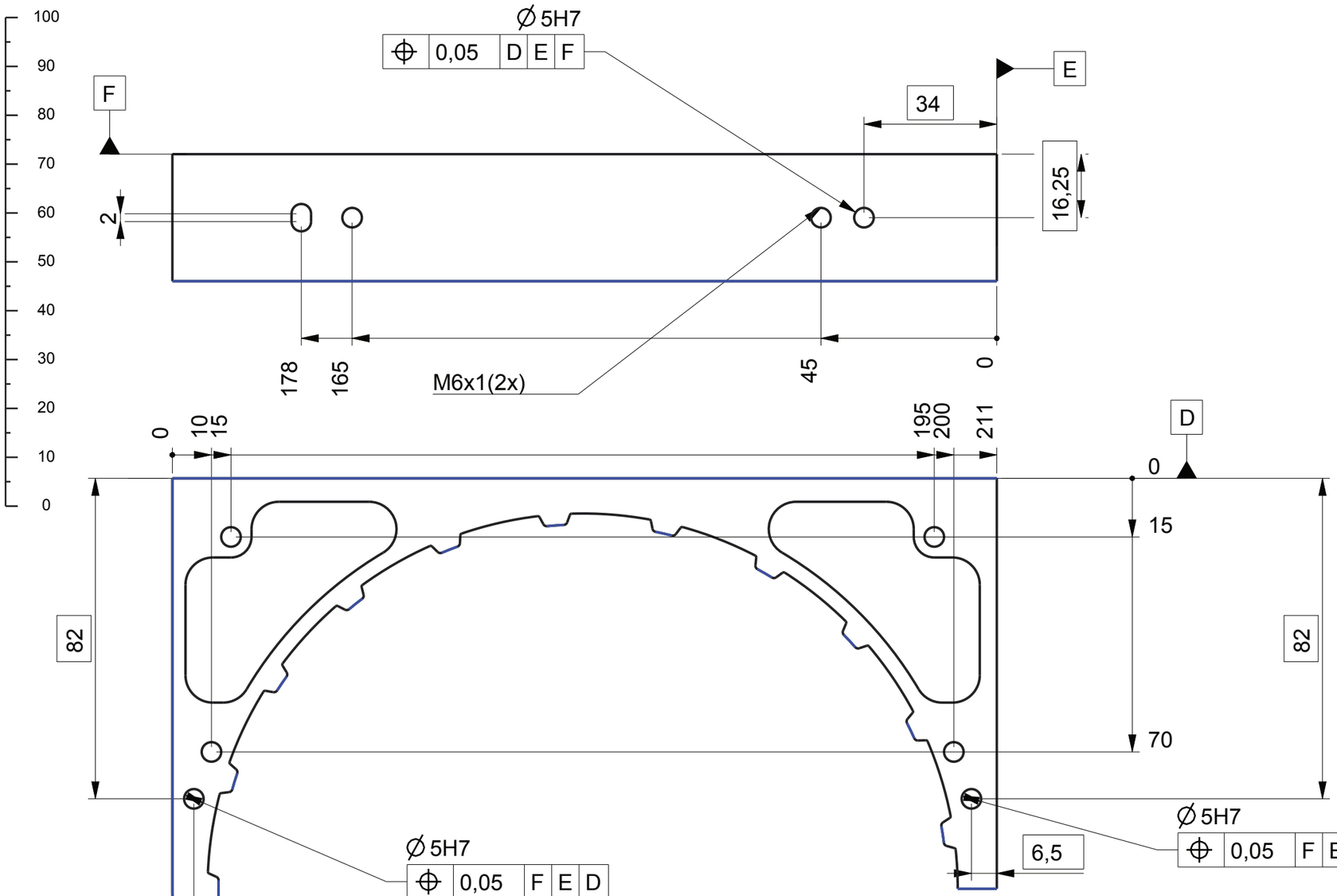

General tolerance unless otherwise stated: DIN ISO 2768 - mH	General surface roughness unless otherwise stated:		
Material: Alu	Date: 2017-05-05	Surf. roughness acc. to ISO 1302	
	Drawn:	CAD system: Creo Parametric	Sheet: 3 of 3
Name	Design Resp.: Rudi Aerts		
	Copied from	Scale: 1,000	Mass: ( )kg
This drawing is property of Punch Powertrain NV and can't be used, copied or shown to third parties without written permission.	Article number	Index	
PUNCH POWERTRAIN NV	Document number: PNSA2103_1	Index: 0	DIN: A3

model name: PNSA2103_1 [PART]

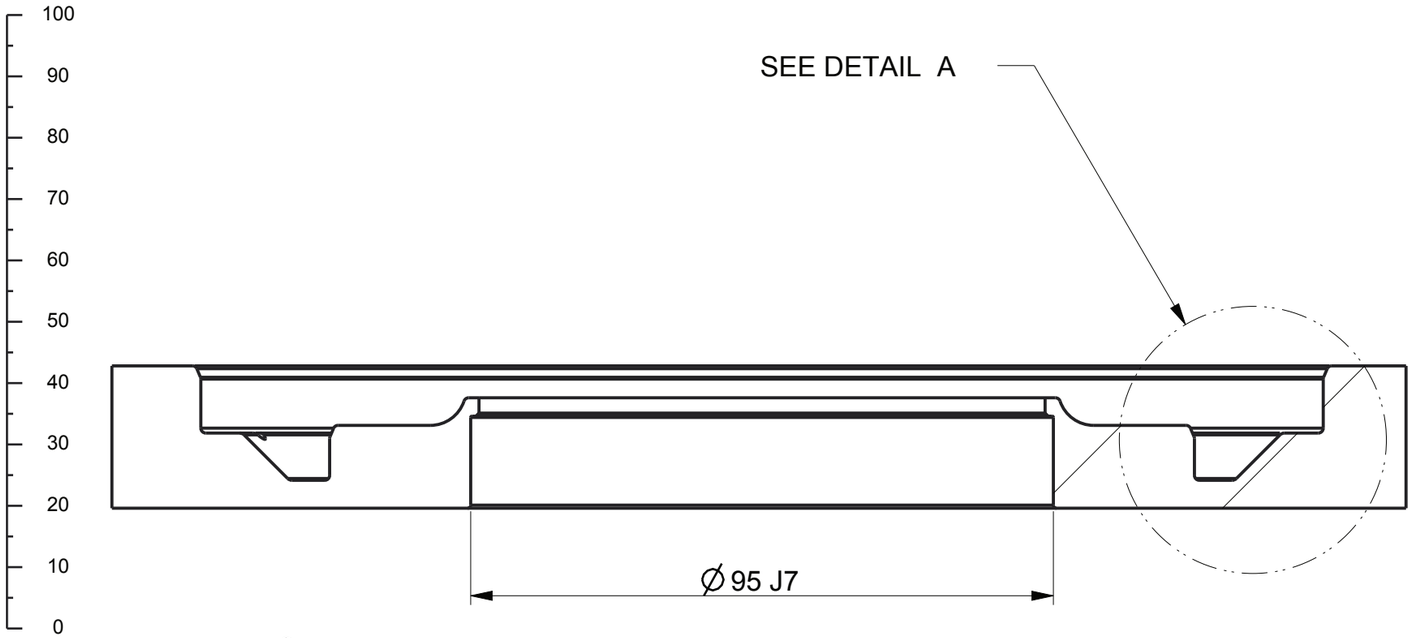

SECTION TOP-TOP

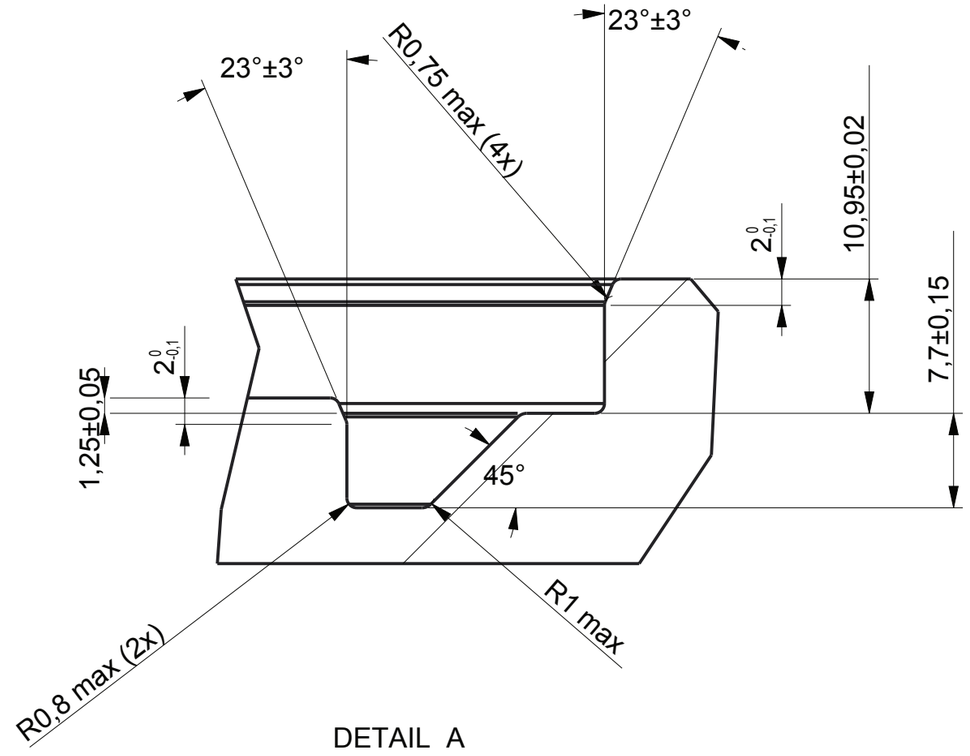

DETAIL A
SCALE 2,000

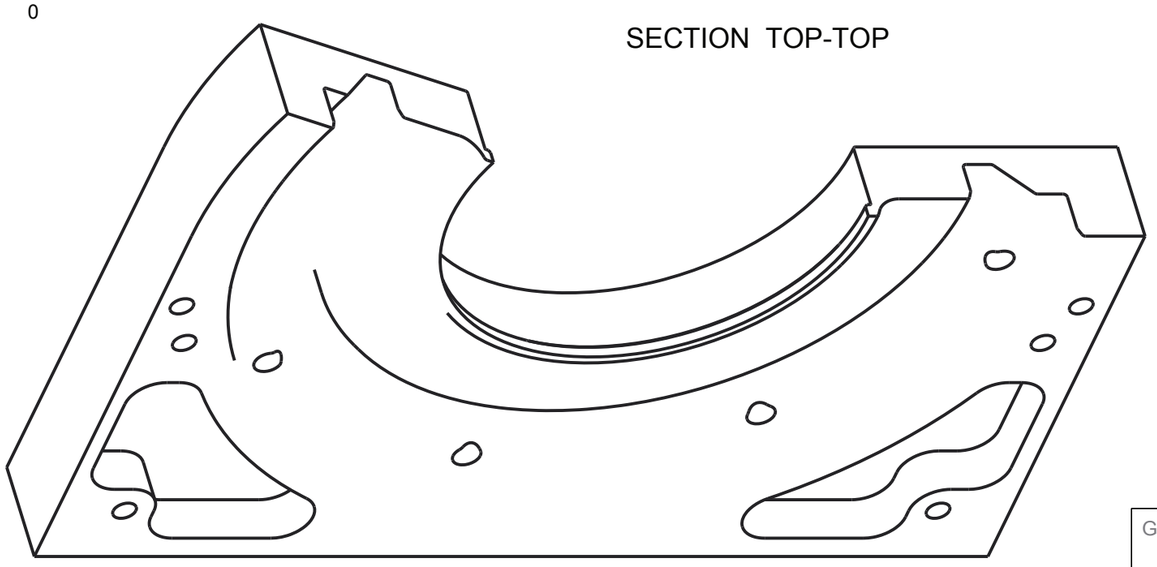

SCALE 0,800

For missing dimensions, please check 3D file and apply general dimensional tolerances
Surface treatment: Black anodising

General tolerance unless otherwise stated: DIN ISO 2768-mH	General surface roughness unless otherwise stated:		
Material: Alu	Date: 26-Apr-17	Surf. roughness acc. to ISO 1302	
	Drawn: Pedro Almeida	CAD system: Creo Parametric	Sheet: 1 of 2
Name: DNR Housing 2	Design Resp.: Rudi Aerts		
	Copied from	Scale: 1,000	Mass: ( )kg
This drawing is property of Punch Powertrain NV and can't be used, copied or shown to third parties without written permission.	Article number: PNSA2103_2	Index: 0	
PUNCH POWERTRAIN NV	Document number: PNSA2103_2	Index: 1	DIN: A3

model name: PNSA2103_2 [PART]

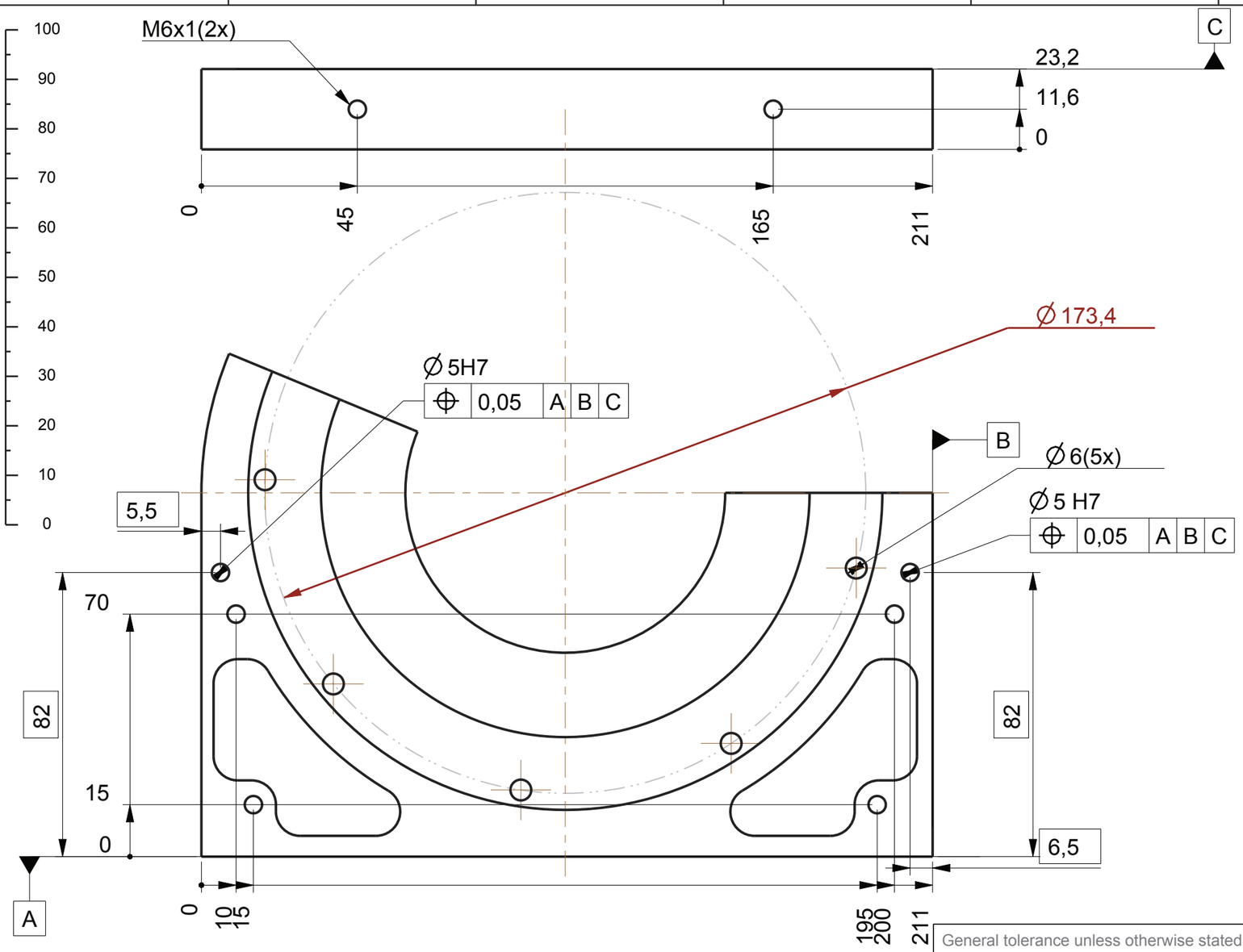

SCALE 0,700

General tolerance unless otherwise stated: DIN ISO 2768 - mH	General surface roughness unless otherwise stated:		
Material: Alu	Date: 26-Apr-17	Surf. roughness acc. to ISO 1302	
	Drawn: Pedro Almeida	CAD system: Creo Parametric	Sheet: 2 of 2
Name: DNR Housing 2	Design Resp.: Rudi Aerts		
	Copied from	Scale: 1,000	Mass: ( )kg
This drawing is property of Punch Powertrain NV and can't be used, copied or shown to third parties without written permission.	Article number: PNSA2103_2	Index: 0	
PUNCH POWERTRAIN NV	Document number: PNSA2103_2	Index: 1	DIN: A3

model name: PNSA2103_2 [PART]

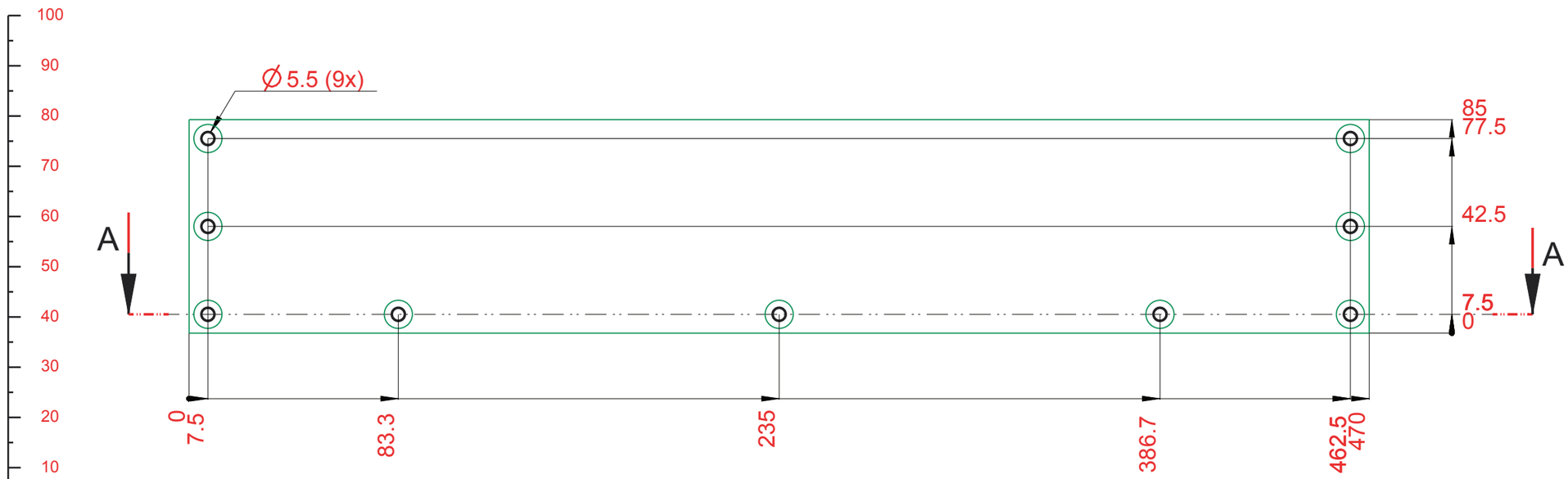

1:2

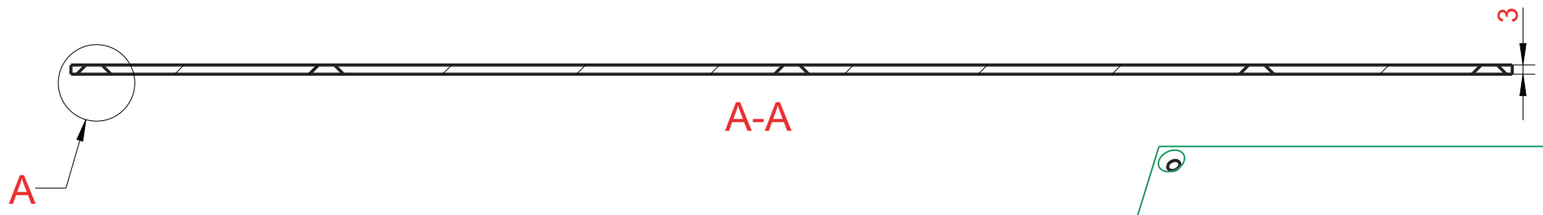

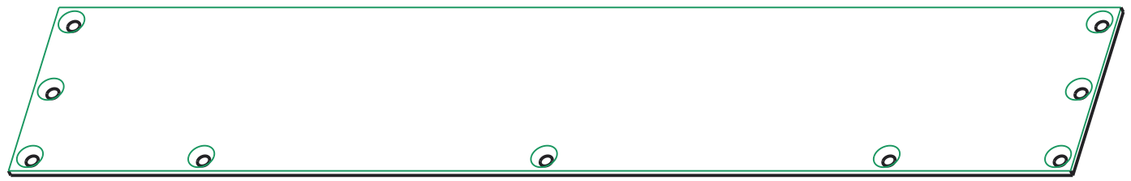

1:2.5

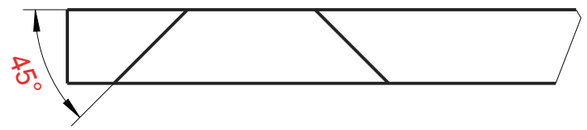

A
4:1

For missing dimensions, please check 3D file and apply general dimensional tolerances
Surface treatment: Black anodising

General tolerance unless otherwise stated: DIN ISO 2768 - mH	General surface roughness unless otherwise stated:			
Material: Alu	Date: 30-May-17		Surf. roughness acc. to ISO 1302	
	Drawn: Pedro Almeida		CAD system: Creo Parametric	Sheet: 1 of 1
Name: Side cover	Design Resp.: Rudi Aerts			
	Copied from		Scale: 1:1	Mass: ( )kg
This drawing is property of Punch Powertrain NV and can't be used, copied or shown to third parties without written permission.	Article number: PNSA2107		Index: 0	
PUNCH POWERTRAIN NV	Document number: PNSA2107		Index: 0	DIN: A3

model name: PNSA2107 [PART]

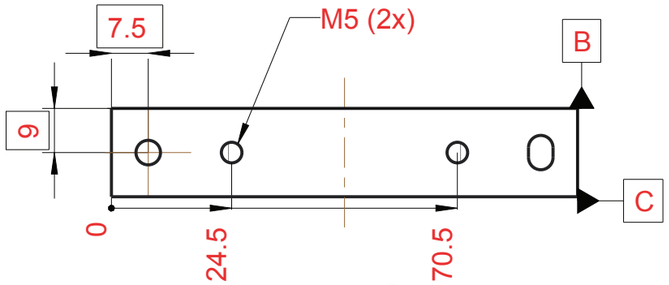

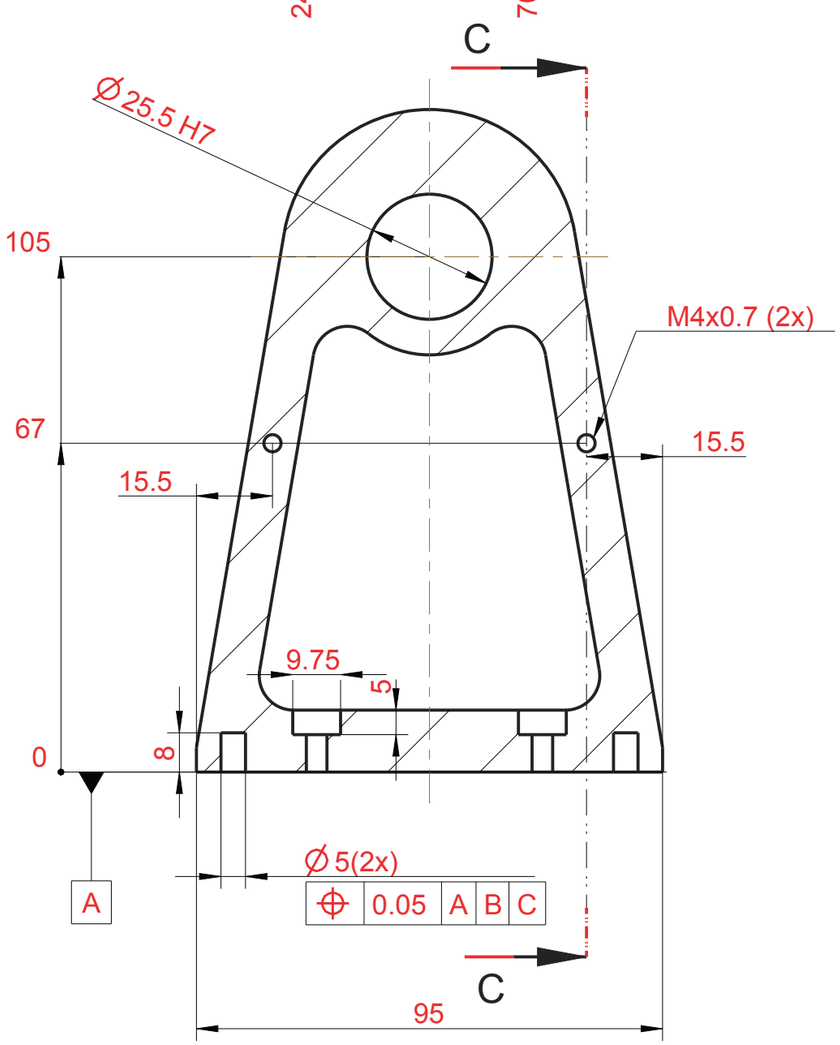

A-A
1:1.25

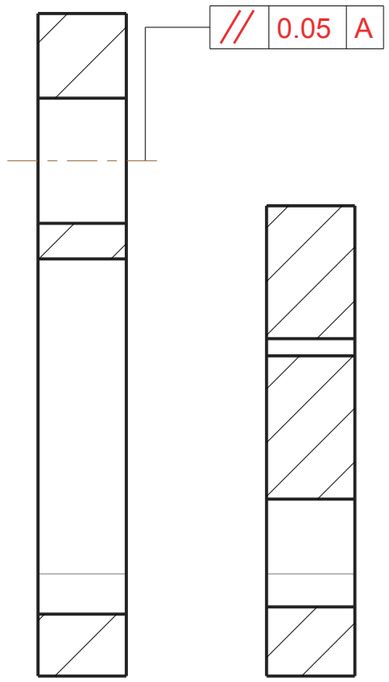

B-B

C-C

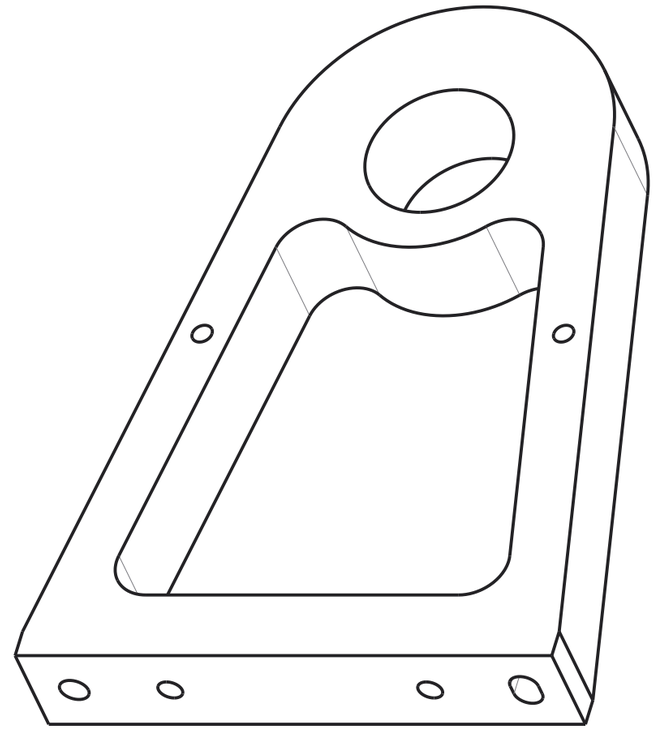

For missing dimensions, please check 3D file and apply general dimensional tolerances
Surface treatment: Black anodizing

General tolerance unless otherwise stated: ISO 2768 - mH	General surface roughness unless otherwise stated:		
Material: Alu	Date: 16-May-17	Surf. roughness acc. to ISO 1302	
	Drawn: Pedro Almeida	CAD system: Creo Parametric	Sheet: 1 of 1
	Design Resp.: Rudi Aerts		
Name: BUSHING SUPPORT	Copied from	Scale: 1:1	Mass: ( )kg
This drawing is property of Punch Powertrain NV and can't be used, copied or shown to third parties without written permission.	Article number: PNSA2701	Index: 0	
PUNCH POWERTRAIN NV	Document number: PNSA2701	Index: 1	DIN: A3

model name: PNSA2701 [PART]

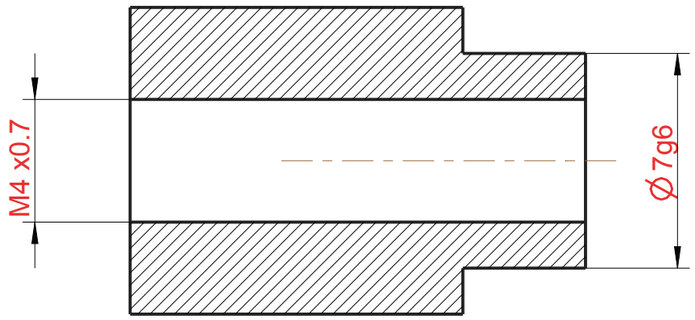

FRONT-FRONT
5:1

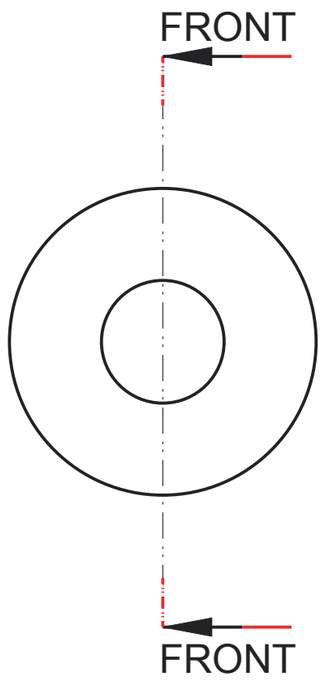

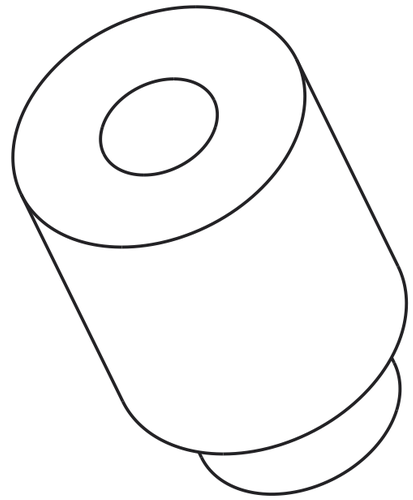

5:1

For missing dimensions, please check the 3D file and apply general dimensional tolerances
Surface treatment: Black anodising

General tolerance unless otherwise stated: DIN ISO 2768 - mH	General surface roughness unless otherwise stated:		
Material: Alu	Date: 27-Apr-17	Surf. roughness acc. to ISO 1302	
	Drawn: Pedro Almeida	CAD system: Creo Parametric	Sheet: 1 of 1
Name: Ball transfer unit adapter	Design Resp.: Rudi Aerts		
	Copied from	Scale: 1:1	Mass: ( )kg
This drawing is property of Punch Powertrain NV and can't be used, copied or shown to third parties without written permission.	Article number: PNSA1203_3	Index: 0	
PUNCH POWERTRAIN NV	Document number: PNSA1203_3	Index: 0	DIN: A3

model name: PNSA1203_3 [PART]

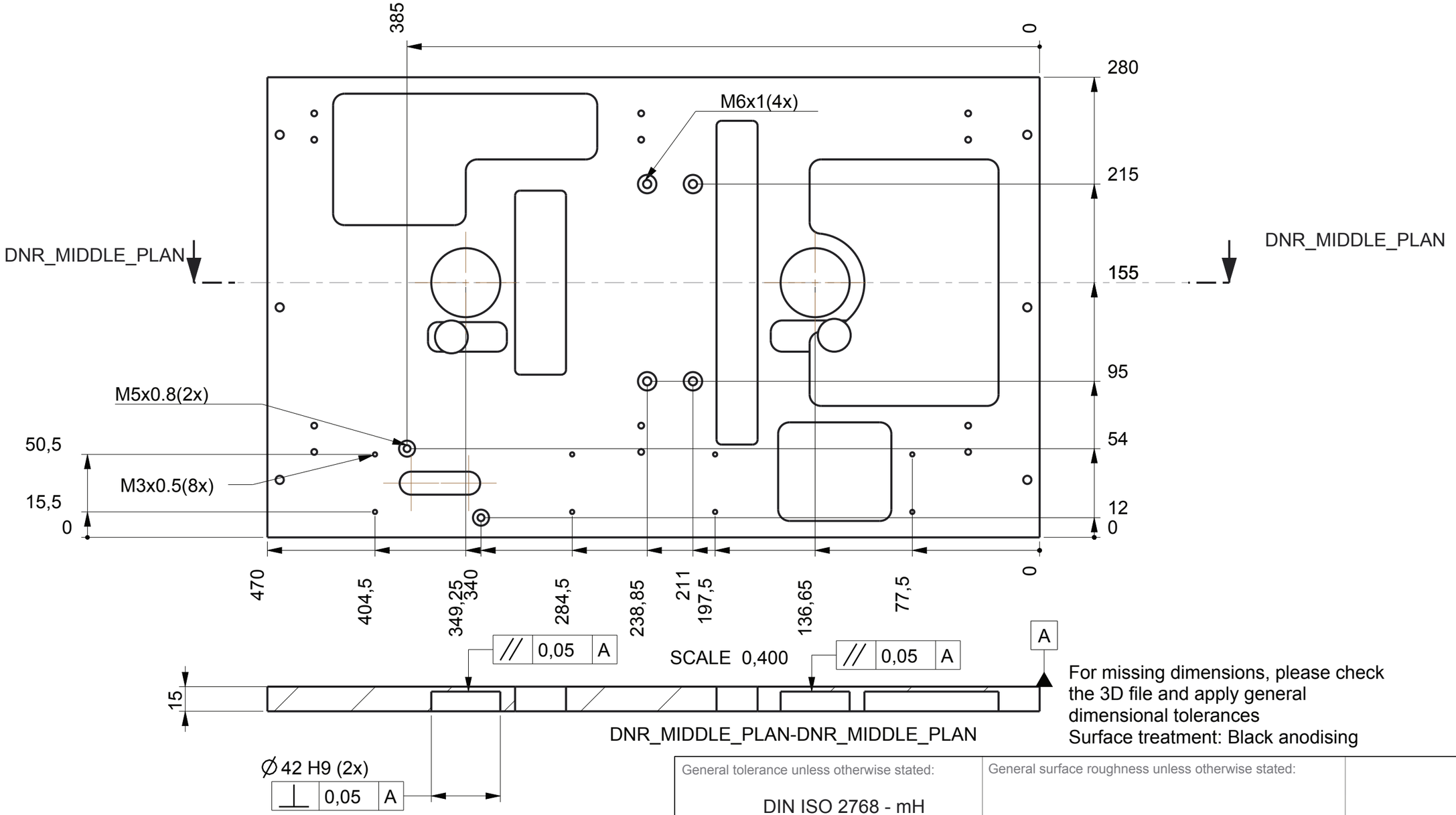

For missing dimensions, please check the 3D file and apply general dimensional tolerances
Surface treatment: Black anodising

General tolerance unless otherwise stated: DIN ISO 2768 - mH	General surface roughness unless otherwise stated:		
Material: Alu	Date: 29-June-17	Surf. roughness acc. to ISO 1302	
	Drawn: Pedro Almeida	CAD system: Creo Parametric	Sheet: 1 of 6
Name: Main plate	Design Resp.: Rudi Aerts	Copied from	Scale: 1,000 / Mass: ( )kg
This drawing is property of Punch Powertrain NV and can't be used, copied or shown to third parties without written permission.	Article number: PNSA2101	Index: 0	
PUNCH POWERTRAIN NV	Document number: PNSA2101	Index: 0	DIN: A3

model name: PNSA2101 [PART]

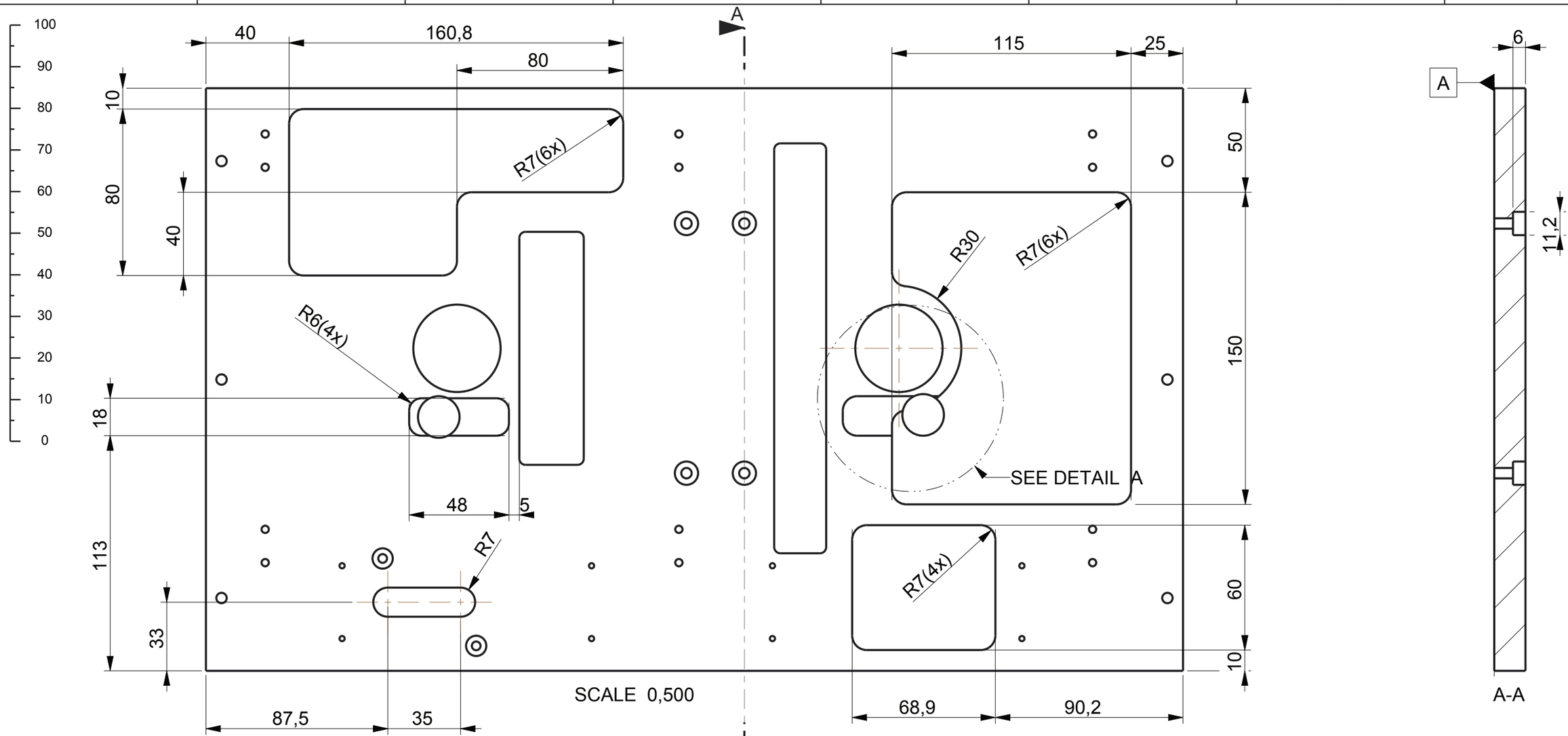

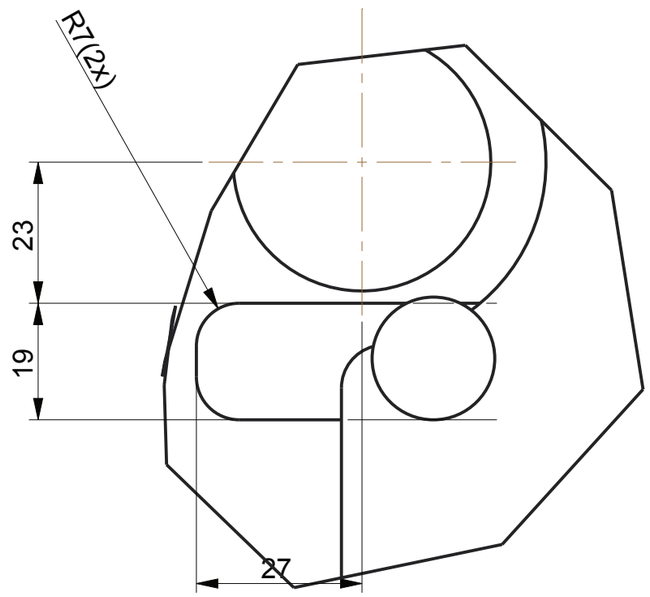

DETAIL A
SCALE 1,000

General tolerance unless otherwise stated: DIN ISO 2768 - mH	General surface roughness unless otherwise stated:		
Material: Alu	Date: 29-June-17	Surf. roughness acc. to ISO 1302	
	Drawn: Pedro Almeida	CAD system: Creo Parametric	Sheet: 2 of 6
Name: Main Plate	Design Resp.: Rudi Aerts		
	Copied from	Scale: 1,000	Mass: ( )kg
This drawing is property of Punch Powertrain NV and can't be used, copied or shown to third parties without written permission.	Article number: PNSA2101	Index: 1	
PUNCH POWERTRAIN NV	Document number: PNSA2101	Index: 1	DIN: A3

model name: PNSA2101 [PART]

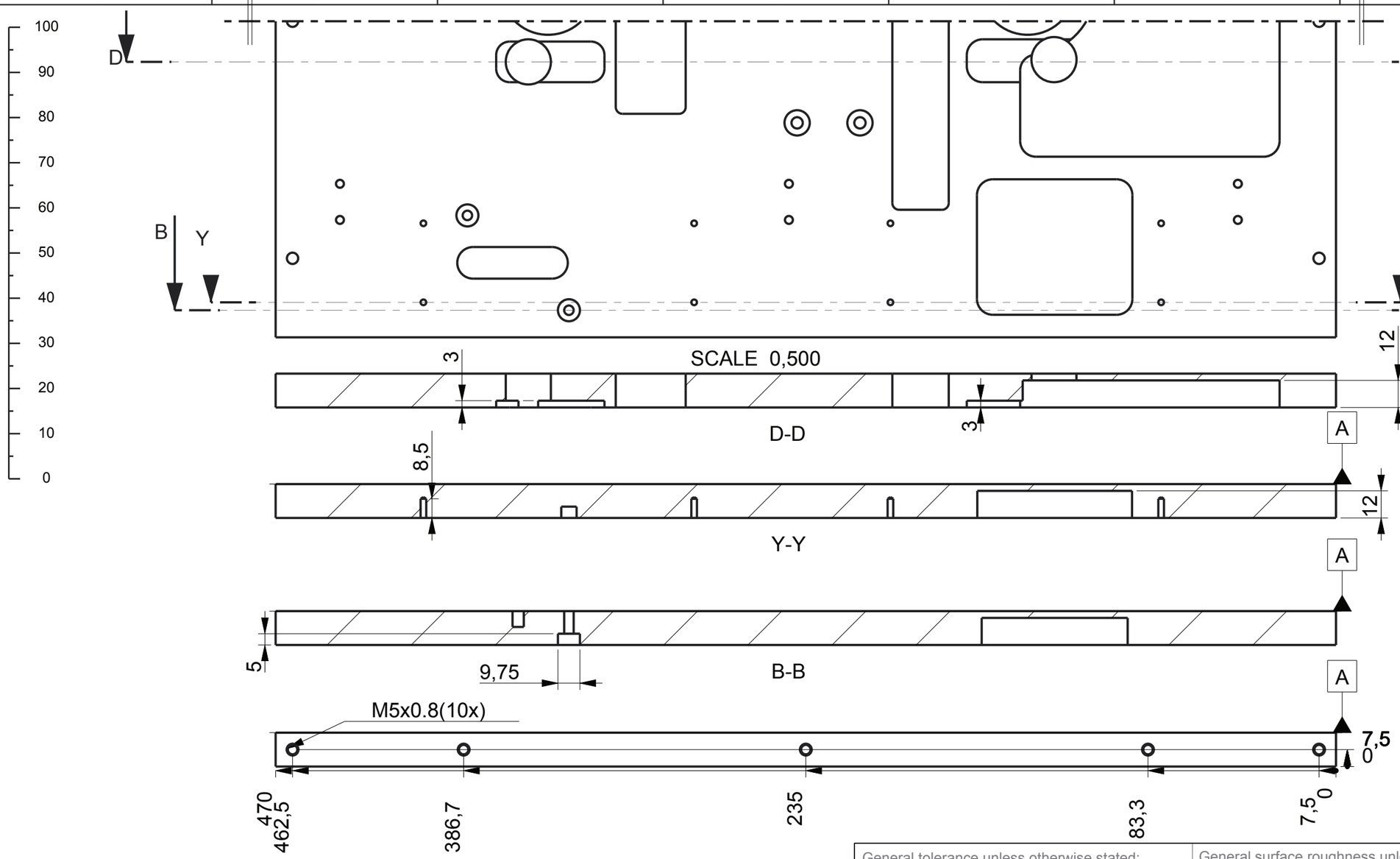

General tolerance unless otherwise stated: DIN ISO 2768 - mH	General surface roughness unless otherwise stated:		
Material: Alu	Date: 29-June-17	Surf. roughness acc. to ISO 1302	
	Drawn: Pedro Almeida	CAD system: Creo Parametric	Sheet: 3 of 6
Name: Main plate	Design Resp.: Rudi Aerts		
	Copied from	Scale: 1,000	Mass: ( )kg
This drawing is property of Punch Powertrain NV and can't be used, copied or shown to third parties without written permission.	Article number: PNSA2101	Index: 1	
PUNCH POWERTRAIN NV	Document number: PNSA2101	Index: 1	DIN: A3

model name: PNSA2101 [PART]

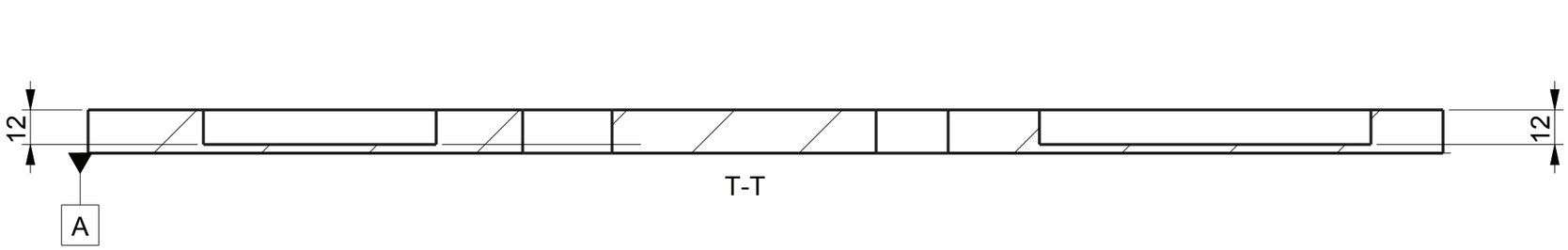

T-T

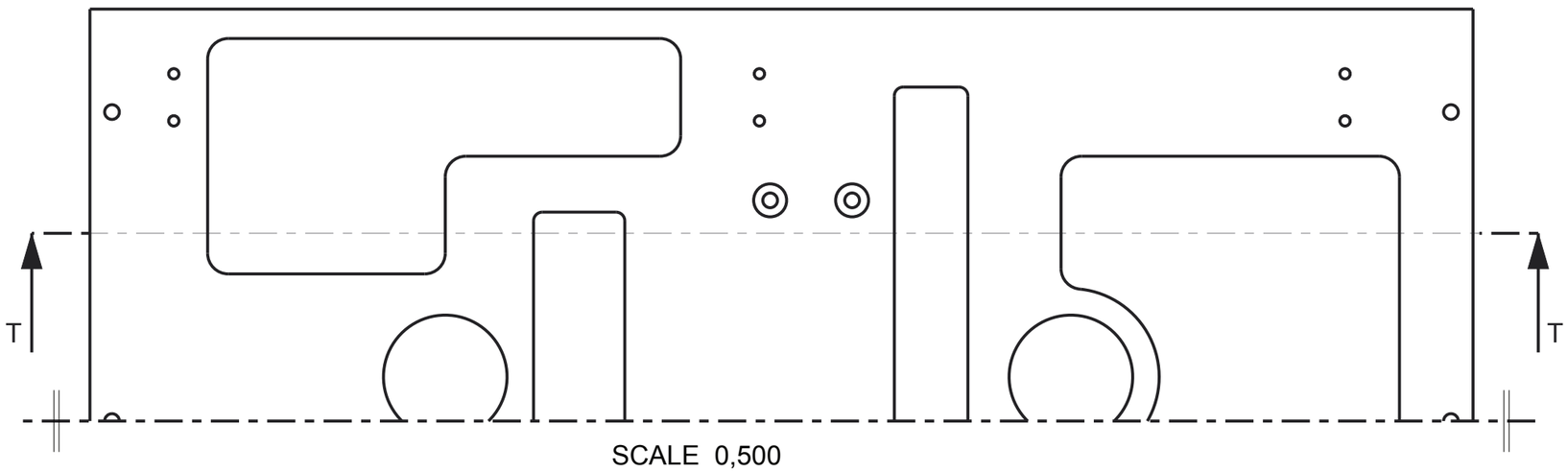

SCALE 0,500

General tolerance unless otherwise stated: DIN ISO 2768 - mH	General surface roughness unless otherwise stated:		
Material: Alu	Date: 29-June-17	Surf. roughness acc. to ISO 1302	
	Drawn: Pedro Almeida	CAD system: Creo Parametric	Sheet: 4 of 6
Name: Main plate	Design Resp.: Rudi Aerts		
	Copied from	Scale: 1,000	Mass: ( )kg
This drawing is property of Punch Powertrain NV and can't be used, copied or shown to third parties without written permission.	Article number: PNSA2101	Index: 1	
PUNCH POWERTRAIN NV	Document number: PNSA2101	Index: 1	DIN: A3

model name: PNSA2101 [PART]

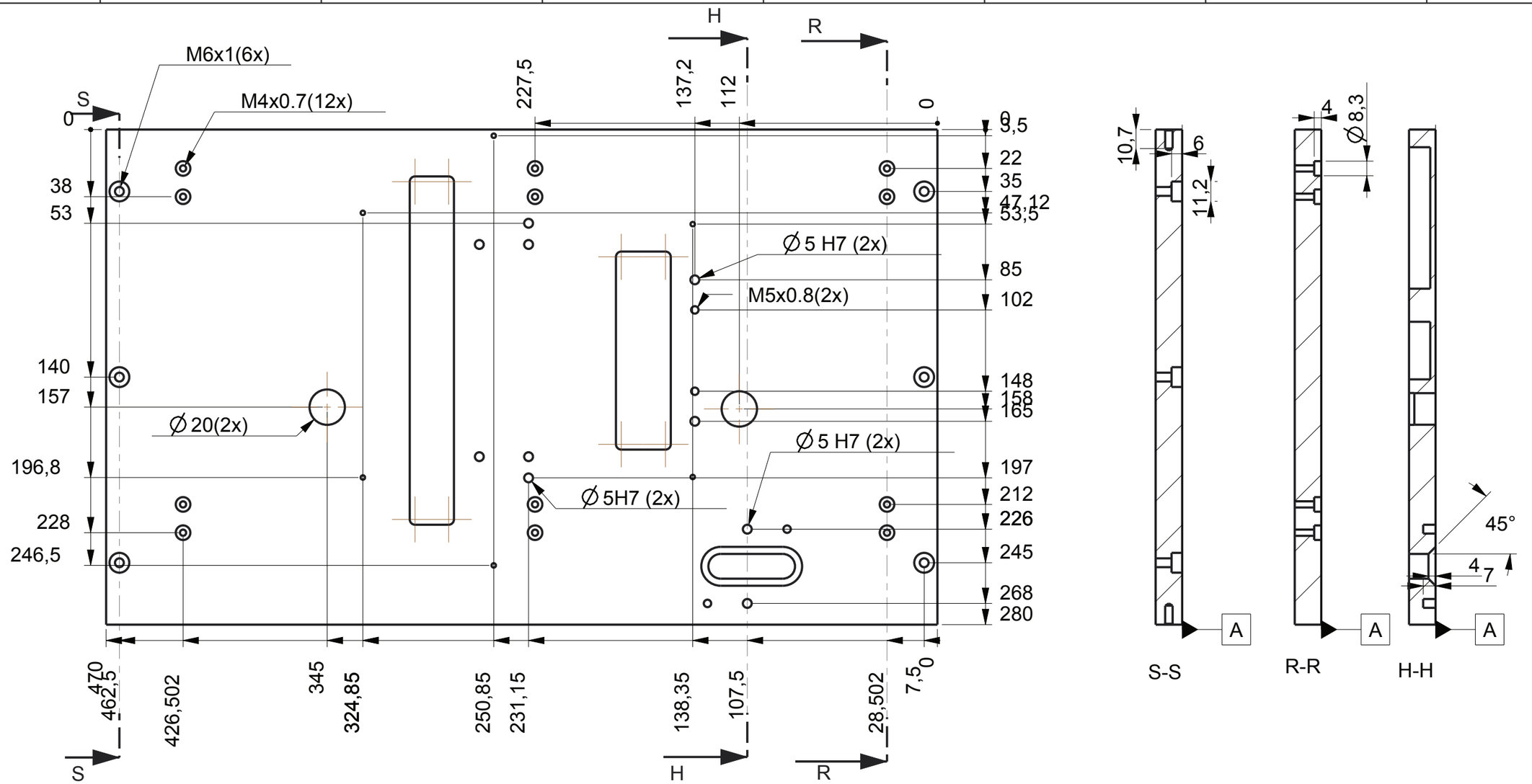

SCALE 0,400

General tolerance unless otherwise stated: DIN ISO 2768 - mH	General surface roughness unless otherwise stated:		
Material: Alu	Date: 29-June-17	Surf. roughness acc. to ISO 1302	
	Drawn: Pedro Almeida	CAD system: Creo Parametric	Sheet: 5 of 6
	Design Resp.: Rudi Aerts		
Name: Main plate	Copied from	Scale: 1,000	Mass: ( )kg
This drawing is property of Punch Powertrain NV and can't be used, copied or shown to third parties without written permission.	Article number: PNSA2101	Index: 1	
PUNCH POWERTRAIN NV	Document number: PNSA2101	Index: 1	DIN: A3

model name: PNSA2101 [PART]

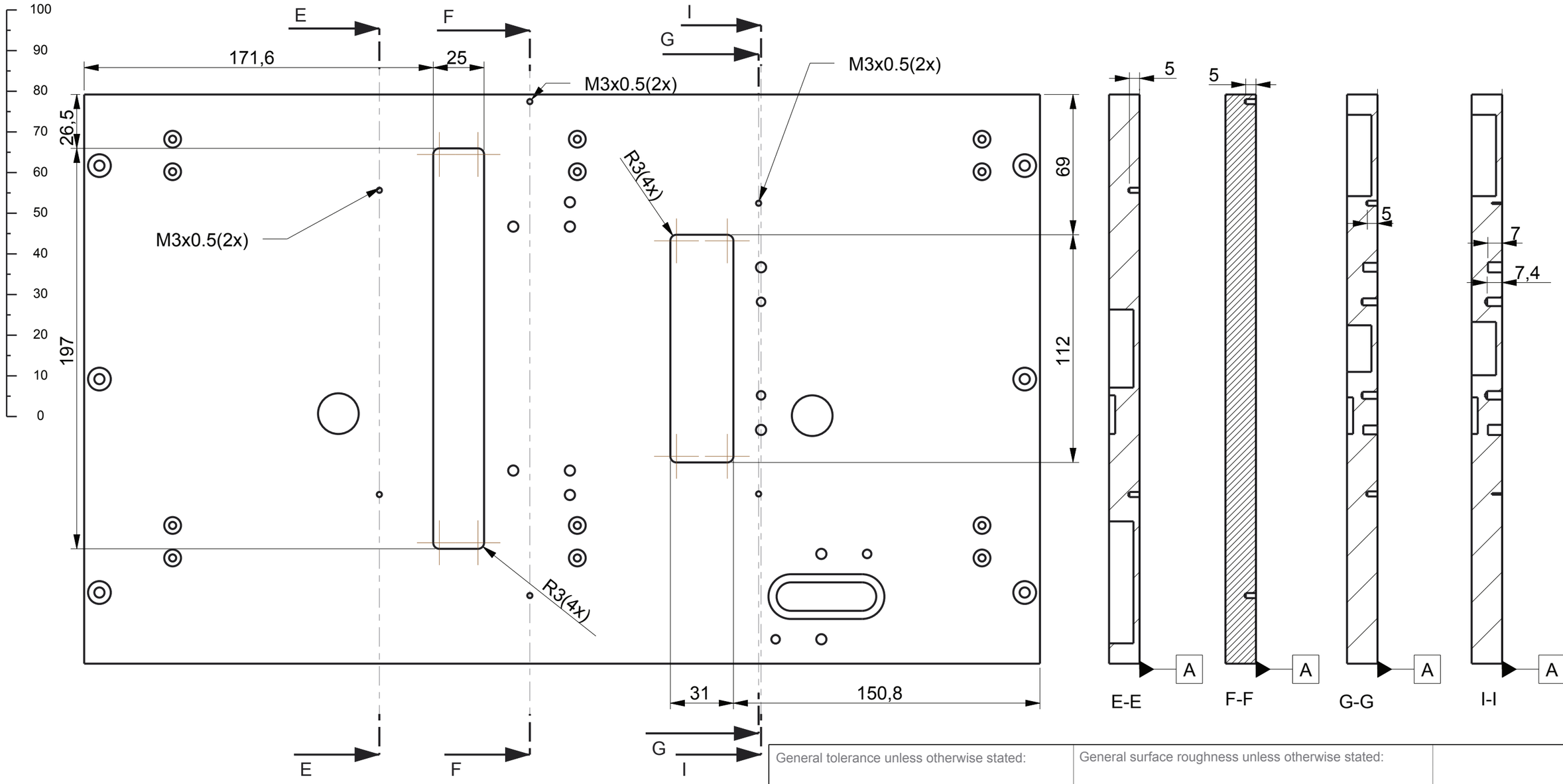

General tolerance unless otherwise stated: DIN ISO 2768 - mH	General surface roughness unless otherwise stated:		
Material: Alu	Date: 29-June-17	Surf. roughness acc. to ISO 1302	
	Drawn: Pedro Almeida	CAD system: Creo Parametric	Sheet: 6 of 6
Name: Main plate	Design Resp.: Rudi Aerts	Copied from	Scale: 1,000 / Mass: ( )kg
This drawing is property of Punch Powertrain NV and can't be used, copied or shown to third parties without written permission.	Article number: PNSA2101	Index: 1	
PUNCH POWERTRAIN NV	Document number: PNSA2101	Index: 1	DIN: A3

model name: PNSA2101 [PART]

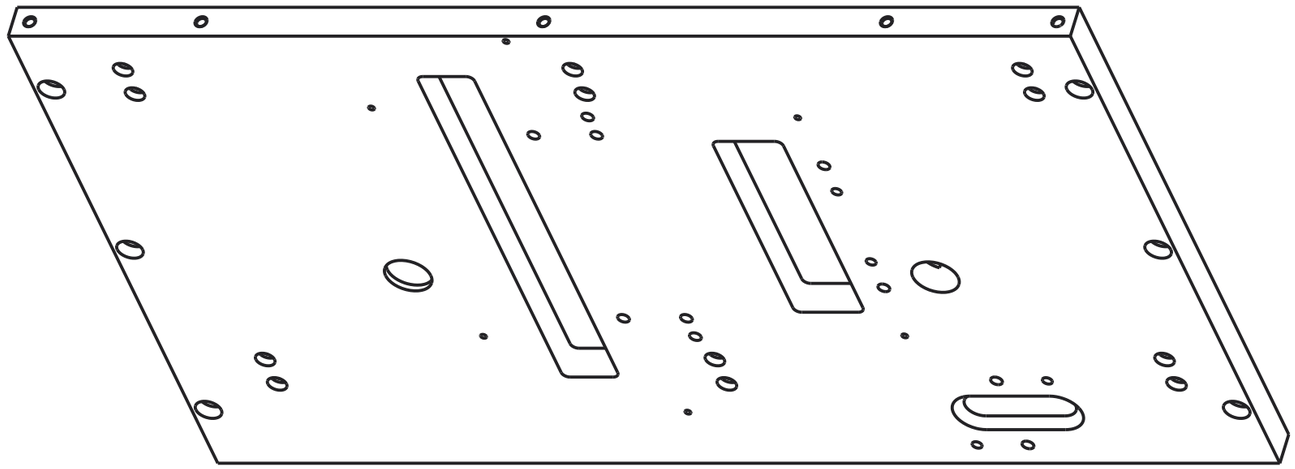

SCALE 0,400

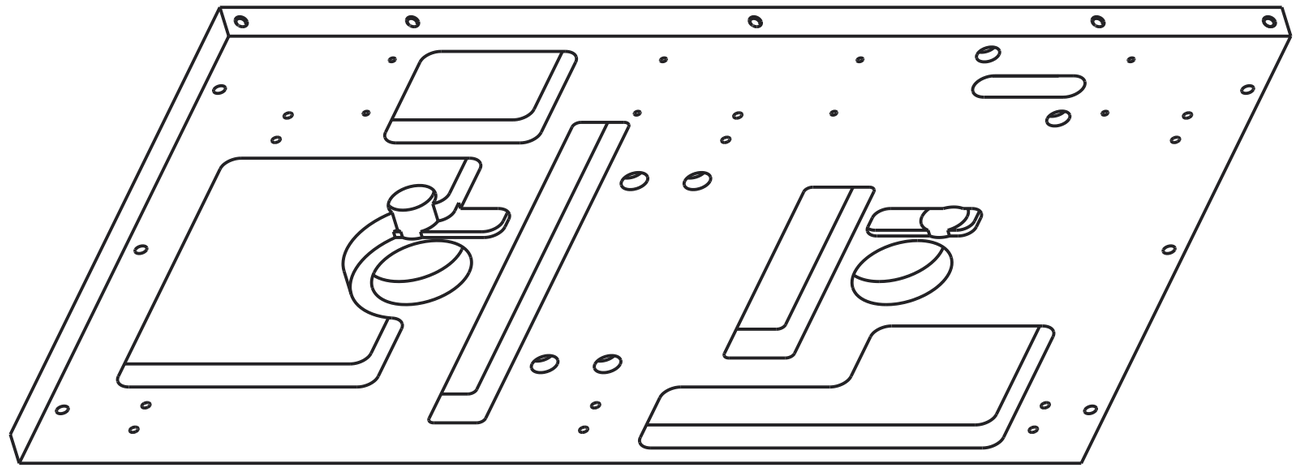

SCALE 0,400

General tolerance unless otherwise stated:	General surface roughness unless otherwise stated:	

Material: Alu	Date: 29-June-17		Surf. roughness acc. to ISO 1302	
	Drawn: Pedro Almeida		CAD system: Creo Parametric	Sheet: 7 of 7
	Design Resp.: Rudi Aerts			
Name: Main plate	Copied from: PNSA2101	Scale: 1,000	Mass: ( )kg	
This drawing is property of Punch Powertrain NV and can't be used, copied or shown to third parties without written permission.	Article number: PNSA2101	Index: 1		
PUNCH POWERTRAIN NV	Document number: PNSA2101	Index: 1	DIN: A3	

model name: PNSA2101 [PART]

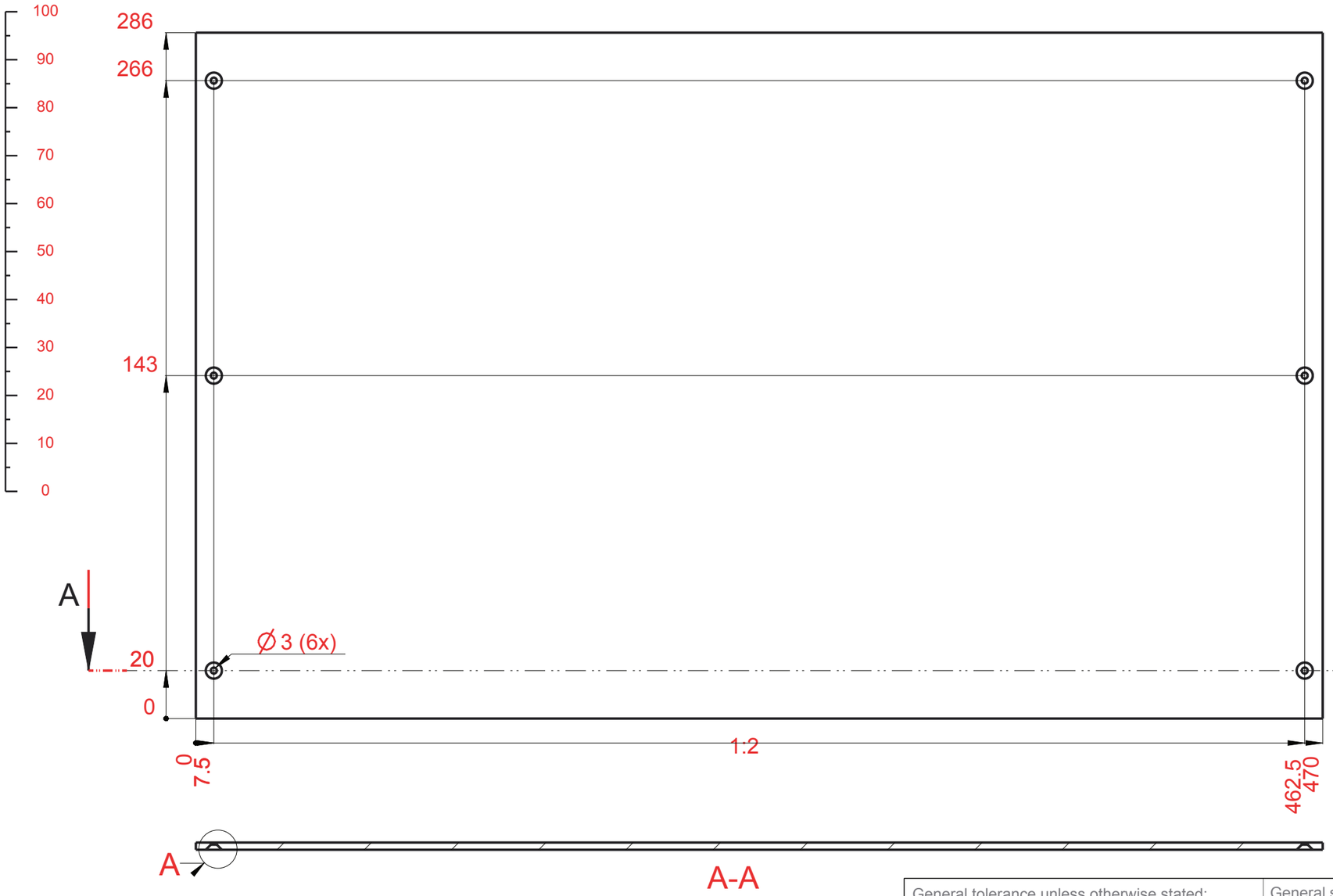

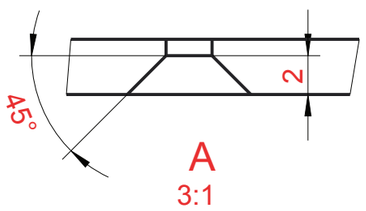

For missing dimensions, please check 3D file and apply general dimensional tolerances

General tolerance unless otherwise stated: ISO 2768 - mH	General surface roughness unless otherwise stated:		
Material: Transparent Plastic	Date: 22-May-17	Surf. roughness acc. to ISO 1302	
	Drawn: Pedro Almeida	CAD system: Creo Parametric	Sheet: 1 of 1
Name: Bottom cover	Design Resp.: Rudi Aerts		
	Copied from	Scale: 1:1	Mass: ( )kg
This drawing is property of Punch Powertrain NV and can't be used, copied or shown to third parties without written permission.	Article number: PNSA290	Index: 0	
PUNCH POWERTRAIN NV	Document number: PNSA290	Index: 0	DIN: A3

model name: PNSA290 [PART]

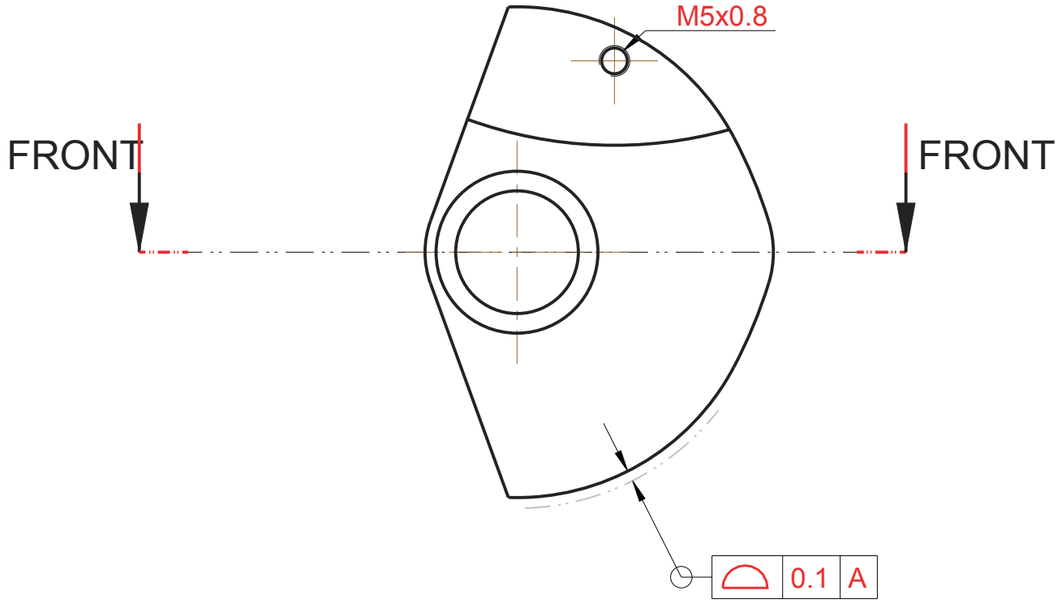

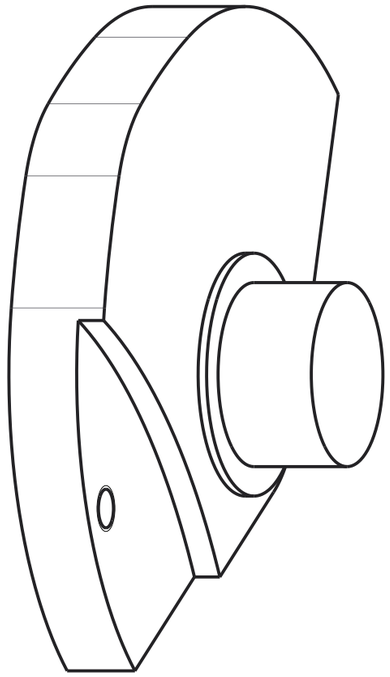

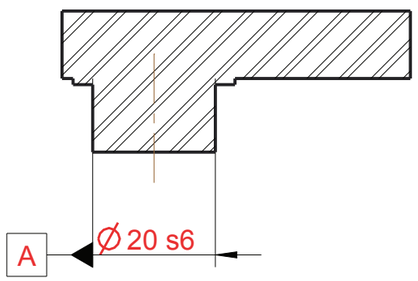

FRONT-FRONT

1.5:1

For missing dimensions, please check 3D file and apply general dimensional tolerances
Min. hardness: 45 HRC
Surface treatment: Chemically black

General tolerance unless otherwise stated: DIN ISO 2768 - mH	General surface roughness unless otherwise stated:			
Material: Steel	Date: 27-Apr-17		Surf. roughness acc. to ISO 1302	
	Drawn: Pedro Almeida		CAD system: Creo Parametric	Sheet: 1 of 1
Name: FWD cam	Design Resp.: Rudi Aerts			
	Copied from		Scale: 1:1	Mass: ( )kg
This drawing is property of Punch Powertrain NV and can't be used, copied or shown to third parties without written permission.	Article number		Index: 0	
PUNCH POWERTRAIN NV	Document number: PNSA3306_1		Index: 0	DIN: A3

model name: PNSA3306_1 [PART]

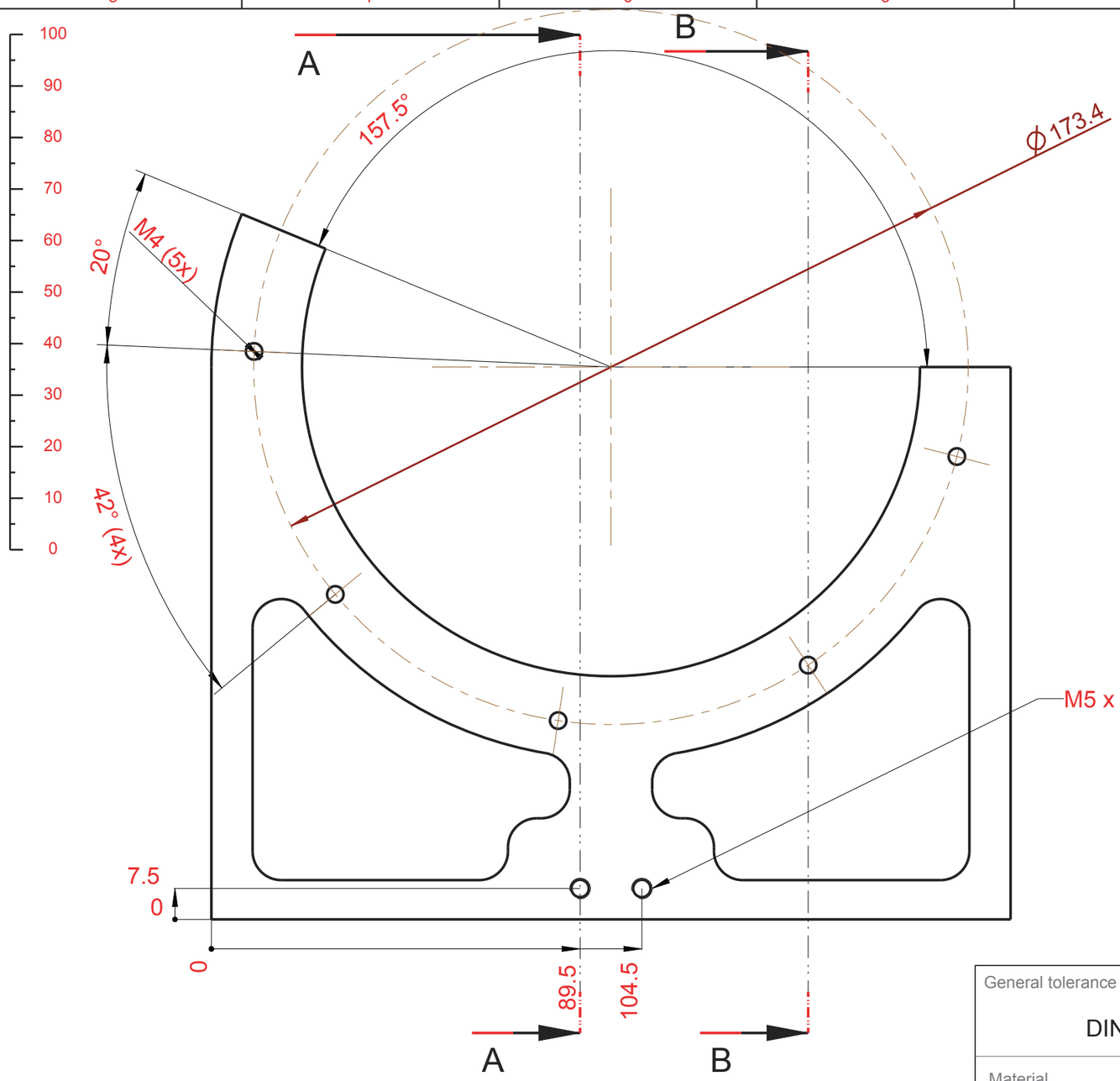

1:1.25

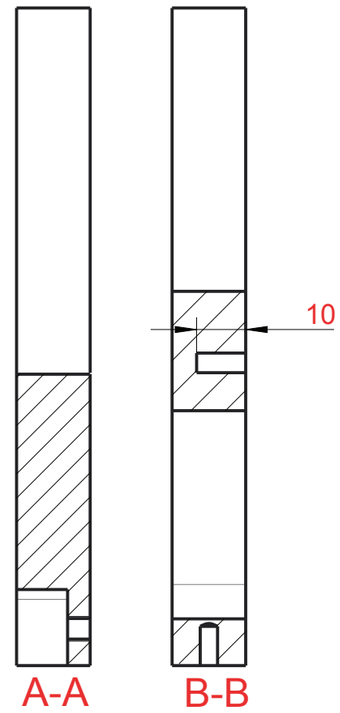

For missing dimensions, please check
3D file and apply general
dimensional tolerances
Surface treatment: Black anodized

General tolerance unless otherwise stated: DIN ISO 2768 - mH	General surface roughness unless otherwise stated:		
Material: Alu	Date: 28-Apr-17	Surf. roughness acc. to ISO 1302	
	Drawn: Pedro Almeida	CAD system: Creo Parametric	Sheet: 1 of 3
	Design Resp.: Rudi Aerts		
Name: Reverse pressing plate	Copied from	Scale: 1:1	Mass: ( )kg
This drawing is property of Punch Powertrain NV and can't be used, copied or shown to third parties without written permission.	Article number	Index: 0	
PUNCH POWERTRAIN NV	Document number: PNSA3401_1	Index: 0	DIN: A3

model name: PNSA3401_1 [PART]

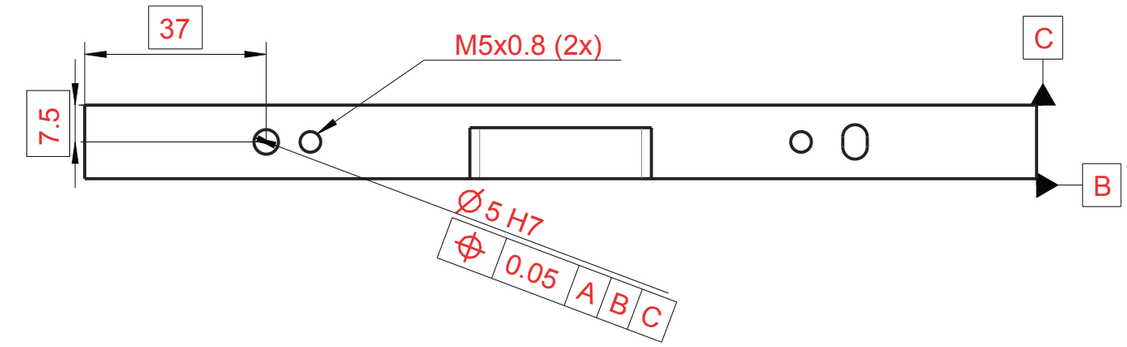

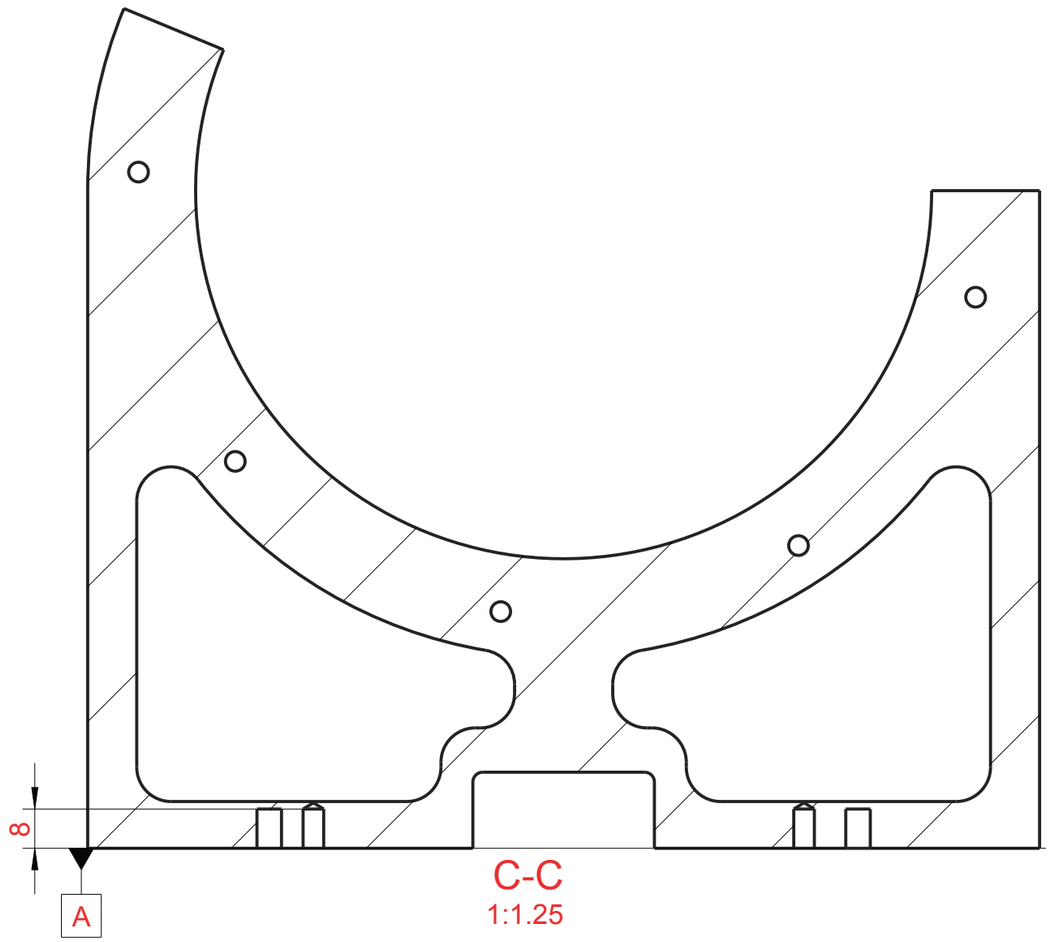

C-C
1:1.25

General tolerance unless otherwise stated: DIN ISO 2768 - mH	General surface roughness unless otherwise stated:		
Material: Alu	Date: 28-Apr-17	Surf. roughness acc. to ISO 1302	
	Drawn: Pedro Almeida	CAD system: Creo Parametric	Sheet: 2 of 3
Name: Reverse pressing plate	Design Resp.: Rudi Aerts	Copied from	Scale: 1:1 / Mass: ( )kg
This drawing is property of Punch Powertrain NV and can't be used, copied or shown to third parties without written permission.	Article number: PNSA3401_1	Index: 0	
PUNCH POWERTRAIN NV	Document number: PNSA3401_1	Index: 0	DIN: A3

model name: PNSA3401_1 [PART]

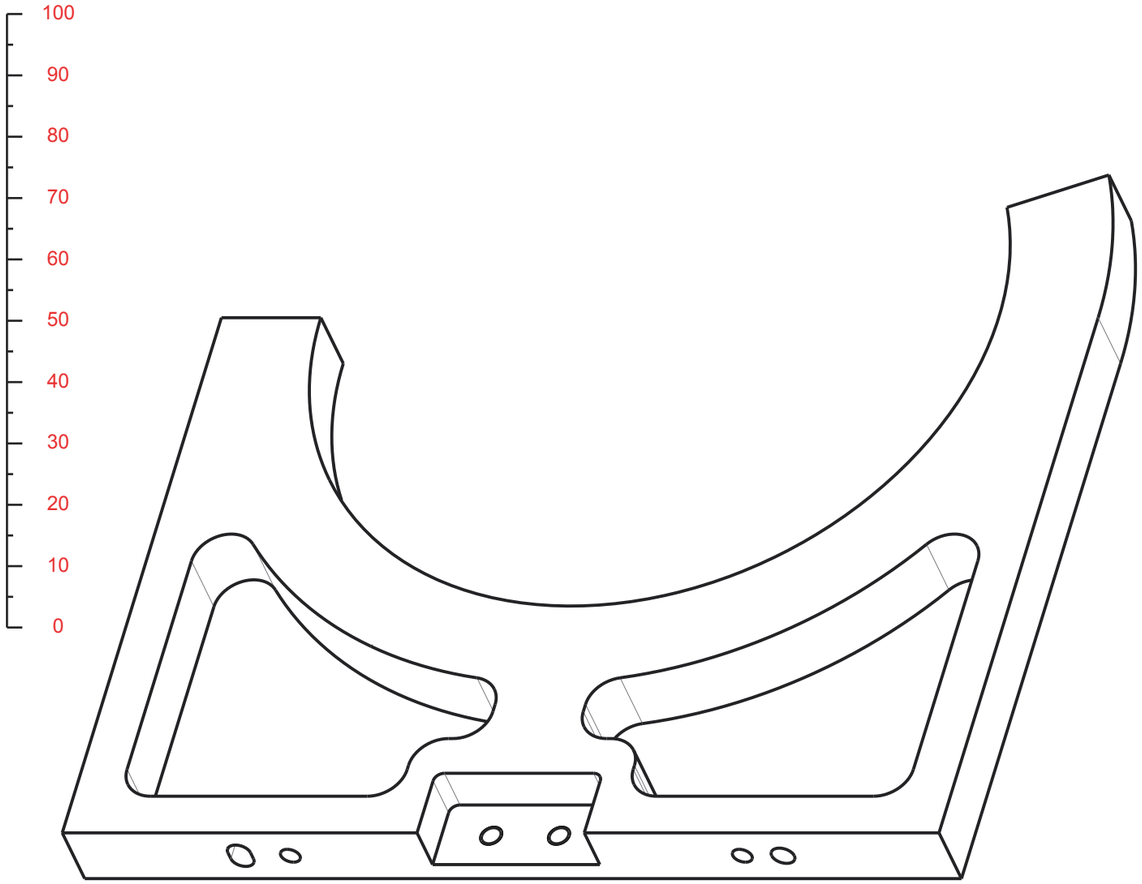

1:1.25

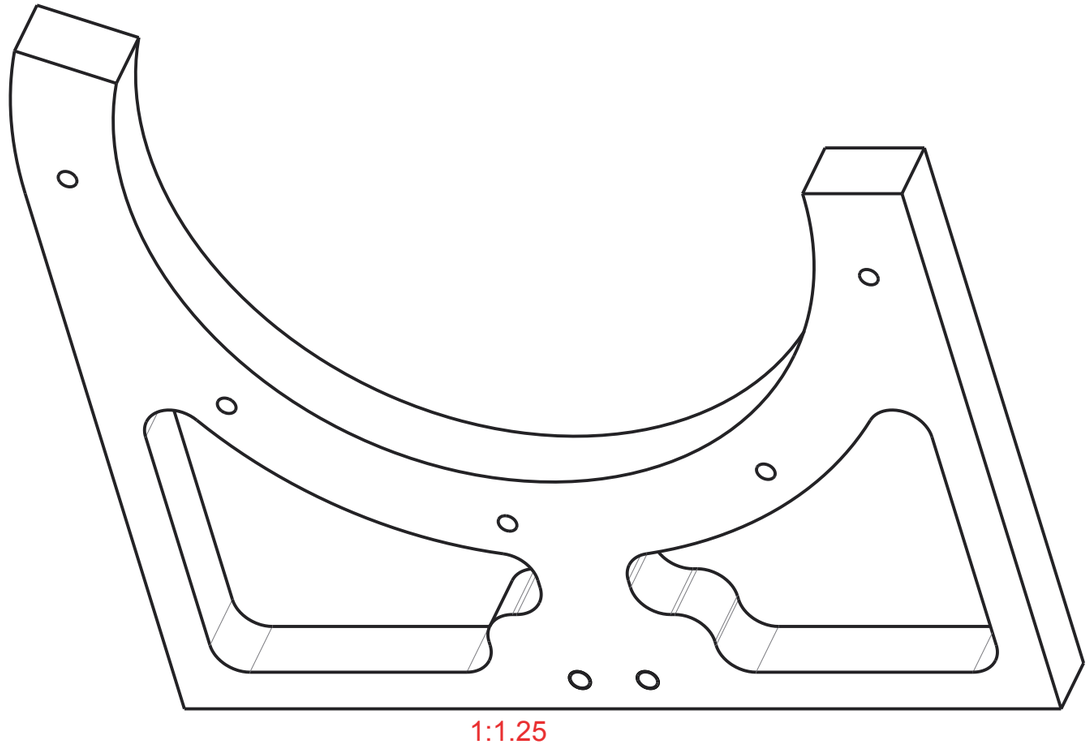

1:1.25

General tolerance unless otherwise stated: DIN ISO 2768 - mH	General surface roughness unless otherwise stated:		
Material: Alu	Date: 28-Apr-17	Surf. roughness acc. to ISO 1302	
	Drawn: Pedro Almeida	CAD system: Creo Parametric	Sheet: 3 of 3
Name: Reverse pressing plate	Design Resp.: Rudi Aerts		
	Copied from: PNSA3401_1	Scale: 1:1	Mass: ( )kg
This drawing is property of Punch Powertrain NV and can't be used, copied or shown to third parties without written permission.	Article number: PNSA3401_1	Index: 0	
PUNCH POWERTRAIN NV	Document number: PNSA3401_1	Index: 0	DIN: A3

model name: PNSA3401_1 [PART]

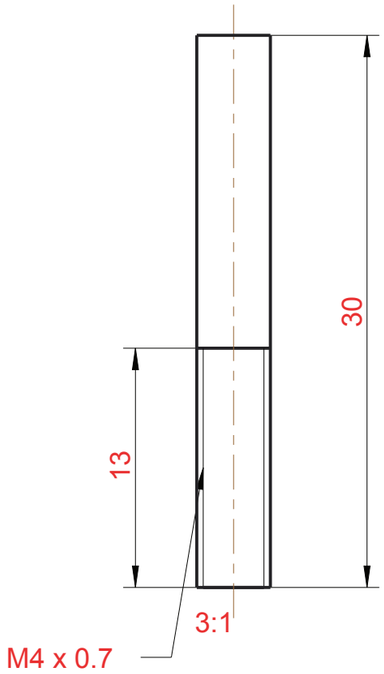

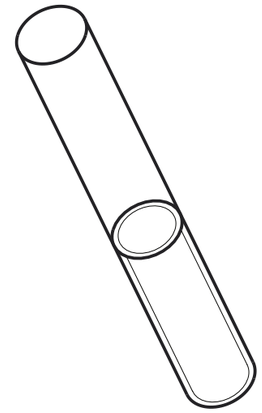

3:1

For missing dimensions, please check 3D file and apply general dimensional tolerances
Surface treatment: Chemically black

General tolerance unless otherwise stated: DIN ISO 2768 - mH	General surface roughness unless otherwise stated:			
Material: Steel	Date: 28-Apr-17		Surf. roughness acc. to ISO 1302	
	Drawn: Pedro Almeida		CAD system: Creo Parametric	Sheet: 1 of 1
Name: Pin	Design Resp.: Rudi Aerts			
	Copied from: PNSA3401_2		Scale: 1:1	Mass: ( )kg
This drawing is property of Punch Powertrain NV and can't be used, copied or shown to third parties without written permission.	Article number: PNSA3401_2		Index: 0	
PUNCH POWERTRAIN NV	Document number: PNSA3401_2		Index: 0	DIN: A3

model name: PNSA3401_2 [PART]

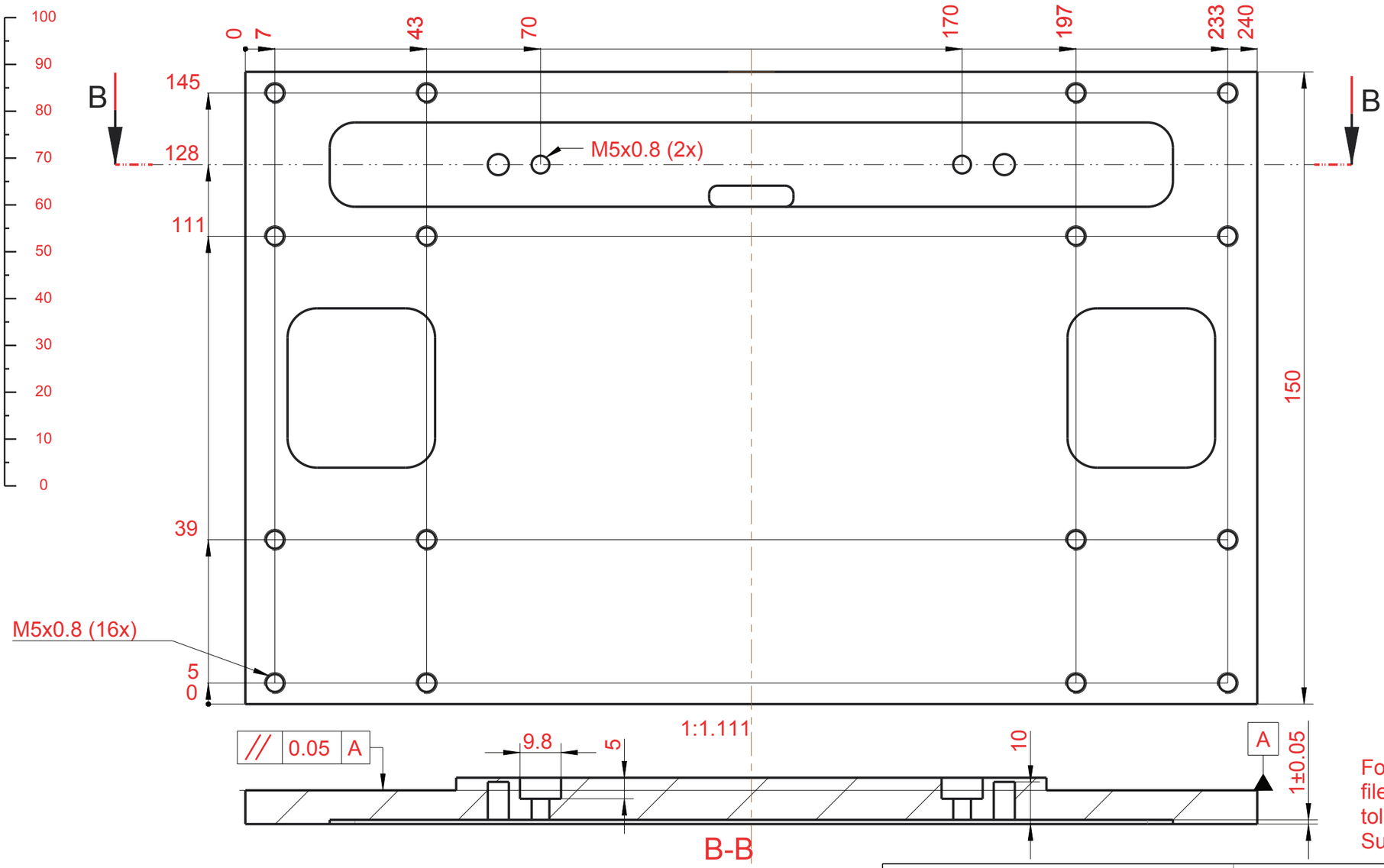

For missing dimensions, please check 3D file and apply general dimensional tolerances
Surface treatment: Black anodising

General tolerance unless otherwise stated: DIN ISO 2768 - mH	General surface roughness unless otherwise stated:		
Material: Alu	Date: 05-July-17	Surf. roughness acc. to ISO 1302	
	Drawn: Pedro Almeida	CAD system: Creo Parametric	Sheet: 1 of 3
Name: Reverse plate	Design Resp.: Rudi Aerts		
	Copied from	Scale: 1:1	Mass: ( )kg
This drawing is property of Punch Powertrain NV and can't be used, copied or shown to third parties without written permission.	Article number	Index: 0	
PUNCH POWERTRAIN NV	Document number: PNSA3402_1	Index: 1	DIN: A3

model name: PNSA3402_1 [PART]

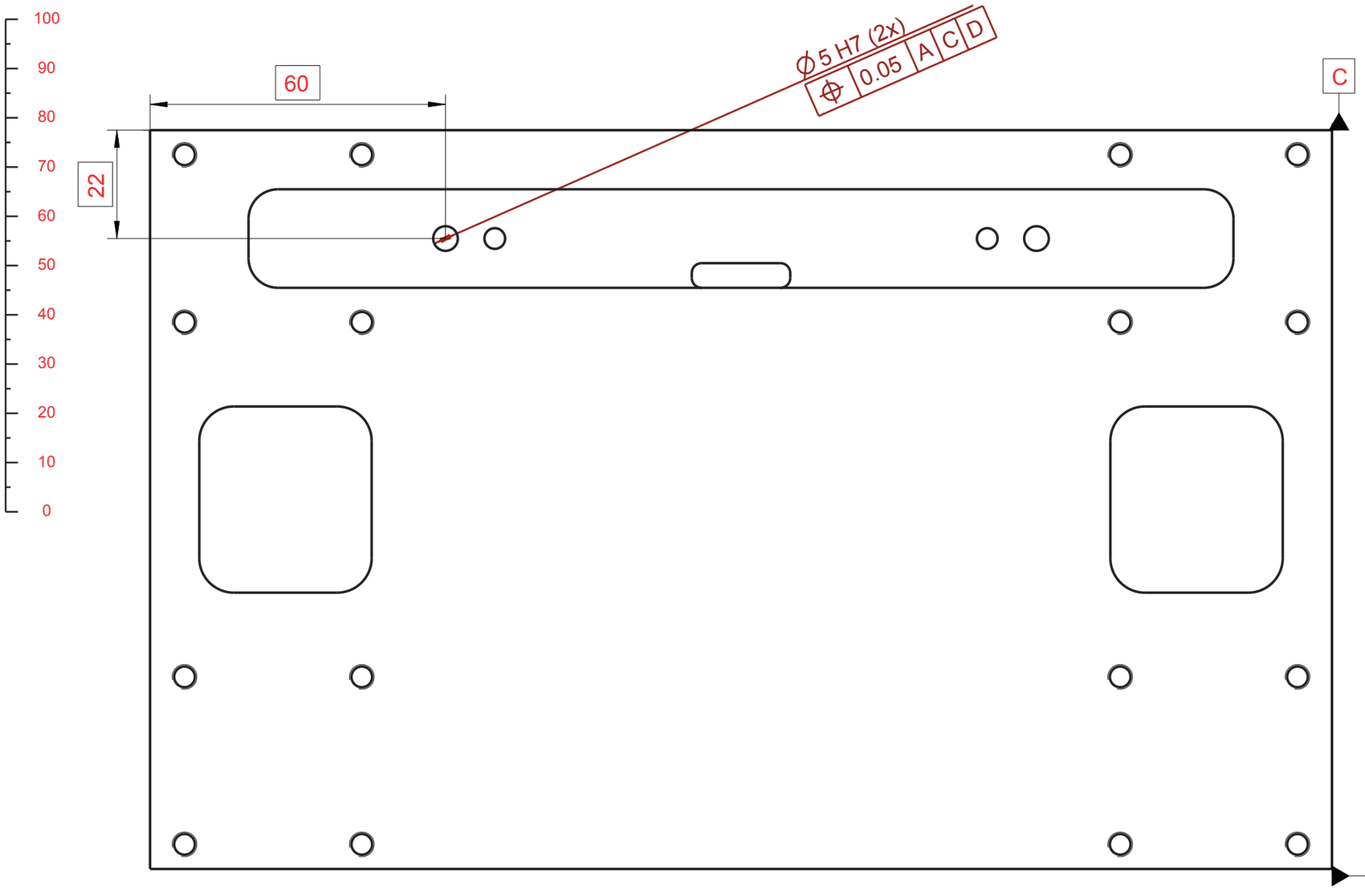

For missing dimensions, please check 3D file and apply general dimensional tolerances
Surface treatment: black anodising

General tolerance unless otherwise stated: DIN ISO 2768 - mH	General surface roughness unless otherwise stated:		
Material: Alu	Date: 05-July-17	Surf. roughness acc. to ISO 1302	
	Drawn: Pedro Almeida	CAD system: Creo Parametric	Sheet: 2 of 3
Name: Reverse plate	Design Resp.: Rudi Aerts		
	Copied from: PNSA3402_1	Scale: 1:1	Mass: ( )kg
This drawing is property of Punch Powertrain NV and can't be used, copied or shown to third parties without written permission.	Article number: PNSA3402_1	Index: 0	
PUNCH POWERTRAIN NV	Document number: PNSA3402_1	Index: 1	DIN: A3

model name: PNSA3402_1 [PART]

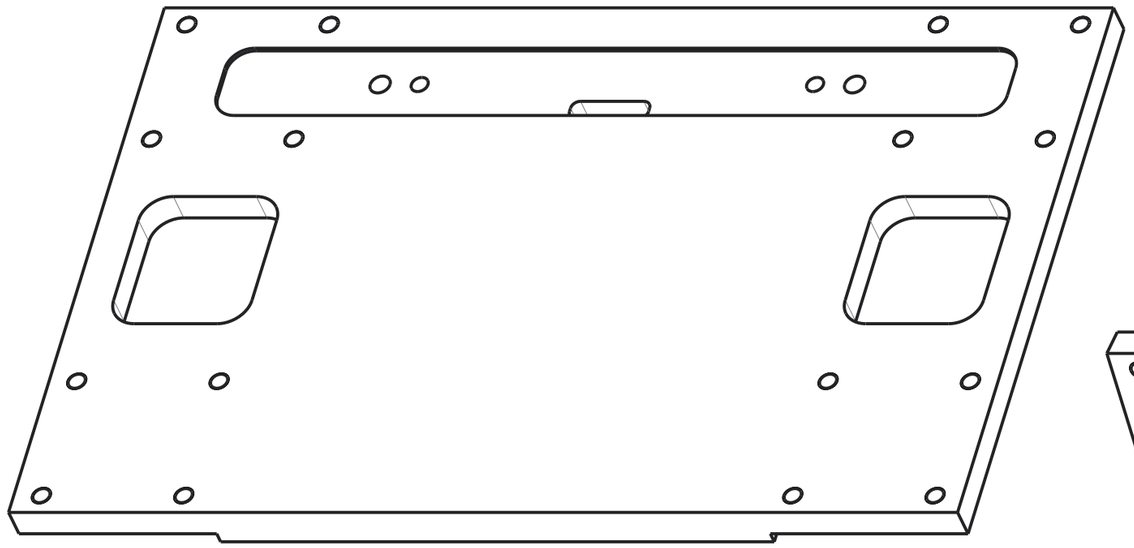

1:1.429

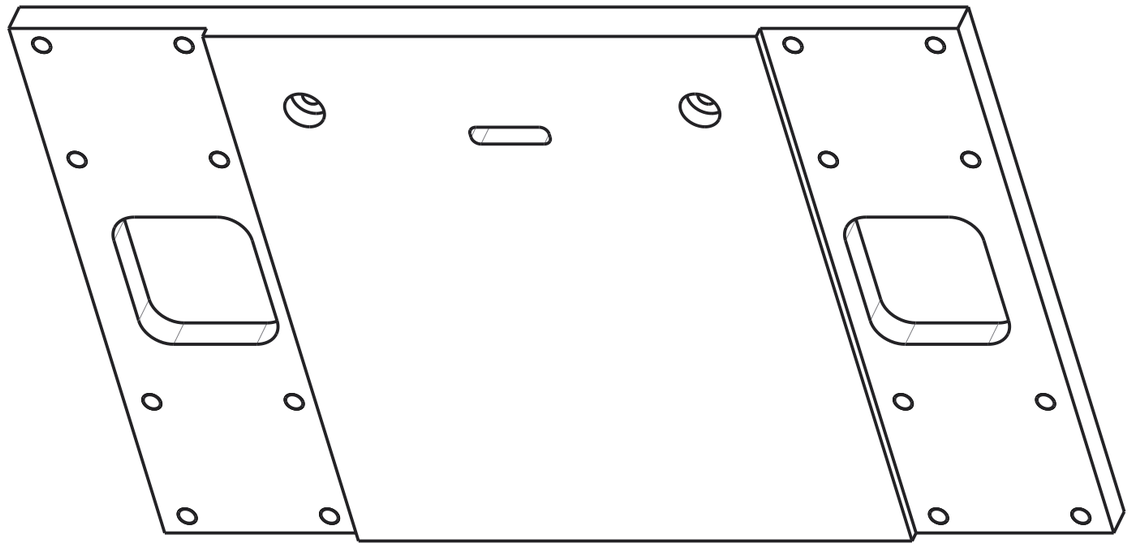

1:1.429

For missing dimensions, please check 3D file and apply general dimensional tolerances
Surface treatment: Black anodising

General tolerance unless otherwise stated: DIN ISO 2768 - mH	General surface roughness unless otherwise stated:	

Material: Alu	Date: 05-July-17		Surf. roughness acc. to ISO 1302	
	Drawn: Pedro Almeida		CAD system: Creo Parametric	Sheet: 3 of 3
Name: Reverse plate	Design Resp.: Rudi Aerts			
	Copied from: PNSA3402_1		Scale: 1:1	Mass: ( )kg
This drawing is property of Punch Powertrain NV and can't be used, copied or shown to third parties without written permission.	Article number: PNSA3402_1		Index: 0	
PUNCH POWERTRAIN NV	Document number: PNSA3402_1		Index: 1	DIN: A3

model name: PNSA3402_1 [PART]

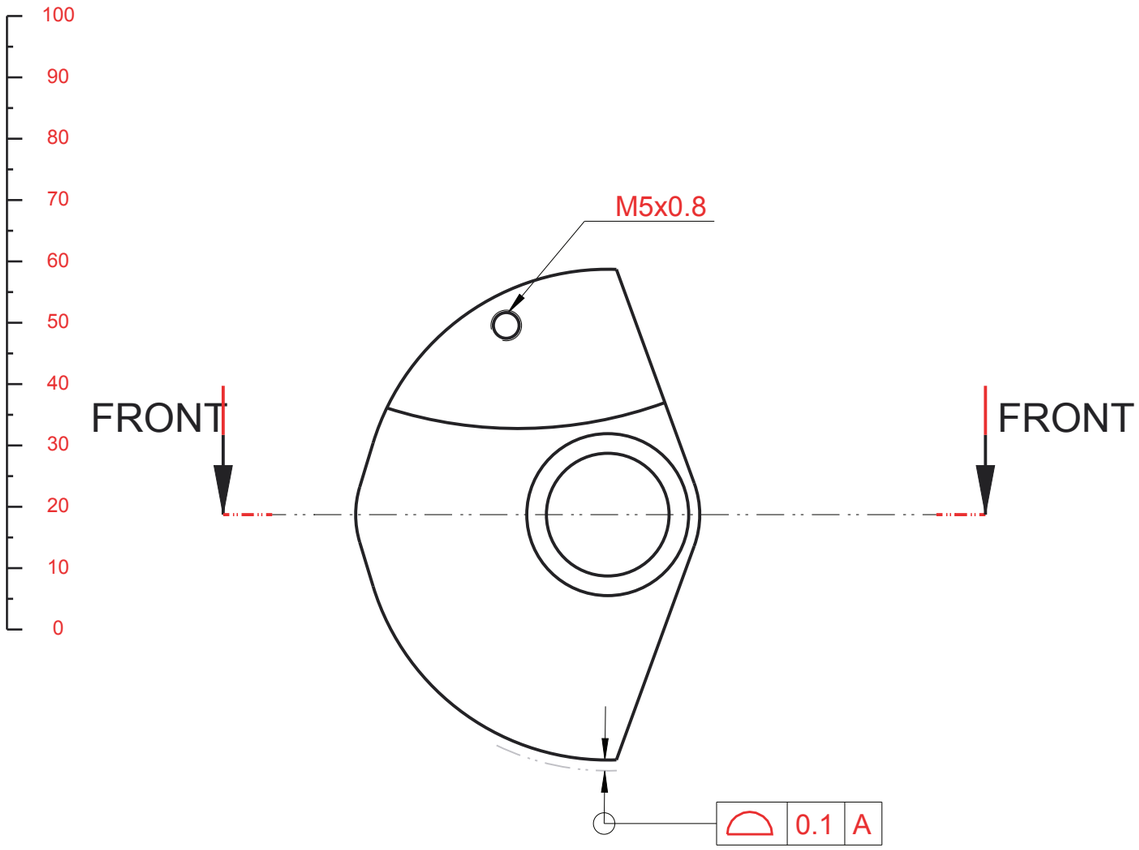

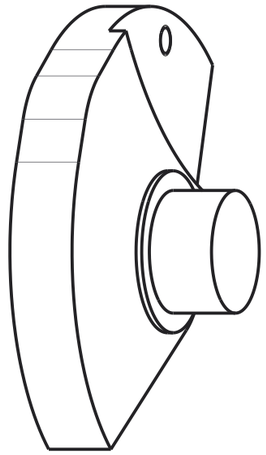

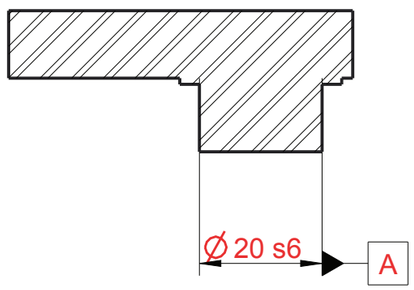

FRONT-FRONT

For missing dimensions, please check 3D file and apply general dimensional tolerances
Min. Hardness: 45 HRC
Surface treatment: Chemically black

General tolerance unless otherwise stated: DIN ISO 2768 - mH	General surface roughness unless otherwise stated:			
Material: Steel	Date: 27-Apr-17		Surf. roughness acc. to ISO 1302	
	Drawn: Pedro Almeida		CAD system: Creo Parametric	Sheet: 1 of 1
Name: Reverse cam	Design Resp.: Rudi Aerts		Copied from	Scale: 1:1 / Mass: ( )kg
This drawing is property of Punch Powertrain NV and can't be used, copied or shown to third parties without written permission.	Article number: PNSA3403_1		Index: 0	
PUNCH POWERTRAIN NV	Document number: PNSA3403_1		Index: 0	DIN: A3

model name: PNSA3403_1 [PART]

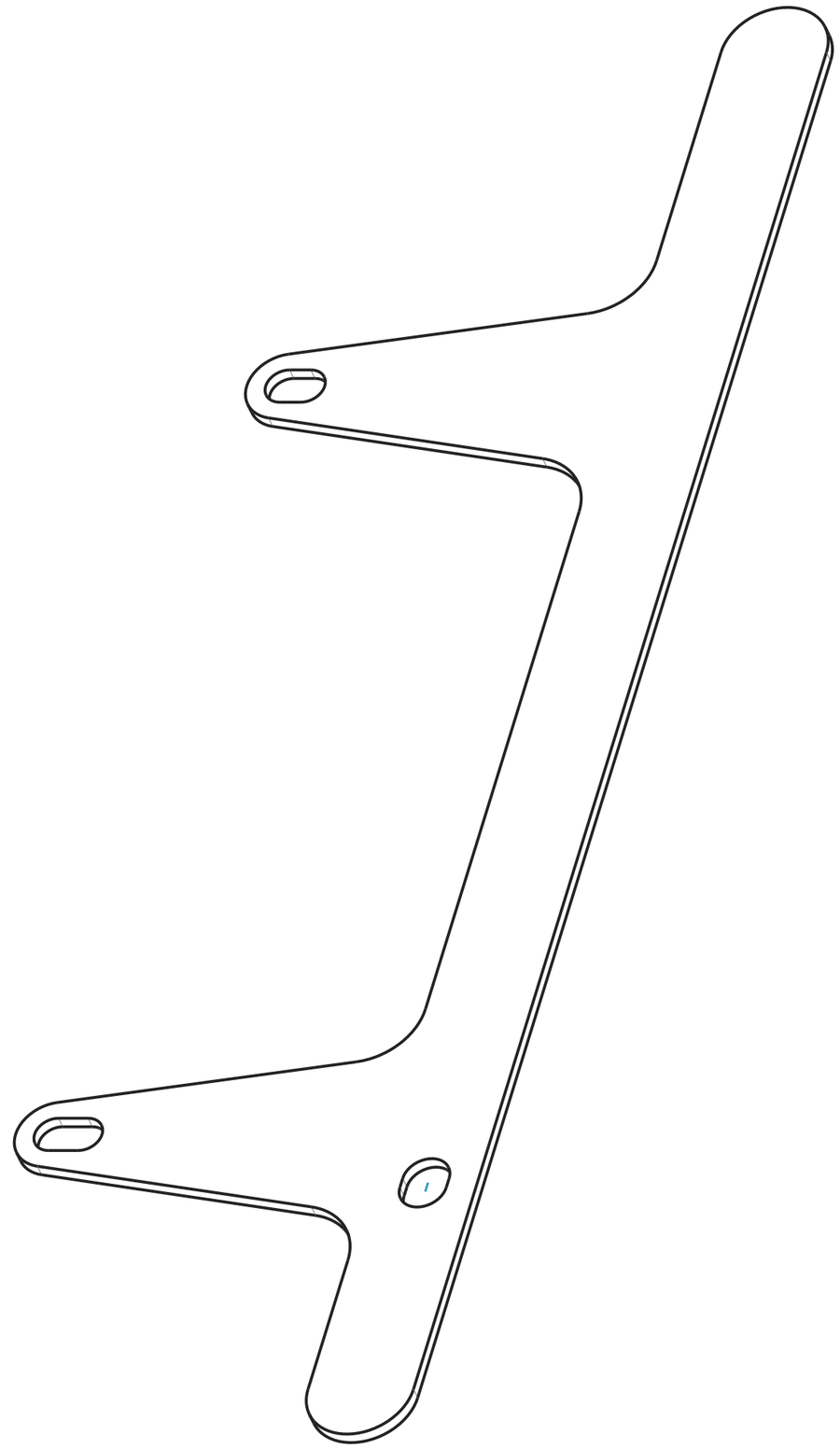

1:1.25

For missing dimensions, please check 3D file and apply general dimensional tolerances

General tolerance unless otherwise stated: DIN ISO 2768 - mH	General surface roughness unless otherwise stated:		
Material: Steel	Date: 19-May-17	Surf. roughness acc. to ISO 1302	
	Drawn: Pedro Almeida	CAD system: Creo Parametric	Sheet: 1 of 1
	Design Resp.: Rudi Aerts		
Name: Transmission plate	Copied from: PNSA3601	Scale: 1:1	Mass: ( )kg
This drawing is property of Punch Powertrain NV and can't be used, copied or shown to third parties without written permission.	Article number: PNSA3601	Index: 0	
PUNCH POWERTRAIN NV	Document number: PNSA3601	Index: 0	DIN: A3

model name: PNSA3601 [PART]

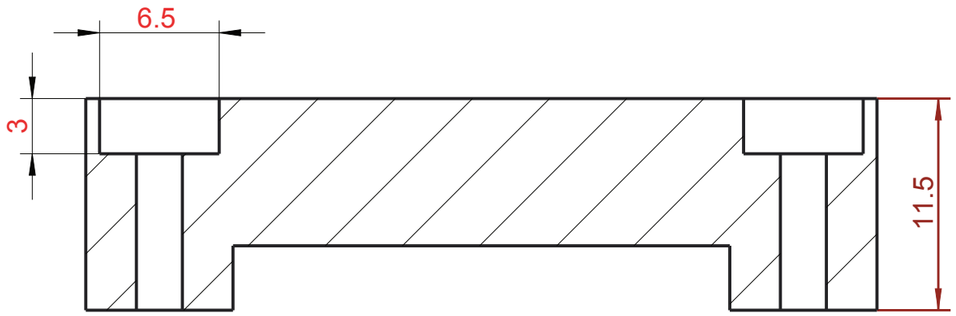

A-A

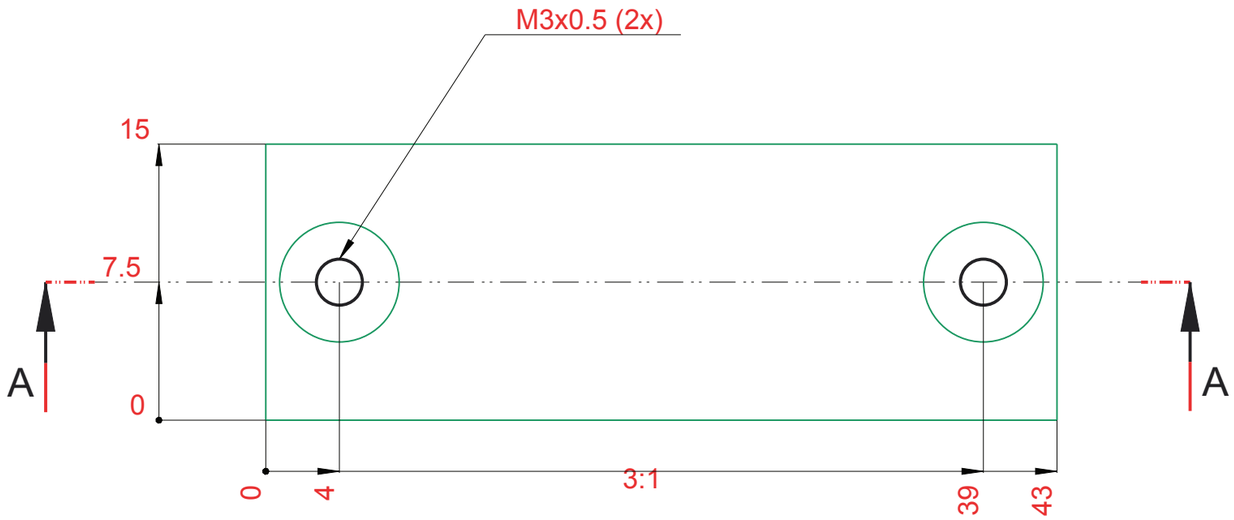

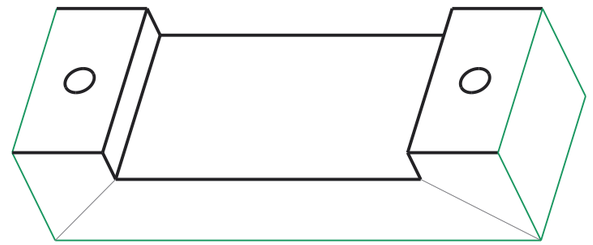

2:1

For missing dimensions, please check 3D file and apply general dimensional tolerances

General tolerance unless otherwise stated: DIN ISO 2768 - mH	General surface roughness unless otherwise stated:			
Material: Alu	Date: 18-May-17	Surf. roughness acc. to ISO 1302		
	Drawn: Pedro Almeida	CAD system: Creo Parametric	Sheet: 1 of 1	
Name: Transmission plate blocks	Design Resp.: Rudi Aerts			
	Copied from: PNSA3608	Scale: 1:1	Mass: ( )kg	
This drawing is property of Punch Powertrain NV and can't be used, copied or shown to third parties without written permission.	Article number: PNSA3608	Index: 0		
PUNCH POWERTRAIN NV	Document number: PNSA3608	Index: 0	DIN: A3	

model name: PNSA3608 [PART]

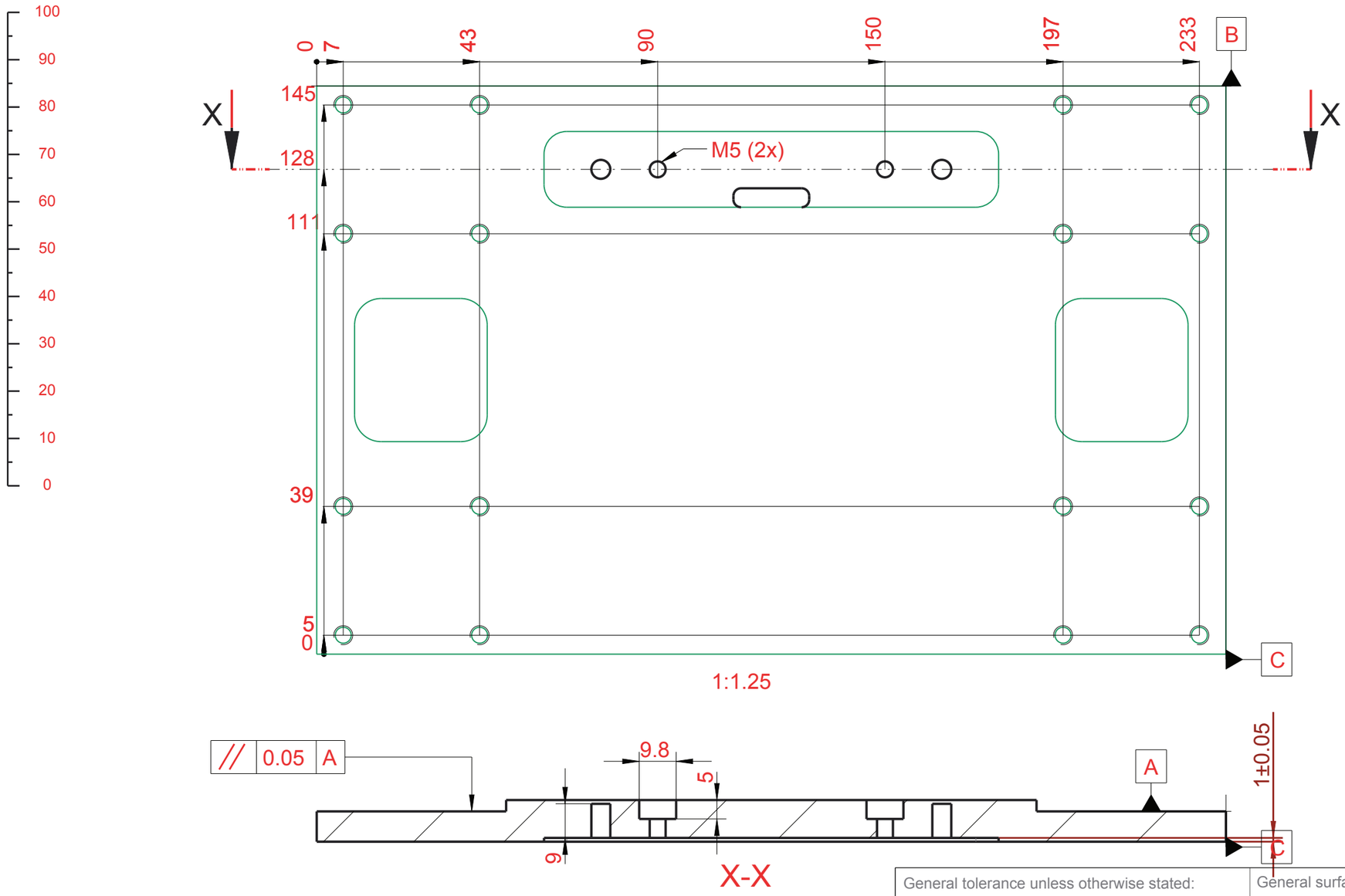

For missing dimensions, please check 3D file and apply general dimensional tolerances
Surface treatment: Black anodising

General tolerance unless otherwise stated: DIN ISO 2768 - mH	General surface roughness unless otherwise stated:		
Material: Alu	Date: 28-Apr-17	Surf. roughness acc. to ISO 1302	
	Drawn: Pedro Almeida	CAD system: Creo Parametric	Sheet: 1 of 1
Name: FWD plate	Design Resp.: Rudi Aerts		
	Copied from	Scale: 1:1	Mass: ( )kg
This drawing is property of Punch Powertrain NV and can't be used, copied or shown to third parties without written permission.	Article number: PNSA3701	Index: 0	
PUNCH POWERTRAIN NV	Document number: PNSA3701	Index: 0	DIN: A3

model name: PNSA3701 [PART]

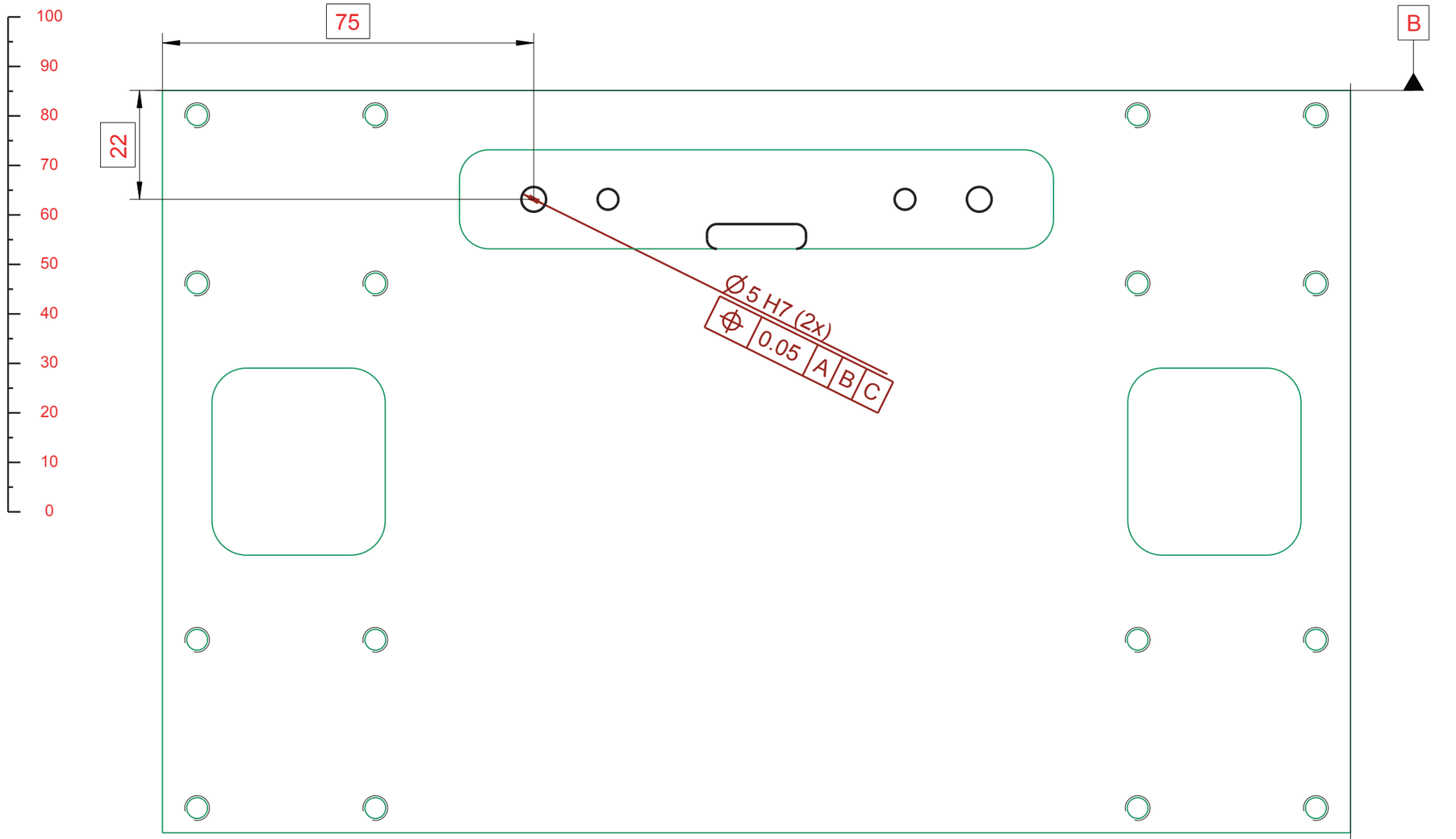

For missing dimensions, please check 3D file and apply general dimensional tolerances

General tolerance unless otherwise stated:	General surface roughness unless otherwise stated:	

Material: Alu	Date: 28-Apr-17		Surf. roughness acc. to ISO 1302	
	Drawn: Pedro Almeida		CAD system: Creo Parametric	Sheet: 2 of 2
Name: FWD Plate	Design Resp.: Rudi Aerts			
	Copied from: PNSA3701		Scale: 1:1	Mass: ( )kg
This drawing is property of Punch Powertrain NV and can't be used, copied or shown to third parties without written permission.	Article number: PNSA3701		Index: 0	
PUNCH POWERTRAIN NV	Document number: PNSA3701		Index: 0	DIN: A3

model name: PNSA3701 [PART]

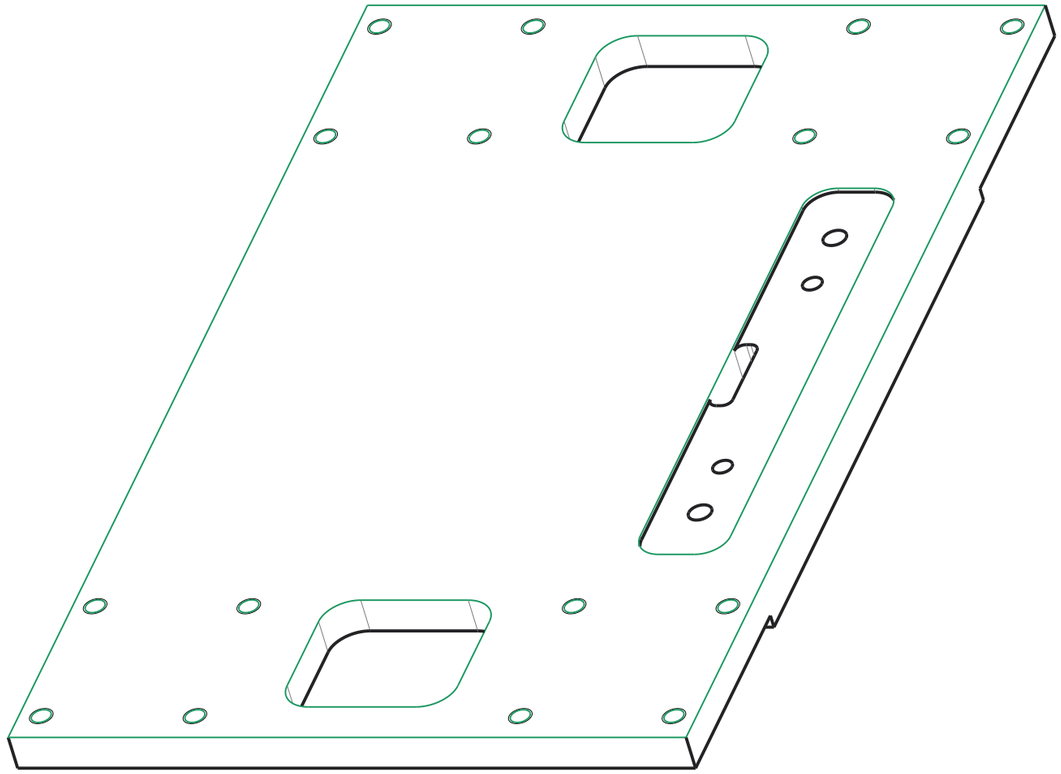

1:1.25

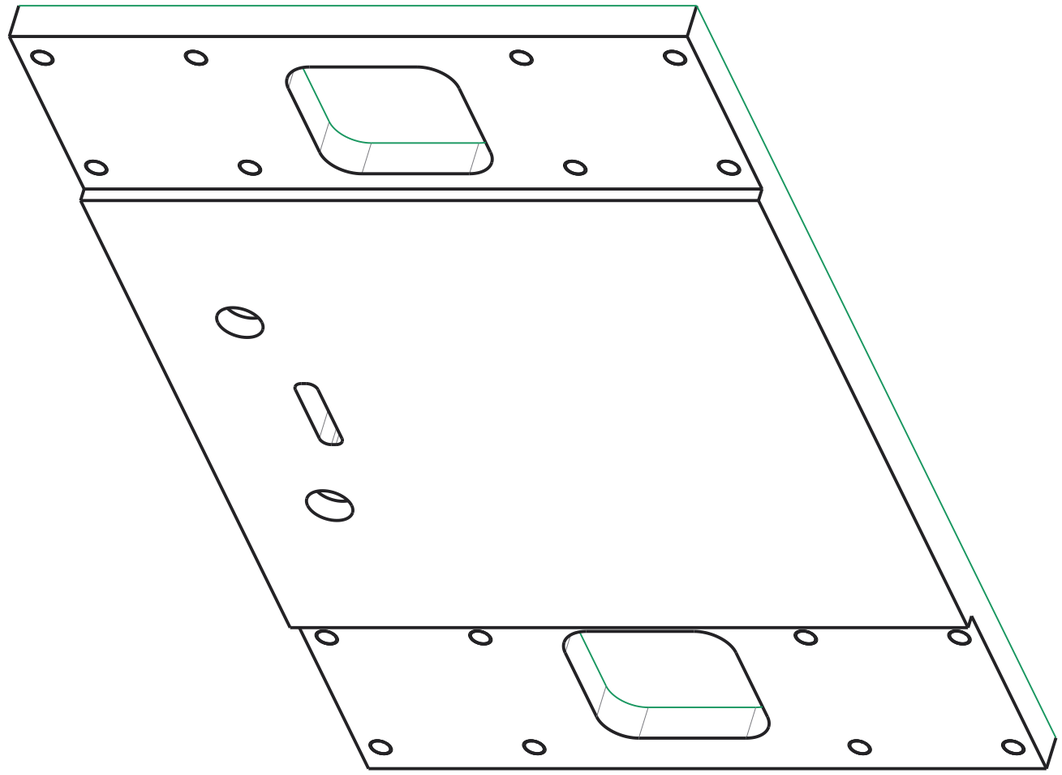

1:1.25

For missing dimensions, please check 3D file and apply general dimensional tolerances

General tolerance unless otherwise stated:	General surface roughness unless otherwise stated:		
Material: Alu	Date: 28-Apr-17	Surf. roughness acc. to ISO 1302	
	Drawn: Pedro Almeida	CAD system: Creo Parametric	Sheet: 3 of 3
	Design Resp.: Rudi Aerts		
Name: FWD Plate	Copied from: PNSA3701	Scale: 1:1	Mass: ( )kg
This drawing is property of Punch Powertrain NV and can't be used, copied or shown to third parties without written permission.	Article number: PNSA3701	Index: 0	
PUNCH POWERTRAIN NV	Document number: PNSA3701	Index: 0	DIN: A3

model name: PNSA3701 [PART]

For missing dimensions, please check 3D file and apply general dimensional tolerances
Surface treatment: Black anodising

General tolerance unless otherwise stated: DIN ISO 2768 - mH	General surface roughness unless otherwise stated:		
Material: Alu	Date: 28-Apr-17	Surf. roughness acc. to ISO 1302	
	Drawn: Pedro Almeida	CAD system: Creo Parametric	Sheet: 1 of 1
Name: Selector shaft	Design Resp.: Rudi Aerts		
	Copied from	Scale: 1:1	Mass: ( )kg
This drawing is property of Punch Powertrain NV and can't be used, copied or shown to third parties without written permission.	Article number: PNSA3102_2	Index: 0	
PUNCH POWERTRAIN NV	Document number: PNSA3102_2	Index: 0	DIN: A3

model name: PNSA3102_2 [PART]

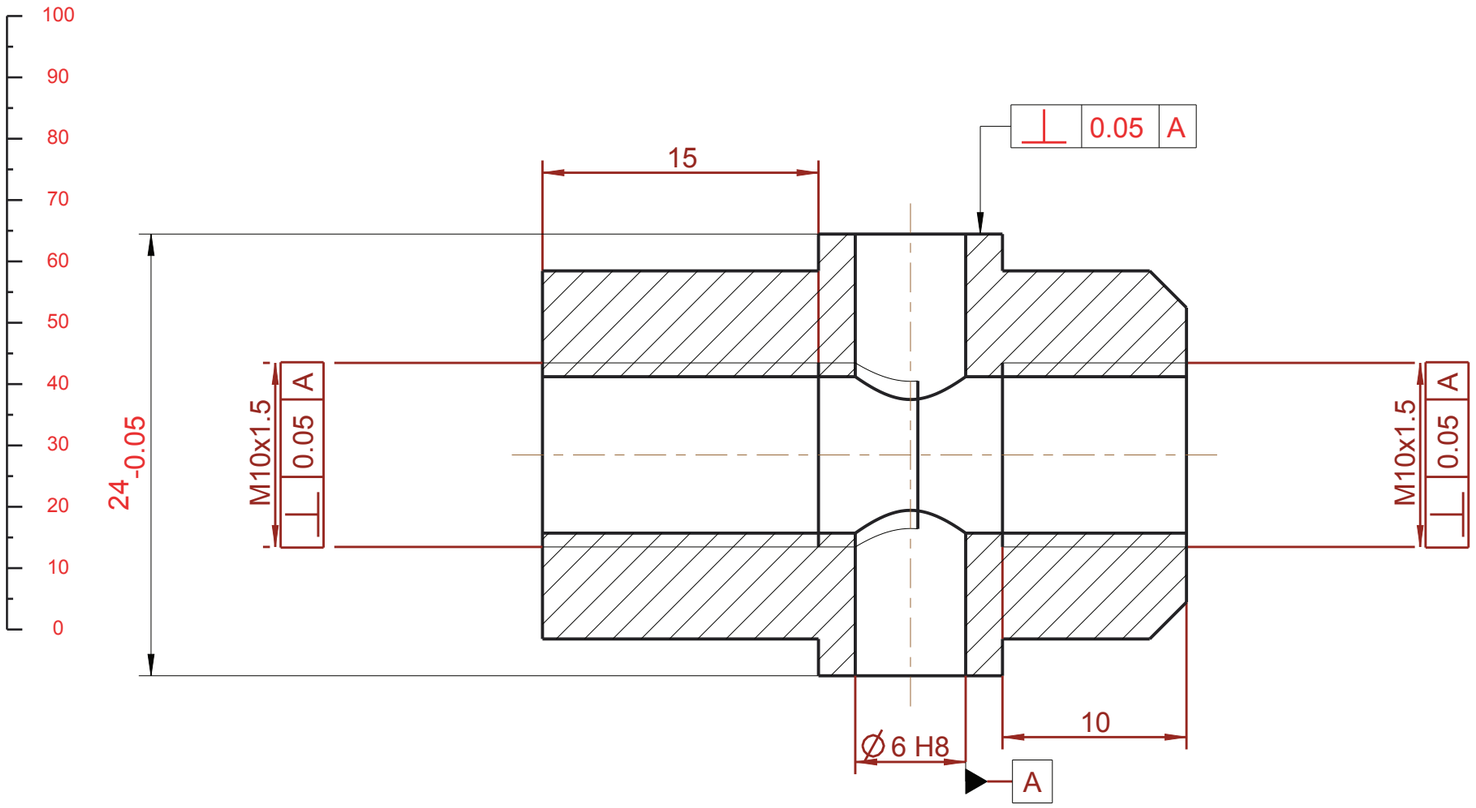

A-A

3:1

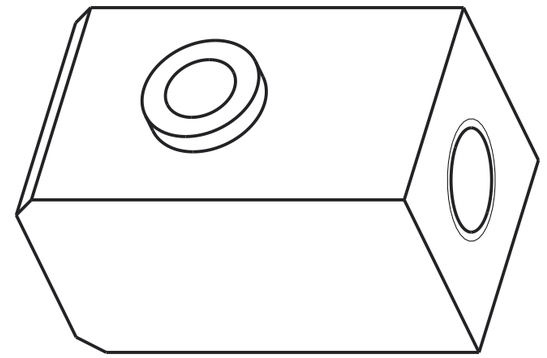

2:1

For missing dimensions, please check 3D file and apply general dimensional tolerances

General tolerance unless otherwise stated: DIN ISO 2768 - mH	General surface roughness unless otherwise stated:		
Material: Alu	Date: 27-Apr-17	Surf. roughness acc. to ISO 1302	
	Drawn: Pedro Almeida	CAD system: Creo Parametric	Sheet: 1 of 1
Name: Joining	Design Resp.: Rudi Aerts		
	Copied from	Scale: 1:1	Mass: ( )kg
This drawing is property of Punch Powertrain NV and can't be used, copied or shown to third parties without written permission.	Article number: PNSA3102_5	Index: 0	
PUNCH POWERTRAIN NV	Document number: PNSA3102_5	Index: 0	DIN: A3

model name: PNSA3102_5 [PART]

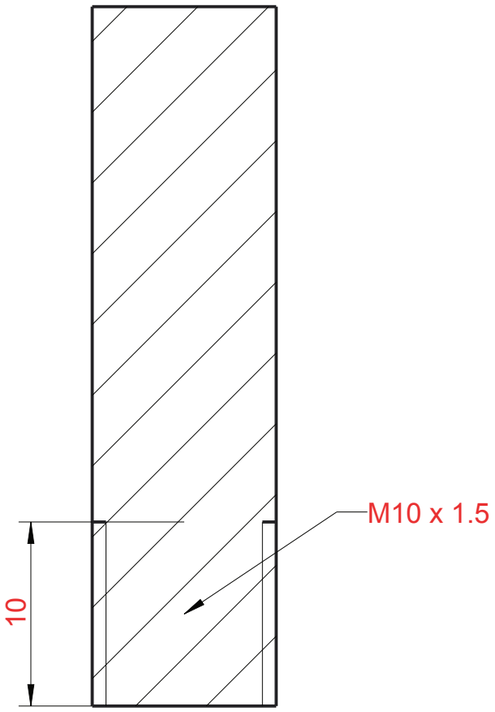

RIGHT-RIGHT
3:1

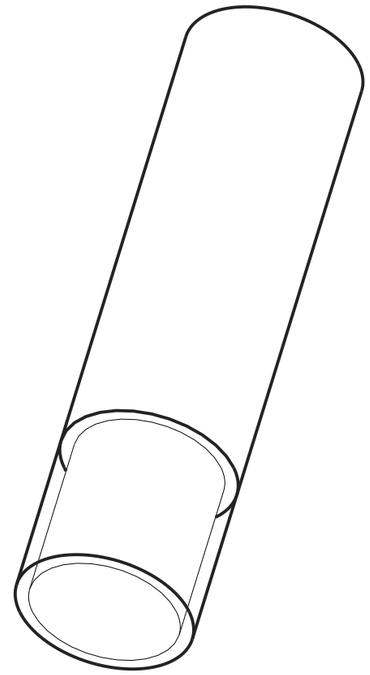

3:1

For missing components, please check 3D file and apply general dimensional tolerances

General tolerance unless otherwise stated: DIN ISO 2768 - mH	General surface roughness unless otherwise stated:		
Material: Alu	Date: 28-Apr-17	Surf. roughness acc. to ISO 1302	
	Drawn: Pedro Almeida	CAD system: Creo Parametric	Sheet: 1 of 1
Name: Secondary shaft	Design Resp.: Rudi Aerts	Copied from	Scale: 1:1 / Mass: ( )kg
This drawing is property of Punch Powertrain NV and can't be used, copied or shown to third parties without written permission.	Article number: PNSA3102_6	Index: 0	
PUNCH POWERTRAIN NV	Document number: PNSA3102_6	Index: 0	DIN: A3

model name: PNSA3102_6 [PART]

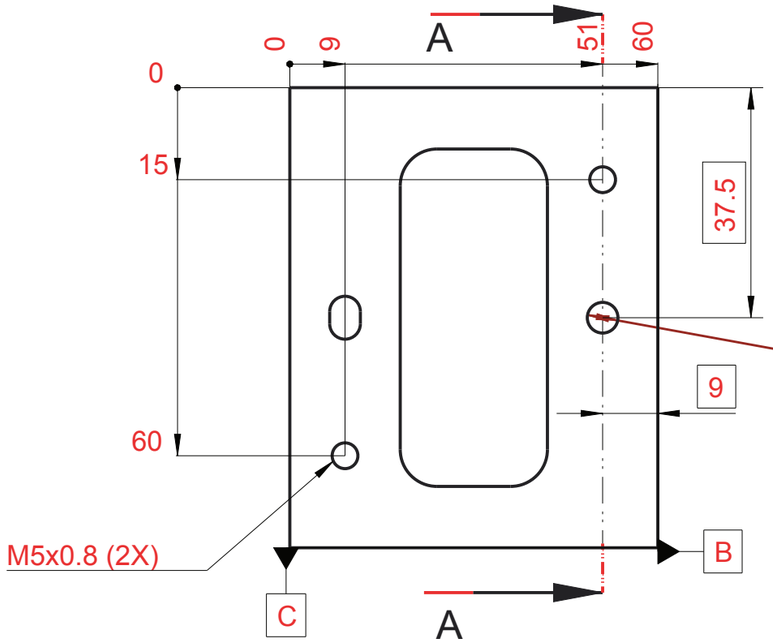

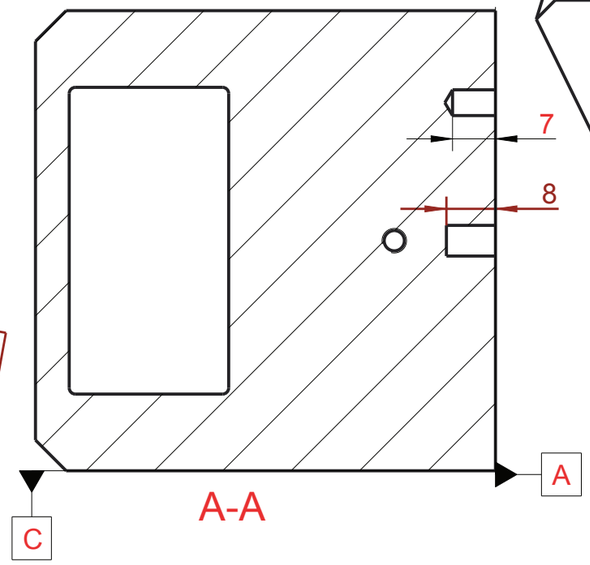

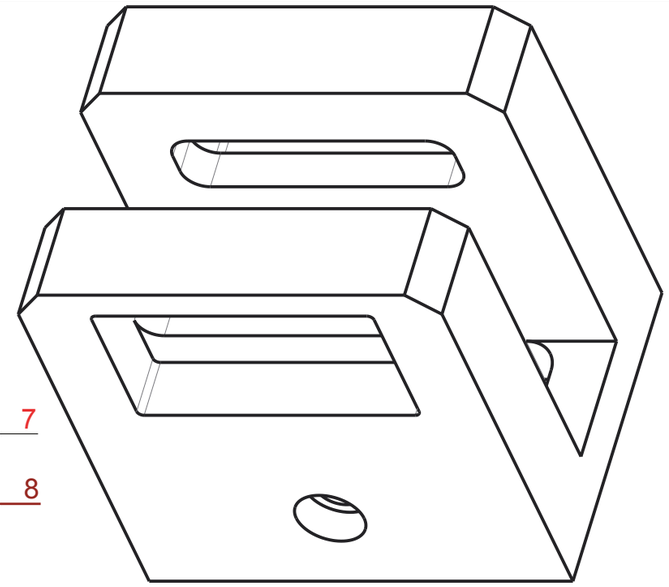

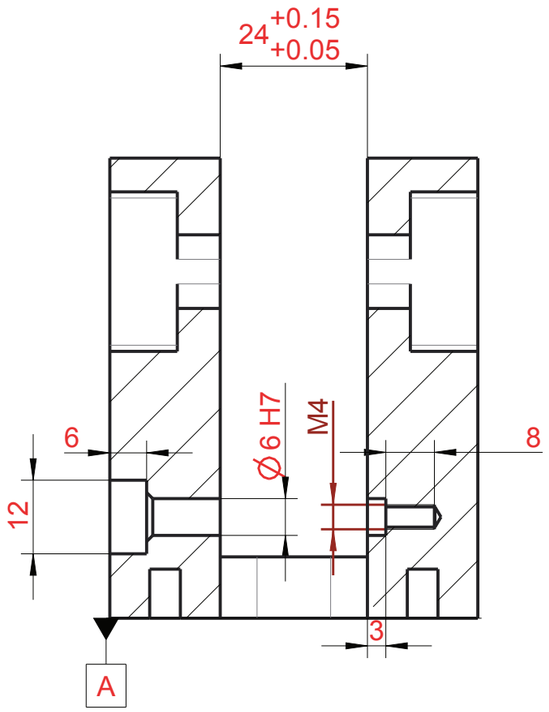

X-X

For missing dimensions, please check 3D file and apply general dimensional tolerances

General tolerance unless otherwise stated: DIN ISO 2768 - mH	General surface roughness unless otherwise stated:			
Material: Alu	Date: 09-May-17	Surf. roughness acc. to ISO 1302		
	Drawn: Pedro Almeida	CAD system: Creo Parametric	Sheet: 1 of 1	
Name: PNSA3102_11	Design Resp.: Rudi Aerts			
	Copied from	Scale: 1:1	Mass: ( )kg	
This drawing is property of Punch Powertrain NV and can't be used, copied or shown to third parties without written permission.	Article number: PNSA3102_11	Index: 0		
PUNCH POWERTRAIN NV	Document number: PNSA3102_11	Index: 0	DIN: A3	

model name: PNSA3102_11 [PART]

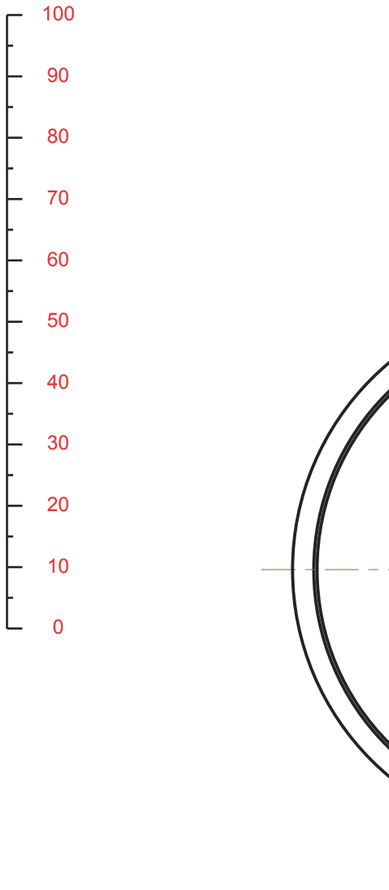

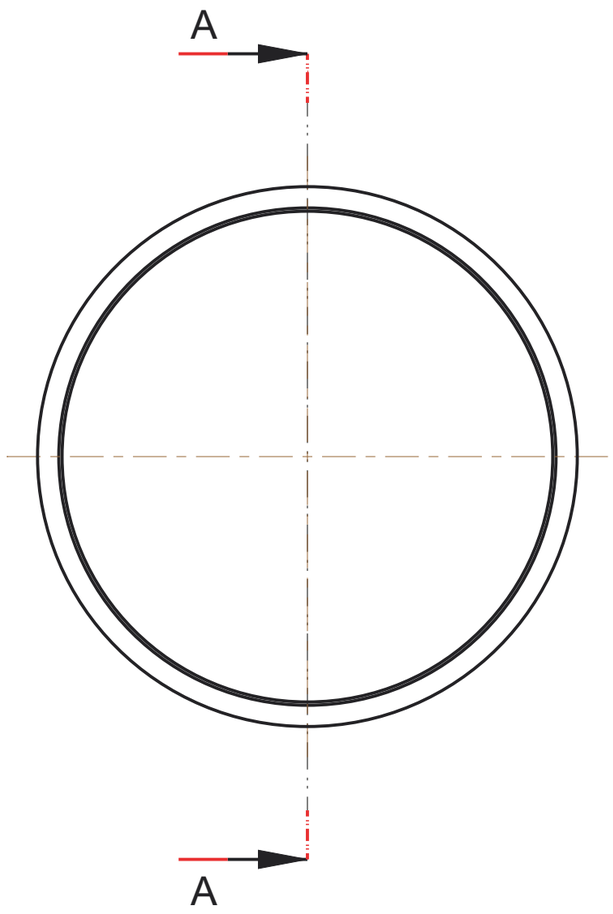

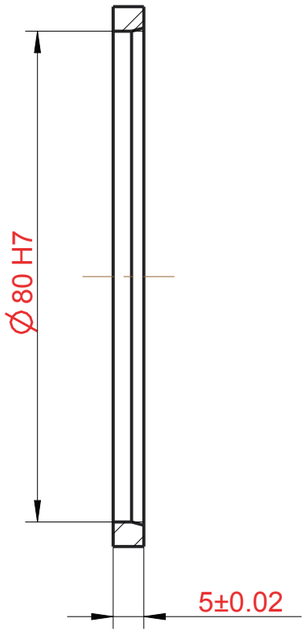

A-A

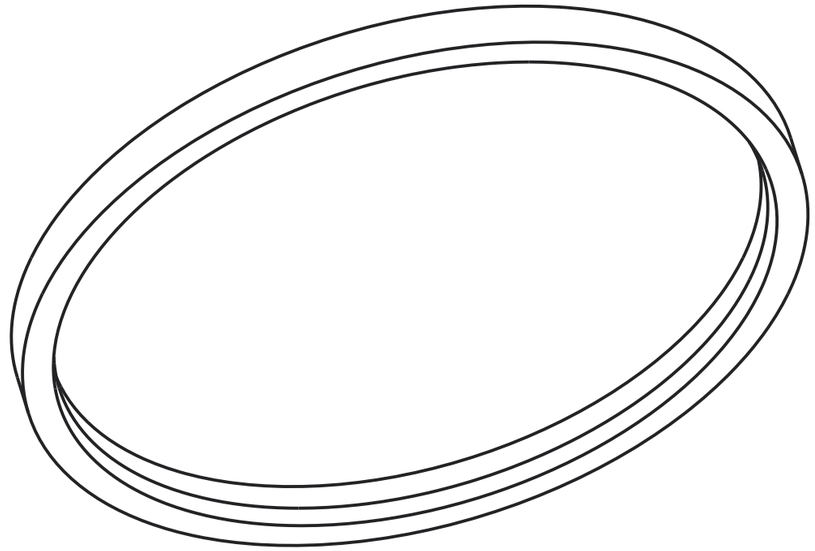

1.5:1

For missing dimensions, please check 3D file and apply general dimensional tolerances
Surface treatment: Chemically black
Hardness: Equal or higher to the Ball transfer units

General tolerance unless otherwise stated: ISO 2768 - mH	General surface roughness unless otherwise stated:		
Material: Steel	Date: 06-May-17	Surf. roughness acc. to ISO 1302	
	Drawn: Pedro Almeida	CAD system: Creo Parametric	Sheet: 1 of 1
	Design Resp.: Rudi Aerts		
Name: RING	Copied from: PNSA3302_1	Scale: 1:1	Mass: ( )kg
This drawing is property of Punch Powertrain NV and can't be used, copied or shown to third parties without written permission.	Article number: PNSA3302_1	Index: 0	
PUNCH POWERTRAIN NV	Document number: PNSA3302_1	Index: 0	DIN: A3

model name: PNSA3302_1 [PART]

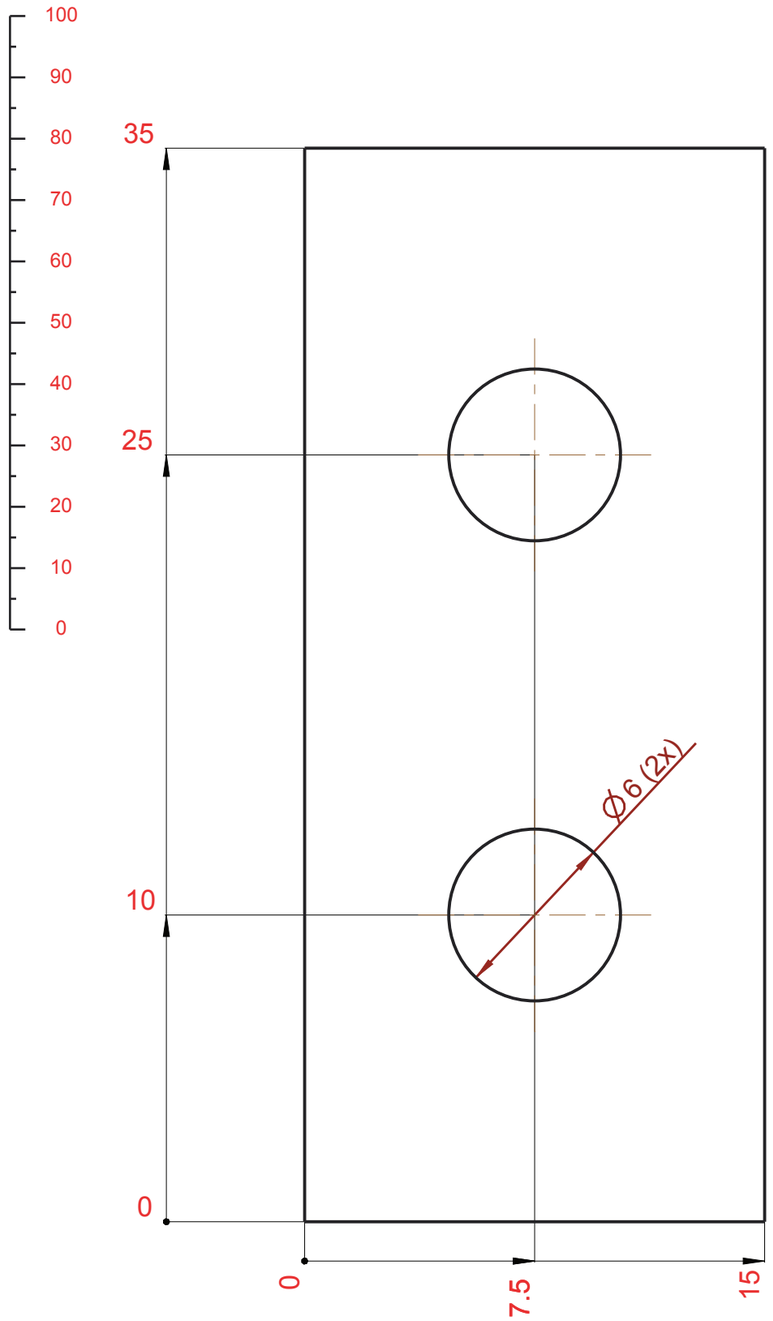

5:1

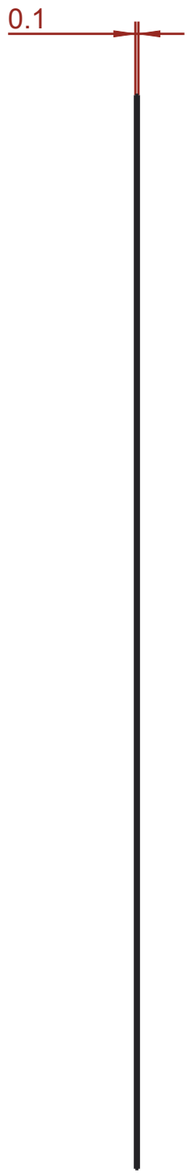

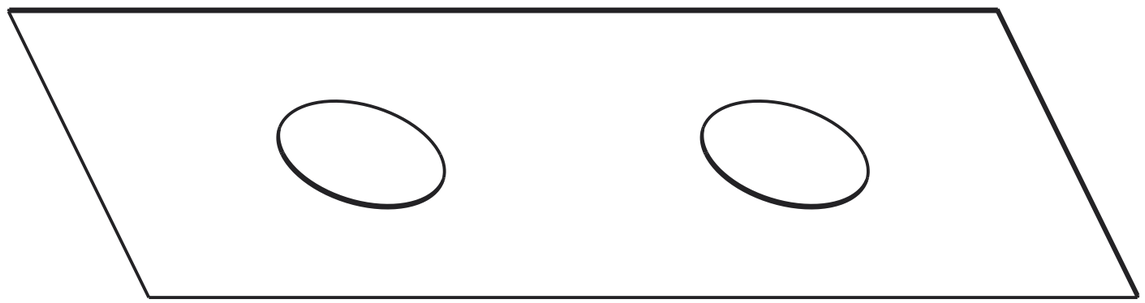

5:1

General tolerance unless otherwise stated: DIN ISO 2768 - mH	General surface roughness unless otherwise stated:		
Material: Alu	Date: 30-May-17	Surf. roughness acc. to ISO 1302	
	Drawn: Pedro Almeida	CAD system: Creo Parametric	Sheet: 1 of 1
Name: Shim	Design Resp.: Rudi Aerts		
	Copied from	Scale: 1:1	Mass: ( )kg
This drawing is property of Punch Powertrain NV and can't be used, copied or shown to third parties without written permission.	Article number: PNSA3302_3	Index: 0	
PUNCH POWERTRAIN NV	Document number: PNSA3302_3	Index: 0	DIN: A3

model name: PNSA3302_3 [PART]

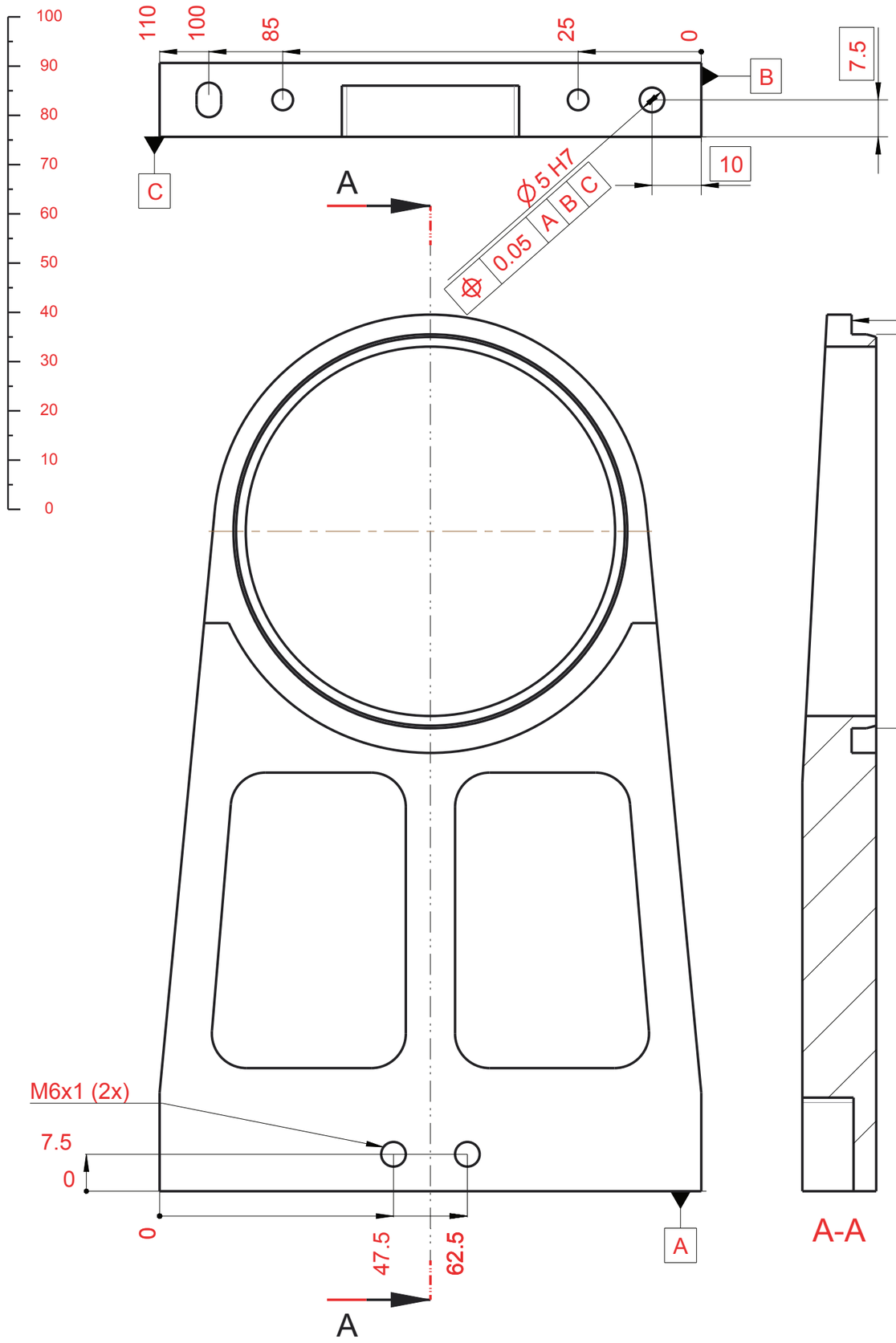

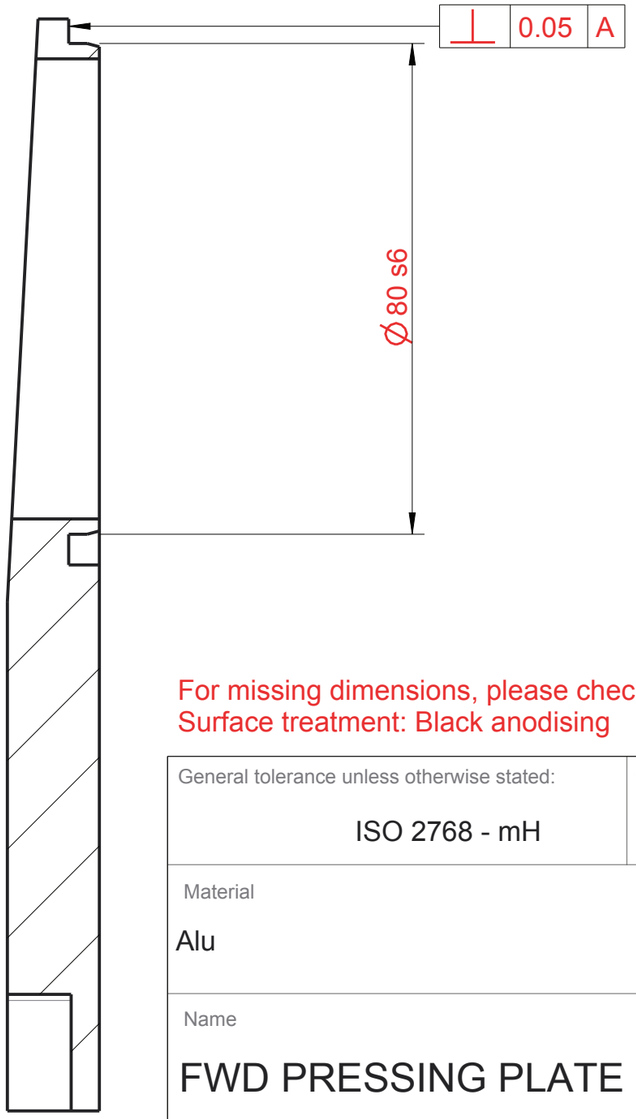

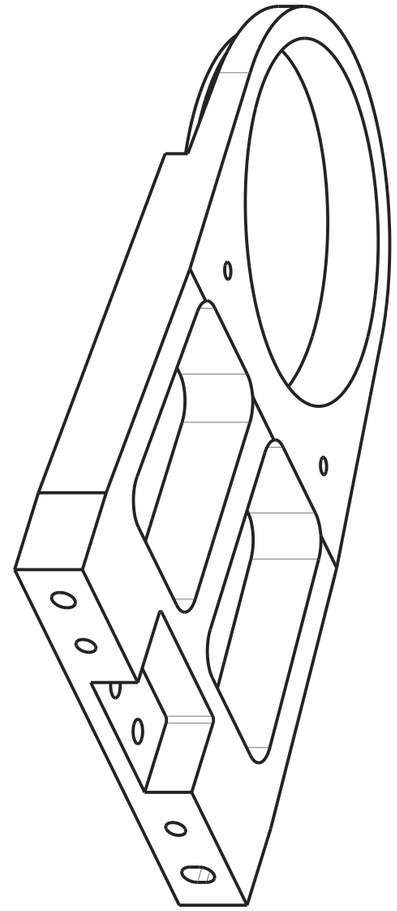

1:1.25

For missing dimensions, please check 3D file and apply general dimensional tolerances
Surface treatment: Black anodising

General tolerance unless otherwise stated:	General surface roughness unless otherwise stated:	
ISO 2768 - mH		

Material: Alu	Date: 05-July-17		Surf. roughness acc. to ISO 1302	
	Drawn: Pedro Almeida		CAD system: Creo Parametric	Sheet: 1 of 2
	Design Resp.: Rudi Aerts			
Name: FWD PRESSING PLATE	Copied from		Scale: 1:1	Mass: ( )kg
This drawing is property of Punch Powertrain NV and can't be used, copied or shown to third parties without written permission.	Article number: PNSA3302_5		Index: 0	
PUNCH POWERTRAIN NV	Document number: PNSA3302_5		Index: 1	DIN: A3

model name: PNSA3302_5 [PART]

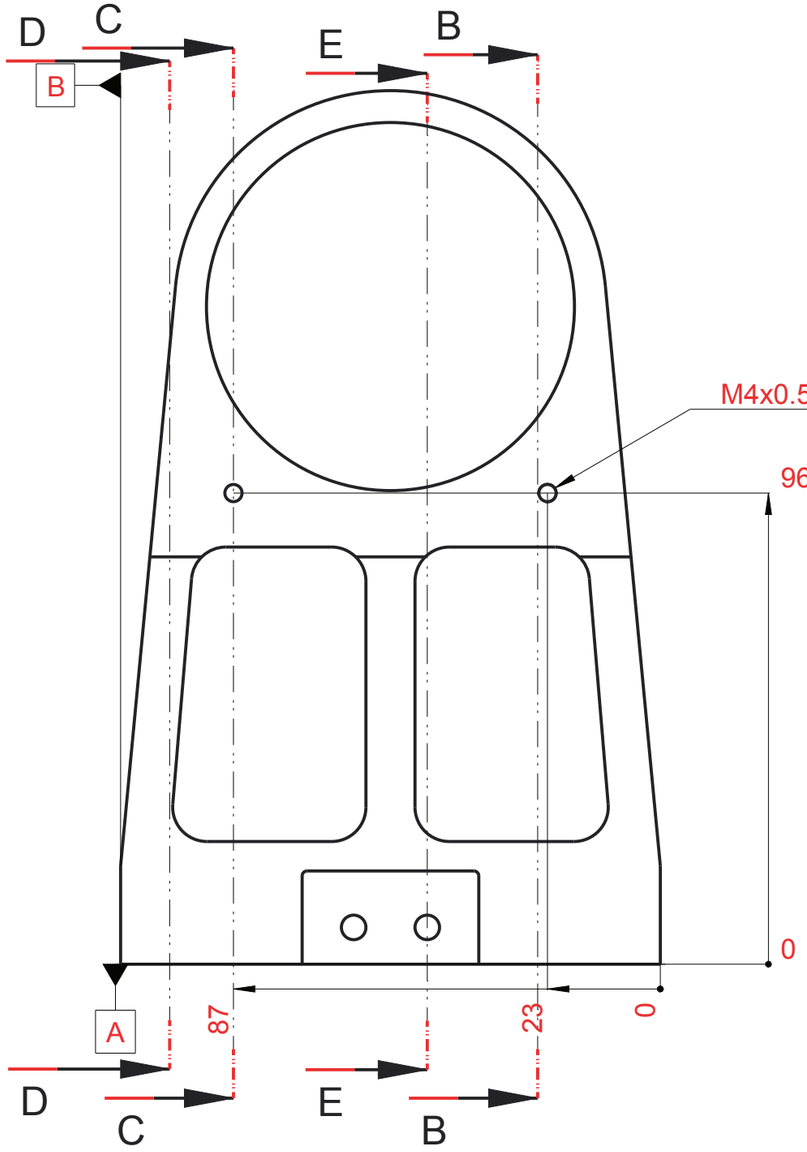

1:1.25

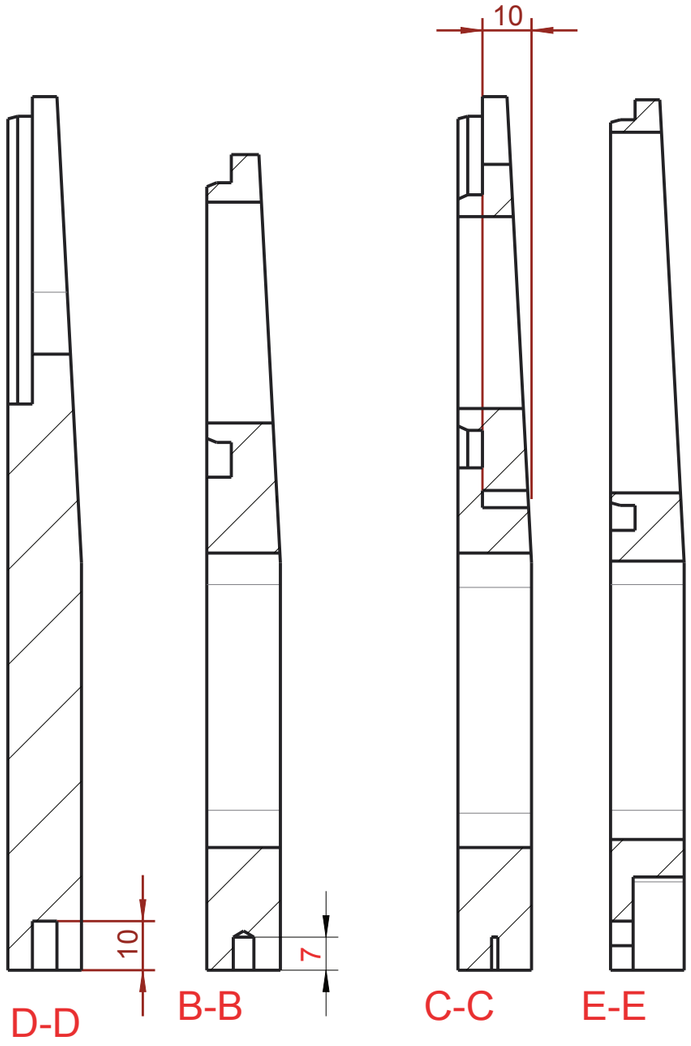

For missing dimensions, please check 3D file and apply general dimensional tolerances
Surface treatment: Black anodising

General tolerance unless otherwise stated: ISO 2768 - mH	General surface roughness unless otherwise stated:		
Material: Alu	Date: 05-July-17	Surf. roughness acc. to ISO 1302	
	Drawn: Pedro Almeida	CAD system: Creo Parametric	Sheet: 2 of 2
Name: FWD PRESSING PLATE	Design Resp.: Rudi Aerts	Copied from: PNSA3302_5	Scale: 1:1 / Mass: ( )kg
This drawing is property of Punch Powertrain NV and can't be used, copied or shown to third parties without written permission.	Article number: PNSA3302_5	Index: 0	
PUNCH POWERTRAIN NV	Document number: PNSA3302_5	Index: 1	DIN: A3

model name: PNSA3302_5 [PART]

6.42 Technical drawings of assemblies of the showcase model

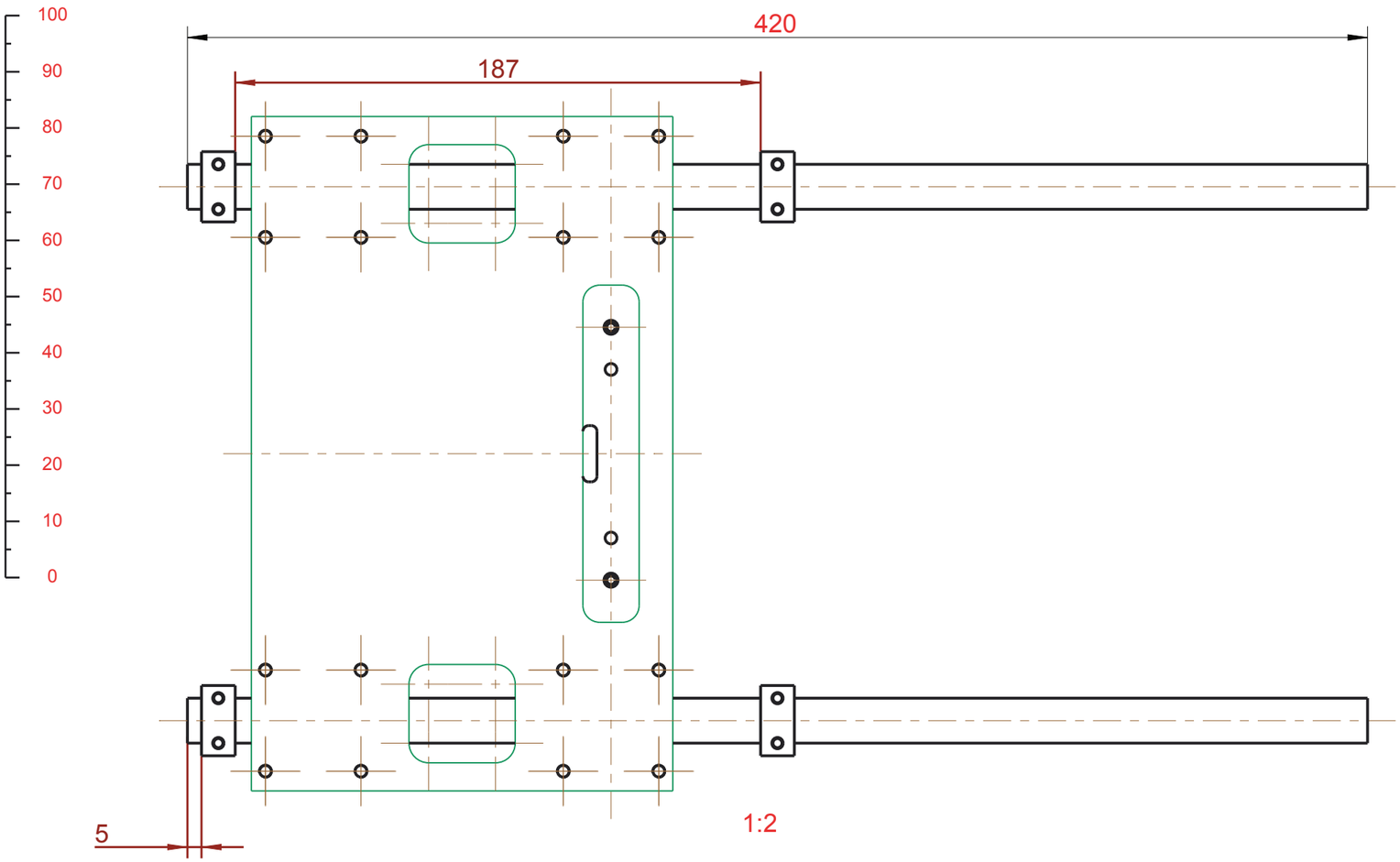

1:2

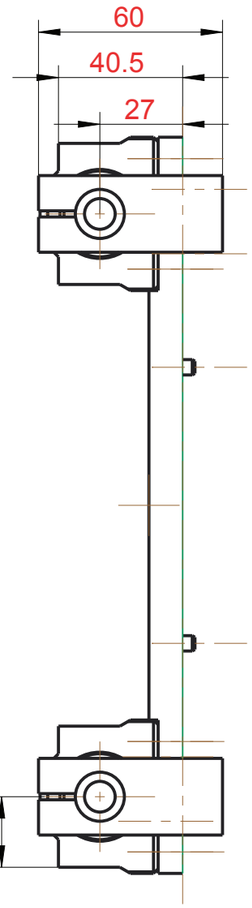

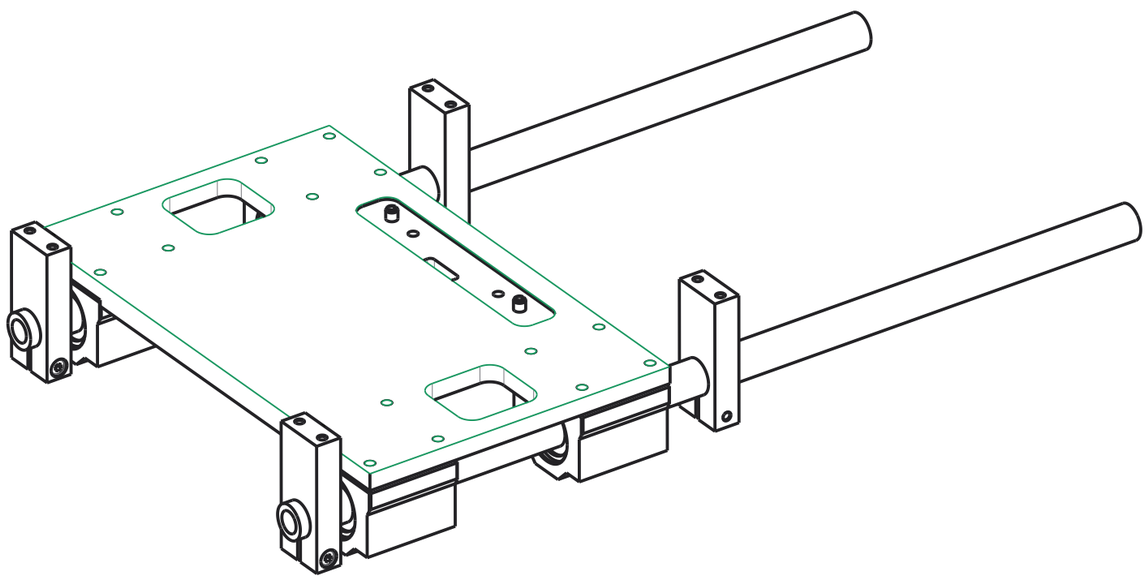

1:2.5

General tolerance unless otherwise stated:	General surface roughness unless otherwise stated:		
Material	Date: 28-June-17	Surf. roughness acc. to ISO 1302	
	Drawn: Pedro Almeida	CAD system: Creo Parametric	Sheet: 1 of 2
	Design Resp.: Rudi Aerts		
Name: FWD guiding system	Copied from: PNSA370	Scale: 1:1	Mass: ( )kg
This drawing is property of Punch Powertrain NV and can't be used, copied or shown to third parties without written permission.	Article number: PNSA370	Index: 0	
PUNCH POWERTRAIN NV	Document number: PNSA370	Index: 0	DIN: A3

model name: PNSA370 [ASSEM]

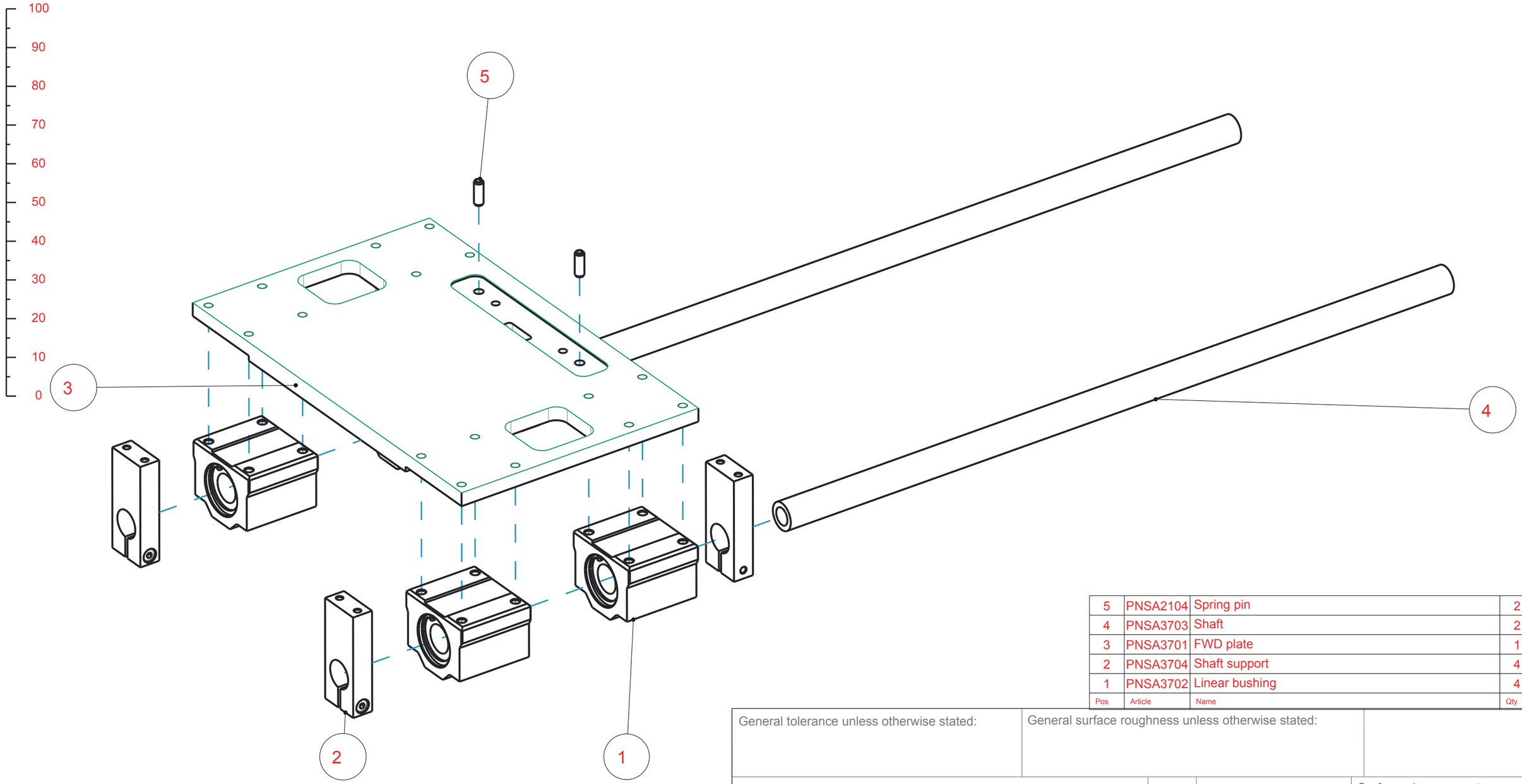

1:2

Pos	Article	Name	Qty
5	PNSA2104	Spring pin	2
4	PNSA3703	Shaft	2
3	PNSA3701	FWD plate	1
2	PNSA3704	Shaft support	4
1	PNSA3702	Linear bushing	4

General tolerance unless otherwise stated:	General surface roughness unless otherwise stated:		
Material	Date: 28-June-17	Surf. roughness acc. to ISO 1302	
	Drawn: Pedro Almeida	CAD system: Creo Parametric	Sheet: 2 of 2
	Design Resp.: Rudi Aerts		
Name: FWD guiding system	Copied from: PNSA370	Scale: 1:1	Mass: ( )kg
This drawing is property of Punch Powertrain NV and can't be used, copied or shown to third parties without written permission.	Article number: PNSA370	Index: 0	
PUNCH POWERTRAIN NV	Document number: PNSA370	Index: 0	DIN: A3

model name: PNSA370 [ASSEM]

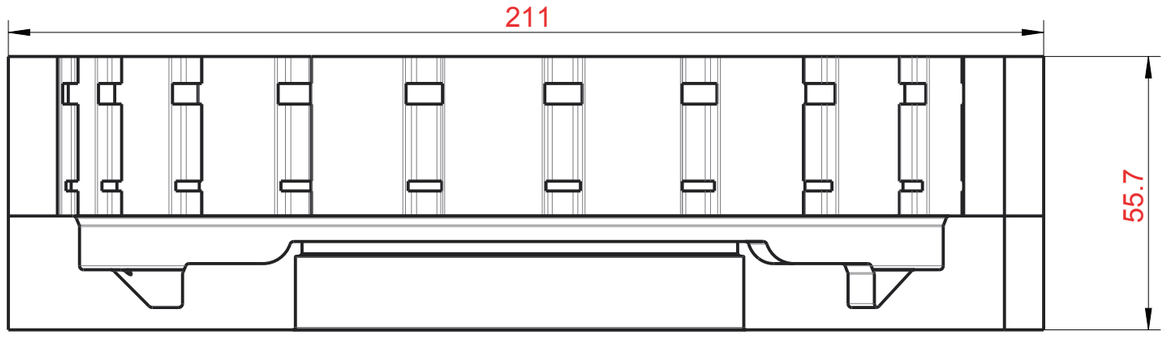

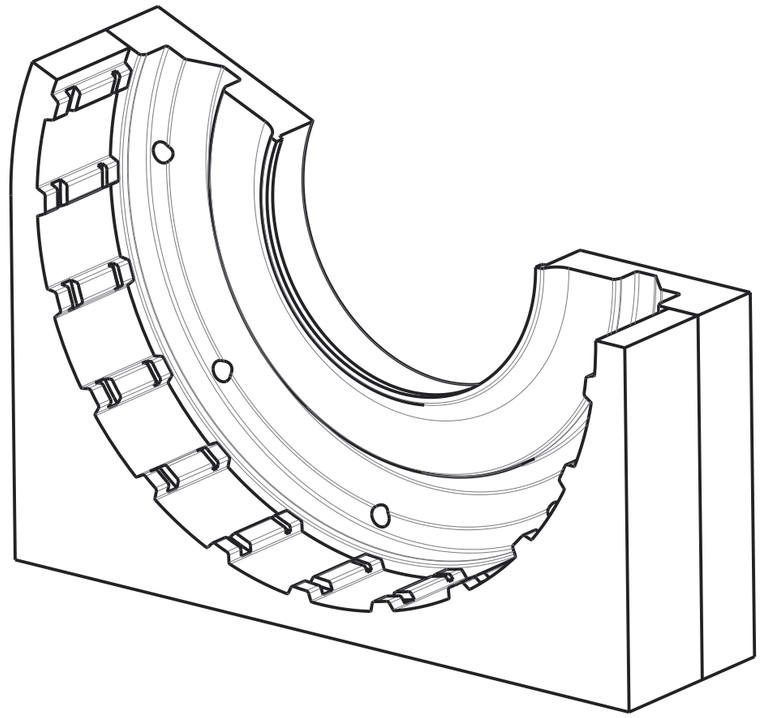

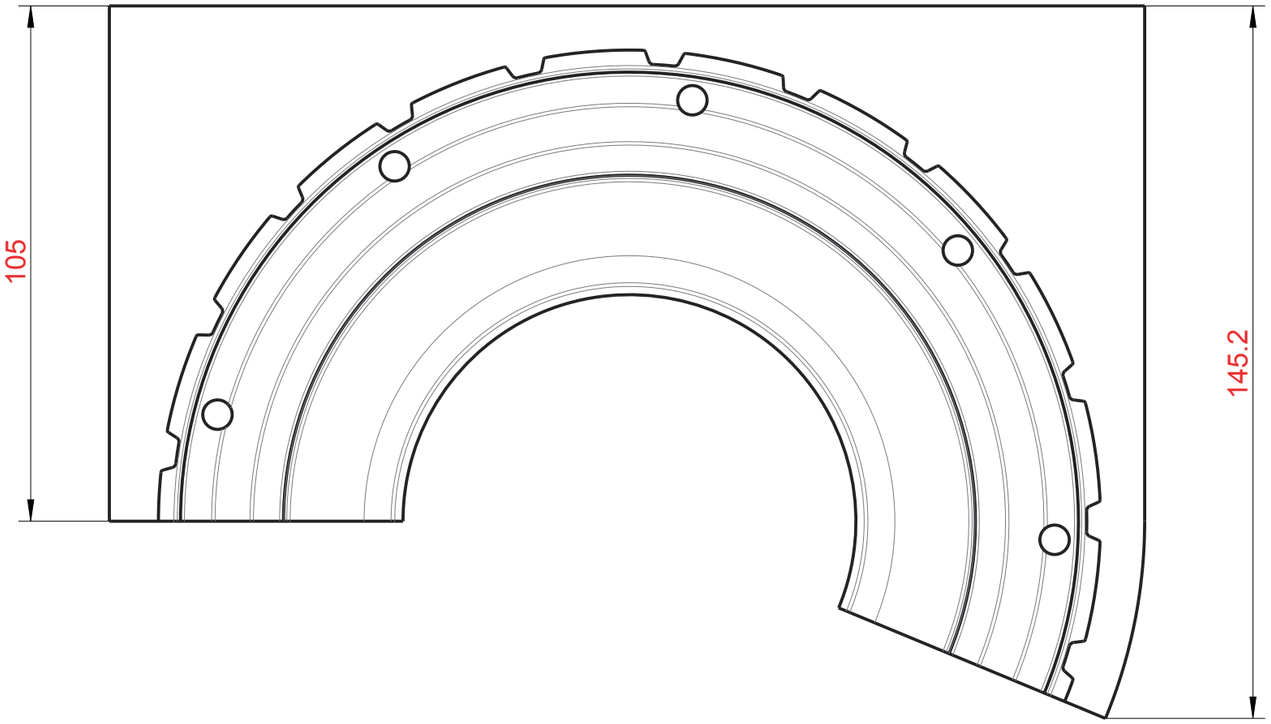

1:1.25

1:1.667

General tolerance unless otherwise stated:	General surface roughness unless otherwise stated:			
Material	Date	28-June-17	Surf. roughness acc. to ISO 1302	
	Drawn	Pedro Almeida	CAD system: Creo Parametric	Sheet: 1 of 2
Name: DNR Housing	Design Resp.	Rudi Aerts		
	Copied from: PNSA2103		Scale: 1:1	Mass: ( )kg
This drawing is property of Punch Powertrain NV and can't be used, copied or shown to third parties without written permission.	Article number: PNSA2103		Index: 0	
PUNCH POWERTRAIN NV	Document number: PNSA2103		Index: 0	DIN: A3

model name: PNSA2103 [ASSEM]

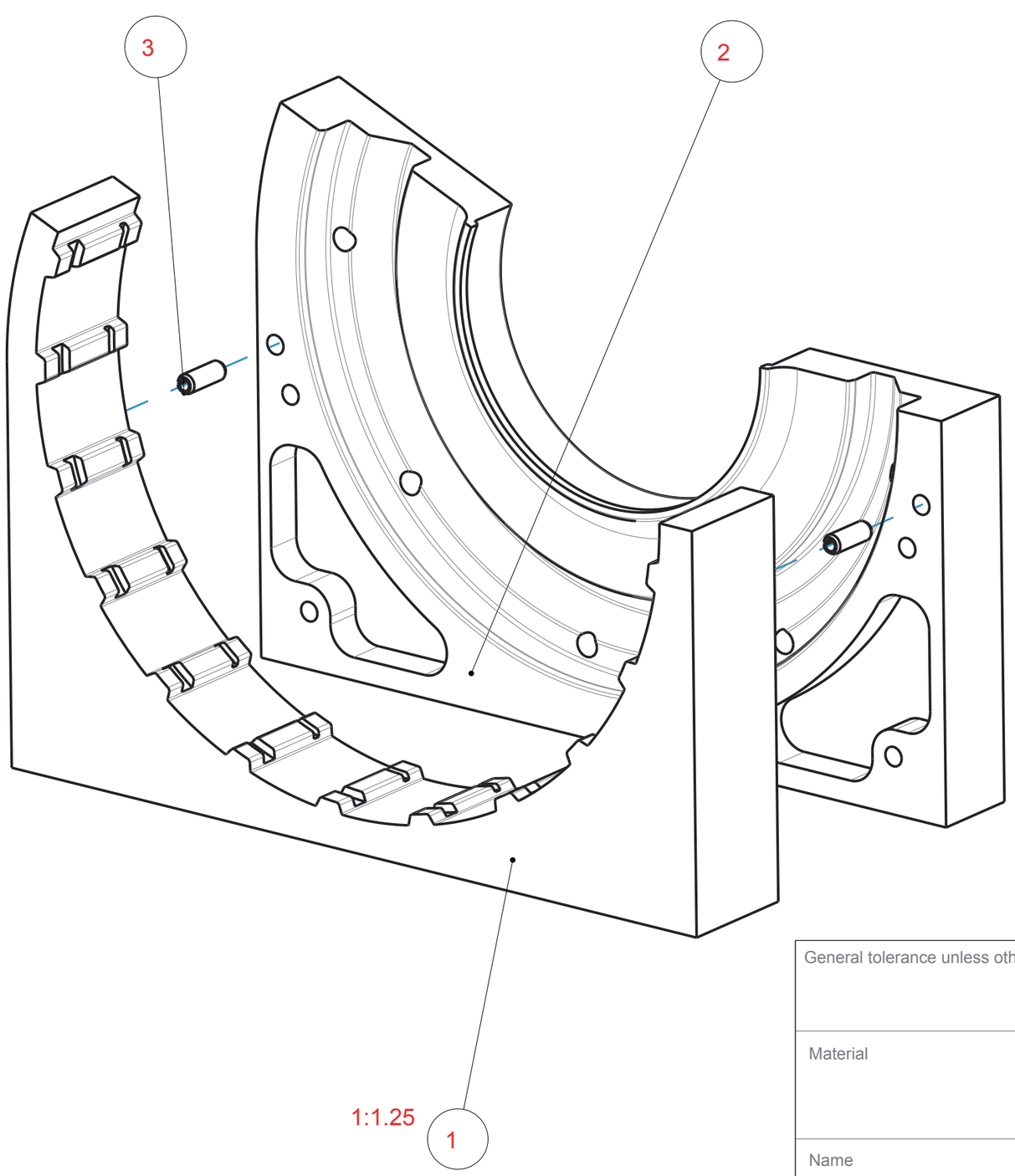

Pos	Article	Name	Qty
3	PNSA2104	Spring pin	2
2	PNSA2103_2	DNR Housing 2	1
1	PNSA2103_1	DNR Housing 1	1

General tolerance unless otherwise stated:

General surface roughness unless otherwise stated:

Material

Name

DNR Housing

PUNCH POWERTRAIN NV

Date	28-June-17	Surf. roughness acc. to ISO 1302	
Drawn	Pedro Almeida	CAD system: Creo Parametric	Sheet: 2 of 2
Design Resp.	Rudi Aerts		
Copied from: PNSA2103		Scale: 1:1	Mass: ( )kg
Article number: PNSA2103		Index: 0	
Document number: PNSA2103		Index: 0	DIN: A3

model name: PNSA2103 [ASSEM]

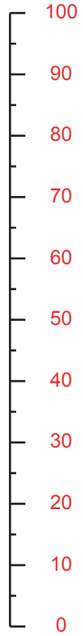

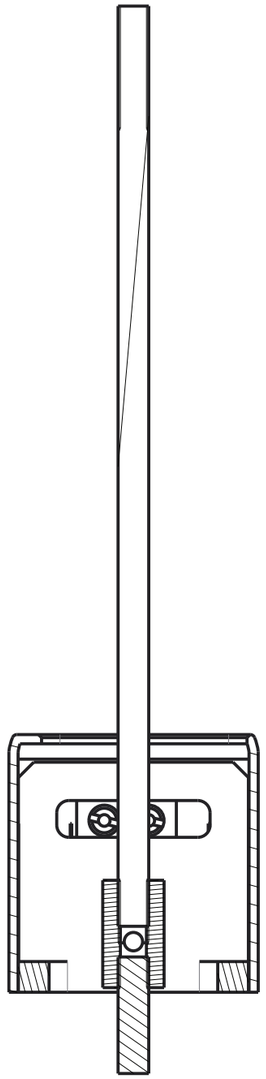

B-B
1:2

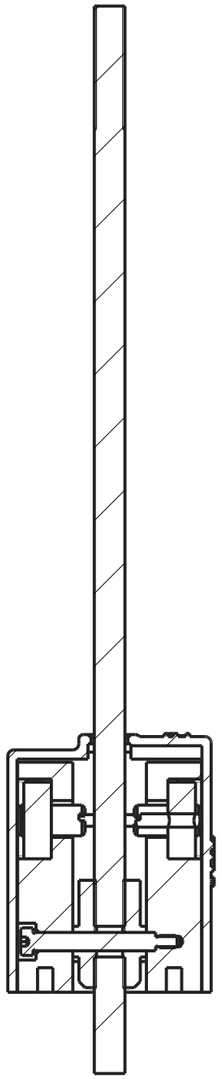

A-A

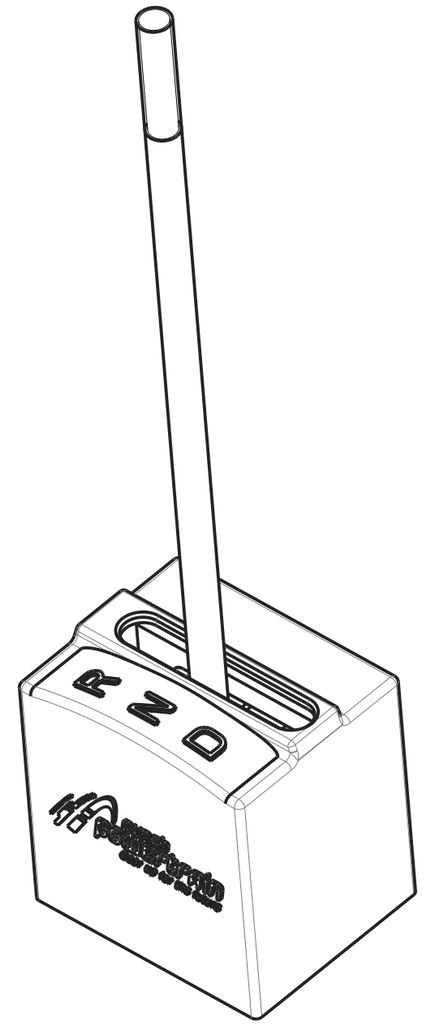

1:1.667

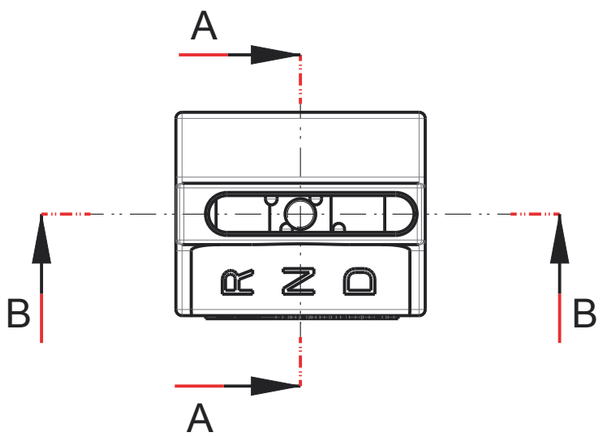

General tolerance unless otherwise stated:	General surface roughness unless otherwise stated:		
Material	Date: 28-June-17		Surf. roughness acc. to ISO 1302
	Drawn: Pedro Almeida		CAD system: Creo Parametric; Sheet: 1 of 2
	Design Resp.: Rudi Aerts		
Name: GEAR SELECTOR	Copied from: PNSA3102	Scale: 1:1	Mass: ( )kg
This drawing is property of Punch Powertrain NV and can't be used, copied or shown to third parties without written permission.	Article number: PNSA3102	Index: 0	
PUNCH POWERTRAIN NV	Document number: PNSA3102	Index: 0	DIN: A3

model name: PNSA3102 [ASSEM]

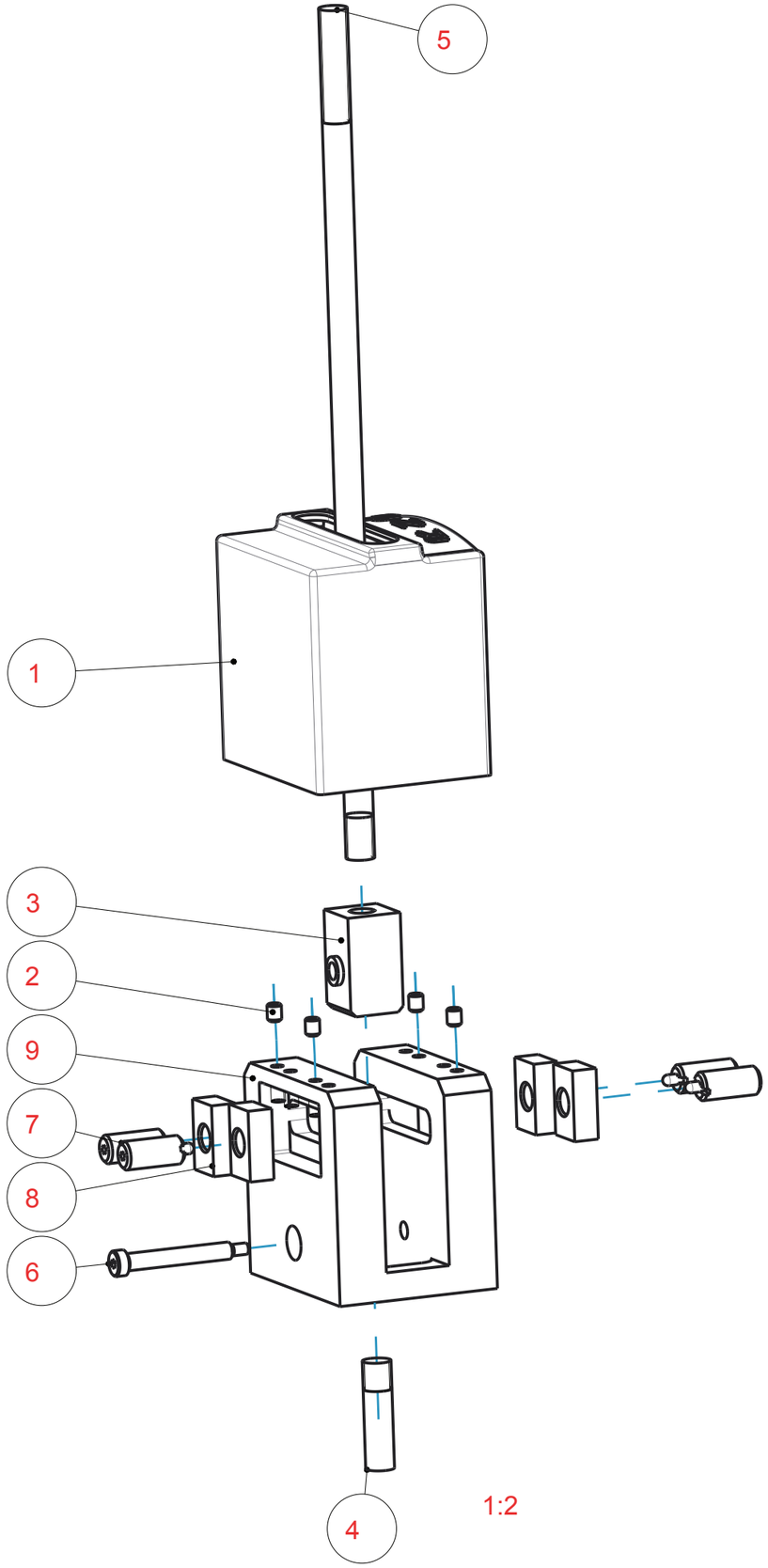

1:2

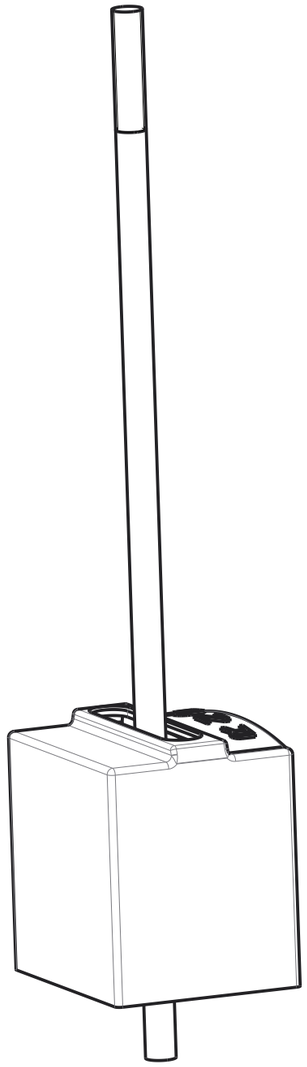

1:2

Pos	Article	Name	Qty
9	PNSA3102_11	Support	1
8	PNSA3102_13	Square nut	4
7	PNSA3102_10	Spring plunger	4
6	PNSA3102_12	Shoulder screw	1
5	PNSA3102_2	Selector shaft	1
4	PNSA3102_6	Secondary shaft	1
3	PNSA3102_5	Joining	1
2	PNSA3102_14	Hex socket set escrew	4
1	PNSA3102_1	Cover	1

General tolerance unless otherwise stated:

General surface roughness unless otherwise stated:

Material

Name

GEAR SELECTOR

PUNCH POWERTRAIN NV

Date	28-June-17	Surf. roughness acc. to ISO 1302	
Drawn	Pedro Almeida	CAD system: Creo Parametric	Sheet: 2 of 2
Design Resp.	Rudi Aerts		
Copied from: PNSA3102		Scale: 1:1	Mass: ( )kg
Article number: PNSA3102		Index: 0	
Document number: PNSA3102		Index: 0	DIN: A3

model name: PNSA3102 [ASSEM]

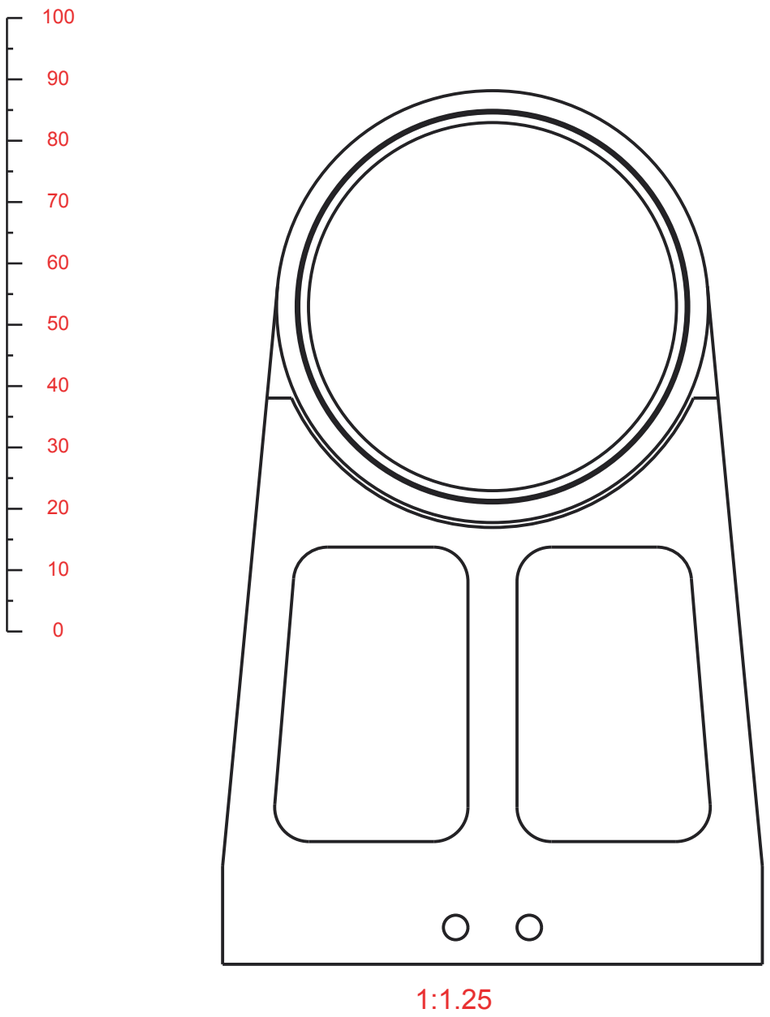

1:1.25

1:1.25

MIDDLE_PLANE-MIDDLE_PLANE

General tolerance unless otherwise stated:	General surface roughness unless otherwise stated:		
Material	Date	28-June-17	Surf. roughness acc. to ISO 1302
	Drawn	Pedro Almeida	CAD system: Creo Parametric; Sheet: 1 of 2
Name: FWD pressing plate	Design Resp.	Rudi Aerts	
	Copied from: PNSA3302	Scale: 1:1	Mass: ( )kg
This drawing is property of Punch Powertrain NV and can't be used, copied or shown to third parties without written permission.	Article number: PNSA3302	Index: 0	
PUNCH POWERTRAIN NV	Document number: PNSA3302	Index: 0	DIN: A3

model name: PNSA3302 [ASSEM]

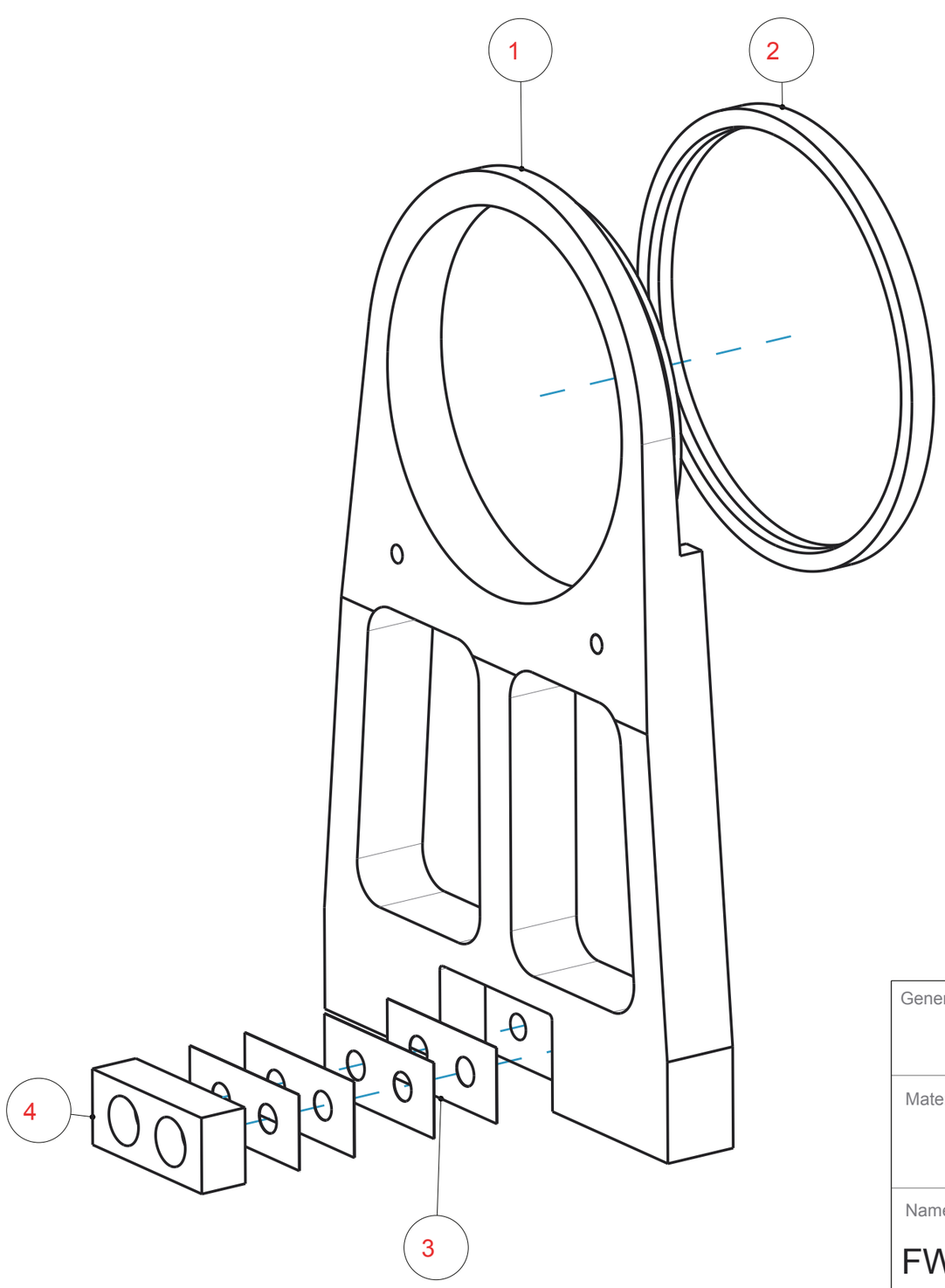

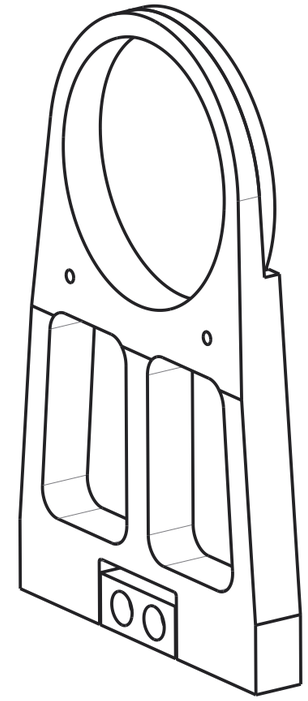

1:1.667

Pos	Article	Name	Qty
4	PNSA3302_2	Stopper	1
3	PNSA3302_3	Shrim	4
2	PNSA3302_1	Ring	1
1	PNSA3302_5	Pressing plate	1

General tolerance unless otherwise stated:

General surface roughness unless otherwise stated:

Material

Name

FWD pressing palte

Date: 28-June-17

Surf. roughness acc. to ISO 1302

Drawn: Pedro Almeida

Design Resp.: Rudi Aerts

CAD system: Creo Parametric

Sheet: 2 of 2

Copied from: PNSA3302

Scale: 1:1

Mass: ( )kg

Article number: PNSA3302

Index: 0

Document number: PNSA3302

Index: 0

DIN: A3

PUNCH POWERTRAIN NV

model name: PNSA3302 [ASSEM]

Shoulder screw will be fastened later during the assembly on the showcase

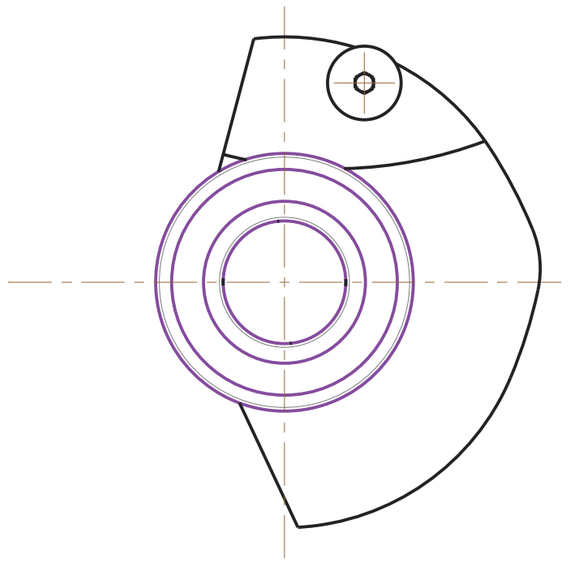

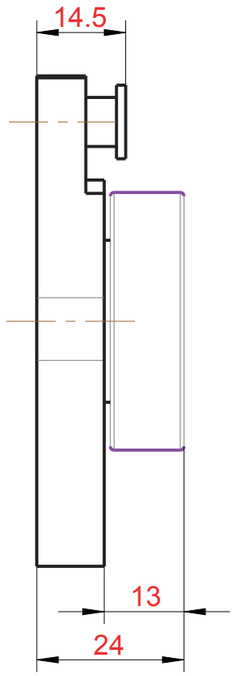

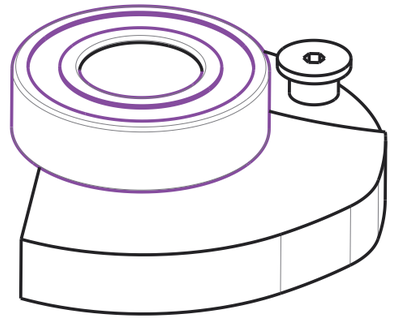

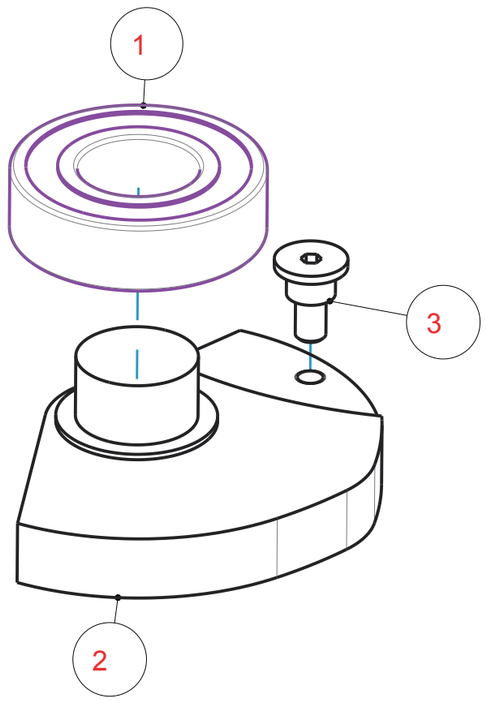

Pos	Article	Name	Qty
3	PNSA3403_3	Shoulder screw	1
2	PNSA3306_1	FWD cam	1
1	PNSA3306_4	Bearing	1

General tolerance unless otherwise stated:

General surface roughness unless otherwise stated:

Material

Name

FWD cam system

PUNCH POWERTRAIN NV

Date	28-June-17	Surf. roughness acc. to ISO 1302	
Drawn	Pedro Almeida	CAD system: Creo Parametric	Sheet: 1 of 1
Design Resp.	Rudi Aerts		
Copied from: PNSA3306		Scale: 1:1	Mass: ( )kg
Article number: PNSA3306		Index: 0	
Document number: PNSA3306		Index: 0	DIN: A3

model name: PNSA3306 [ASSEM]

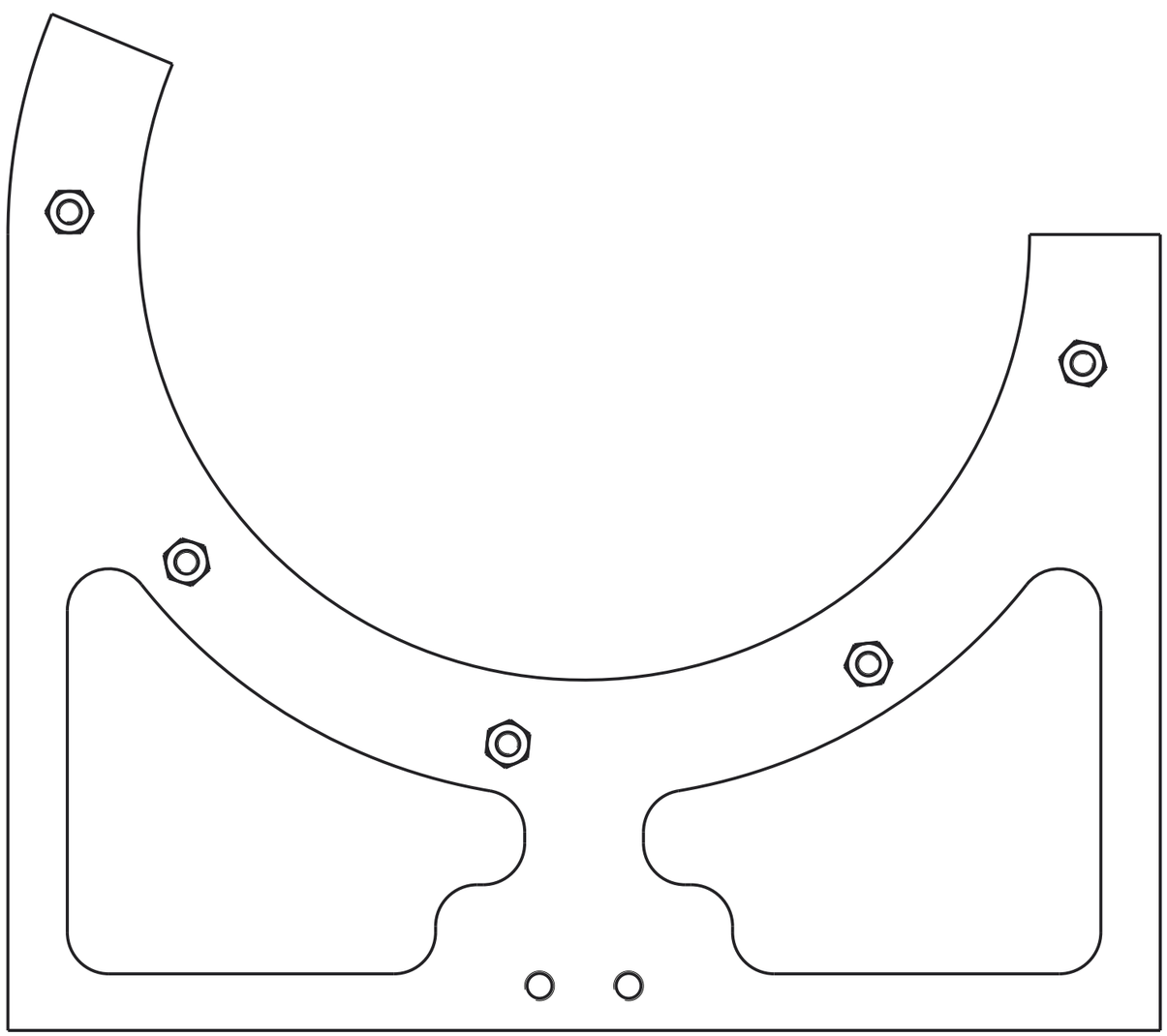

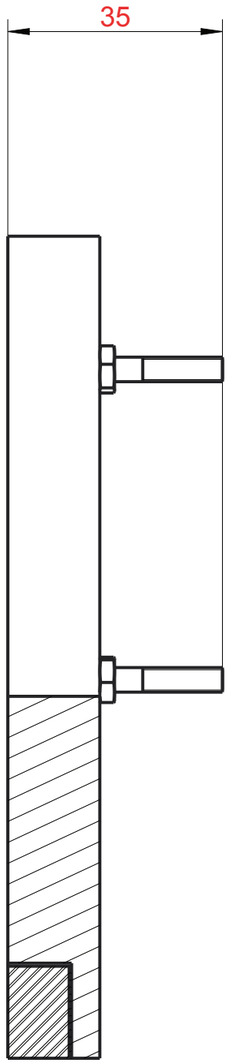

X-X

General tolerance unless otherwise stated:	General surface roughness unless otherwise stated:		
Material	Date: 28-June-17	Surf. roughness acc. to ISO 1302	
	Drawn: Pedro Almeida	CAD system: Creo Parametric	Sheet: 1 of 2
	Design Resp.: Rudi Aerts		
Name: REV pressing plate	Copied from: PNSA3401	Scale: 1:1	Mass: ( )kg
This drawing is property of Punch Powertrain NV and can't be used, copied or shown to third parties without written permission.	Article number: PNSA3401	Index: 0	
PUNCH POWERTRAIN NV	Document number: PNSA3401	Index: 0	DIN: A3

model name: PNSA3401 [ASSEM]

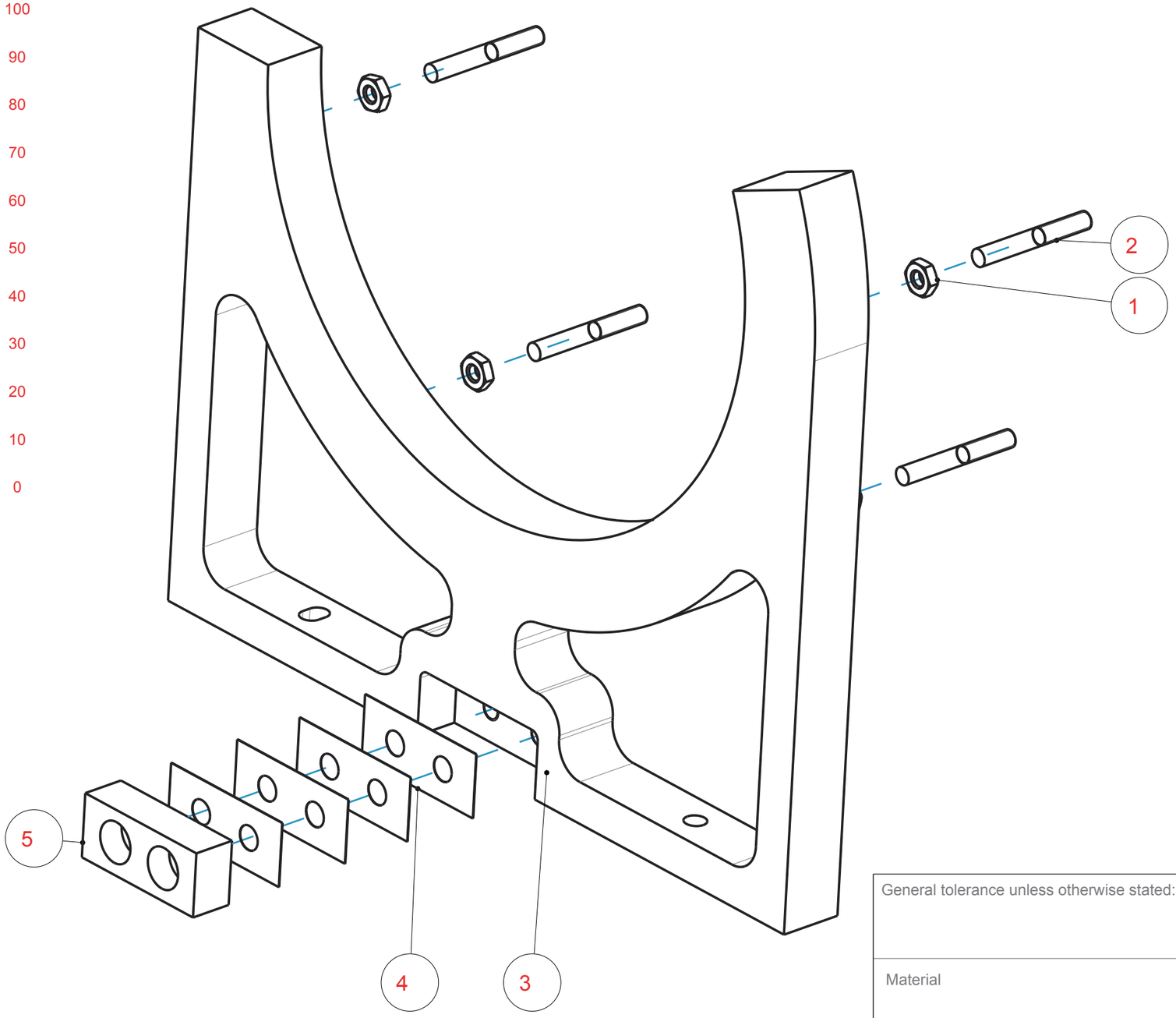

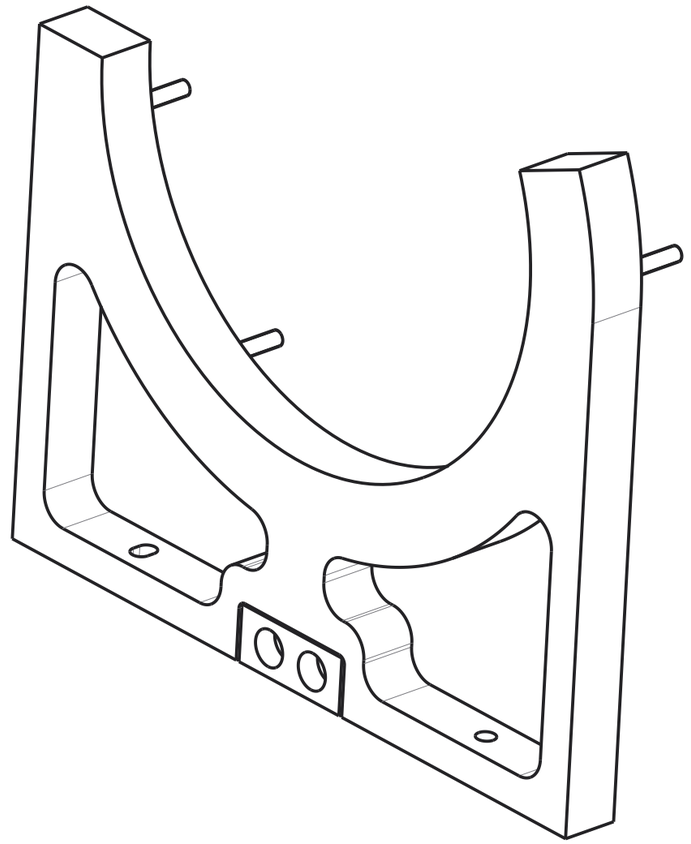

1:1.429

Pos	Article	Name	Qty
5	PNSA3302_2	Stopper	1
4	PNSA3302_3	Shrim	4
3	PNSA3401_1	Reverse pressing plate	1
2	PNSA3401_2	Pin	5
1	PNSA3401_3	Nut	5

General tolerance unless otherwise stated:

General surface roughness unless otherwise stated:

Material

Name

REV pressing plate

PUNCH POWERTRAIN NV

Date	28-June-17	Surf. roughness acc. to ISO 1302	
Drawn	Pedro Almeida	CAD system: Creo Parametric	Sheet: 2 of 2
Design Resp.	Rudi Aerts		
Copied from: PNSA3401		Scale: 1:1	Mass: ( )kg
Article number: PNSA3401		Index: 0	
Document number: PNSA3401		Index: 0	DIN: A3

model name: PNSA3401 [ASSEM]

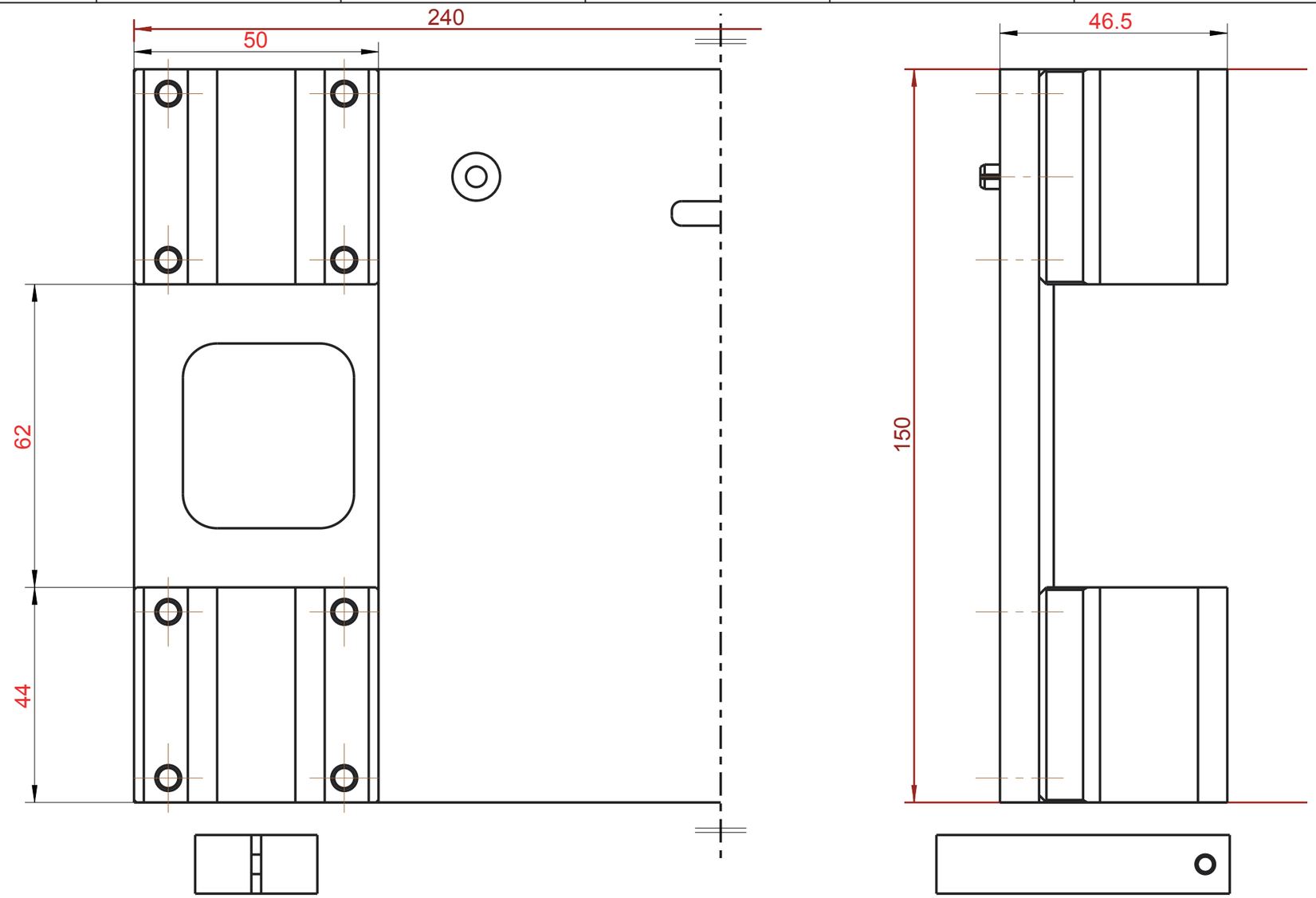

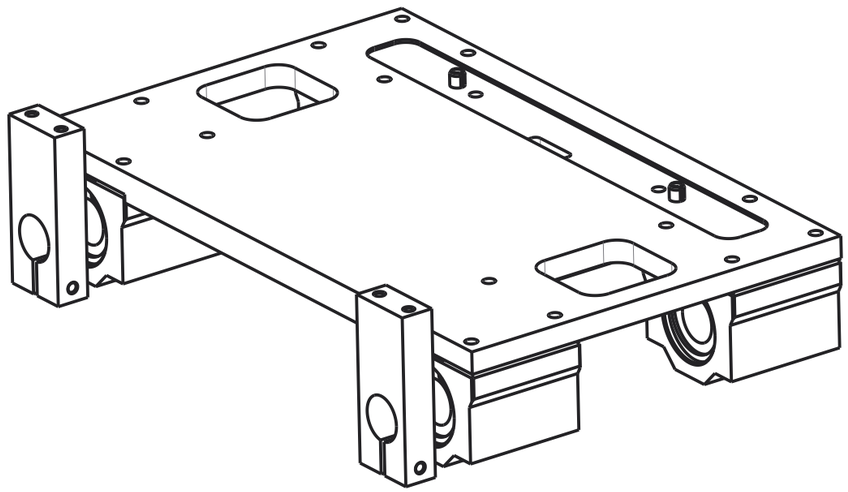

1:2

Shaft supports are free. They are presented on the drawing because they will be assembled at the showcase at the same time of the guiding plate system

General tolerance unless otherwise stated:	General surface roughness unless otherwise stated:	
Material	Date: 28-June-17	Surf. roughness acc. to ISO 1302
	Drawn: Pedro Almeida	CAD system: Creo Parametric; Sheet: 1 of 2
	Design Resp.: Rudi Aerts	
Name: REV guiding system	Copied from: PNSA3402	Scale: 1:1; Mass: ( )kg
This drawing is property of Punch Powertrain NV and can't be used, copied or shown to third parties without written permission.	Article number: PNSA3402	Index: 0
PUNCH POWERTRAIN NV	Document number: PNSA3402	Index: 0; DIN: A3

model name: PNSA3402 [ASSEM]

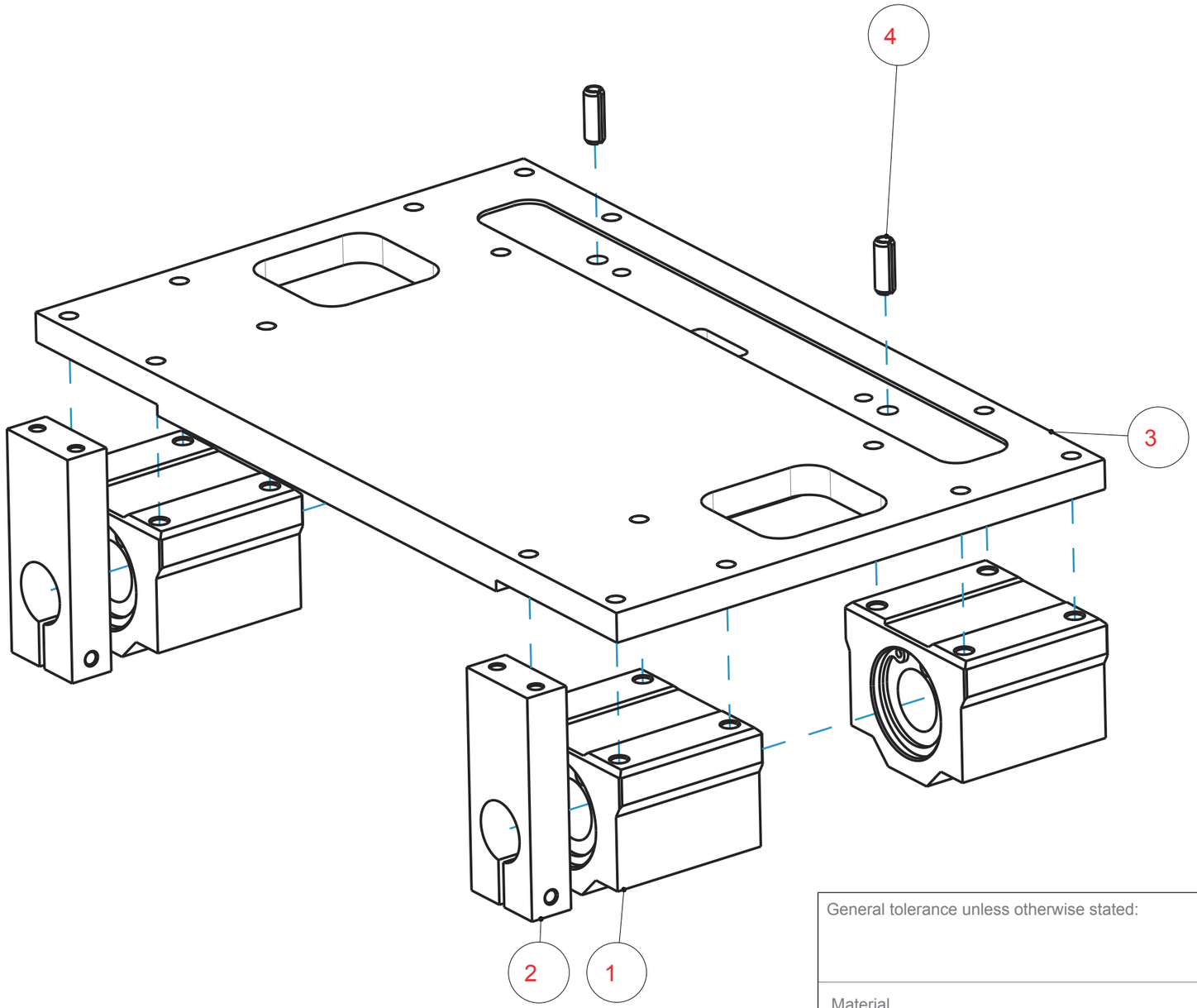

1:1.25

Pos	Article	Name	Qty
4	PNSA2104	Spring pin	2
3	PNSA3402_1	Reverse plate	1
2	PNSA3704	Shaft support	2
1	PNSA3702	Linear bushing	4

General tolerance unless otherwise stated:

General surface roughness unless otherwise stated:

Material

Name

REV guiding system

PUNCH POWERTRAIN NV

Date	28-June-17	Surf. roughness acc. to ISO 1302	
Drawn	Pedro Almeida	CAD system: Creo Parametric	Sheet: 2 of 2
Design Resp.	Rudi Aerts		
Copied from: PNSA3402		Scale: 1:1	Mass: ( )kg
Article number: PNSA3402		Index: 0	
Document number: PNSA3402		Index: 0	DIN: A3

model name: PNSA3402 [ASSEM]

Shoulder screw will be fastened later, during the assembly on the showcase

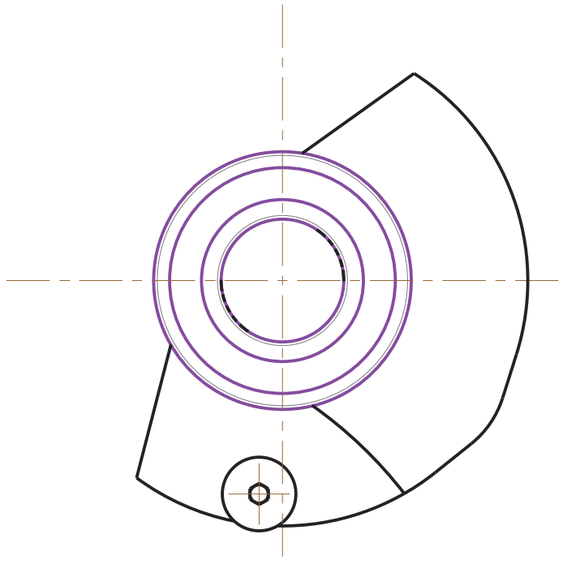

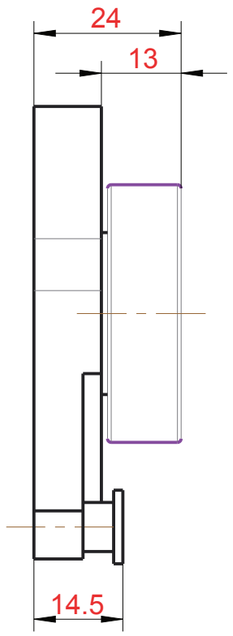

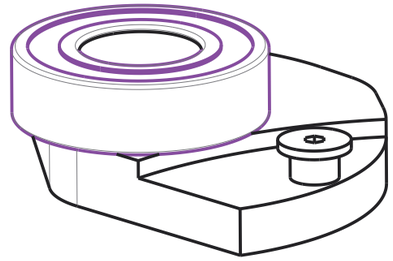

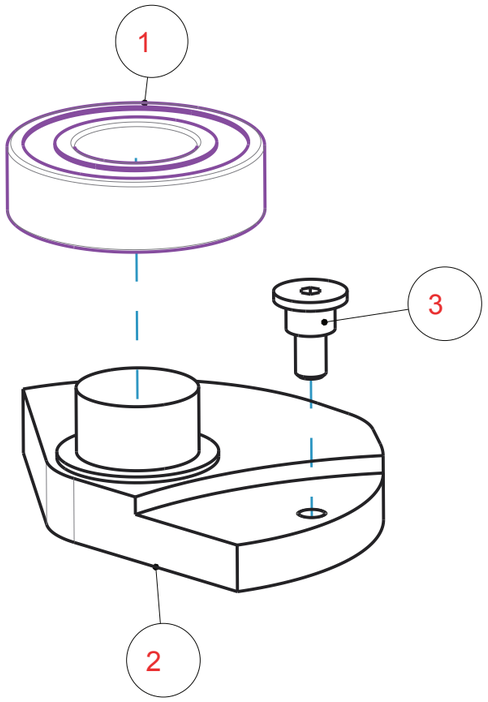

Pos	Article	Name	Qty
3	PNSA3403_3	Shoulder screw	1
2	PNSA3403_1	Reverse cam	1
1	PNSA3306_4	Bearing	1

General tolerance unless otherwise stated:	General surface roughness unless otherwise stated:		
Material	Date: 28-June-17	Surf. roughness acc. to ISO 1302	
	Drawn: Pedro Almeida	CAD system: Creo Parametric	Sheet: 1 of 1
Name: REV cam system	Design Resp.: Rudi Aerts		
	Copied from: PNSA3403	Scale: 1:1	Mass: ( )kg
This drawing is property of Punch Powertrain NV and can't be used, copied or shown to third parties without written permission.	Article number: PNSA3403	Index: 0	
PUNCH POWERTRAIN NV	Document number: PNSA3403	Index: 0	DIN: A3

model name: PNSA3403 [ASSEM]

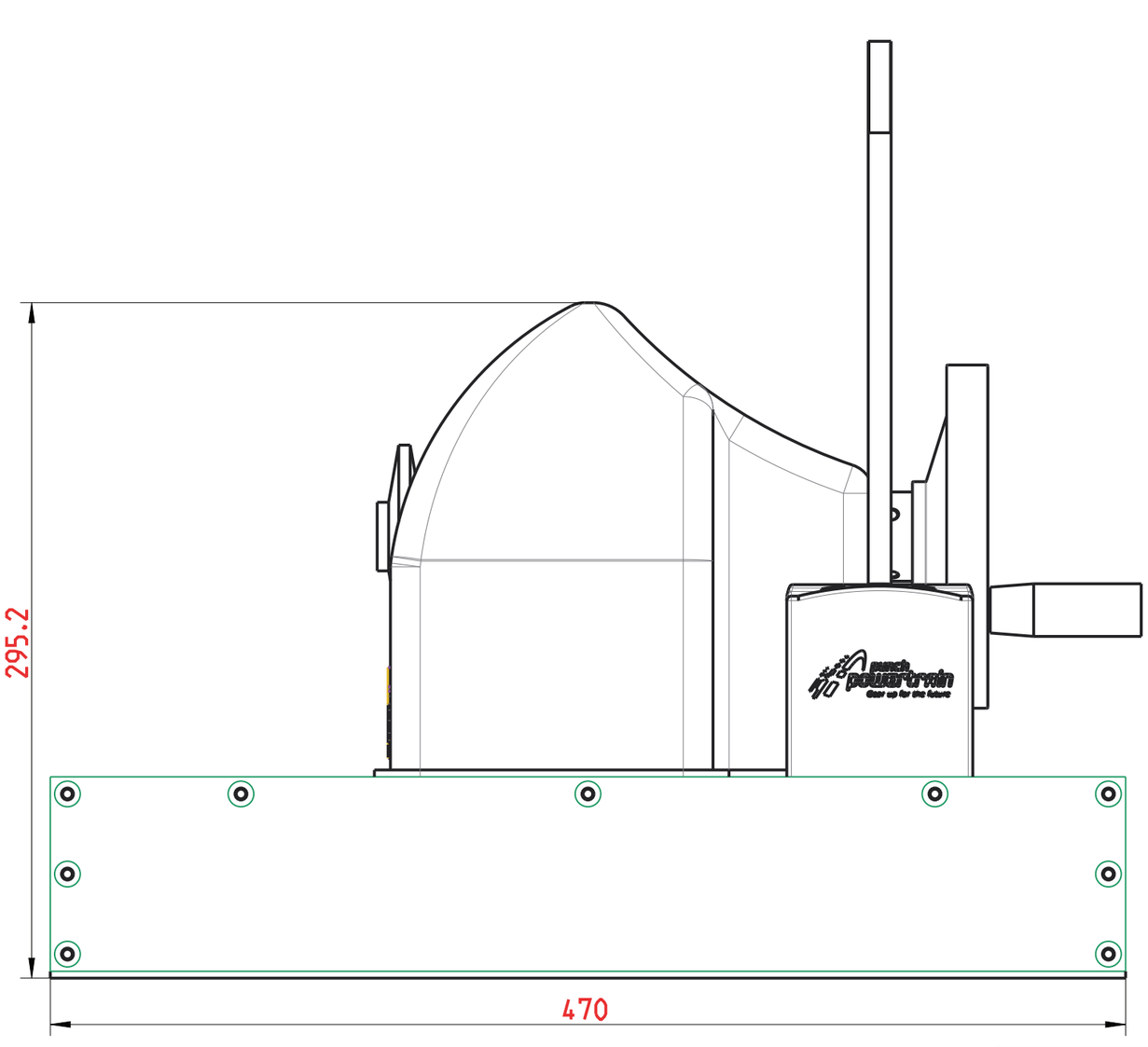

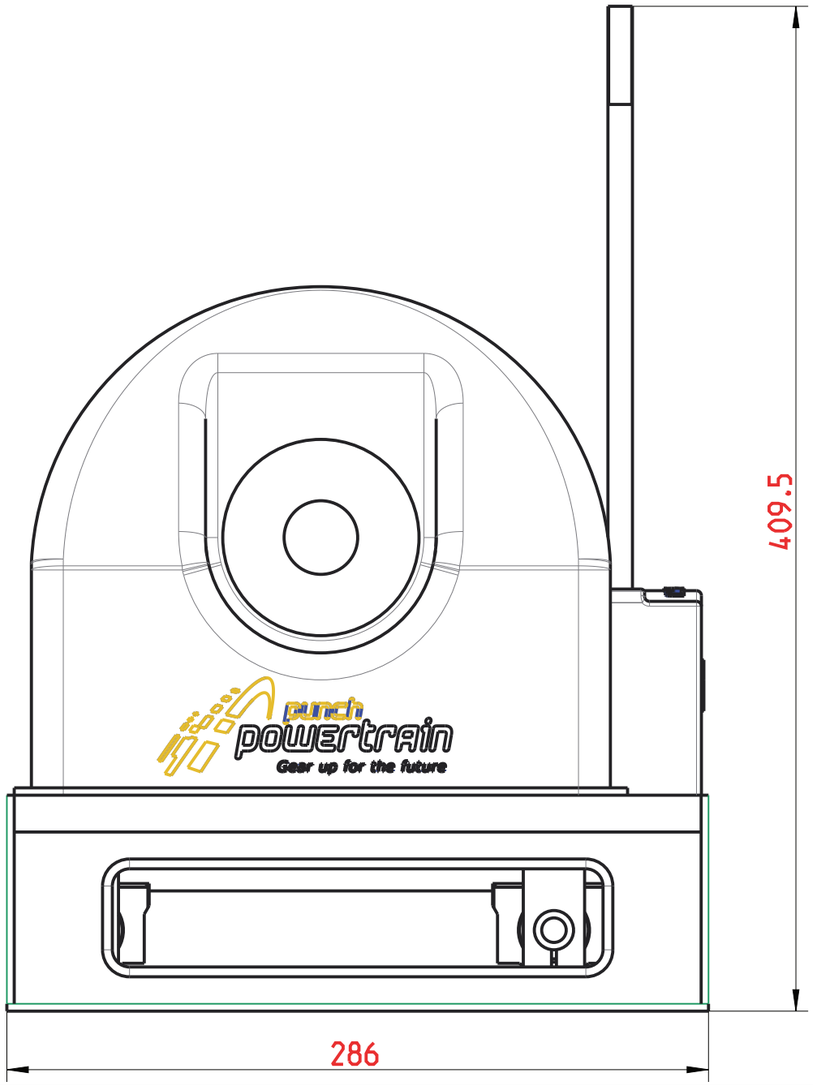

1:2.5

General tolerance unless otherwise stated:	General surface roughness unless otherwise stated:		
Material	Date: 17-July-17		Surf. roughness acc. to ISO 1302
	Drawn: Pedro Almeida	CAD system: Creo Parametric	Sheet: 1 of 7
	Design Resp.: Rudi Aerts		
Name: DNR Showcase	Copied from: T22661	Scale: 1:1	Mass: (22.6)kg
This drawing is property of Punch Powertrain NV and can't be used, copied or shown to third parties without written permission.	Article number: T22661	Index: 0	
PUNCH POWERTRAIN NV	Document number: DNR_SHOWCASE	Index: 0	DIN: A3

model name: SHOWCASE [ASSEM]

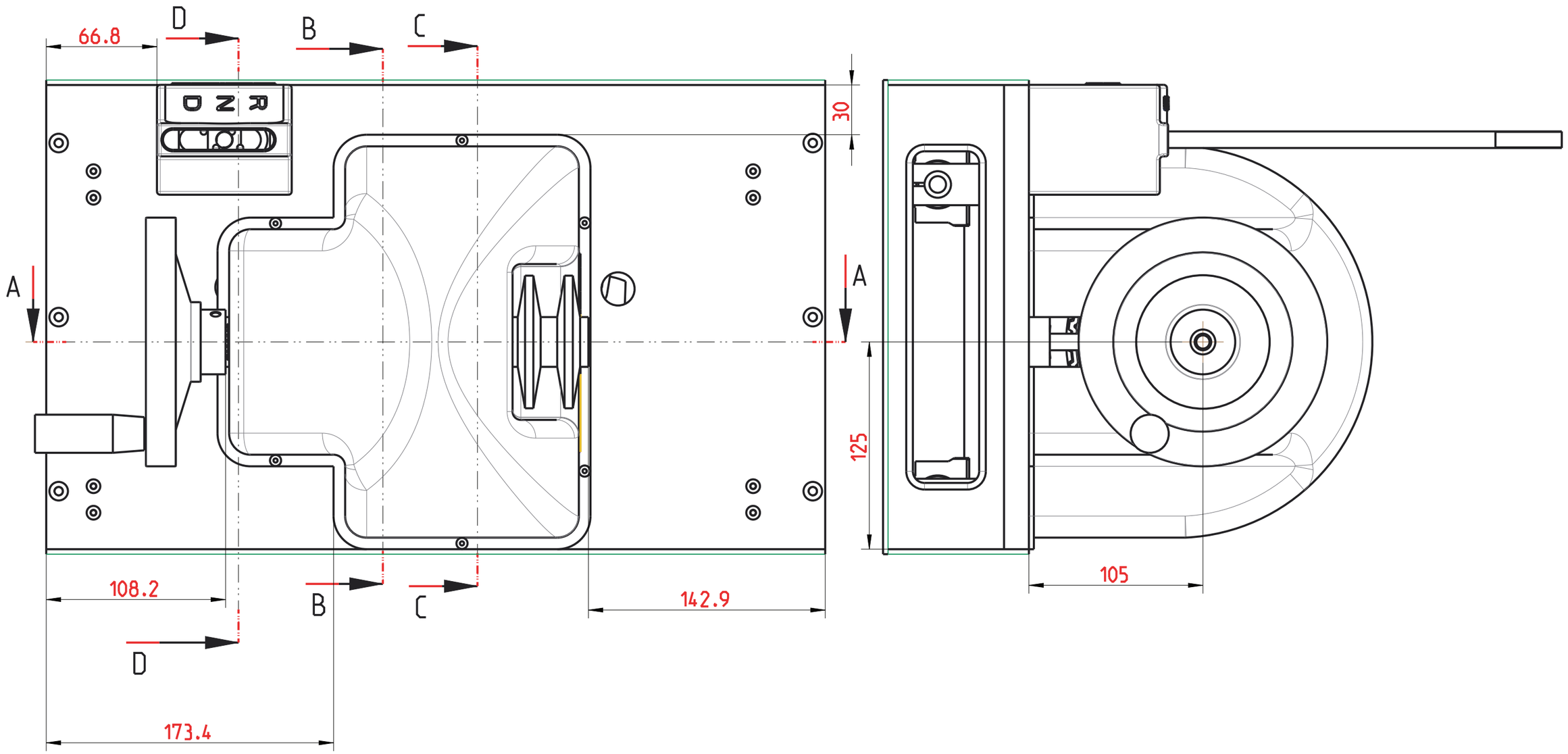

General tolerance unless otherwise stated:	General surface roughness unless otherwise stated:		
Material	Date	17-July-17	Surf. roughness acc. to ISO 1302
	Drawn	Pedro Almeida	CAD system: Creo Parametric; Sheet: 2 of 7
Name: DNR Showcase	Design Resp.	Rudi Aerts	
	Copied from: T22661	Scale: 1:1	Mass: (22.6)kg
This drawing is property of Punch Powertrain NV and can't be used, copied or shown to third parties without written permission.	Article number: T22661	Index: 0	
PUNCH POWERTRAIN NV	Document number: DNR_SHOWCASE	Index: 0	DIN: A3

model name: SHOWCASE [ASSEM]

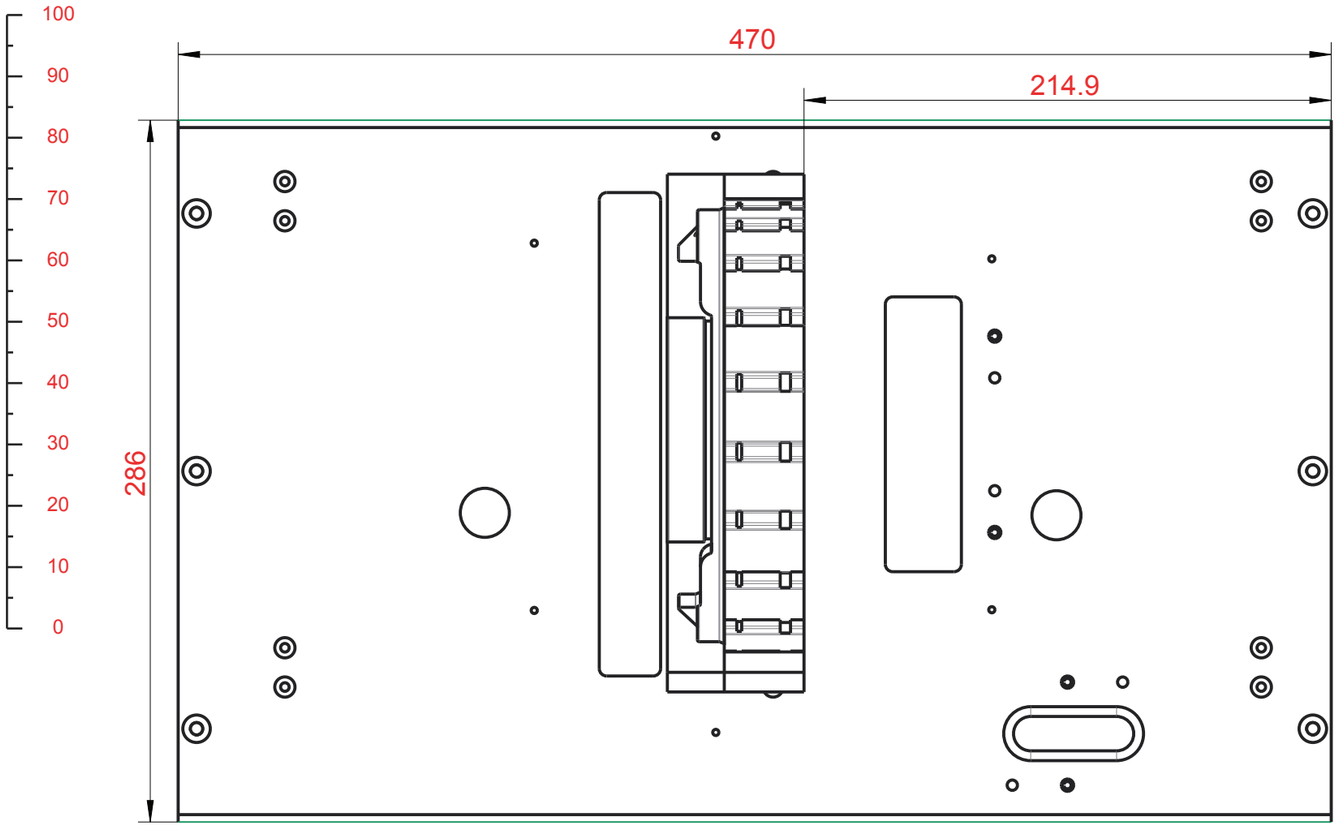

1:2.5

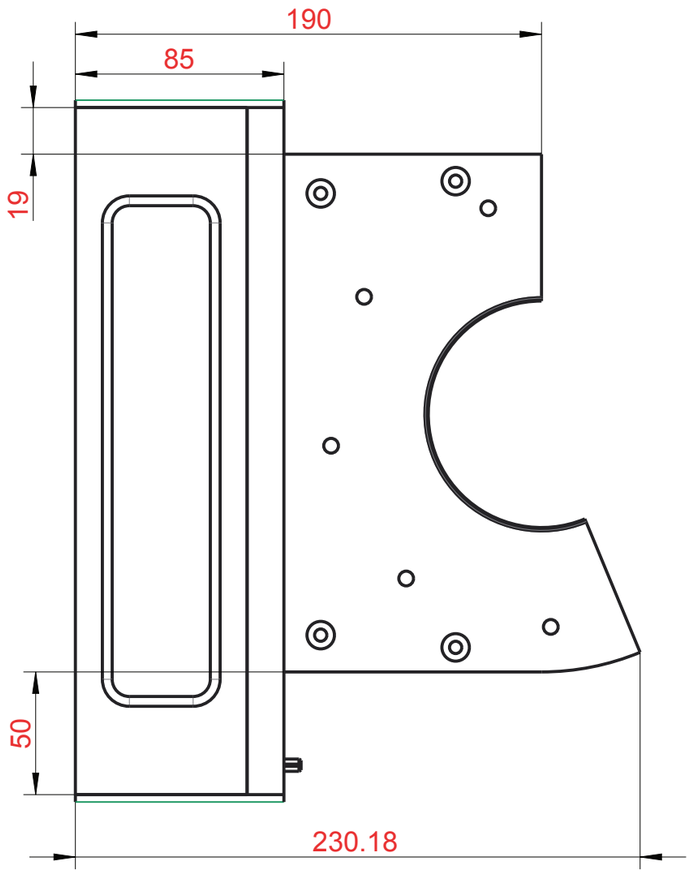

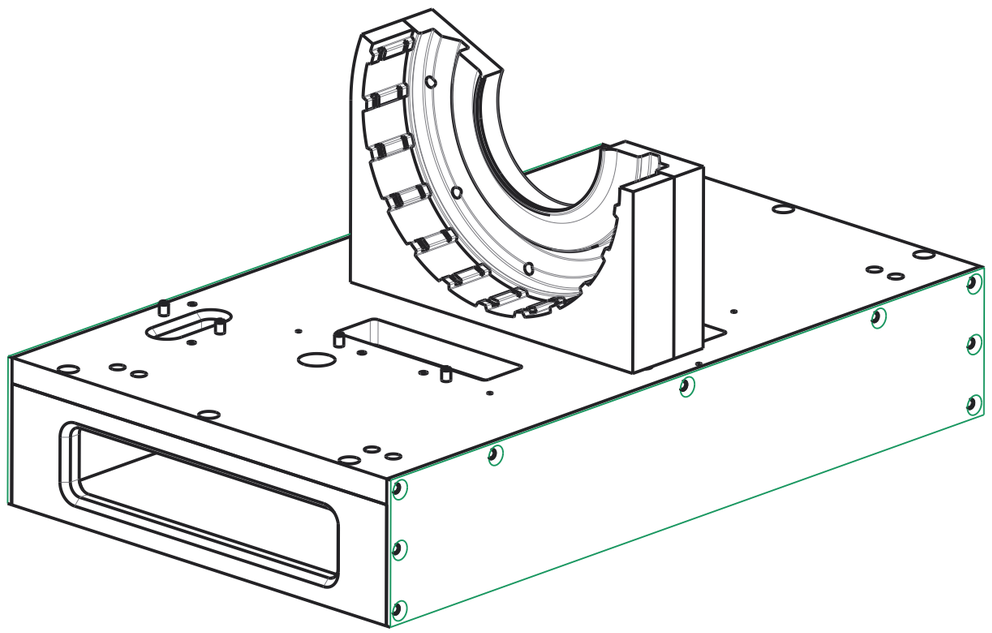

1:3.333

General tolerance unless otherwise stated:	General surface roughness unless otherwise stated:		
Material	Date: 28-June-17	Surf. roughness acc. to ISO 1302	
	Drawn: Pedro Almeida	CAD system: Creo Parametric	Sheet: 1 of 2
Name: Platform	Design Resp.: Rudi Aerts		
	Copied from: PNSA210	Scale: 1:1	Mass: ( )kg
This drawing is property of Punch Powertrain NV and can't be used, copied or shown to third parties without written permission.	Article number: PNSA210	Index:	
PUNCH POWERTRAIN NV	Document number: PNSA210	Index: 0	DIN: A3

model name: PNSA210 [ASSEM]

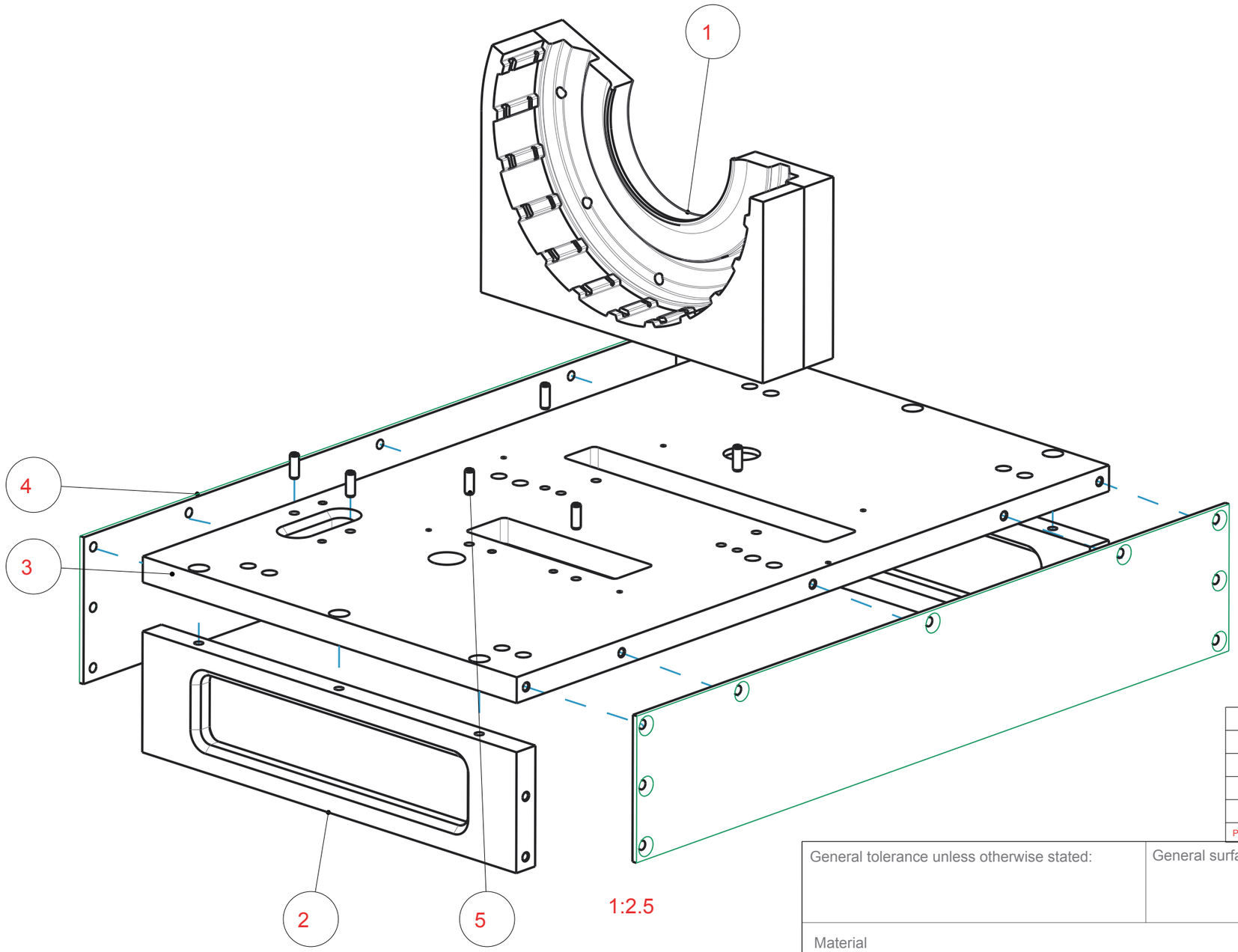

Pos	Article	Name	Qty
5	PNSA2104	Spring pin	6
4	PNSA2107	Side cover	2
3	PNSA2101	Main plate	1
2	PNSA2102	Leg	2
1	PNSA2103	DNR Housing	1

General tolerance unless otherwise stated:

General surface roughness unless otherwise stated:

Material

Name

Platform

PUNCH POWERTRAIN NV

Date	28-June-17	Surf. roughness acc. to ISO 1302	
Drawn	Pedro Almeida	CAD system: Creo Parametric	Sheet: 2 of 2
Design Resp.	Rudi Aerts		
Copied from: PNSA210		Scale: 1:1	Mass: ( )kg
Article number: PNSA210		Index: 0	
Document number: PNSA210		Index: 0	DIN: A3

model name: PNSA210 [ASSEM]

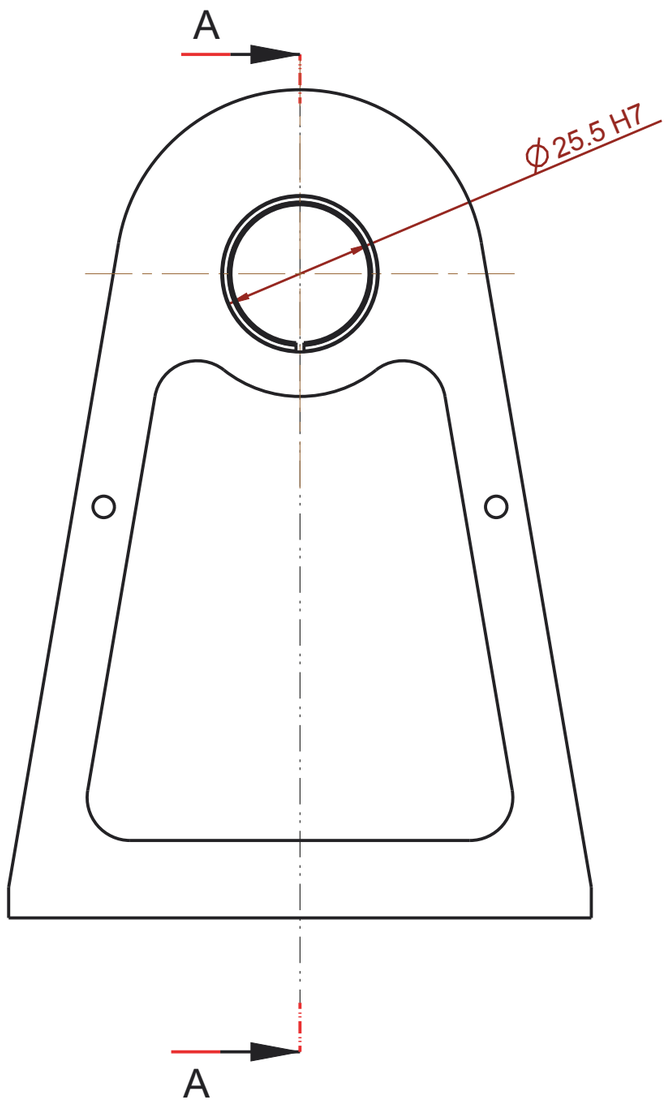

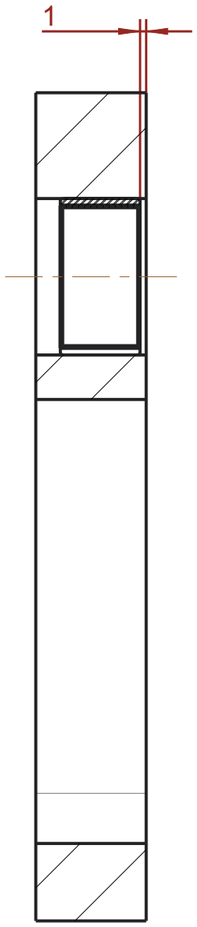

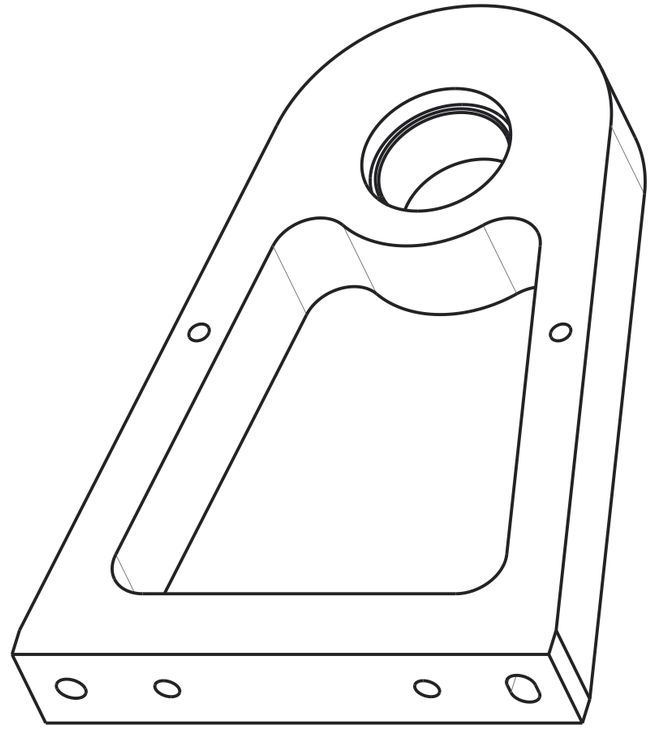

General tolerance unless otherwise stated:	General surface roughness unless otherwise stated:		
Material	Date	17-July-17	Surf. roughness acc. to ISO 1302
	Drawn	Pedro Almeida	CAD system: Creo Parametric; Sheet: 1 of 2
Name: Bushing support	Design Resp.	Rudi Aerts	
	Copied from: PNSA270	Scale: 1:1	Mass: ( )kg
This drawing is property of Punch Powertrain NV and can't be used, copied or shown to third parties without written permission.	Article number: PNSA270	Index: 0	
PUNCH POWERTRAIN NV	Document number: PNSA270	Index: 1	DIN: A3

model name: PNSA270 [ASSEM]

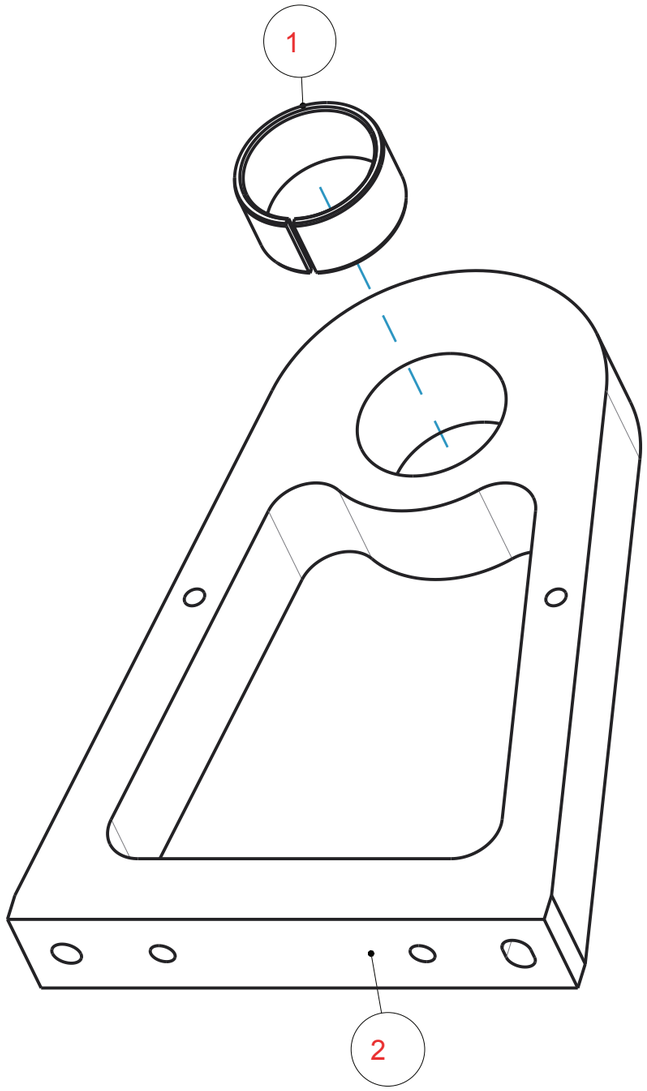

Pos	Article	Name	Qty
2	PNSA2701	Bushing support	1
1	541179_DES001	Bearing Bush Plate Stator	1

General tolerance unless otherwise stated:

General surface roughness unless otherwise stated:

Material

Name

Bushing support

PUNCH POWERTRAIN NV

Date	17-July-17	Surf. roughness acc. to ISO 1302	
Drawn	Pedro Almeida	CAD system: Creo Parametric	Sheet: 2 of 2
Design Resp.	Rudi Aerts		
Copied from: PNSA270		Scale: 1:1	Mass: ( )kg
Article number: PNSA270		Index: 0	
Document number: PNSA270		Index: 1	DIN: A3

model name: PNSA270 [ASSEM]

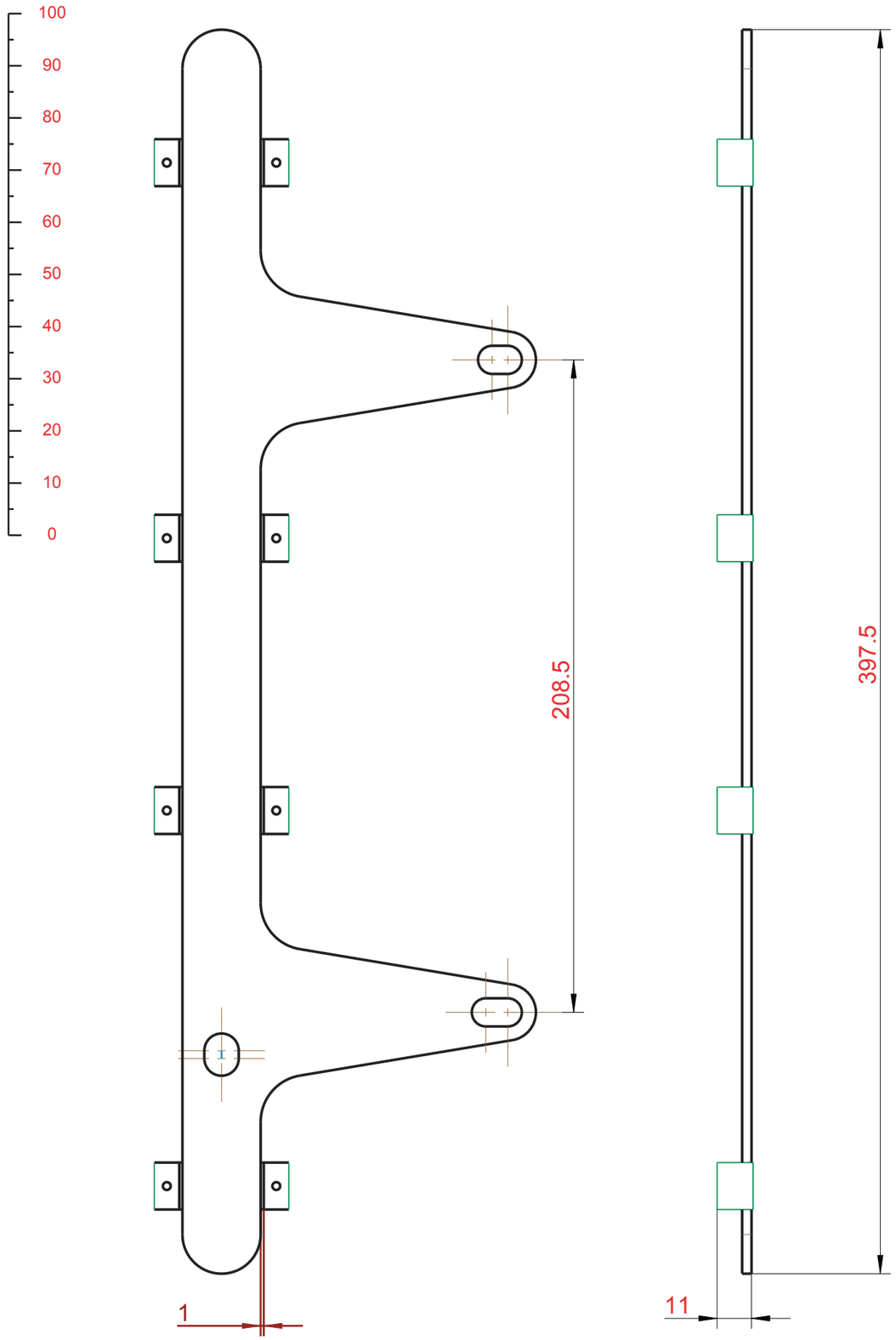

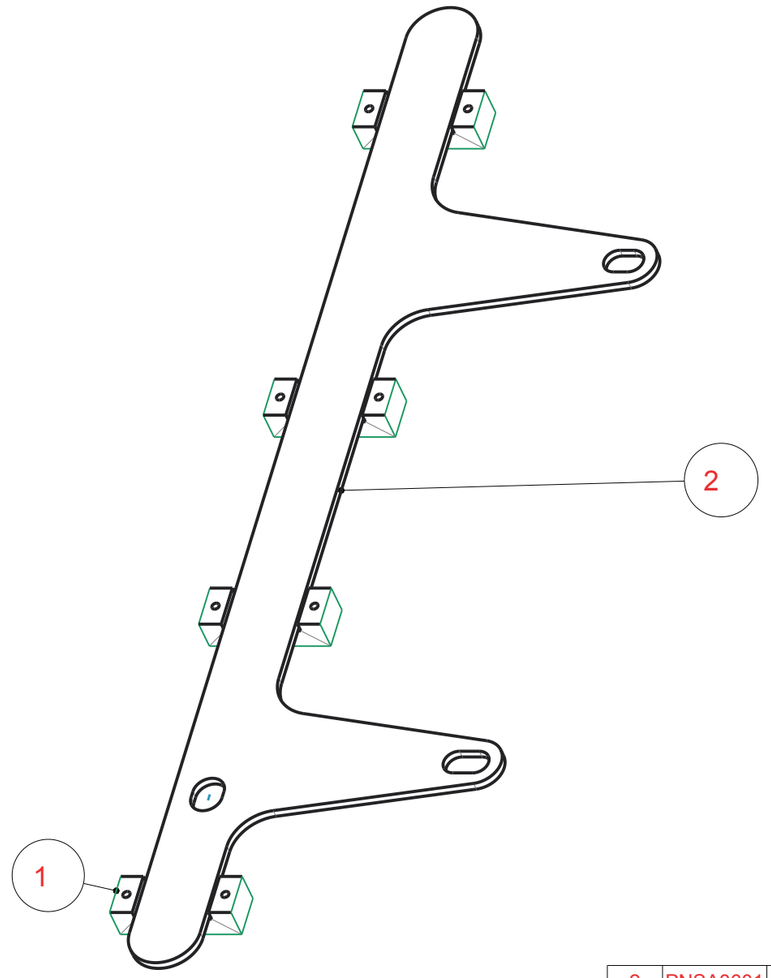

1:2

Pos	Article	Name	Qty
2	PNSA3601	Main	1
1	PNSA3608	Guide	4

General tolerance unless otherwise stated:	General surface roughness unless otherwise stated:		
Material	Date: 17-July-17	Surf. roughness acc. to ISO 1302	
	Drawn: Pedro Almeida	CAD system: Creo Parametric	Sheet: 1 of 1
	Design Resp.: Rudi Aerts		
Name: Lever system	Copied from: PNSA360	Scale: 1:1	Mass: ( )kg
This drawing is property of Punch Powertrain NV and can't be used, copied or shown to third parties without written permission.	Article number: PNSA360	Index: 0	
PUNCH POWERTRAIN NV	Document number: PNSA360	Index: 0	DIN: A3

model name: PNSA360 [ASSEM]